Protection of Works of Art from Photochemical Smog

Glen R. Cass

James R. Druzik

Daniel Grosjean

William W. Nazaroff

Paul M. Whitmore

Cynthia L. Wittman

JUNE 1988

Environmental Quality Laboratory
California Institute of Technology
Pasadena, California 91125

The Getty Conservation Institute
Scientific Program
4503 Glencoe Avenue
Marina del Rey, California 90292-6537

Final Report Submitted to
The Getty Conservation Institute

PROTECTION OF WORKS OF ART FROM PHOTOCHEMICAL SMOG

by

Glen R. Cass, James R. Druzik, Daniel Grosjean,
William W. Nazaroff, Paul M. Whitmore and Cynthia L. Wittman

June, 1988

Environmental Quality Laboratory
California Institute of Technology
Pasadena, California 91125

TABLE OF CONTENTS

TABLE OF CONTENTS

TABLE OF CONTENTS

TABLE OF CONTENTS

TABLE OF CONTENTS

TABLE OF CONTENTS

ACKNOWLEDGEMENTS

Thanks are due to Dr. Frank D. Preusser and the staff of the Getty Conservation Institute for technical advice throughout the course of this project.

The natural colorants used in this work were made available with the cooperation of a large number of individuals. Eugene Farrell and Richard Newman of the Harvard University Art Museums, and Gary Wade Alden of the Balboa Art Conservation Center provided pigments used traditionally in Western pictorial art. The Japanese silk cloths were dyed by Mr. S. Yamazaki and were made available through Dr. K.M. Kashiwagi of the Kyoritsu Women's University, Tokyo. Dr. Takeo Kadokura and Dr. Kunio Yoshizumi are also to be thanked for their help with sample acquisition in Japan. The aigami sample and woodblock prints from an illustrated poetry book were provided by Mrs. Keiko Keyes. The Munsell conversion calculations were performed using a computer program supplied by Max Saltzman and Dr. Fred Billmeyer. Discussions with Mr. Saltzman were helpful in the spectroscopic analyses of the pigments. The authors also wish to acknowledge the assistance of Dr. Helmut Schweppe, whose advice and reference materials aided the thin layer chromatographic identification of the natural colorants.

Solvent extractions needed to prepare samples for mass spectrometry analysis were carried out by Dr. Scott Boyce of the California Institute of Technology. The mass spectrometry analyses were performed by Drs. Dilip K. Sensharma and John Wells, Department of Chemistry, University of California, Los Angeles. The XRF analyses of the inorganic constituents of the pigments tested were performed at NEA, Inc., Portland, OR.

The program of indoor/outdoor ozone concentration measurements in southern California museums was conducted with the help of Mark Adams and Christine Tiller of the California Institute of Technology. The assistance of the staff of each of the museum sites tested is sincerely appreciated; without access to these

facilities, this research project could not have been completed. Dr. Fred Shair of Caltech made available the laboratory facilities needed for the SF_6 tracer tests used to determine the air exchange rates between display cases and the room air.

This project final report and the accompanying eleven journal articles were typed by Dixie Fiedler and Christina Conti. Nancy Tomer drafted the figures.

CHAPTER 1
OZONE AND THE FADING OF ARTISTS' PIGMENTS

INTRODUCTION

Air pollution has been suspected as a possible cause of damage to museum collections for at least one hundred years. As early as 1888, concern over pollution in the London atmosphere led to a systematic investigation of whether or not direct exposure to the combustion exhaust from a burning gas jet would cause artists' pigments to fade (1). Since that time, a number of studies have examined the effects of sulfur oxides air pollutants on leather, paper, calcareous stone, textiles and a few pigments (2). Much less has been said about the effects of photochemically-generated air pollutants like ozone, which is found in Los Angeles, Athens and other cities that experience intense solar radiation in the presence of high population densities.

Ozone is one of the most powerful oxidants found in nature. High levels of atmospheric ozone (O_3) in outdoor urban atmospheres are known to be caused by the combined interaction of sunlight, oxygen, oxides of nitrogen and hydrocarbons (3). Many effects of ozone on materials have been reviewed by Jaffe (4) and by the National Research Council (5). Accordingly, damage to materials has been reported for rubber (6), exterior paint binders (7) and textile fibers (8). Ozone attack on cellulose has been investigated by Katai and Schuerch (9). Within the textile industry, ozone has been implicated in the fading of anthraquinone dyes on nylon and cellulose acetate (10-14).

In the early 1980's, a pilot study was conducted to determine whether or not artists' pigments are affected by exposure to ozone at the concentrations found in urban atmospheres. In the first exploratory test, seventeen artists' watercolor pigment samples and two Japanese woodblock prints were exposed to 0.40 ppm ozone in a controlled test chamber for three months (15). A second study followed in

which the ozone-fastness of 27 modern organic watercolor pigments was examined (16). It was found that several artists' pigments when applied on paper will fade in the absence of light if exposed to an atmosphere containing ozone at the concentrations found in photochemical smog. Alizarin-based watercolors containing 1,2-dihydroxyanthraquinone lake pigments were shown to be particularly sensitive to ozone damage, as were the yellow pigments used in the Japanese woodblock prints tested. Indoor-outdoor ozone measurements made at that time in a Pasadena, California art gallery confirmed that ozone concentrations half as high as those outdoors can be found in art galleries that lack a chemically protected air conditioning system. The identification of ozone-sensitive artists' pigments plus the existence of high ozone levels inside at least one museum argued that further investigation of the hazard to works of art posed by exposure to photochemically-generated air pollutants was warranted.

Objectives and Approach

The objective of the present research project is to provide a comprehensive assessment of the effect of ozone and nitrogen dioxide on the fading of artists' pigments, and to determine the methods that can be used to protect works of art from damage due to atmospheric ozone. In Chapter 2 of this work, the ozone-induced fading of traditional natural organic artists' pigments is studied, based on pigment samples withdrawn from the Forbes collection at Harvard, and elsewhere. Chapter 3 continues with an examination of the ozone fading of traditional Japanese colorants. In Chapters 4, 5, 6 and 7, the mechanisms of the ozone reaction with alizarin lakes, indigos, curcumin and the triphenylmethanes are examined based on gas chromatography/mass spectrometry analysis of the ozone-colorant reaction products. It is shown that the reaction products are indeed consistent with ozone being the cause of the observed destruction of these colorants during the ozone exposure experiments.

Ozone is not the only oxidant present in photochemical smog. Nitrogen dioxide (NO_2) is a somewhat weaker oxidant that is found in high concentrations in urban atmospheres. NO_2 has been shown to redden some blue anthraquinone textile dyes (17,18). In Chapter 8 of this report, the effect of NO_2 on the fading of artists' pigments is examined by means analogous to the earlier ozone exposure experiments.

The existence of a fading hazard to works of art posed by photochemical oxidants depends in part on whether or not the high concentrations of ozone and NO_2 found in outdoor air are transferred to the indoor atmospheres of museums and galleries. In Chapter 9 of this work, a mathematical model is presented for predicting the concentration of chemically reactive air pollutants in indoor air based on outdoor pollutant levels and building design variables. The model is tested by application to the Virginia Steele Scott Gallery at the Huntington Library in San Marino, CA. Close agreement is found between computed and observed indoor O_3 and NO_2 levels. In Chapter 10, a survey of indoor/outdoor ozone concentration relationships in eleven museums, galleries, historical society houses and libraries in Southern California is presented. Advice is offered on estimation of the ozone concentrations in buildings that have not yet been tested, based on analogy to the large variety of building and ventilation system types studied here.

Protection of works of art from damage due to atmospheric ozone is discussed in Chapters 11 and 12. Several categories of control measures are evaluated via laboratory and field experiments, including:

(a) Application of binders or coatings, when appropriate, to protect pigments from reaction with ozone (Chapter 11).

(b) Elimination of pollutants from indoor atmospheres via ventilation system redesign.

(c) Construction of display cases to protect the works.

(d) Framing of paintings, prints and watercolors behind glass.

(e) Selection of ozone-resistant pigments.

While advanced air purification systems indeed can be used to protect collections from ozone damage, a number of inexpensive protective measures also are identified that can be employed effectively.

SUMMARY OF MAJOR FINDINGS

The Ozone Fading of Traditional Natural Organic Colorants

More than 50 samples of traditional natural organic pigments provided from the Forbes collection at Harvard and elsewhere were applied to watercolor paper and then were exposed to 0.397±0.007 ppm ozone at 22°C and 50% RH, in the absence of light, for 12 weeks. This ozone concentration is typical of that found in the Los Angeles atmosphere during a heavy smog episode, and the total ozone dose delivered to the samples is equivalent to about four years of exposure to outdoor air in Los Angeles, or to about eight years inside a typical air conditioned building in that city. The ozone sensitivity of these colorant systems was evaluated by measuring the color changes which occurred progressively over time. Almost all of the organic colorant systems tested showed some fading after ozone exposure, and several colorants (curcumin, dragon's blood, indigo and madder lake) were found to be very ozone-fugitive.

The Ozone Fading of Traditional Japanese Colorants

The colorfastness of several traditional Japanese colorants upon exposure to atmospheric ozone was tested in a chamber exposure experiment. Samples, in the form of colorants applied to paper, dyes on silk cloth, and colorants on a 19th century Japanese woodblock print, were exposed to an atmosphere containing 0.40

ppm ozone at 22°C and 50%RH, in the absence of light, for 12 weeks. Color differences, calculated from the measured diffuse reflectance spectra, were used to assess the rate and extent of the ozone fading. Of the colorants applied to paper, orpiment was the only inorganic pigment that showed severe color loss after ozone exposure. Several organic colorants on paper also reacted, including the widely used plant colorants *ai* (indigo) and *ukon* (turmeric). The woodblock print, produced using the plant-derived colorants *beni* (safflower), *ai* (indigo), *shiō* (gamboge), and *aigami* (dayflower), showed significant ozone fading only in the blue and green areas, which contain *ai*. Several of the dyed silk cloths also exhibited some color change in this experiment, suggesting that prolonged exposure to atmospheric ozone could pose a risk to these materials as well.

Confirmation that Ozone is Indeed the Cause of the Observed Fading Phenomena

As a result of the chamber ozone exposure experiments just described, several families of artists' colorants were identified as being particularly ozone-sensitive. Four colorant families were selected for detailed examination to confirm that the chemical reaction products of the ozone-colorant interaction were indeed consistent with ozone being the actual cause of the observed fading phenomena.

The colorants alizarin, Alizarin Crimson (a calcium-aluminum lake pigment), indigo, dibromoindigo, colorants containing thioindigo and tetrachlorothioindigo, curcumin (1,7-bis(4-hydroxy-3-methoxyphenyl)-1,6-heptadiene-3,5-dione), the triphenylmethane cationic dye Basic Violet 14, and other closely related compounds were deposited on silica gel, cellulose, and Teflon substrates and exposed in the dark to ozone in purified air (~0.4 ppm O_3 for 95 days and ~10 ppm O_3 for 18-80 hours). Exposed and control samples were analyzed by mass spectrometry.

In all cases, the reaction products observed were consistent with the proposition that reaction with ozone is indeed the cause of the observed fading. Alizarin

Crimson reacted with ozone on all substrates, yielding phthalic acid (major), benzoic acid (minor), and other minor and unidentified products. Important substrate-specific effects were observed, with alizarin dye on silica gel and the alizarin lake pigment samples being far more reactive toward ozone than alizarin dye deposited on cellulose, Teflon, or watercolor paper. A chemical mechanism responsible for the fading of these alizarin-related colorants by ozone is suggested that is consistent with the products distribution, the observed reactivity sequence and the observed substrate-specific effects. Under the conditions employed, indigo and dibromoindigo were entirely consumed, and the major reaction products were isatin and isatoic anhydride from indigo and bromoisatin and bromoisatoic anhydride from dibromoindigo. Thioindigo and its chloro derivative also reacted with ozone, though at a slower rate; the corresponding substituted isatins and anhydrides were tentatively identified as reaction products. The major products of the ozone-curcumin reaction included vanillin (4-hydroxy-3-methoxy benzaldehyde) and vanillic acid (4-hydroxy-3-methoxy benzoic acid). Basic Violet 14 reacted to form methyldiaminobenzophenone and other products. These products and the corresponding loss of chromophore (i.e. fading) are consistent with a reaction mechanism involving electrophilic addition of ozone onto the olefinic bonds of the indigos, curcumin and triphenylmethane-derived colorants studied. At least in the case of dibromoindigo, the ozone-indigo reaction products are distinctly different from those produced by the light-induced fading of the same colorant.

The Effect of Nitrogen Dioxide on the Fading of Artists' Pigments

Nitrogen dioxide is a common air pollutant, formed in the atmosphere from the nitric oxide emissions from fuel combustion sources. Samples of organic and inorganic pigments, iron inks on paper, and traditional Japanese textile dyes mordanted onto silk were exposed to 0.50 ppm NO_2 in air for 12 weeks. Ten of the eighteen traditional natural organic colorant samples on paper tested showed

measurable color changes ($\Delta E > 2$) as a result of the NO_2 exposure, as did several of the anthraquinone-based synthetic organic pigments. The arsenic sulfide pigments orpiment and realgar and the iron inks tested showed considerable color changes ($\Delta E > 5$) over the 12 week period. Nine of the 23 Japanese dyed silk cloths changed color by at least 2 ΔE units, including an *Enju* (Japanese pagoda tree-derived) sample that faded by more than 7 ΔE units. An NO_2 dose (concentration times duration of exposure) of the magnitude employed in this experiment would be experienced inside an unprotected museum in downtown Los Angeles over about a 2 year period, and in many other cities within a 5 year to 6 year period.

Measurements and Model Predictions of Ozone and Other Pollutant Concentrations in Museums

A computer-based model for predicting the indoor concentration of photochemically-generated air pollutants was developed as a tool for studying the effect of building design on indoor pollutant exposure. The model accounts for the effects of ventilation, filtration, heterogeneous removal, direct emission and photolytic and thermal chemical reactions. The model was tested by comparison to experimental data taken at the Virginia Steele Scott Gallery on the Huntington Library grounds in San Marino, CA, and the predicted NO, NO_2, and O_3 concentrations were found to closely track the measured data. The model predicts substantial indoor production of several species due to chemical reaction, including HNO_2, HNO_3, NO_3 and N_2O_5. Circumstances in which homogeneous chemistry may assume particular importance are identified and include buildings with glass walls, indoor combustion sources, and direct emission of olefins.

A series of experiments next was conducted to characterize the indoor/outdoor ozone relationships in eleven Southern California museums, galleries, historical houses and libraries. The air quality model described above confirmed that the measured indoor ozone concentrations could be explained

readily given a knowledge of the outdoor ozone concentration and the retention time for air within the building, during which time ozone is depleted by reaction with indoor surfaces.

It was found that buildings with high rates of air exchange with the outdoors but no pollutant removal system show peak indoor ozone concentrations greater than two-thirds as high as those outdoors. Buildings with conventional air conditioning systems that provide for repeated internal recirculation of air through their cooling systems show peak ozone levels about 30% to 40% of those outside. Museums with no forced ventilation system and with slow air infiltration from outdoors (e.g. a converted private mansion) show indoor ozone levels typically 10% to 20% of those outdoors. Museums with well-designed activated carbon air filtration systems show low indoor ozone levels, often less than 10% of the outdoor concentration. The results of this study can be used to estimate indoor ozone levels in buildings that have not yet been tested, and the computer-based models employed here can be used to design building systems that will ensure the maintenance of low indoor ozone concentrations.

Protection of Works of Art from Damage due to Atmospheric Ozone

A chamber exposure experiment was conducted to examine the effect of binders and coatings that might be used to protect artists' pigments from oxidation by ozone. Binder systems studied included acrylics, beeswax, casein, egg tempera, oils, and varnishes. Coatings tested included acrylic emulsions, methacrylates, beeswax, varnishes, shellac, and ethulose (a consolidant). Alizarin Crimson dry pigment airbrushed onto a white painted background with no binder or coating typically faded severely ($\Delta E > 15$) under the conditions of this experiment. In contrast, many of the binder and coating systems tested were capable of limiting the fading of an equivalent Alizarin Crimson sample to a color change of $\Delta E < 1$ during identically the same exposure conditions. Several binders and coatings, however, did

prove to be less effective than others. In particular, many of the acrylic paint binders and acrylic emulsion coatings failed to offer adequate protection to the Alizarin Crimson pigment samples tested.

While selection of protective binders or coatings may be possible at the time that certain works of art are created or restored, in many other cases (e.g., oriental scroll paintings; watercolor paintings) a coating simply cannot be applied without altering the appearance of the object. Therefore a wide variety of other approaches to protecting collections from ozone damage were studied. It was found that activated carbon air purification systems can effectively eliminate more than 90% of the ozone from indoor air under actual museum operating conditions. In addition, lower cost control measures are available. Setting the outdoor make-up air dampers on conventional air conditioning systems to achieve the lowest entrainment of oudoor air consistent with recommended building standards can in some cases reduce indoor ozone levels noticeably. Framing under glass was shown to provide virtually complete protection of a sensitive pigment sample on watercolor paper. Use of display cases, even those that are not tightly sealed, will reduce ozone concentrations greatly by decreasing the air exchange rate near the object and by providing additional surface area near the object at which the ozone will be depleted by surface removal processes. With deliberate forethought, display conditions can be created that will protect museum collections from damage due to atmospheric ozone.

REFERENCES FOR CHAPTER 1

1. N.S. Brommelle, "The Russell and Abney Report on the Action of Light on Watercolors," *Studies in Conservation, 9* (1964), 140-152.

2. N.S. Baer and P.N. Banks, "Indoor Air Pollution: Effects on Cultural and Historic Materials," *Int. J. Museum Manage. Curatorship, 4* (1985), 9-20.

3. J.H. Seinfeld, *Air Pollution: Physical and Chemical Fundamentals* (McGraw-Hill, New York, 1975).

4. L.S. Jaffe, "The Effects of Photochemical Oxidants on Materials," *J. Air Pollut. Control Assoc., 17* (1967), 375-378.

5. "Preservation of Historical Records," Committee on Preservation of Historical Records, National Research Council, National Academy Press, Washington, D.C., 1986.

6. R.G. Newton, "Mechanism of Exposure Cracking of Rubber with a Review of the Influence of Ozone," *J. Rubber Res., 14* (1945), 27-39.

7. G.G. Campbell, G.G. Schurr, D.E. Slawikowski, and J.W. Spence, "Assessing Air Pollution Damage to Coatings," *J. Paint Technol., 46* (1974), 59-71.

8. N. Kerr, M.A. Morris, and S.H. Zeronian, "The Effect of Ozone and Lundering on a Vat-Dyed Cotton Fabric," *Am. Dyest. Rep., 58* (1969), 34-36.

9. A.A. Katai, and C. Schuerch, "Mechanism of Ozone Attack on α-methyl Glucoside and Cellulosic Materials," *J. Polymer Science; Part A-1, 4* (1966), 2683-2703.

10. V.S. Salvin, and R.A. Walker, "Service Fading of Disperse Dyestuffs by Chemical Agents Other than the Oxides of Nitrogen," *Textile Res. J., 25* (1955), 571-585.

11. V.S. Salvin, "Ozone Fading of Dyes," *Textile Chem. Color., 1* (1969), 245-251.

12. N.J. Beloin, "Fading of Dyed Fabrics Exposed to Air Pollutants', *Textile Chem. Color., 5* (1973), 128-133.

13. W.W. Lebensaft, and V.S. Salvin, "Ozone Fading of Anthraquinone Dyes on Nylon and Acetate', *Textile Chem. Color., 4* (1972), 182-186.

14. J.C. Haylock, and J.L. Rush, "Studies on the Ozone Fading of Anthraquinone Dyes on Nylon Fibers," *Textile Res. J., 46* (1976), 1-8.

15. C.L. Shaver, G.R. Cass, and J.R. Druzik, "Ozone and the Deterioration of Works of Art," *Environ. Sci. Technol., 17* (1983), 748-752.

16. K. Drisko, G.R. Cass, P.M. Whitmore, and J.R. Druzik, "Fading of Artists' Pigments due to Atmospheric Ozone," in *Wiener Berichte über Naturwissenschaft in Der Kunst,* Bd. 2/3, 1985/86, ed. A. Vendl, B. Pichler, and J. Weber. (Verlag ORAC, Vienna, 1985/86).

17. F.M. Rowe, and K.A. Chamberlain, "Fading of Dyes on Cellulose Acetate Rayon," *J. Soc. Dyers. Colour., 53* (1937), 268-278.

18. V.S. Salvin, W.D. Paist, and W.J. Myles, "Advances in Theoretical and Practical Studies of Gas Fading," *Am. Dyest. Rep., 41* (1952), 297-302.

CHAPTER 2

THE OZONE FADING OF TRADITIONAL NATURAL ORGANIC COLORANTS ON PAPER

INTRODUCTION

Recent studies have demonstrated that significant amounts of ozone (O_3) present in the outdoor atmosphere can invade a museum environment (1,2). This chemically reactive gaseous air pollutant could prove hazardous to works of art and cultural property, for the damage to organic materials, particularly certain polymers (3), textiles (4), and textile dyes (5), from prolonged ozone exposure has been well documented. Little of this previous work, however, has been concerned specifically with the action of ozone on artists' materials; thus, the extent of the danger to museum collections and works of art has not been fully explored.

In an effort to identify those artists' materials which are vulnerable to ozone attack, chamber exposure studies can be used to determine the colorfastness of artists' pigments exposed to an atmosphere containing ozone. In the first exploratory experiment, reported elsewhere (1), a small number of modern watercolors on paper, representing a variety of organic and inorganic pigments, was exposed to ozone. Subsequently, a second experiment tested the ozone resistance of a more complete selection of modern artists' watercolors (from the Winsor & Newton line) containing organic pigments (6). These two investigations succeeded in targeting the synthetic alizarin lakes and a lake reportedly produced from Basic Violet 14 (a triphenylmethane dye) as being extremely reactive towards ozone.

Almost all the pigments used in modern artists' paints are man-made chemicals, developed in many cases as substitutes for rare, expensive, or unstable natural colorants of plant, animal, or mineral origin. Since works of art which pre-date the development of modern synthetic colorants were produced using these traditional pigments, the pollution resistance of natural coloring agents has a direct bearing on

the preservation of museum collections.

This chapter describes a chamber exposure experiment performed to test the ozone sensitivity of a number of traditional natural colorants. Pigment samples were obtained from collections at the Harvard University Art Museums, the Balboa Art Conservation Center, and the Los Angeles County Museum of Art. The pigments were applied to watercolor paper, and color measurements were made instrumentally at intervals during the exposure test. The samples were exposed at 22°C, 50% RH, and in the absence of light, to 0.40 parts per million (ppm) ozone for 12 weeks. This average ozone concentration, although several times greater than that normally encountered in an indoor environment, was nevertheless within the range observed during a heavy smog episode in an outdoor metropolitan setting (7). The total ozone dose during the 12-week exposure was equivalent to about four years of exposure to outdoor air in Los Angeles, or to about eight years inside a typical air-conditioned building. The relative ozone sensitivity of the natural colorants was determined on the basis of the rate and severity of the color changes that occurred during this ozone exposure.

EXPERIMENTAL

The authenticity of the natural pigments obtained from museum collections was tested by a variety of analytical techniques. Solubility tests and color reactions (8-11) were usually performed first, for not only did these tests provide a great deal of information (often sufficient for a definitive identification), but the solutions generated in these tests could also be used in subsequent analyses. Transmission spectra of pigment solutions were recorded in the 380 nm—700 nm range on a Diano Match Scan II spectrophotometer and were compared to literature results (12) or to spectra of reliable samples obtained from suppliers of artists' materials (Winsor & Newton, Fezandie & Sperrle, Cerulean Blue, A. F. Suter Co.), chemical supply houses (Aldrich, Sigma), and from Prof. Helmut Schweppe. Thin layer chromatography on

polyamide plates was performed according to published procedures (11), and comparison to authentic reference samples permitted differentiation of closely related colorants, such as cochineal and lac lakes, or various yellow lake pigments derived from different plants. The results of these analyses indicate that most of the pigments tested which bear the names of natural colorants were genuine. Only these natural colorants whose chemical compositions could be established were included in the ozone exposure test. The complete list of the natural organic colorants tested is shown in Table 2.1, along with the Color Index designation for each. Also shown are the number of different examples of each colorant which were tested. These multiple samples reportedly represented various shades, manufacturers, or dates of manufacture for a single coloring agent, but this information could not be substantiated in most cases.

Because of the limited availability of many of the natural colorants tested, a technique was developed which allows preparation and study of very small (milligram) quantities of pigment on paper in the absence of any binder. A suspension of pigment in about 1 ml of volatile solvent was airbrushed (Iwata HP-A) onto a 2.5cm x 5cm piece of watercolor paper (cut from larger sheets of Arches 140 lb. hot-pressed paper) through a stainless steel mask with a 1 cm diameter hole. This produced an even, matte 1 cm spot in the center of the paper, and the pigment particles were embedded into the paper securely. Repeated color measurements of a number of control samples were made prior to exposure to verify that routine handling did not produce a measurable color change due to loss of pigment from the samples. (Four colorants—curcumin, dragon's blood, gamboge, and saffron—were applied as dye solutions rather than as pigment suspensions.) An effort was made to produce samples whose reflectance at the wavelength of maximum absorption was about 40%, for at this initial reflectance the color change has been found to be most sensitive to changes in the colorant concentration (13).

Table 2.1. The traditional natural organic colorants tested in this experiment. Also shown are the Color Index designation and the number of different examples of each colorant.

Colorant	Color Index Designation	Number of Samples Tested
Weld Lake	Natural Yellow 2	1
Curcumin	Natural Yellow 3	1
Saffron	Natural Yellow 6	5
Quercitron Lake	Natural Yellow 9	2
Persian Berries Lake	Natural Yellow 14	3
Gamboge	Natural Yellow 24	5
Cochineal Lake	Natural Red 4	4
Madder Lake	Natural Red 9	13
Lac Lake	Natural Red 25	6
Litmus	Natural Red 28	1
Dragon's Blood	Natural Red 31	2
Indigo	Natural Blue 1	6
Van Dyke Brown	Natural Brown 8	1
Sepia	Natural Brown 9	1
Bitumen	Natural Black 6	3
Indian Yellow	none	2

Reflectance spectra were measured using the Diano Match Scan II, with the spot size of the light beam limited to 7 mm using the small-area-view option. This small sample size reduces the signal-to-noise ratio of a measurement and also increases the sensitivity to inhomogeneity of the pigment samples, so a jig was made to hold the paper samples in a reproducible position in front of the sample port of the spectrophotometer. This allowed precision of a few percent in reflectance measurements, or an uncertainty in ΔE of less than about 1 unit. The instrument was calibrated with a standard white tile (referenced to an NBS standard) and, owing to the translucence of the paper samples, this tile was used as a backing during reflectance measurements. The calibration and reflectance spectra were all recorded with the specular beam excluded. Reflectance measurements were made at 2 nm intervals from 380 nm to 700 nm and were stored on floppy disks. Chromaticity coordinates and color differences (using the CIE 1976 L*a*b* formula) were calculated for the CIE Illuminant C (14). Munsell color notations were subsequently calculated from these chromaticity coordinates (15).

The ozone exposure apparatus used is illustrated in Figure 2.1. Briefly, a dry airstream was pumped at a rate of 2.5 lpm through a series of filters to remove existing pollutants. The airstream then was split in half. One half of the flow was saturated with water vapor while the other dry airstream was irradiated by ultraviolet light from mercury vapor lamps housed in commercial ozone generators (Ultra Violet Products SOG-2). The ozonated air and humidifid air were mixed and then admitted to the exposure chamber through a perforated Teflon tube. The ozone concentration inside the chamber was measured continuously with a UV photometric ozone monitor (Dasibi Model 1003 AH), and a computer interfaced to the ozone monitor automatically collected and stored the hourly average ozone concentrations during the course of the exposure.

Samples of all the colorants on paper were prepared and mounted on anodized

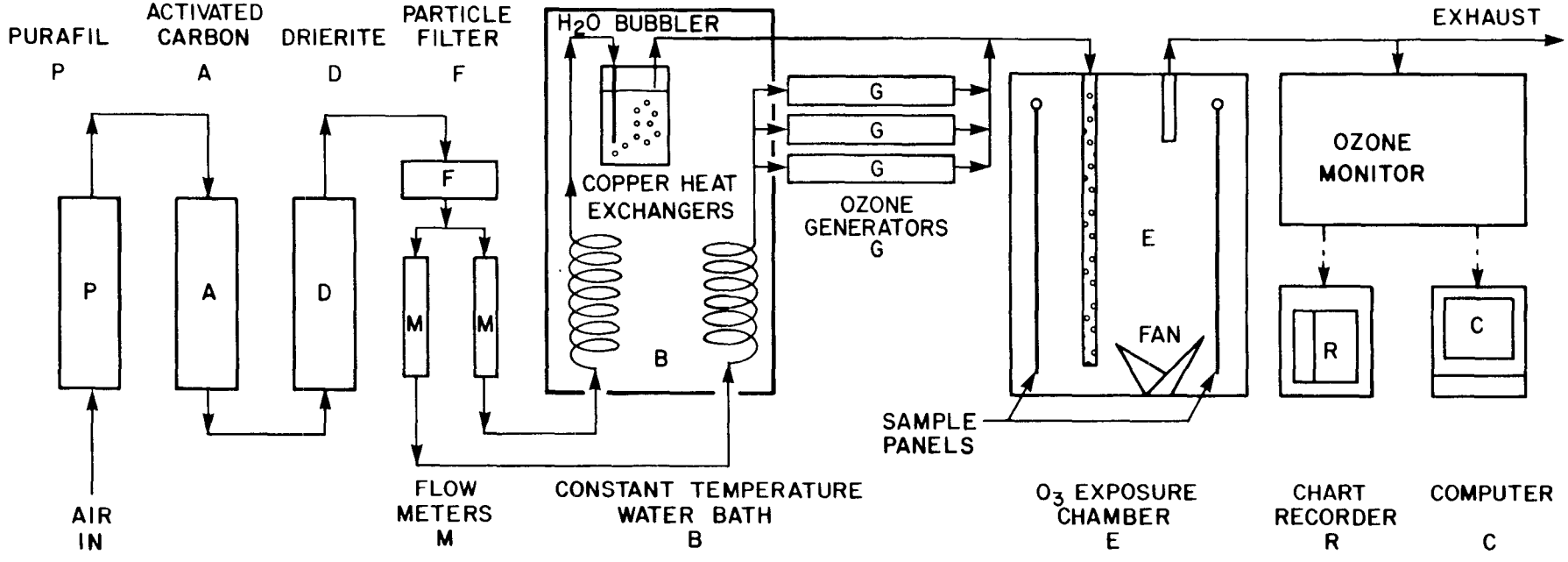

Figure 2.1 Ozone exposure apparatus.

aluminum panels. These panels were hung in the exposure chamber adjacent to the chamber walls, with the samples facing the interior of the box. The colorants were exposed to 0.397 ± .007 parts per million (ppm) ozone at 22°C and 50% RH in the absence of light for 12 weeks. The samples were removed and reflectance spectra recorded after 1, 2, 3, 4, 6, 8, and 12 weeks of exposure.

RESULTS

The fading of an ozone-sensitive colorant system can be characterized by the change in its visible reflectance spectrum upon exposure to ozone. Figure 2.2 illustrates the evolution of the reflectance spectrum of indigo on paper during its 12-week reaction with ozone. Indigo absorbs light across the visible spectrum, giving the indigo/paper system a bluish gray appearance. As the colorant is consumed (and presumably decolorized) by ozone, the reflectance across the visible spectrum increases, and the sample appears a lighter gray (i.e., faded). In this example, the wavelength of maximum reflectance also shifts from 450 nm (blue) to 500 nm (green) during the ozone reaction.

Although the reflectance spectrum contains all the information necessary to characterize the color during an ozone reaction, it is not the most convenient means to quantitatively assess or compare complicated color changes, which could involve shifts in hue as well as lightness. It is common, then, to reduce the spectral information to a set of parameters according to one of several conventions adopted for describing color (14). Table 2.2 utilizes several of these methods to characterize the color under CIE Illuminant C during the ozone exposure of the indigo/paper sample whose reflectance spectrum is shown in Figure 2.2. Two frequently used color notations are the CIE tristimulus values (X, Y, Z) and the CIE chromaticity coordinates and luminous reflectance (x, y, Y). The chromaticity coordinates (x, y) also allow two-dimensional plotting and determination of such aspects of color as the dominant wavelength and purity under a standard illumination source. Figure 2.3

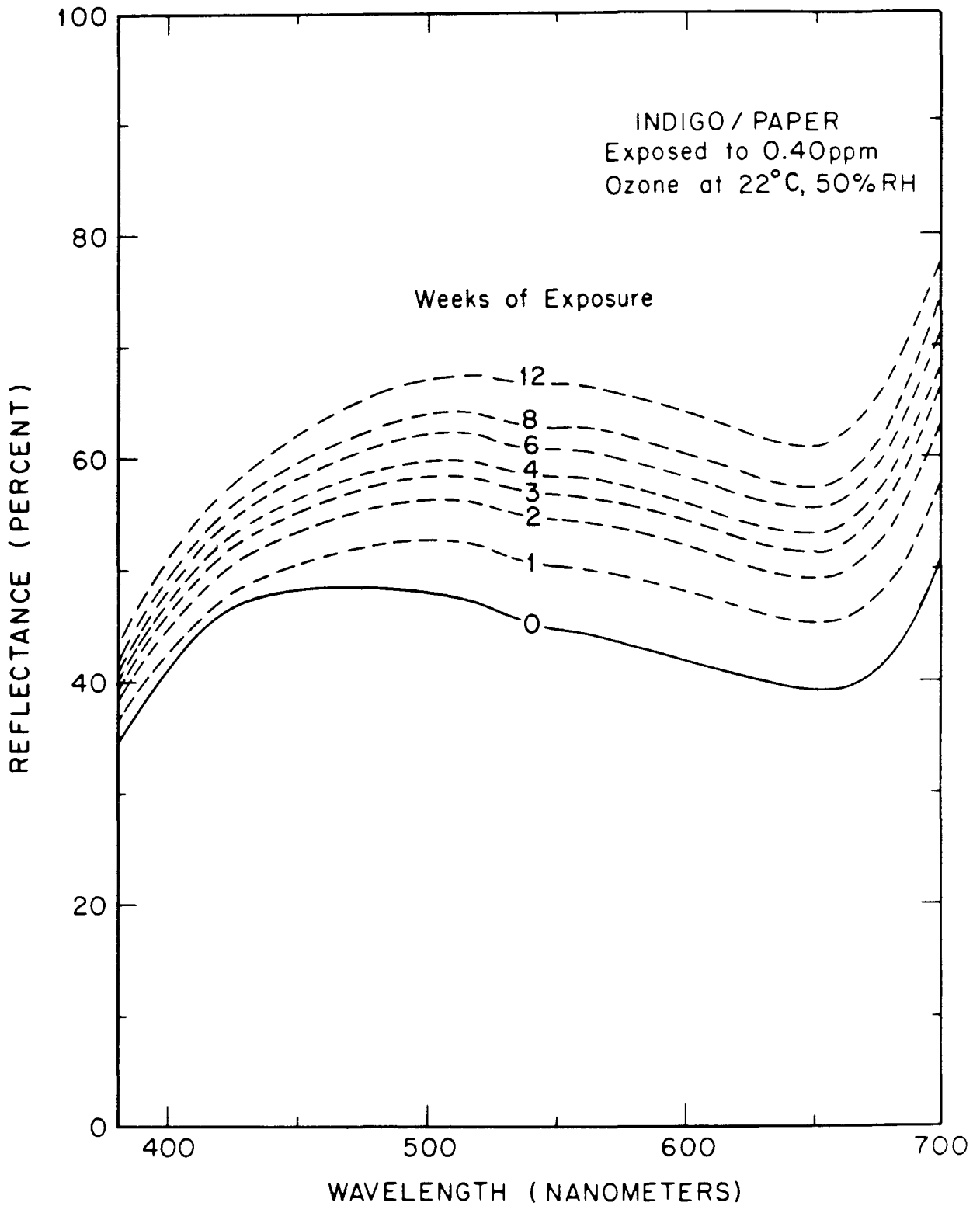

Figure 2.2 Reflectance spectrum of the indigo/paper system at several stages during its exposure to 0.40 ppm ozone at 22°C, 50% RH, in the absence of light.

Table 2.2. Observed color change in indigo/paper system during exposure to 0.40 ppm ozone at 22°C, 50% RH, in the absence of light. CIE tristimulus values (X, Y, Z) and CIE chromaticity coordinates and luminous reflectance (x, y, Y) are calculated for CIE Illuminant C from the measured reflectance spectra. Munsell color notations (hue, value/chroma) are calculated from the tristimulus values. Color differences, ΔE, are calculated using the CIE 1976 L*a*b* formula.

Week	X	Y	Z	x	y	Munsell	ΔE
0	42.17	44.02	56.37	.296	.309	8.1B7.1/1.4	—
1	47.25	49.57	59.40	.302	.317	7.0BG7.4/0.7	4.99
2	50.93	53.42	62.79	.305	.320	2.7BG7.7/0.6	7.40
3	53.00	55.58	64.82	.306	.321	9.6G7.8/0.6	8.67
4	54.51	57.15	66.33	.306	.321	8.0G7.9/0.6	9.56
6	56.81	59.63	68.52	.307	.322	5.2G8.0/0.6	11.05
8	58.67	61.61	70.29	.308	.323	3.8G8.1/0.6	12.18
12	62.01	65.13	73.26	.309	.325	2.5G8.3/0.7	14.20

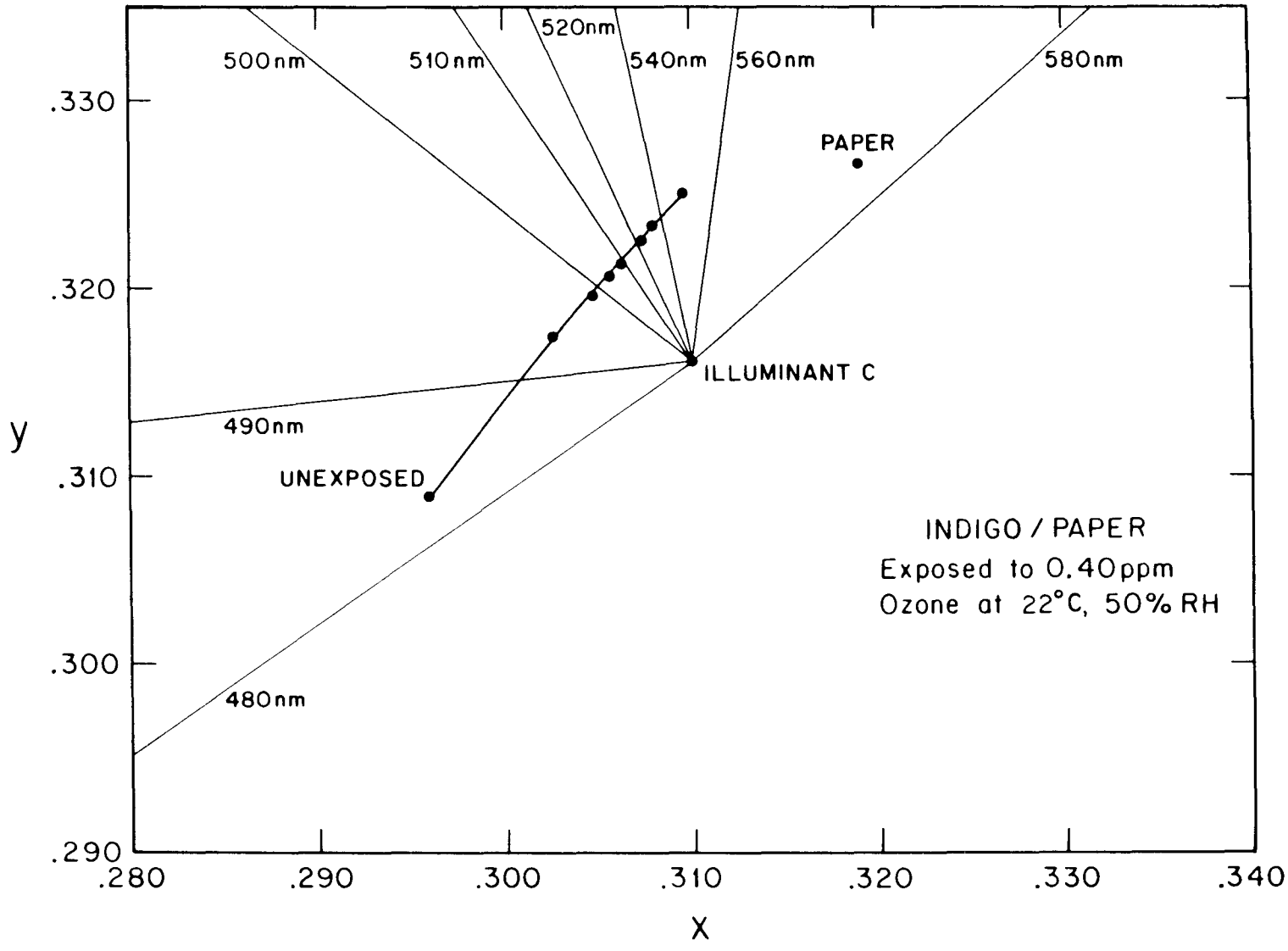

Figure 2.3 Observed color change of the indigo/paper system during its exposure to 0.40 ppm ozone at 22°C, 50% RH, in the absence of light. The CIE chromaticity coordinates (x, y) for CIE Illuminant C are plotted, and the dominant wavelengths of the samples and plain paper are indicated.

illustrates this use, showing the trend toward green (under Illuminant C) as the predominantly blue indigo/paper sample fades toward the yellow hue of the plain paper substrate. (Under this standard illuminant, the plain paper substrate appears yellow, and its color remains unchanged throughout the exposure. The observed yellowing of the indigo/paper sample during ozone exposure probably arises, at least in part, from the optical mixing of the yellow paper and the blue indigo. The possibility that some of this hue shift results from the generation of a yellow reaction product is the subject of further investigation.)

These parameters can also be used to calculate the Munsell notation for the color (15). This system denotes the color in terms of an average observer's perception of its hue, value (lightness), and chroma (saturation or purity). The Munsell description of the indigo/paper color change is easily interpretable in terms of its apparent shift in hue from blue toward green and an increase in its value or lightness. An added advantage of this approach is that a reported color can be visualized easily by referring to the appropriate color chips in the Munsell Book of Color (16).

Finally, a single quantity representing the total perceived color difference between two specimens, combining changes in hue and lightness, can be calculated from two respective sets of tristimulus values (14). In this work the CIE 1976 L*a*b* formula has been used to determine the color difference, ΔE, of a colorant system before and after a given ozone dose, thus providing an approximate indicator of the magnitude or extent of the total color change caused by ozone reaction. (On the average, a ΔE value less than 0.5 is not perceptible, and a ΔE value less than 1 is usually considered a good color match.) The calculated color difference (vs. unexposed sample) during ozone exposure for the indigo/paper system is tabulated in Table 2.2 and illustrated graphically in Figure 2.4.

The results of the 12-week ozone exposure for the other natural

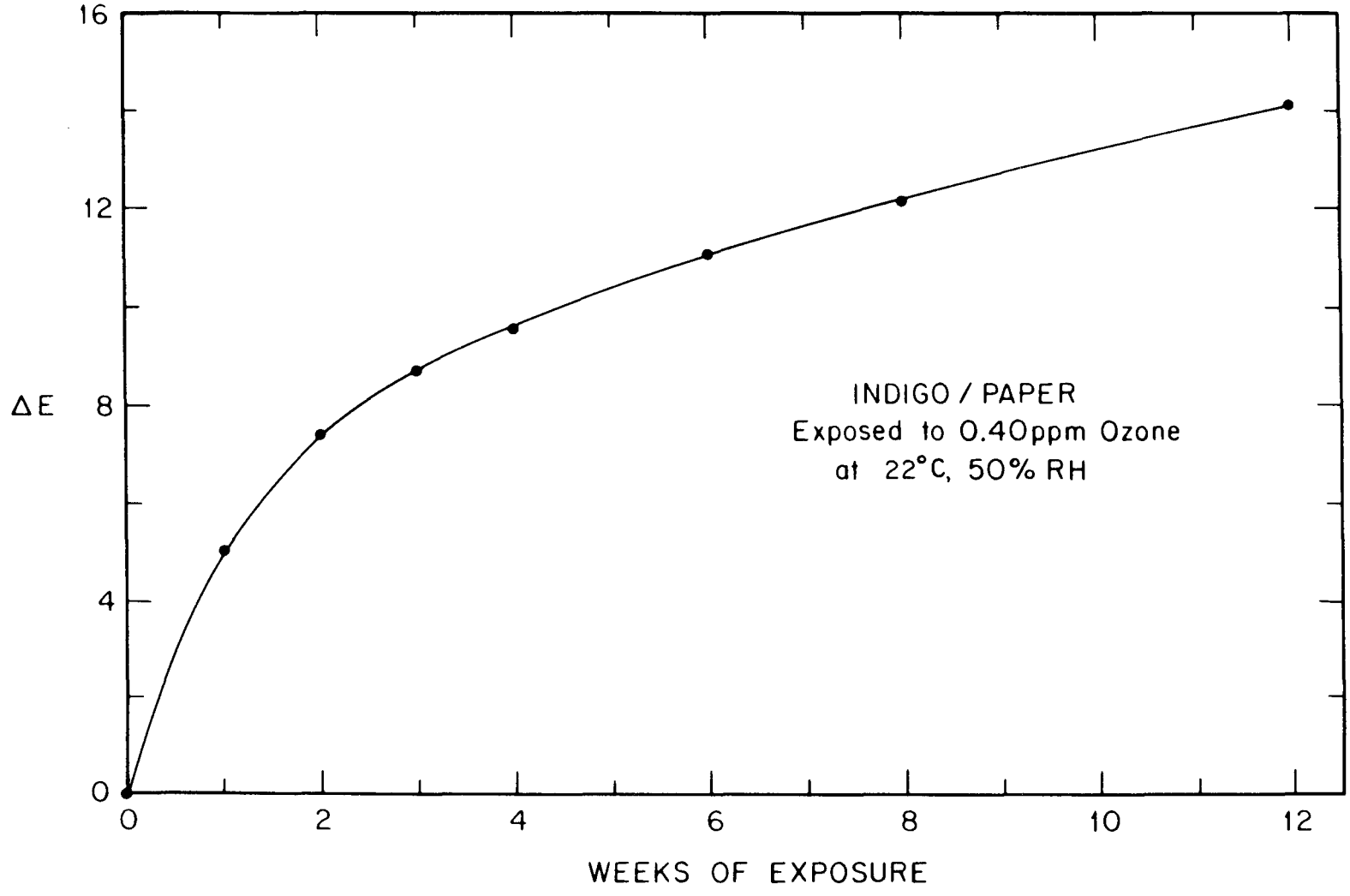

Figure 2.4 Observed color differences (versus unexposed sample) of the indigo/paper system during its exposure to 0.40 ppm ozone at 22°C, 50% RH, in the absence of light. Color differences, ΔE, were calculated for CIE Illuminant C from the measured reflectance spectra using the CIE 1976 L*a*b* formula.

colorant/paper systems are summarized in Table 2.3. Again, the reflectance spectra were measured, and the colors of the samples before and after exposure are described in terms of the calculated tristimulus values, chromaticity coordinates, Munsell notations, and color differences, ΔE. The time dependence of the color changes for all the colorant systems is shown in Figure 2.5. (For those colorants which were represented by samples from several sources, the results are reported for a typical example.)

DISCUSSION

The reaction of ozone with organic materials has been widely studied (17) and has found application in various processes ranging from organic syntheses to water sterilization. It has been determined that, for the most part, ozone attacks organic molecules at carbon-carbon double bonds, both in olefinic (straight carbon chain) and, more slowly, in aromatic (benzene ring) structures. This reaction oxidizes the organic molecule, ultimately cleaving the carbon atom framework at the site of initial ozone attack. Detailed studies of the mechanism of the ozone reaction with alizarin lakes (18) with indigo (19) and with other colorants are presented in Chapters 4-7 that illustrate the chain of events involved. Since these double bonds often form part of the chromophore in organic colorants, their destruction from ozone reaction usually leads to a loss of color. The observed sensitivity of the natural colorants in this study can be rationalized on the basis of this accepted scheme of ozone reaction.

However, the pertinent issue is not whether a particular colorant will react with ozone—if the colorant contains carbon-carbon double bonds, it will react—but rather, how quickly a colorant system will fade upon exposure to ozone at concentrations found in museum environments. The observed ozone fading of a colorant system is actually a very complicated process governed by a variety of factors. First among these is the chemical reactivity of the colorant towards gaseous ozone.

Table 2.3. Observed color change of natural colorant/paper systems upon exposure to 0.40 ppm ozone at 22°C, 50% RH, in the absence of light. CIE tristimulus values (X, Y, Z), chromaticity coordinates (x, y) and calculated Munsell notations (hue, value/chroma) for CIE Illuminant C are reported before and after the 12-week ozone exposure. Color differences between exposed and unexposed samples are calculated using the CIE 1976 L*a*b* formula.

	Weeks of Exposure	X	Y	Z	x	y	Munsell	ΔE
Weld Lake	0	80.47	84.41	75.90	.334	.351	8.3Y9.3/1.9	
	12	82.45	85.93	81.66	.330	.344	7.7Y9.3/1.5	3.35
Curcumin	0	72.61	76.15	28.92	.409	.429	4.6Y8.9/7.9	
	12	83.35	87.16	79.16	.334	.349	7.5Y9.4/1.8	41.77
Saffron	0	76.25	80.21	52.41	.365	.384	5.2Y9.1/4.3	
	12	78.51	82.41	61.04	.354	.371	5.7Y9.2/3.4	6.34
Quercitron Lake	0	74.85	78.96	59.03	.352	.371	6.6Y9.0/3.3	
	12	77.04	81.19	63.10	.348	.367	6.8Y9.1/3.0	2.10
Persian Berries Lake	0	76.93	82.85	54.10	.360	.387	8.8Y9.2/4.3	
	12	78.14	84.00	62.40	.349	.373	9.1Y9.2/3.3	6.77
Gamboge	0	75.03	77.87	60.33	.352	.365	4.3Y9.0/3.1	
	12	77.70	80.78	66.86	.345	.358	4.8Y9.1/2.6	3.57
Cochineal Lake	0	62.16	53.09	58.64	.357	.305	8.3RP7.6/6.2	
	12	65.42	57.58	62.90	.352	.310	9.1RP7.9/5.4	4.60
Madder Lake	0	76.57	69.68	78.61	.341	.310	8.2RP8.6/4.4	
	12	81.36	78.66	86.81	.330	.319	4.0R9.0/2.5	9.95
Lac Lake	0	58.92	54.08	62.17	.336	.309	7.4RP7.7/4.0	
	12	65.89	62.68	69.58	.333	.316	1.6R8.2/2.9	6.88
Litmus	0	76.82	78.80	88.49	.315	.323	8.2Y9.0/0.3	
	12	81.37	83.47	91.24	.318	.326	5.5Y9.2/0.6	2.70
Dragon's Blood	0	63.38	57.55	43.07	.386	.351	2.5YR7.9/5.3	
	12	75.77	75.29	67.68	.346	.344	7.9YR8.8/2.5	17.19
Indigo	0	42.17	44.02	56.37	.296	.309	8.1B7.1/1.4	
	12	62.01	65.13	73.26	.309	.325	1.5G8.3/0.7	14.20
Van Dyke Brown	0	49.86	49.38	44.29	.347	.344	8.1YR7.4/2.3	
	12	52.24	51.88	47.05	.346	.343	8.2YR7.6/2.3	1.58
Sepia	0	48.66	49.18	47.02	.336	.340	0.5Y7.4/1.6	
	12	50.80	51.34	49.23	.336	.339	0.4Y7.5/1.6	1.32
Bitumen	0	59.55	60.22	52.52	.346	.350	0.9Y8.1/2.3	
	12	65.02	65.99	60.54	.339	.345	1.0Y8.4/2.0	3.76
Indian Yellow	0	71.97	75.47	31.95	.401	.421	4.6Y8.8/7.2	
	12	73.46	76.94	34.23	.398	.417	4.5Y8.9/6.9	1.95

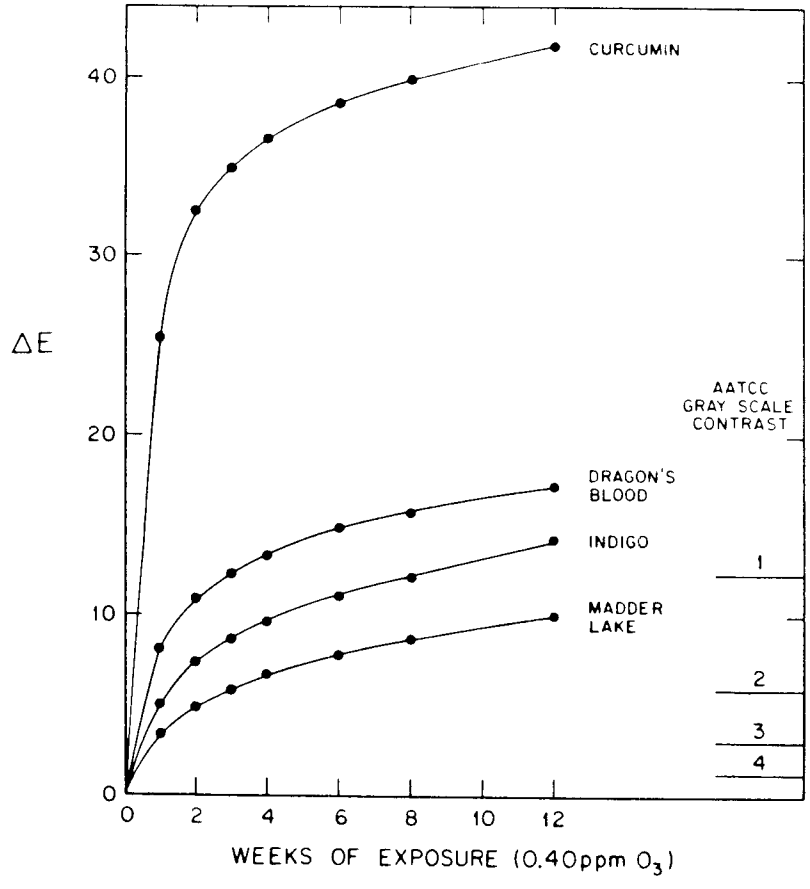

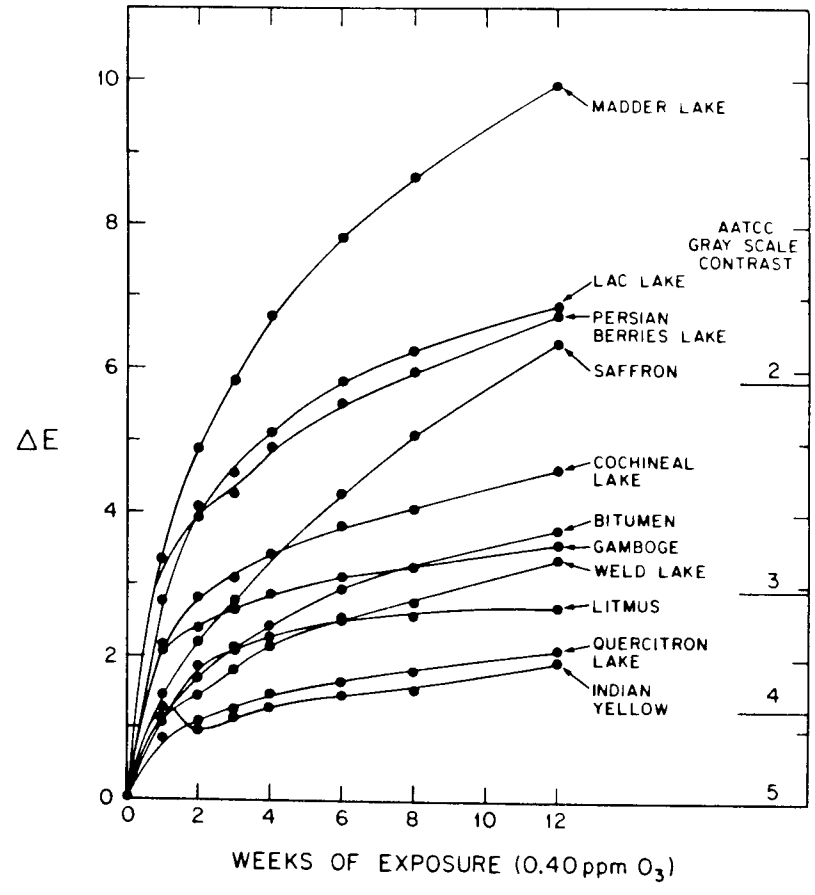

Figure 2.5 Plot of the observed color changes of natural colorant/paper systems during exposure to 0.40 ppm ozone at 22°C, 50% RH, in the absence of light. Color differences, ΔE, were calculated for CIE Illuminant C using the CIE 1976 L*a*b* equation. Measured color differences for the AATCC Gray Scale are also indicated for reference. Color changes are shown for a) very reactive, and b) moderately reactive, colorant systems (note different scales for vertical axes).

This property depends on the molecular structure of the colorant, particularly on the number and types of chemical bonds and atomic sites vulnerable to ozone attack. Often the chemical reactivity of a colorant can be altered by processing during manufacture (with included additives or particle coatings, or by variations in particle shape or size); during application (through interaction with mordants or substrates, through control of the colorant concentration or degree of aggregation, and through the use of binders or coatings); or during the aging of a museum piece (which could experience extensive oxidation or other chemical degradation in reactions with light, the atmosphere, and pollutants). Finally, the color change produced upon ozone reaction of the colorant system is related in a complicated way to the colorant particle size, shape, concentration, and optical properties, as well as to the physical structure of the colorant system.

The thorough investigation of all these factors on the ozone fading behavior of museum pieces is beyond the scope of the present study. However, to the extent that these factors could be controlled during sample preparation, the physical structure of the colorant systems should be uniform enough to allow meaningful comparisons of the ozone sensitivity of the colorants. In addition, some colorant samples were available from several sources (see Table 2.1), and these materials, representing different manufacturers, formulations, or eras, were tested and compared. In nearly every case, different samples of a colorant demonstrated only slight variations in ozone reactivity, suggesting that the formulation, particle size distribution, and aging history probably played relatively minor roles in determining the ozone resistance of the colorant systems in this study. The sole exception to this trend was observed in the sample of "Burnt Madder Lake," which, unlike the other madder lakes, was practically inert towards ozone ($\Delta E < 1$ after 12 weeks). The reason for this lack of reactivity is unclear, but it could be the result of prior oxidation of the pigment in a charring process (9), which might render the product

less susceptible to further oxidation by ozone.

The results of this exposure test are summarized in Table 2.4, in which the most ozone-sensitive colorants on paper have been identified on the basis of their (average) rates of fading and the extent to which they had faded after the 12-week ozone reaction. Since the ozone exposure was relatively mild and of short duration (representing an ozone dose equivalent to only a few years inside a museum), it is possible to differentiate only among the most reactive colorant systems. The time dependence of the ozone fading, shown in Figure 2.5, was qualitatively the same for all the reactive colorant systems. In these cases, rapid fading began almost immediately upon exposure to ozone, with the largest color changes (as measured by ΔE) occurring during the first week. Subsequent weeks of ozone exposure produced successively smaller color changes. By the end of 12 weeks, most of the colorants are fading at a rate that if extrapolated to longer exposure times would still not alter the relative rank ordering among the colorants tested based on total color change (ΔE) observed in response to a given ozone exposure. Because of this ordering of the time dependence of the ozone fading, the colorant systems can be grouped according to the extent of fading after 12 weeks into rather arbitrary categories of Very Reactive ($\Delta E > 9$ after 12 weeks at 0.40 ppm ozone), Reactive ($\Delta E = 3 - 8$ after 12 weeks), and borderline cases ($\Delta E = 1 - 3$ after 12 weeks but with a monotonic increase in ΔE value over time). The remaining colorant systems showed no definite color change after the 12-week exposure and are termed "Unreactive" towards this ozone dose.

The interpretation of the observed fading rates in terms of the chemical reaction kinetics requires knowledge of the relation between the measured spectral reflectances and the concentrations of the colorants in these reactive systems. This connection has been made previously in the study of acrylic paint layers (13) and glazes (20) using a computer color-matching formula based on a simplified

Table 2.4. Classification of the natural colorant/paper systems according to their observed fading during the 12-week exposure to 0.40 ppm ozone at 22°C, 50% RH, in the absence of light. (See text for the criteria upon which these categories were based.)

Very Reactive:	Curcumin
	Dragon's Blood
	Indigo
	Madder Lake
Reactive:	Bitumen (Asphaltum)
	Cochineal Lake
	Gamboge
	Lac Lake
	Persian Berries Lake
	Saffron
	Weld Lake
Possibly Reactive:	Indian Yellow
	Litmus
	Quercitron Lake
Unreactive:	Van Dyke Brown
	Sepia

Kubelka-Munk analysis. However, the application of such an approximate theoretical treatment based on a model of a thick, homogeneous paint layer, having smooth boundaries and whose color changes only from reduction of the colorant concentration, is inappropriate for the analysis of the ozone fading of the colorant systems in this study. The optical absorption and scattering properties of these samples, comprised of pigment particles embedded to some depth in the paper, are very complex compared to those of a thick, well-characterized paint layer. Further, by its nature the decolorization of the samples by ozone reaction involves alteration of the pigment particles themselves (not just their concentration), possibly leaving the particles coated with colorless ozone reaction products (which would alter their optical properties), or distorting and eventually decreasing the pigment particle size distribution. These effects will in turn change the optical response of the colorant system in a very complicated way throughout the course of the ozone exposure. Clearly, a more complete theoretical formalism and more thorough characterization of the colorant systems are needed before the chemical kinetic details of the ozone reaction can be inferred from color measurements alone.

For now, then, the ozone fading results are presented to illustrate the effect of prolonged ozone exposure on the appearance of these colorant systems. The apparent slowing of the observed ozone fading of these freshly prepared colorant samples suggests the possibility of very different ozone fading kinetics for older works of art, which may have experienced substantial oxidation due to atmospheric or photo-oxidation over the years and in which the rapid initial reaction (or reactions) may already have been completed. Exposure testing of aged samples is necessary to explore these variables. Nevertheless, there is compelling evidence prompting the routine protection of works of art containing natural colorants from prolonged exposure to atmospheric ozone.

CONCLUSION

The ozone-induced fading rate of a number of traditional natural organic colorants applied on paper has been examined. Samples were exposed in an environmental chamber to an atmospheric ozone dose equivalent to approximately six to eight years of residence in a conventional air-conditioned building in Los Angeles. Previous studies of the ozone sensitivity of modern synthetic artists' pigments showed that a large number of these materials were relatively stable towards an ozone dose of the magnitude employed here. By contrast, almost all of the traditional natural colorants tested in this work showed some degree of fading after exposure to ozone. This procedure was successful in identifying many natural colorant/paper systems which should be considered ozone-fugitive, and a few (curcumin, dragon's blood, madder lake, and indigo) which are very ozone-sensitive. While these results are strictly applicable only to other similar colorant systems (such as watercolors or pastel drawings), at present this study should nevertheless be useful as a guide in the judgment of those natural colorants which, in other applications, warrant particular observation or precautions.

REFERENCES FOR CHAPTER 2

1. Shaver, C. L., Cass, G. R., and Druzik, J. R., "Ozone and the Deterioration of Works of Art," *Environmental Science and Technology, 17* (1983), 748-752.

2. Davies, T. D., Ramer, B., Kaspyzok, G. and Delany, A. C., "Indoor/Outdoor Ozone Concentrations at a Contemporary Art Gallery," *J. Air Pollution Control Assoc., 31* (1984), 135-137.

3. Stephens, K. E. and Beatty, C. L., "Effects of Ozone on the Physical Properties of Butadiene and Styrene/Butadiene Copolymers," *Polymeric Materials Science and Engineering, 47* (1982), 277-281.

4. Jaffe, L., "The Effects of Photochemical Oxidants on Materials," *J. Air Pollution Control Assoc., 17* (1967), 375-378.

5. Haylock, J. C. and Rush, J. L., "Studies on the Ozone Fading of Anthraquinone Dyes on Nylon Fibers," *Textile Research Journal,* (January, 1976), 1-8.

6. Drisko, K., Cass, G. R., Whitmore, P. M., and Druzik, J. R., "Fading of Artists' Pigments due to Atmospheric Ozone," in *Wiener Berichte über Naturwissenschaft in der Kunst,* Bd. 2/3, 1985/86, ed. A. Vendl, B. Pichler, and J. Weber. (Verlag ORAC, Vienna, 1985/86)

7. Hunt, W. F., Curran, T. C., Faoro, R. B., Frank, N. H., and Mask, E., *National Air Quality and Emissions Trends Report, 1981,* document EPA-450/4-83-011 (U.S. Environmental Protection Agency, Research Triangle Park, 1983).

8. Weber, F. W., *Artists' Pigments* (Van Nostrand, New York, 1923).

9. Gettens, R. J. and Stout, G. L., *Painting Materials* (Van Nostrand, New York, 1942).

10. "Colour Index," 3rd edition, revised, Society of Dyers and Colourists, Bradford, Yorkshire, England, 1971, Vols. 3 and 4.

11. Schweppe, H., "Identification of Dyes on Old Textiles," *J. American Institute for Conservation, 19* (1980), 14-23.

12. Billmeyer, F. W., Jr., Kumar, R., and Saltzman, M., "Identification of Organic Colorants in Art Objects by Solution Spectrophotometry," *J. Chem. Educ., 58* (1981), 307-313.

13. Johnston-Feller, R., Feller, R. L., Bailie, C. W., and Curran, M., "The Kinetics of Fading: Opaque Films Pigmented with Alizarin Lake and Titanium Dioxide," *J. American Institute for Conservation, 23* (1984) 114-129.

14. Billmeyer, F. W., Jr. and Saltzman, M., *Principles of Color Technology,* 2nd edition (John Wiley and Sons, New York, 1981).

15. "Standard Method of Specifying Color by the Munsell System," Designation D 1535-80, American Society for Testing and Materials, Philadelphia, Pennsylvania, 1980.

16. "Munsell Book of Color," Macbeth Division of Kollmorgen Corp., Baltimore, Maryland, 1976.

17. Bailey, P. S., *Ozonation in Organic Chemistry,* Vols. 1 & 2 (Academic Press, New York, 1978 and 1982).

18. Grosjean, D., Whitmore, P. M., De Moor, C. P., Cass, G. R., and Druzik, J. R., "Fading of Alizarin and Related Artists' Pigments by Atmospheric Ozone: Reaction Products and Mechanisms," *Environmental Science and Technology 21* (1987), 635-643.

19. Grosjean, D., Whitmore, P. M., Cass, G. R., and Druzik, J. R., "Ozone Fading of Natural Organic Colorants: Mechanisms and Products of the Reaction of Ozone with Indigos," *Environmental Science and Technology 22* (1988), 292-298.

20. Johnston-Feller, R., and Bailie, C., "An Analysis of the Optics of Paint Glazes: Fading," in N. S. Brommelle and G. Thomson, *Science and Technology in the Service of Conservation* (International Institute for Conservation, London, 1982) 180-185.

CHAPTER 3

THE OZONE FADING OF TRADITIONAL JAPANESE COLORANTS

INTRODUCTION

Initial experiments, exploring the ozone resistance of a variety of modern artists' watercolors, identified two pigments in current use, alizarin crimson and a triphenylmethane lake, that were very ozone-sensitive (1,2). In Chapter 2, the ozone sensitivity of many traditional natural organic colorants applied to paper was examined (3). The colorants tested included most of the widely used organic colorants found in pre-20th century Western pictorial art (4). These materials proved to be generally fugitive upon ozone exposure, with several (curcumin, dragon's blood, indigo, and madder lake) demonstrating extreme ozone sensitivity.

The present chapter extends the assessment of the risk of ozone damage to art works by exploring the ozone fading of traditional colorants used in Japanese painting, woodblock prints, and textiles. Some of the natural colorants tested previously also saw use in the Orient, but, in addition, a remarkable variety of other coloring agents, many derived from indigenous plants, were utilized in the production of Japanese works of art and costumes. The light-fastness of some of these traditional Japanese colorants has been examined (5); the ozone-fastness of these materials also should be an important consideration in the preservation of this type of object.

TRADITIONAL JAPANESE COLORANTS: HISTORICAL BACKGROUND

Our knowledge of the materials and techniques used in Japanese painting, woodblock printing, and dyeing is incomplete. Many art historical discussions of these crafts mention technical details only incidentally; these references often are undocumented and may be based upon folklore. A few scholarly investigations (in English) exist, however, and the list of some of the most important traditional

colorants in Table 3.1 is drawn from several of these.

Evidence of the first development of pictorial art in ancient Japan is quite sparse. The earliest examples would appear to be simple line drawings and decorative designs on vases and bells dating from the 1st century A.D. (6). Murals of the 3rd century, found in tombs of nothern Kyushu, seem to be the oldest surviving paintings, and analyses of the pigments show these works to have been created using mainly colored earths (red and yellow ochres, "green rock," white clay, and a black manganese-containing mineral, probably pyrolusite) (7).

The introduction of Buddhism from China to Japan in the 6th century eventually brought with it traditional Chinese painting materials and methods. Thus, in a 7th century Japanese painted mural were found, in addition to the ochres and clays of the pre-Buddhist works, colored minerals and synthetic pigments, notably malachite, azurite, cinnabar, vermilion, red lead, and litharge (7). One thousand years later, in *ukiyo-e* paintings on paper and silk, the basic palette was much the same, with the occasional addition of several other inorganic pigments, such as shell white, lead white, smalt, ultramarine, and copper greens (8-10). By the 17th century, a few organic colorants also saw use in Japanese paintings, notably gamboge, indigo, and a red (possibly madder, cochineal, lac, or safflower) (8,9).

The dyeing of textile materials, particularly silk, is also a very ancient craft in Japan (11). As early as the 4th century, textiles were being dyed with *akane,* from the native Japanese madder plant, and with indigo, imported from China. A number of other natural dyes, derived from plants native to Japan or imported from China or Southeast Asia, were common by the 8th century, and the standard procedures for their use were being detailed in Japanese documents such as *Engishiki,* published in 927 A.D. In these ancient times, textile dyes were derived almost exclusively from plant sources, with inorganic pigments being used only rarely (12) and insect dyes such as cochineal being used only after their introduction from

Table 3.1. Some traditional Japanese colorants

Color	Japanese name	Main constituent	Common name/source
Inorganic/synthetic			
White	*Gofun*	$CaCO_3$	shell white
	Enpaku	$2Pb(CO_3)\cdot Pb(OH)_2$	lead white
Red	*Shu*	HgS	vermilion
	Tan	Pb_3O_4	red lead
Yellow	*Sekiō*	As_1S_3	orpiment
	Ōdo	Fe oxides/clay	yellow ochre
	?	PbO	litharge (massicot)
Green	*Rokushō*	$CuCO_3\cdot Cu(OH)_2$	malachite
	Ichiban rokushō	$Cu(C_2H_3O_2)_2\cdot 2Cu(OH)_2$	verdigris
Blue	*Iwa gunjō*	$2CuCO_3\cdot Cu(OH)_2$	azurite
	Hana-konjō	K, CO(Al), silicate	smalt
	Gunjō	$Na_8Al_6Si_6O_{24}S_4$	ultramarine
	Bero-ai	$Fe_4[Fe(CN)_6]_3$	Prussian blue
Brown	*?*	hydrated Fe, Mg oxides	umber
Black	*Sumi*	carbon	lampblack
Organic			
Red	*Beni*	carthamin	safflower petals
	Enji	carminic acid	cochineal insects
	Shiko	laccaic acid	lac insect exudate
	Akane	pseudopurpurin	Japanese madder root
	Suo	brazilein	Red bud wood
	Yenji		*Mirabilis jalapa*
Yellow	*Shiō*	gambogic acid	gamboge resin
	Ukon	curcumin	turmeric root
	Kuchi nashi	crocin	Cape jasmine
	Kihada	berberine	Japanese yellow wood
	Kariyasu	arthraxin	*Miscanthus* grass
	Enju	rutin	Japanese pagoda tree
	Yama-momo	myricitrin	*Myrica rubia*
	Yamahaji	fustin	Japanese sumac
	Woren	berberine	*Coptis japonica*
	Zumi	cyanin	*Pyrus toringo* bark
Blue	*Ai*	indigotin	*Polygonum tinstorium* root
	Aigami	malonyl awobanin	*Commelina communis* petals
Purple	*Shikon*	shikonin	*Lithospermum erythrorhizos* root

China in the 17th or 18th century (8).

The multi-colored woodblock prints of the Edo period (1600-1868), most notably those of the *ukiyo-e* schools, were the culmination of a long tradition in Japan that had its roots in the block printing technology used to produce book illustrations. The earliest example of a Japanese woodblock print dates from 1162 A.D., and documentary evidence indicates that prior to this time such prints were produced to illustrate Buddhist religious texts (13). Woodblock illustrations in printed books were common by the early 17th century (14). Printed in black-and-white outlines until this time, hand-coloring of these designs by the artists, printers, or owners became popular by 1630. Readily available painter's materials were used in these illustrations: at first, *tan* (red lead) and a green; in later years other colors, hand-applied, were added to this basic color scheme (14).

By the late 17th century, the art of single-sheet woodblock prints *(ichimai-e)* was developing as an outgrowth of this illustration form. As with the book illustrations, the first single-sheet prints were produced in black-and-white *(sumizuri-e)* using only lampblack ink *(sumi).* Color soon was included in these prints, utilizing materials borrowed from the traditional painting and dyeing crafts. Hand-coloring of the prints was the natural approach at first, and *tan* was once again used as the sole or dominant colorant in these first color sheets *(tan-e),* with the later addition of yellow (possibly orpiment, gamboge, turmeric, or jasmine), green, and blue (13). In 1715, *beni-e* sheets were produced, hand-colored with a soft rose pink, *beni* (safflower) (15). A technical study of a number of these hand-colored prints found a few inorganic pigments (shell white, red lead, iron oxide, and, rarely, orpiment and malachite), materials of the painter's craft, and a number of plant dyes (indigo and safflower, probably mixed with some rice starch for body) from the dyer's traditional materials (16).

The public's demand for color in these woodblock prints, and the difficulty and

expense of hand-coloring, prompted the development of the technique of printing colors from blocks. Early examples of such block-printed color sheets, dating from 1740-1744, were created using *beni* and a green (possibly verdigris) (17). These prints are called *benizuri-e* ("*beni*-printed sheets"), distinguishing them from *beni-e* (sheets hand-colored with *beni*). Later, yellow, blue, and other colors were included, but since each color required a separate block to be cut, these early prints usually exhibit a restricted range of colors.

Beginning around 1764, however, the patronage of wealthy connoisseurs fostered the flourishing of the "brocade print" *(nishiki-e),* the multi-colored woodblock prints that have come to represent the fulfillment of this form (18). For the artist, expense and trouble were no longer obstacles, and the finest in materials (wooden blocks, papers, and colorants) and an increased number of color blocks (as many as ten) provided the artist with the means for an enormous range of expression.

The exact identities, sources, preparations, and applications of the various colorants used on these woodblock prints are for the most part unknown. Technical studies of the colorants are rare, for the sampling and identification of these materials is often quite difficult (16). Feller et al. (5) were able to identify several colorants present on a number of 19th century prints using the spectral reflectances of these materials. The colorants identified in that work all were derived from plants: *ai* (indigo), *aigami* (dayflower), and *beni* (safflower). According to other sources (15,19), these three colorants, along with *shiō* (gamboge), *ukon* (turmeric), and perhaps *shikon* (from *Lithospermum* root), *kuchinashi* (jasmine), and *ki* or *zumi* (from the bark of *Pyrus toringo*), were the most common natural organic colorants on Japanese prints of the 18th and 19th centuries. The inorganic colorants that saw use were *tan* (red lead), *shu* (vermilion), *benigara* (iron oxide), *sekiō* (orpiment), *gunjō* (ultramarine), *gofun* (shell white), and *enpaku* (lead white). Another source (20) mentions that textile dyes were also at the disposal of the woodblock printers,

in which case a number of other colorants, such as *enju* (Japanese pagoda tree), *kihada* (Japanese yellow wood), and *akane* (Japanese madder), might also be found on these prints. Other colorants such as *bero-ai* (Prussian blue) and aniline dyes were used after their introduction to Japan, and the latter half of the 19th century saw an increased number of Western materials used in the production of Japanese prints. The distinction between native Japanese materials and imported technology has always been blurred, but after the opening of Japan to Western technology in the mid-19th century, the age of the traditional materials was on the decline.

From this review of the history of Japanese colorants, one can see that the pigments of the Japanese painting tradition were predominantly inorganic (derived from natural earths and minerals or synthetic compounds), with the occasional use of a small number of organic colorants. In contrast, textile dyeing grew out of the use of organic dyes, extracted from plants (both native and imported) and, occasionally, from insects. Inorganic pigmentation of cloth was uncommon.

The materials used in the production of color prints were selected from these other crafts. A small number of inorganic pigments were often included, especially in the early development of the color print. However, the color printing process required coloring agents of very little body; the addition of a little rice starch thus allowed use of many of the dye extracts that were applied to textiles. The beauty of these color prints derives in large part from the variety and richness of the plant dyes used.

TRADITIONAL JAPANESE COLORANTS: CHEMISTRY

Nearly all of the inorganic earths and minerals (both natural and synthetic) used in traditional Japanese pictorial arts have counterparts, identical in chemical nature, that were used in Western painting. Thus, these inorganic pigments have been studied extensively (mainly in the context of their applications in Western art),

and much is known about their chemical compositions and properties (21). Most of these compounds are insoluble metal salts (oxides, carbonates, sulfides, etc.) and have been found to be stable to light and air. Two exceptions are litharge and orpiment, which may convert to more stable oxides upon exposure to light, air, and humidity. Others of these pigments, notably those containing lead or copper, may react to form black sulfides when placed in contact with sulfur-containing pigments or when exposed to sulfur-containing air pollutants. Finally, the mercuric sulfide, vermilion, has been observed to blacken upon exposure to light, a phenomenon attributed to a change in crystalline form rather than to a chemical alteration (22). The action of oxidizing air pollutants such as ozone on most of these materials has not, to our knowledge, been explored.

In contrast to these inorganic pigments, the plant dyes that saw use as coloring agents in Japanese textiles and woodblock prints are, for the most part, peculiar to the Orient, having been extracted from native plants. In general, natural dye extracts are complex mixtures of chemical compounds. The extraction, separation, and characterization of the components in these plant extracts constitute an active area of current research (23-25).

The coloring matters present in plant materials usually fall into one of several chemical classes (26,27). The most notable colorant in living plants is chlorophyll a, belonging to a class of molecules called porphyrins. This compound, however, is not important as an artist's colorant. Another group of plant dyes is the carotenoids, polyenes whose molecular structures are built around combinations of isoprene units. These compounds give rise to much of the yellow coloration in plant leaves and flowers. One such carotenoid is crocin, the major dye constituent of the Japanese *kuchinashi* (11).

The largest group of plant colorants is the flavonoid class, which includes the flavones, flavonols, and anthocyanins. The yellow-colored flavones and flavonols

occur in many leaves, woods, and flowers. Examples of these compounds are fustin, from the wood of the Japanese sumac *(yamahaji),* and rutin, from flowers of the Japanese pagoda tree *(enju).* The red, blue, and purple colorations of flowers, fruits, and foliage are the result of the presence of anthocyanins. Other compounds whose structures are related to the flavonoids, such as carthamin and brazilein, are also important dyestuffs in Japanese crafts. The occurrence of these various flavonoids in different plant species has been extensively studied by a number of authors, and several excellent review articles are available (11,28,29).

A number of other chemical classes are represented in the colorants that are derived from the roots, bark, or wood of certain plants (30). Quinones, for example, occur in madder root (which contains the anthraquinones, pseudopurpurin and alizarin, among others) and in the root of the Japanese borage plant *Lithospermum erythrorhizon* (from which the naphthoquinone dye, *shikonin,* is derived). (Incidentally, the major components of the insect dyes, cochineal and lac, are also anthraquinone compounds.) Turmeric root yields the diaroylmethane dye, curcumin. Alkaloids, natural compounds whose chemical structures contain nitrogen atoms, are found in extracts of the roots of *Polygonum tinctorium* (indigotin) and *Coptis japonica* (berberine) (11).

The major plant colorants described here usually exist in the plants as chemical derivatives of the parent dye compound and are components of a complex mixture with other dyes, carbohydrates, and various biological compounds. Because many of these dyestuffs play a role in the carbohydrate biochemistry of the living plant, the colorants commonly occur as compounds with sugar molecules (for example, as glycosides or gentiobiosides). Some colorants, such as the anthocyanins, exist in cationic forms and naturally occur as salts with an organic base. Tannins, both hydrolyzable and condensed, often are found in plant materials, and these can participate in the vegetable dyeing process (even when they are not intentionally

used as a dye or mordant). The presence of tannins in the vegetable dyeing usually leads to a dulling of the color, i.e., a reduction of chroma (31). Colorants can also complex together in the plant. In certain flowers, for example, anthocyanins can bind with other flavonoids. This usually results in the anthocyanin hue becoming more blue (26).

The chemical structures of these natural organic colorants can be greatly altered by the various extraction, separation, and mordanting/laking procedures that are performed in the production of a dyed textile or woodblock print. The breakdown of the natural compounds into soluble forms often involves freeing the dye molecules from the carbohydrates, tannins, or anions with which they are compounded in the plant. The additional treatment of the dye extracts, according to a variety of dyeing recipes, can further convert the dye components to other forms. Finally, the fixing of the vegetable dye to a textile fiber or the formation of an insoluble pigment is usually effected by complexing the dye with a metal ion. Few of these chemical transformations are fully understood, and the ultimate chemical structure of the colorant as it exists on the fabric or pigment is still an open question.

Even though the molecular structures of many colorant systems have not yet been established, the chemical alterations resulting from various preparations can nevertheless manifest themselves in the appearance and stability of the pigment or dyed textile. It is well known that the color of dyed cloth or pigments depends on the metal ion involved in the mordanting or laking process. In addition, the presence of other substances (minor dye constituents, tannins, etc.), either as impurities or as intentional additions, can affect the hue or chroma of the final product. Of particular relevance to this study, the chemical reactivities of the colorant systems, as demonstrated in light (32,33) or ozone (34) fading studies, also have been found to be critically dependent on the preparation of the colorant and its application.

Because the ozone reactivity of a colorant system does depend on the materials and procedures used in its production, a judgment of the ozone sensitivity of works of art created in historical times must involve the testing of either authentic materials or materials that duplicate authentic preparations. In some cases, such as for Japanese textiles dyed with vegetable dyes, the identity of the plant materials and the dyeing techniques have been recorded in historical documents; modern reproduction of authentic cloths is thus feasible. In other instances, such as the application of vegetable colorants on Japanese woodblock prints, similar records rarely exist, and technical studies may be difficult. These circumstances call for the testing of authentic works containing the relevant colorant systems, if such samples are available.

The ozone fading study described in this chapter involved both of these types of samples. Dry pigments and watercolor paints were tested as thin applications on paper. These materials included a number of the more common inorganic and organic colorants found on pre-19th century Japanese prints and paintings. Little or no binder was used for these colorants, so these samples are perhaps more directly analogous to the hand-colored or printed color woodblock prints of the Edo period and to any scroll or screen paintings done as light washes on paper. A woodblock print from a 19th century Japanese poetry book also was tested, which allowed both the examination of plant colorants in an authentic artist's application, as well as the testing of a colorant system that had already undergone some natural aging (presumably including photo- or atmospheric oxidation). Finally, a number of silk cloths also were included, having been recently prepared in Japan employing traditional materials and dyeing techniques. This experiment, then, provides a survey of the ozone fading hazard to a number of colorants that one might expect to encounter on a wide variety of Japanese works of art.

EXPERIMENTAL

Samples of dry pigments and watercolors were obtained from the pigment collection at the Center for Conservation and Technical Studies at Harvard University, and include litharge (massicot), orpiment, Prussian blue, verdigris, vermilion, cochineal lake, gamboge, indigo, lac lake, and madder lake. One colorant (curcumin) was acquired from Aldrich Chemical Company. The colorant powders were analyzed to authenticate their chemical compositions, using spectrophotometric or chromatographic techniques for organic colorants (described elsewhere (3)) and X-ray diffraction for the inorganic colorants. (Products of the ozone reaction of inorganic colorants also were identified using X-ray diffraction.) The sample of *aigami* was provided by Mrs. Keiko Keyes as a soaked paper, from which the colorant could be extracted with water. The reflectance spectrum of this colorant on paper was sufficient for identification by comparison to published data (5). Suspensions or solutions of these colorants were airbrushed onto hot-pressed watercolor paper using a previously discussed technique (3). Colorants were applied to achieve a reflectance of approximately 40% at the wavelength of maximum absorption, for this depth of shade has been found to provide the largest color change upon ozone reaction of this type of sample.

Diffuse reflectance spectra were recorded using a Diano Match Scan II spectrophotometer, with the sampling area 7 mm in diameter. Reflectance data were referenced to a standard white tile (calibrated against an NBS standard), which also was used as a backing for the paper samples during the measurements. From the reflectance spectra, tristimulus values and color differences, ΔE (from the CIE 1976 L*a*b* formula) (35), were calculated for CIE Illuminant C. Munsell notations (for CIE Illuminant C) were subsequently calculated from the tristimulus values (36). Details of this protocol are to be found elsewhere (3).

The Japanese woodblock print included in this test was a page from an illus-

trated poetry book, "A View of Osaka," (artist unknown) loaned by Mrs. Keyes. This book was produced circa 1810 in *fukuro-tōji* format (37), i.e., with two illustrations printed side-by-side on each sheet of paper. Each sheet was folded in half with the prints facing outward, and the unfolded ends were sewn together to form the spine of the book. In this experiment, the book was unbound, and a single page was chosen that contained all of the various colorants. The colorants on this print survived in relatively good condition by being protected in the book, but several areas were marred by serious wear and insect damage. The ozone fading test could be performed only on the entire print: masking of portions of the print to protect them from ozone exposure proved impossible. However, the accuracy of the color measurement technique allowed the establishment of the ozone sensitivity with only minor color changes. The ozone exposure experiment was designed to be terminated before the overall appearance of the print was severely damaged.

Reflectance spectra of 7 mm diameter areas on the print again were measured on the Match Scan II spectrophotometer. The page first was mounted between a 3/8-inch thick, foam-filled mounting board and a Mylar sheet that had several 7 mm holes marked and cut in it. This Mylar template also had registration marks for reproducible placement over the print. Square holes cut in the backing board behind the target areas allowed placement of the standard reflectance white tile directly behind the print during the color measurement. The entire assembly was held on an easel against the front of the spectrophotometer, and, using a mirror, the marked holes in the Mylar template could be viewed through the sample port and accurately positioned. Reproducibility of color measurements on the print using this technique was excellent, with resultant uncertainties in ΔE being less than about 1 unit. For the ozone exposure, the print was removed from this assembly and mounted on an anodized aluminum panel for convenient handling.

The colorants on the print were identified from their reflectance spectra by

comparison with previously published results (5). The red areas were colored with *beni* (safflower), the blue with *ai* (indigo); the green was *ai* plus a yellow (either overprinted or printed with a mixture of colorants), and the purple areas contained *aigami* (dayflower) and a red. The intense red-orange fluorescence of the red areas under ultraviolet illumination was further evidence for the presence of *beni.* The reflectance spectra of the yellow areas were not sufficient to identify the colorant, so microchemical color reactions were employed. A small amount of the yellow colorant was transferred from a damaged portion of one of the other book pages to a piece of filter paper wetted with a small drop of methanol and pressed against the print. This solubility of the colorant in methanol and the subsequent color tests performed on the filter paper spot [orange with NaOH solution, indicating either curcumin or gamboge (38), and a negative boric acid test—thus curcumin was not present (39)] all are consistent with the yellow colorant's being *shiō* (gamboge). The *beni, ai, aigami,* and *shiō* were all common organic colorants used on prints of the early 19th century. The ozone sensitivity of these colorants was tested by following the color changes of these materials during ozone exposure on 17 colored areas (3 or 4 examples of each hue) on several different regions of the page.

The dyed Japanese textiles were silk cloths prepared by Mr. Seiju Yamazaki using traditional materials and formulas and were acquired with the help of Dr. K. M. Kashiwagi. The dyes and mordants, listed in Table 3.2, were specified by the dyer, and no further chemical analysis was attempted. One-inch square swatches of the silk cloths were sewn to 2.5cm x 5cm pieces of watercolor paper for convenient handling. Color measurements were performed as for the colorant/paper samples.

The ozone exposure apparatus and its operation have been detailed in Chapter 2 (1,3). Briefly, an air stream is purified with a series of filters, ozonized with a short-wavelength ultraviolet lamp, and humidified, before finally being admitted to

Table 3.2. Natural colorant/mordant combinations for silk cloths tested.

Color	Natural dye	Mordant
Yellow	*Enju* (Japanese pagoda tree)	Al
	Kariyasu (Miscanthus)	Al
	Kariyasu (Miscanthus)	Cu
	Kihada (Japanese yellow wood)	Al
	Kuchi nashi (Jasmine)	Al
	Ukon (Turmeric)	Al
	Ukon (Turmeric)	Acetic acid
	Woren (*Coptis japonica*)	None
	Yamahaji (Japanese sumac)	Al
	Yama-momo (*Myrica rubia*)	Al
	Zumi (Mustard)	Al
	Shiō (Orpiment, As_2S_3)	None
Red	*Seiyo akane* (Western madder)	Al
	Akane (Japanese madder)	Al
	Enji (Cochineal)	Sn
	Shiko (Lac)	Al
	Suo (Sappanwood)	Al
	Beni (Safflower)	None
Blue	*Ai* (Indigo)	None
Green	*Ai* + *enju*	Al
	Ai + *kariyasu*	Al
	Ai + *kihada*	Al
Violet	*Shikon* (Lithospermum)	Al

a light-tight, stainless steel and glass chamber. The samples, mounted on anodized aluminum panels and hanging adjacent to the interior walls of the chamber, were exposed to 0.40 parts per million (ppm) ozone at 22°C, 50% RH, in the absence of light, for 12 weeks. Ozone concentrations were measured continuously with a UV photometric ozone monitor, and hourly average concentrations were calculated automatically and stored on a computer. The reflectance spectra of the samples were recorded before the exposure and at intervals during the exposure. Color differences (between spectra of samples before and after exposure) were calculated from the reflectance measurements. The extent and rate of the color changes were used to judge the ozone sensitivity of the colorants in the various forms.

RESULTS AND DISCUSSION

The results for the colorants and watercolors applied to paper are shown in Table 3.3. The results for some of the natural organic colorants are from an earlier experiment and have been published previously (3), but they are presented here because of their relevance to the present study. Among the organic colorants tested, curcumin, indigo, madder lake, and lac lake are all quite sensitive to ozone exposure. Detailed studies of the mechanics of the ozone reaction with indigo, curcumin, and with an alizarin lake (a synthetic pigment related to the madder lakes) are presented in Chapters 4-6 and confirm that reaction with ozone is indeed the agent causing the observed fading (34, 40). The remaining organics—cochineal lake, gamboge, and *aigami*—show measurable but somewhat lesser fading upon exposure to the same ozone dose. The gum binder present in the gamboge and indigo watercolor paints seems to have little effect on the observed ozone sensitivity of the colorants: the relatively insensitive colorant gamboge shows only a very slight color change when applied as a watercolor, and the very ozone-fugitive indigo fades rapidly even in the form of a watercolor wash.

Table 3.3. Observed color change of colorant/paper systems under CIE Illuminant C after exposure to 0.40 ppm ozone. Munsell notation (hue, value/chroma) calculated from tristimulus values.

Colorant	Weeks of Exposure	X	Y	Z	Munsell	ΔE
Litharge (massicot)	0	76.90	79.61	72.10	4.8Y9.0/1.9	
	12	79.14	82.00	74.32	5.0Y9.1/1.9	1.08
Orpiment	0	72.01	75.31	50.69	4.7Y8.8/4.1	
	12	81.96	84.77	82.79	5.8Y9.3/1.4	20.01
Prussian blue	0	44.00	47.86	72.51	8.8B7.3/4.0	
	12	46.41	50.82	77.07	8.3B7.5/4.2	2.13
Verdigris	0	70.86	75.27	84.35	3.3G8.8/0.9	
	12	73.10	77.96	87.33	4.0G9.0/1.0	1.42
Vermilion	0	65.60	60.23	56.18	8.4R8.1/4.1	
	12	66.97	61.50	57.50	8.3R8.1/4.1	0.69
Aigami (watercolor)	0	52.31	55.27	67.63	0.2B7.8/1.1	
	12	55.98	58.85	70.27	6.3BG8.0/0.8	2.49
Cochineal lake[a]	0	62.16	53.09	58.64	8.3RP7.6/6.2	
	12	65.42	57.58	62.90	9.1RP7.9/5.4	4.60
Curcumin[a]	0	72.61	76.15	28.92	4.6Y8.9/7.9	
	12	83.35	87.16	79.16	7.5Y9.4/1.8	41.77
Gamboge (powder)[a]	0	75.03	77.87	60.33	4.3Y9.0/3.1	
	12	77.70	80.78	66.86	4.8Y9.1/2.6	3.57
Gamboge (watercolor)	0	79.55	85.07	63.87	9.6Y9.3/3.2	
	12	79.95	85.35	65.68	9.6Y9.3/3.1	1.34
Indigo (powder)[a]	0	42.17	44.02	56.37	8.1B7.1/1.4	
	12	62.01	65.13	73.26	1.5G8.3/0.7	14.20
Indigo (watercolor)	0	52.25	54.49	70.53	9.4B7.7/1.7	
	12	77.24	79.87	87.16	4.6GY9.1/0.6	16.25
Lac lake[a]	0	58.92	54.08	62.17	7.4RP7.7/4.0	
	12	65.89	62.68	69.58	1.6R8.2/2.9	6.88
Madder lake[a]	0	76.57	69.68	78.61	8.2RP8.6/4.4	
	12	81.36	78.66	86.81	4.0R9.0/2.5	9.95

[a]Results previously reported in Ref. 3.

Of the inorganic colorants tested, only orpiment shows an ozone reaction, and the fading here is very rapid. The product of the ozone reaction of orpiment was the arsenic oxide, As_2O_3, in its cubic crystal structure (arsenolite). This conversion of orpiment, As_2S_3, to the more stable oxide, As_2O_3, seems to occur slowly even in the absence of ozone. (In fact, two of the three samples of "orpiment" obtained for this study proved to be predominantly the oxide.) Although this reaction occurs under normal exposure to oxygen, light, and humidity, examination of an orpiment/paper sample that was not exposed to ozone showed that this natural conversion to the oxide was very slow compared to the reaction during ozone exposure. Most of the color change observed in this experiment, then, can be attributed to the ozone reaction, or ozone-assisted oxidation, of this mineral pigment.

The Japanese woodblock print tested in this study contained four coloring agents, all plant-derived organic colorants: *beni* (safflower), *ai* (indigo), *aigami* (dayflower), and *shiō* (gamboge). Three of these colorants—the *ai, aigami,* and *shiō*—also were tested as fresh preparations on watercolor paper, as described above. This comparison presents the opportunity to judge the relevance of these colorant/paper systems in assessing the ozone sensitivity of aged, authentic artists' applications.

The measured ozone fading of a typical example of each color on the print is shown in Table 3.4. Definite color changes were observed only for the blue and green areas, both containing *ai.* It is clear from the changes in the reflectance spectra of the green areas that at least part of the color change is due to consumption of the blue component of the colorant mixture (i.e., the *ai*). The remaining colorants—*beni, shiō*, and *aigami* (in the purple areas)—showed very little reactivity towards ozone. The results for each color were consistent over the entire print: all of the blue and green areas showed relatively large ΔE values, and all of the red, yellow, and purple areas produced color differences of less than about 2 units after

Table 3.4. Observed color change of color areas on the Japanese woodblock under CIE Illuminant C after exposure to 0.40 ppm ozone. Munsell notation (hue, value/chroma) calculated from tristimulus values.

Color area (colorant)	Weeks of Exposure	X	Y	Z	Munsell	ΔE
Red (*benī*)	0	34.04	28.42	17.44	1.1YR5.9/6.6	
	12	34.98	29.30	18.16	1.1YR5.9/6.5	0.81
Blue (*ai*)	0	20.49	22.06	25.81	1.3BG5.2/1.0	
	12	23.88	25.65	27.85	1.3G5.6/1.0	4.79
Yellow (*shiō*)	0	45.27	46.20	31.05	3.1Y7.2/3.7	
	12	46.86	47.89	32.76	3.1Y7.3/3.7	1.18
Green (*ai* + yellow)	0	13.13	14.46	16.62	9.5G4.3/1.3	
	12	1.86	17.53	19.38	5.6G4.7/1.4	4.37
Purple (*aigami* + red)	0	20.43	19.45	17.75	3.6YR5.0/2.1	
	12	21.91	20.92	19.16	3.8YR5.1/2.1	1.66

ozone exposure.

The observed ozone sensitivity of the indigo and the lesser extent of fading for the gamboge and dayflower are all consistent with the conclusions of the colorant/paper study. The ΔE values for the indigo present on the woodblock print were somewhat less than those encountered for the prepared indigo/paper samples; these differences may be due either to variations in chemical purity, sample preparation, or colorant concentration or to the prior aging of the colorant on the print. In any case, the consideration of indigo as an ozone-sensitive colorant appears valid even for a specimen that has seen a rather long history of natural aging.

In the first part of this experiment, the systematic applications of colorants on paper allowed an approximate comparison of the relative ozone sensitivities of the various colorants. In contrast, the dyed silk cloths included in this test were not uniformly prepared, for they differed both in mordant and in depth of shade. Because of this, the ozone exposure of these textiles, rather than providing a measure of the relative ozone sensitivities of the colorants, should be viewed only as a survey of the ozone fading hazard for this type of material.

The results in Table 3.5 show the color changes for those colorant systems that faded to a measurable extent upon exposure to ozone. Not surprisingly, among the textiles that reacted were those that were dyed with *ai* (indigo), either alone or in combination with one of the yellow plant dyes. Also showing evidence of ozone fading were the purple *shikon,* the red-orange *akane,* and several yellow plant dyes. Although some of these color changes were relatively slight and the color differences for the materials not listed in Table 3.5 were even smaller (ΔE less than 2 units), these results, nevertheless, suggest that prolonged exposure of traditional Japanese dyed textiles to atmospheric ozone presents a risk of damage to their colorants.

Table 3.5. Observed color change of dyed silk cloths under CIE Illuminant C after exposure to 0.40 ppm ozone.[a] Munsell notation (hue, value/chroma) calculated from tristimulus values.

Dye/mordant	Weeks of Exposure	X	Y	Z	Munsell	ΔE
Akane/Al	0	26.15	29.68	15.21	2.0YR6.0/7.6	
	12	40.82	34.38	18.33	2.7YR6.4/7.3	4.36
Ai	0	7.37	7.22	16.93	5.1PB3.1/4.7	
	12	8.70	8.76	20.08	4.1PB3.4/5.0	3.78
Ai + *enju*/Al	0	29.25	34.84	12.95	3.0GY6.4/6.6	
	12	32.92	38.64	14.03	2.6GY6.7/6.9	4.11
Ai + *kariyasu*/Al	0	9.19	10.99	11.73	6.7G3.8/2.4	
	12	12.08	14.68	13.78	2.3G4.4/2.9	7.74
Ai + *kihada*/Al	0	11.89	14.38	8.16	5.6GY4.3/4.0	
	12	17.45	20.62	9.10	3.1GY5.1/5.0	12.95
Shikon/Al	0	9.23	8.01	12.75	7.3P3.3/2.8	
	12	12.25	10.76	16.69	7.5P3.8/3.0	5.17
Kuchinashi/Al	0	31.27	28.76	5.81	0.1Y5.9/9.2	
	12	34.97	32.14	6.04	0.1Y6.2/9.8	4.98
Yamahaji/Al	0	45.80	46.01	26.44	2.2Y7.2/4.8	
	12	48.87	49.21	28.65	2.3Y7.4/4.8	2.06
Yama-momo/Al	0	30.79	30.60	19.00	1.4Y6.0/3.9	
	12	33.51	33.24	21.05	1.1Y6.3/3.9	2.21
Zumi/Al	0	37.87	37.89	16.42	2.6Y6.6/6.0	
	12	40.87	41.10	18.27	2.8Y6.9/6.0	2.40

(a) All dyed cloth samples listed in Table 3.2 were tested. Results are given here only for those samples showing a noticeable color change ($\Delta E > 2$) after ozone exposure.

CONCLUSIONS

This study and the others in this series were based upon a chamber experiment, an attempt to simulate in a relatively short time the chemical reactions expected to occur during a prolonged exposure to atmospheric ozone under natural conditions. As pointed out in prior reports (3), the ozone concentration used in this work is equal to that observed for short periods in a polluted urban environment. The total ozone dose administered to the samples in this test is equivalent to that which would be encountered within about four years outdoors or about eight years in a typical air-conditioned indoor environment. The results of this exposure study suggest that the risk of ozone damage to a wide range of Japanese works of art and artifacts (particularly prints and costumes containing natural colorants) is significant, and protection of these objects from prolonged ozone exposure would be a prudent precaution.

REFERENCES FOR CHAPTER 3

1. Shaver, C.L., Cass, G.R., and Druzik, J.R., "Ozone and the Deterioration of Works of Art," *Environmental Science and Technology, 17* (1983) 748-752.

2. Drisko, K., Cass, G.R., Whitmore, P.W., and Druzik, J.R., "Fading of Artists' Pigments due to Atmospheric Ozone," in *Wiener Berichte über Naturwissenschaft in der Kunst,* Bd. 2/3, 1985/86, ed. A. Vendl, B. Pichler, and J. Weber, pp. 66-87, Verlag ORAC, Vienna (1986).

3. Whitmore, P.M., Cass, G.R., and Druzik, J.R., "Ozone Fading of Traditional Natural Organic Colorants on Paper," *J. Amer. Inst. Cons., 26* (1987) 45-58.

4. Mayer, R., *The Artist's Handbook of Materials and Techniques,* Viking Press, New York (1981).

5. Feller, R.L., Curran, M., and Bailie, C., "Identification of Traditional Organic Colorants Employed in Japanese Prints and Determination of Their Rates of Fading," in *Japanese Woodblock Prints: A Catalogue of the Mary A. Ainsworth Collection,* Allen Memorial Art Museum, Oberlin, OH (Reprint from Indiana University Press, 1984).

6. Terukazu, A., *Japanese Painting,* Albert Skira, Lausanne, Switzerland (1961).

7. Yamasaki, K., "Pigments Employed in Old Paintings of Japan," in *Archaeological Chemistry,* ed. by M. Levey, American Chemical Society, Washington, D.C. (1967) 347-365.

8. Gettens, R., "Japanese Paintings: Technical Studies at the Freer Gallery of Art," in *Conservation and Restoration of Pictorial Art,* ed. by N. Brommelle and P. Smith, Butterworths, London (1976) 241-252.

9. Fitzhugh, E., "A Pigment Census of *Ukiyo-e* Paintings in the Freer Gallery of Art," *Ars Orientalis, 11* (1979) 27-38.

10. Winter, J., "'Lead White' in Japanese Paintings," *Studies in Conservation, 26* (1981) 89-101.

11. Hayashi, K., "Chemical Procedure for the Determination of Plant Dyes in Ancient Japanese Textiles," in *International Symposium on the Conservation and Restoration of Cultural Property,* Tokyo National Research Institute of Cultural Properties (1979) 39-50.

12. Nasu, Y., Nakazawa, F., and Kashiwagi, M., "Emission and Excitation Spectra of Natural Yellow Dyes on Silk Fabrics Before and After Fading," *J. Soc. Dyers and Colourists, 101* (1985) 173-176.

13. Stern. H.P., *Master Prints of Japan,* Harry N. Abrams, Inc., New York (1969?) 13.

14. Chibbett, D., *The History of Japanese Printing and Book Illustration,* Kodansha International Ltd., Tokyo (1977) 29-38, 118-119.

15. Turk, F.A., *The Prints of Japan,* Arco Publications, Worcester, MA (1966) 39-66.

16. Grove, N., in Appendix to *Ukiyo-e Prints and Paintings: The Primitive Period, 1680-1745,* Donald Jenkins, The Art Institute of Chicago, Chicago, IL (1971) 128.

17. Munsterberg, H., *The Japanese Print: A Historical Guide,* Weatherhill, New York (1982) 39.

18. Lane, R., *Images from the Floating World: The Japanese Print,* G.P. Putnam's Sons, New York (1978) 99-102.

19. Yoshida, T., and Yuki, R., *Japanese Print-Making: A Handbook of Traditional and Modern Techniques,* Charles E. Tuttle Co., Rutland, VT (1966) 54-55.

20. Schraubstadter, C., *Care and Repair of Japanese Prints,* Idlewild Press, Cornwall-on-Hudson, New York (1948).

21. Wehlte, K., *The Materials and Techniques of Painting,* Van Nostrand Reinhold, New York (1982) 51-168.

22. Gettens, R.J., Feller, R.L., and Chase, W.J., "Vermilion and Cinnabar," *Studies in Conservation, 17* (1972) 45-69.

23. Obara, H., and Onodera, J., "Structure of Carthamin," *Chem. Letters* (1979) 201-204.

24. Goto, T., Kondo, T., Tamura, H., and Takase, S., "Structure of Malonylawobanin, the Real Anthocyanin Present in Blue-colored Flower Petals of *Commelina communis*," *Tetrahedron Lett., 24* (1983) 4863-4866.

25. Andersen, O.M., and Francis, G.W., "Simultaneous Analysis of Anthocyanins and Anthocyanidins on Cellulose Thin Layers," *J. Chromatography, 318* (1985) 450-454.

26. Alkema, J., and Seager, S.L., "The Chemical Pigments of Plants," *J. Chem. Ed., 59* (1982) 183-186.

27. Sequin-Frey, M., "The Chemistry of Plant and Animal Dyes," *J. Chem. Ed., 58* (1981) 301-305.

28. Geissman, T.A., ed., *The Chemistry of Flavonoid Compounds,* Macmillian Co., New York (1962).

29. Harborne, J.B., *Comparative Biochemistry of the Flavonoids,* Academic Press, London (1967).

30. Mayer, F., and Cook, A.H., *The Chemistry of Natural Coloring Matters*, Reinhold, New York (1943).

31. Kashiwagi, K.M., "Color Characteristics of Traditional Vegetable Dyeing," *Textile Res. J., 43* (1973) 404-408.

32. Padfield, T., and Landi, S., "The Light Fastness of the Natural Dyes," *Studies in Conservation, 11* (1966) 181-193.

33. Crews, P., "The Influence of Mordant on the Lightfastness of Yellow Natural Dyes," *J. Am. Inst. Cons., 21* (1982) 43-58.

34. Grosjean, D., Whitmore, P.M., De Moor, C.P., Cass, G.R., and Druzik, J.R. "Fading of Alizarin and Related Artists' Pigments by Atmospheric Ozone: Reaction Products and Mechanisms," *Environmental Science and Technology, 21* (1987) 635-643.

35. Billmeyer, F.W., Jr. and Saltzman, M., *Principles of Color Technology*, 2nd edition, John Wiley and Sons, New York (1981).

36. "Standard Method of Specifying Color by the Munsell System," Designation D1535-80, American Society for Testing and Materials, Philadelphia (1980).

37. Hillier, J., and Smith, L., *Japanese Prints: 300 Years of Albums and Books*, British Museum Publications, Ltd., London (1980) 14.

38. "Colour Index," 3rd edition, revised, Society of Dyers and Colourists, Bradford, Yorkshire, England, 1971, Vol. 4

39. Lee, D.L., Bacon, L., and Daniels, V., "Some Conservation Problems Encountered with Turmeric on Ethnographic Objects," *Studies in Conservation, 30* (1985) 184-188.

40. Grosjean, D., Whitmore, P.M., Cass, G.R., and Druzik, J.R., "Ozone Fading of Natural Organic Colorants: Mechanisms and Products of the Reaction of Ozone with Indigos," *Environmental Science and Technology, 22* (1988) 292-298.

CHAPTER 4

FADING OF ALIZARIN AND RELATED ARTISTS' PIGMENTS BY ATMOSPHERIC OZONE: REACTION PRODUCTS AND MECHANISMS

INTRODUCTION

The experiments described in Chapters 2 and 3 plus prior experiments performed on modern synthetic organic artists' pigments (1,2) show that several categories of artists' pigments will fade substantially when exposed, in the dark, to air containing 0.3 ppm-0.4 ppm of ozone over a period of three months. These levels of ozone are occasionally recorded in urban air during photochemical smog episodes, and an ozone dose equivalent to these experiments (concentration multiplied by duration of exposure) would be accumulated by exposure to outdoor air over a three- to five-year period in many parts of the world. Organic pigments that were particularly ozone-fugitive included alizarin red pigments containing lakes of the polycyclic aromatic compound 1,2-dihydroxyanthraquinone (and their natural counterpart, the madder lakes), blue-violet pigments containing substituted triphenylmethane lakes, heterocyclic compounds such as indigo, and yellow coloring agents containing polyfunctional, polyunsaturated compounds such as curcumin (1-3).

Given the structural diversity of these ozone-fugitive pigments, several types of chemical reactions must be involved in the initial ozone attack and the subsequent pathways resulting in the loss of chromophore, i.e., pigment fading. These reactions have received only very limited attention in the case of textile dyes (4,5) and have not been studied in the case of artists' pigments. The chemical mechanism of the reaction of ozone with selected pigments thus will be investigated with an eye toward confirming that ozone is indeed the cause of the fading observed during the ozone exposure experiments. As an aid to the elucidation of the corresponding reaction mechanisms, "model" compounds will be included in this investigation consisting of simple structural homologues of the pigments studied. In addition, parameters such as

ozone concentration, ozone exposure time, and nature of the substrate will be examined. These factors are expected to play a role in the heterogeneous reactions taking place when exposing substrate-deposited organic pigments to gaseous ozone.

In this chapter, we describe our results for alizarin (1,2-dihydroxyanthraquinone) and for Alizarin Crimson, a calcium-aluminum lake representative of a number of alizarin derivatives employed in the formulation of artists' pigments. Results of companion studies of the reaction of ozone with curcumin, indigos, triphenylmethanes and related compounds are described in Chapters 5-7 (6,7).

EXPERIMENTAL METHODS

A summary of the matrix of experiments carried out and of the corresponding analyses is given in Table 4.1.

Compounds Studied

This study focused on alizarin and on the watercolor pigment, Winsor and Newton's 002 Alizarin Crimson. Also included in this study was the simple structural homologue anthraquinone (MW = 208, CAS number 84-65-1, purity $\geq$ 97%). The structure of alizarin (1,2-dihydroxyanthraquinone, MW = 240, CAS number 72-48-0, CI number 58000) was verified by mass spectrometry analysis (8) of the reference compound (purity $\geq$ 97%) obtained from Aldrich Chemicals Co., Milwaukee, Wisconsin. The Alizarin Crimson pigment is prepared as a lake by precipitating alizarin as an aluminum complex according to the tentative structure shown in Figure 4.1. X-ray fluorescence analysis confirmed that aluminum and calcium were the major inorganic components, in agreement with the lake structure given in Figure 4.1. However, the commercially prepared sample used here contained more aluminum than calcium (relative abundance 6:1 on a molar basis, versus 1:1 for the structure given in Figure 4.1, reflecting the likely addition of alumina during the laking process) and also contained silicon, phosphorus, sulfur, chlorine, and barium (abundances relative to calcium, on a molar basis,

Table 4.1 Matrix of experiments

	Alizarin	Anthra-quinone	Alizarin Crimson
Ozone exposure mode:			
long term to low O_3	+		+
short term to high O_3	+	+	+
Substrate:			
silica gel	+		+
cellulose	+		+
Teflon filter	+	+	+
Sample extraction:			
methylene chloride	+		+
methanol	+		+
none (direct MS analysis)	+	+	+
Mass spectrometry analysis:sup(a)			
probe--electron impact (EI)	+		
probe--chemical ionization (CI)	+	+	+
GC--electron impact	+		+

(a) Include, for all compounds, the analysis of control (unexposed) samples and of all appropriate solvent and substrate blanks.

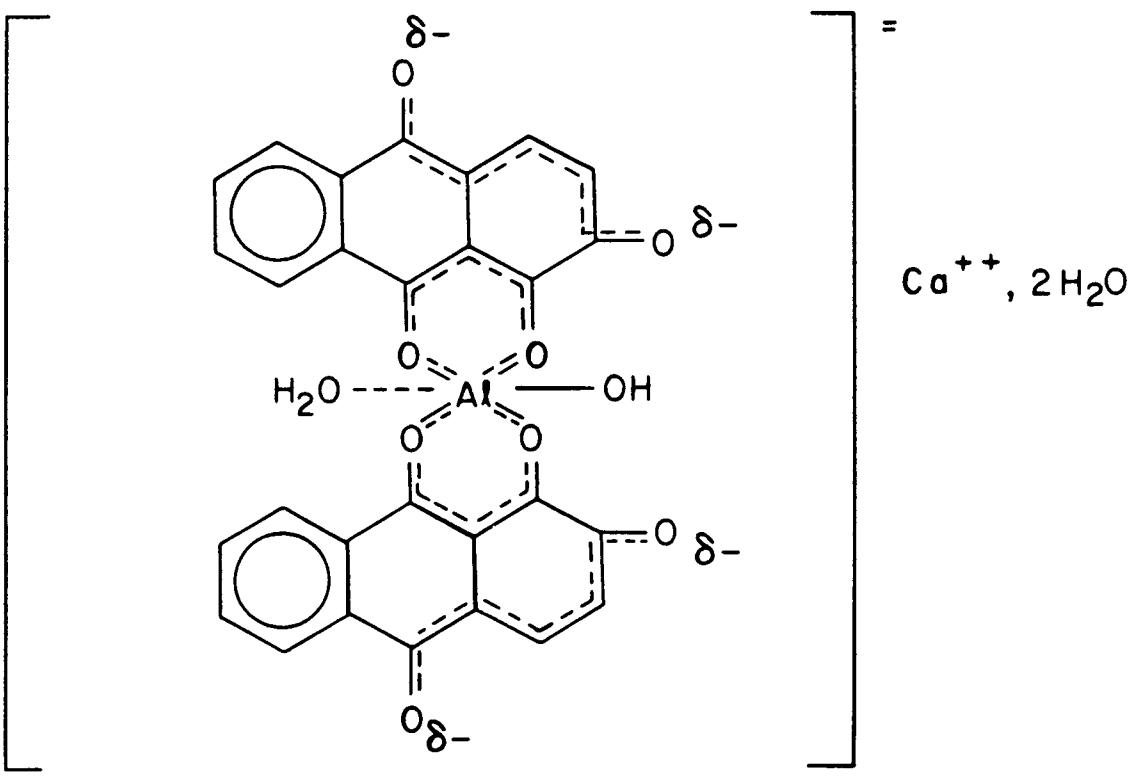

Figure 4.1 Probable structure of Alizarin Crimson (calcium-aluminum lake of alizarin). From references (1) and (27).

of 0.12, 0.67, 0.04, 0.03, and 0.06, respectively). Mineral impurities, e.g., alumina, silicate, phosphate, etc., were obviously present in the sample.

Ozone Exposure Protocols

Two types of experiments were carried out, one involving long-term exposure to low concentrations of ozone and the other involving shorter term exposure to higher ozone concentrations. The long-term exposure protocol involved two substrates, cellulose and silica gel; while a third substrate, Teflon, was employed in the short-term exposure experiments.

For the long-term exposures, the compounds were airbrushed on 50×200 mm thin layer chromatography (TLC) plates, both silica gel (0.25 mm thickness Silica Gel G with calcium sulfate binder, Analtech Co.) and cellulose (0.5 mm thickness, no binder, Analtech Co.). Two samples, each containing ~100 mg of compound per TLC plate, were prepared for each compound on both silica gel and cellulose. The first sample was used as control and was stored between glass plates sealed with Teflon tape and wrapped in aluminum foil in the dark prior to solvent extraction and analysis. The second sample was exposed for 95 days to 0.356 ± 0.108 ppm of ozone in purified air in the absence of light, at constant temperature (22°C) and humidity (RH = $49.5 \pm 1.9\%$). The ozone concentration inside the exposure chamber was monitored continuously during the experiment using a Dasibi model 1003-AH ultraviolet photometer. The exposure chamber consisted of a 55 liter vessel admitting ozonated air at a constant rate of 2.5 liters per minute through a perforated Teflon tube with an in-line particulate filter. The matrix air was purified using a Purafil bed (to remove SO_2 and NO_2) and an activated charcoal filter (to remove ozone and reactive hydrocarbons) and subsequently humidified and ozonated using a Pen-ray ultraviolet lamp. Details of the experimental protocol have been described in Chapter 2.

Since the observation of fading (loss of chromophore) provided the impetus for this study of colorant-ozone reaction products and mechanisms, it is important to be

able to associate color changes in the samples with the consumption of colorant materials by chemical reaction. The samples intended for chemical analysis were very heavily coated (~100 mg of compound per TLC plate) and thus appear much darker than would be used in a watercolor artist's work. With such a thick pigment layer, it was possible that ozone would react with only the upper surface of the deposit and that such a superficial attack might not lead to observable fading of the samples. In order to draw a direct comparison between the ozone exposure conditions used here and the fading of light washes of colorant on different substrates, additional samples were prepared on silica gel and cellulose TLC plate substrates and on watercolor paper. These lightly loaded samples will be referred to as "optical" samples to distinguish them from the heavily loaded "analytical" samples intended for chemical reaction product identification studies. The optical samples plus examples of blank TLC plates and blank watercolor paper were divided in half, with one half of each sample placed in the long-term ozone exposure chamber alongside the analytical samples, while the second half was stored in the dark to serve as an unexposed control. The color of the ozone-exposed and control samples was specified using the Munsell system of color notation (9). Munsell matches were made by a human observer using the illumination provided by a Macbeth Spectra Light booth under the daylight setting in accordance with ASTM standard methods (10). The tristimulus value of each exposed and control optical sample was measured using a Diano Matchscan II reflectance spectrophotometer, and the total color difference, ΔE, between exposed and control optical samples was computed using the CIE 1976 L*a*b* formula. The reflectance spectra of the Alizarin Crimson and alizarin dye control optical samples on cellulose and on silica gel substrates are given in Figure 4.2.

Each sample for the short-term, high ozone concentration exposures consisted of about 10 mg of the neat compound, supported on a 47 mm diameter, 0.5 μm pore size, Teflon membrane filter (Membrana Corp.). Through this filter, mounted in a Teflon in-

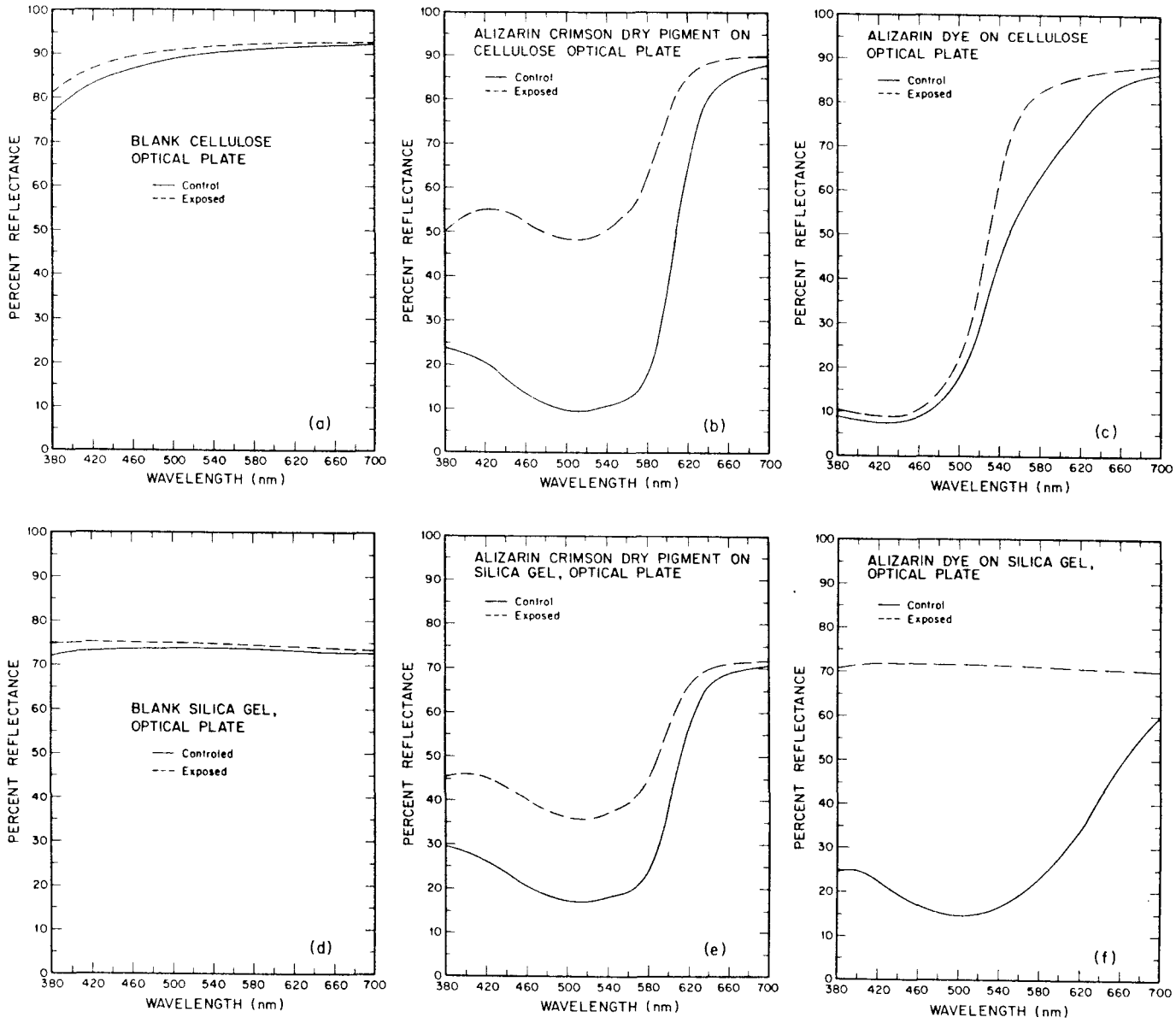

Figure 4.2 Reflectance spectra of ozone-exposed and control samples of Alizarin Crimson dry pigment powder and alizarin dye on silica gel and on cellulose TLC plates.

line filter holder, passed an airstream that had been purified by Purafil and activated carbon beds and ozonated with a Pen-ray ultraviolet lamp. Samples were exposed, one at a time, to ozone for 18-80 hours at 24°C and a relative humidity $\leq$ 40%, in the absence of light. At a flow rate of 1 lpm, the ozone concentrations, subsequently determined by dynamic dilution and UV photometric detection, were approximately 10 ppm.

Samples Preparation

In the absence of well-established protocols, we examined several methods for sample recovery following exposure to ozone. Taking into account the requirements for sample analysis by either insertion probe mass spectrometry (for which both solid and liquid samples are suitable) or by gas chromatography/mass spectrometry (liquid samples only), and considering the usual trade-offs between solvent extraction and direct sample analysis (e.g., possibility of solvent extract concentration for increased detection limits versus possible loss of information due to poor recovery of one or more reaction products), we elected to analyze both total (solid) samples and solvent extracts. Thus, samples from the short-term exposures were obtained simply by scraping the deposits off the Teflon filters, and samples from the long-term exposures were prepared as concentrated solvent extracts using high-purity methylene chloride and methanol (Soxhlet extraction for 18 hours with 150 mL of solvent followed by a two-step extract concentration to 1 mL using a rotary evaporator). All control and ozone-exposed samples were stored in the dark at refrigerator temperature in glass vials with Teflon-lined caps prior to analysis.

Mass Spectrometry Analysis

MS analyses were carried out (a) by direct insertion probe with electron impact ionization (probe-EI), (b) by direct insertion probe with chemical ionization using methane as reagent gas (probe-CI), and (c) by gas chromatography/mass spectrometry with electron impact ionization (GC-EIMS). Several sample extracts were also screened

by GC alone prior to MS analysis. Experimental conditions were as follows: (a) probe-EI: Kratos Scientific Instrument model MS-25 hexapole, double focusing magnetic sector instrument, electron energy 70 eV, probe temperature 250°C, source temperature 200°C, acceleration potential 2 kV; (b) probe-CI: MS-25 instrument, reagent gas (methane) pressure ~0.1 torr, reagent gas flow rate 30 mL min^{-1}, probe temperature 300°C, source temperature 320°C, electron energy 100 eV, acceleration potential 2 kV; (c) GC-EIMS: Hewlett-Packard HP 5710A gas chromatograph equipped with a J&W Scientific DB-5 fused silica capillary column (30 m long, film thickness 0.25 μm), column temperature = 70 to 300°C at 8°C/minute, injection temperature = 250°C, injection volume = 1 μL with 1:30 split ratio, interface temperature = 300°C, mass spectrometer parameters same as for probe-CI analyses. Finally, a limited number of analyses were carried out by fast atom bombardment (FAB) using a modified Associated Electrical Industries (AEI) model MS 902 mass spectrometer.

RESULTS AND DISCUSSION

Color Changes due to Exposure to Ozone

The color changes that resulted from the long-term, low-level ozone exposure experiment are summarized in Table 4.2, organized according to colorant and substrate. Each of the colorant systems was observed to fade on all of the substrates tested, while the appearance of the blank TLC plates and blank watercolor paper was changed by the ozone exposure experiment only to the extent of a very slight bleaching (see Figures 4.2ad). Reagent alizarin applied to watercolor paper and to cellulose appears to be yellow-red in hue; while when applied to the silica gel TLC plates in a light wash, the sample plus substrate combination takes on a red-purple hue that more closely resembles an alizarin lake. This difference between alizarin dye on cellulose and on silica gel can be examined by comparing Figures 4.2cf. The sample of alizarin dye on silica gel has a minimum in its reflectance spectrum at 500 nm that is similar to that observed

Table 4.2. Observed color change in reagent alizarin and Alizarin Crimson pigment samples as a function of substrate after exposure to 0.356 ppm O_3 at 49.5% RH for 95 days in the absence of light.

COLORANT AND SUBSTRATE	Munsell Notation[a]		Tristimulus Value[b]						Color Difference[c]
	Control	O_3 Exposed	Control			O_3 Exposed			
Alizarin			X	Y	Z	X	Y	Z	ΔE
Watercolor Paper[d]	7.5YR 6.7/10	10YR 7.8/11.2	45.04	39.49	10.55	61.92	57.57	14.42	16.77
Cellulose TLC Plate (Optical)[e]	9.5YR 7.4/10.8	2.0Y 8.4/10.8	53.38	49.97	11.07	65.30	64.70	13.46	13.75
Cellulose TLC Plate (Analytical)[e]	8.5YR 7/13.6	8.5YR 7.7/13.2							
Silica Gel TLC Plate (Optical)	8.5RP 5.3/5.6	7.5PB 8.7/0.8	25.31	20.98	21.07	69.40	70.95	84.33	41.27
Silica Gel TLC Plate (Analytical)	5.0YR 4.1/7.6	8.5Y 8.7/2.4							
Alizarin Crimson Dry Powder									
Watercolor Paper	10RP 5.7/11.2	5.0R 9.1/2.4	42.93	30.95	28.69	80.92	80.73	87.35	48.42
Cellulose TLC Plate (Optical)	9.5RP 5.2/11.6	8.5RP 8.2/5.6	32.98	21.20	17.42	65.83	59.05	61.95	42.64
Cellulose TLC Plate (Analytical)	4.5R 3.2/11.2	1.0R 4.7/11.2							
Silica Gel TLC Plate (Optical)	8.0RP 5.7/8	7.0RP 7.4/5.6	33.91	25.59	25.27	49.79	43.67	48.20	20.40
Silica Gel TLC Plate (Analytical)	4.5R 3/11.2	1.25R 4.2/11.6							
Alizarin Crimson Tube Watercolor[d]									
Watercolor Paper	9.0RP 6.2/11.2	9.0RP 6.8/10.4	43.33	30.73	28.32	50.47	39.21	39.07	11.26
Cellulose TLC Plate (Optical)	9.0RP 5.5/10.4	8.0RP 6.5/9.2	34.92	23.89	21.82	45.21	34.27	34.27	12.31
Cellulose TLC Plate (Analytical)	10RP 5.4/9.6	8.5RP 6.2/8.8							
Silica Gel TLC Plate (Optical)	10RP 4.7/12.4	7.5RP 6.6/9.2	28.13	17.37	12.98	43.31	33.96	35.05	26.67
Silica Gel TLC Plate (Analytical)	2.5R 4/12.8	9.5RP 4.7/11.2							
Blanks									
Blank Watercolor Paper			85.13	87.16	97.47	86.62	88.65	100.69	1.15
Blank Cellulose TLC Plate			88.05	90.15	101.36	89.41	91.49	104.71	1.26
Blank Silica Gel TLC Plate			71.67	73.33	86.55	72.77	74.37	88.45	0.69

(a) Munsell matches are by a human observer using a Macbeth Spectra Light Booth under the daylight setting according to ASTM standards.

(b) Tristimulus Values (X,Y,Z) are reported for CIE Illuminant C.

(c) Color differences between the control and exposed samples are calculated using the CIE 1976 $L^*a^*b^*$ formula.

(d) Included for relevance to artists; no chemistry.

(e) For distinction between optical versus analytical samples, see text.

for the Alizarin Crimson pigment. The combination of reagent alizarin on silica gel is also much more ozone-fugitive than reagent alizarin on cellulose or on watercolor paper. In Figure 4.2c, it is seen that after ozone exposure the strong absorption of alizarin dye on cellulose between 380-500 nm has changed very little, suggesting that most of the colorant material remains on the plate. In the case of alizarin dye on silica gel shown in Figure 4.2f, the plate after ozone exposure has virtually the same optical characteristics as the unexposed TLC plate in Figure 4.2d, suggesting that virtually all of the alizarin dye placed on the silica gel TLC plate has reacted to form nearly colorless products.

Mass Spectra of Reactants

The EI and CI spectra of alizarin and anthraquinone were recorded and are discussed in detail elsewhere (8). Attempts to obtain EI and CI spectra of the Winsor and Newton's Alizarin Crimson sample were not successful. This was probably due to the ionic character of the compound and to its exceedingly low vapor pressure even at high probe temperature (350°C). Attempts to obtain a fast atom bombardment (FAB) spectrum of the Alizarin Crimson were also unsuccessful.

Substrate and Solvent Effects

Mass spectra of control samples were recorded for the three compounds studied. These control samples consisted of methanol and methylene chloride extracts of the silica gel and cellulose deposits not exposed to ozone. Unexposed Teflon filter deposits were also included. As noted before for the starting materials, no structural information could be recovered from the Alizarin Crimson control samples. Impurities identified by GC-EI analysis of methanol extracts of Alizarin Crimson deposited on cellulose and on silica gel included anthraquinone, 4-hydroxy xanthone:

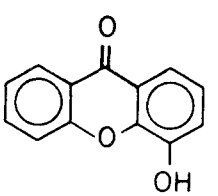

2-butoxyethanol, terephthalic acid (benzene 1,4-dicarboxylic acid), and several phthalates. These compounds were only identified as "best matches" with the computerized library of EI spectra. No attempt was made to confirm this information by recording the spectra of the corresponding pure compounds, except for anthraquinone. For all of the other samples, the control sample mass spectra were identical to those of the starting materials, thus indicating (a) reasonable recovery by solvent extraction and (b) no substrate-promoted or solvent-promoted change in chemical composition in the absence of ozone.

Product Identification: Definitions and Limitations

Reaction products that could go undetected in our conditions include (a) compounds of molecular weight higher than 517 (the upper limit of the spectrometer mass scan), e.g., polymeric reaction products; (b) compounds of very low vapor pressure, no detectable amounts of which could be introduced into the instrument source at the maximum probe temperature; (c) products formed in very low yields of $< 0.1\%$, since the spectrometer does not record mass fragments whose intensity is less than 0.1% of that of the base peak; and (d) volatile products that were no longer present on the substrate at the end of the exposure experiment.

Within these constraints, product identification was deemed (a) *positive* when the sample mass spectrum was identical to that of an authentic sample recorded under the same conditions *and* the sample was analyzed using at least two of the three sample introduction modes, i.e., probe-EI, probe-CI, and GC-EI; (b) *probable:* same as above but only one method used; (c) *possible:* same as above but the spectrum obtained by probe insertion contained information from several products with possible overlap; and (d) *tentative* when no authentic sample was available for comparison and the structure of the product was derived solely from interpretation of its CI and EI mass spectra.

Anthraquinone

Experimental findings are summarized in Table 4.3 for anthraquinone, alizarin, and Alizarin Crimson. There was no evidence for reaction of ozone with Teflon-deposited anthraquinone in the short-term exposure experiment. The sample and control spectra were identical to that of pure anthraquinone. As an impurity in Alizarin Crimson (see experimental section), anthraquinone was also exposed to ozone on silica gel, cellulose, and Teflon and was found again in the corresponding exposed samples.

Alizarin

Results obtained for alizarin were substantially different for different substrates. In the short-term exposure on Teflon and the long-term exposure on cellulose, there was no evidence for reaction between ozone and alizarin. In contrast, nearly all of the alizarin was consumed on silica gel. In this case, the exposed samples contained no detectable amounts of alizarin as measured by probe-EI and GC-EI, and an estimated 4% of the initial amount could be detected by probe-CI. The major reaction product was phthalic acid or phthalic anhydride. These two compounds cannot be distinguished by mass spectrometry due to rapid loss of water from phthalic acid in the instrument source, i.e., $C_6H_4(COOH)_2 \rightarrow H_2O$ + phthalic anhydride. Authentic samples of phthalic acid and phthalic anhydride gave identical mass spectra in both EI and CI modes (Table 4.4), in agreement with literature data (11).

Other products could not be identified. The probe-EI spectrum contained only one fragment at m/z = 163, which is typical of methyl phthalates (i.e., loss of OH from COOH - C_6H_4 – $\underset{\underset{O}{\|}}{C}OCH_3$, 180 - 17 = 163) and may indicate some reaction between the methanol solvent and phthalic acid during sample extraction. The chromatogram of the GC-EI sample contained, besides phthalic acid and/or phthalic anhydride, three peaks whose EI spectra suggest phthalate-type structures (first GC peak: m/z = 149 [11%], 105 [17%], 104 [81%], and 76 [base peak]; second GC peak: m/z = 178 [1%], 177 [16%], 149

Table 4.3. Alizarin and related compounds: Summary of experimental findings

Compound	Ozone Exposure Mode	Substrate	Extraction Solvent	Mass Spectrometry Analysis	Sample composition after ozone exposure	
					Reactant	Products and comments
Alizarin	short-term to high O_3 (SH), 80 hours	Teflon	none	CI	present	no evidence for reaction
	long-term to low O_3 (LL)	cellulose	CH_3OH	EI,CI	present	no evidence for reaction
	LL	silica gel	CH_3OH	EI,CI,GC-EI	~96% consumed	phthalic anhydride and/or acid (major); two unidentified phthalate-type compounds (GC-EI); several unidentified peaks (CI)
Anthraquinone	SH, 24 hours	Teflon	none	CI	present	no evidence for reaction
Alizarin Crimson	SH, 18 hours	Teflon	none	CI	--	phthalic anhydride and/or acid (major); benzoic acid (minor); several unidentified peaks
	LL	silica gel	CH_3OH	GC-EI	--	phthalate-type compounds, inconclusive
		cellulose	CH_3OH, CH_2Cl_2	CI	--	phthalic anhydride and/or acid (major); benzoic acid (minor); several unidentified fragments (see text for tentative structures)

Table 4.4. EI and CI spectra of phthalic acid [$C_6H_4(COOH)_2$, MW = 166] and phthalic anhydride [$C_6H_4(CO)_2O$, MW = 148]

Electron Impact				Chemical Ionization (Methane)			
m/z	abundance,%		fragment	m/z	abundance,%		fragment
	acid	anhydride			acid	anhydride	
149	0.2	0.2	—	177	~1	~1	M + 29
148	8	8	$M^{+\cdot}$	167	< 0.1	0	(a)
104	90	90	$M - CO_2$	163	5	5	M + 15
76	100	100	$C_6H_4^+$	150	8	8	—
74	24	24	$C_6H_2^+$	149	100	100	MH^+
50	75	75	$C_4H_2^+$				
				123	5	5	$MH - C_2H_2$?
				105	5	5	$MH - CO_2$
				104	15	14	$M - CO_2$,MH–COOH

(a) Would be MH^+ of acid, M_1 = 166.

[base peak], 105 [17%], 104 [21%], and 93 [15%]; third GC peak: m/z = 223 [1%], 205 [1%], 149 [base peak], 105 [4%], 104 [11%], and 76 [17%]). The computerized search of EI literature data yielded di-(butoxyethyl) phthalate as a reasonable match for the third GC peak and was inconclusive for the first two GC peaks. While computerized libraries of EI mass spectra contain literature data for thousands of compounds, they do not necessarily include those of interest for this work (e.g., alizarin is not listed in our EI library file). The probe-CI spectra contained unidentified peaks at m/z = 209 (~1%), 179 (1%), 133 (13%), 101 (12%), 99 (11%), 77 (10%), and 76 (10%), where the abundances given in parentheses are relative to that of m/z = 149, the base peak of phthalic anhydride. The fragments of m/z = 76 and 77 may originate from many organic compounds and have little diagnostic value. The small m/z = 209 peak may indicate source contamination by anthraquinone (MW = 208). The peak at m/z = 179 was also seen at m/z = 178 in the GC-EI analysis with a phthalate-like fragmentation pattern. The fragments m/z = 133, 101, and 99 may originate either from three unknown products of MW = 132, 100, and 98, respectively, or from a single product of MW = 132 with MH-32 and MH-34 fragments (e.g., MH-O_2, MH-2OH).

Alizarin Crimson

There was evidence for substantial reaction between ozone and Alizarin Crimson on all three substrates. All exposed samples contained phthalic anhydride (or phthalic acid) as the major product, along with smaller amounts of benzoic acid whose base peak (m/z = 123) was 8-11% of the base peak for phthalic anhydride (m/z = 149).

Other product fragments were also present, with abundances ranging from 2 to 17% of that of m/z = 149 and with substantial differences among substrates. Samples exposed on silica gel yielded no high mass fragments (with the exception of the anthraquinone impurity) and numerous low mass fragments (base peak m/z = 41) from which no useful information could be derived. CI spectra of samples exposed on cellulose contained peaks at m/z = 257, 239, 171, 139, 129, 125, 111, 109, and 97. Those

exposed on Teflon contained peaks at m/z = 229, 175, 155, 147, 133, 119, 113, 109, and 97. Of these, only two peaks are common to the Teflon and cellulose samples, m/z = 109 and 97. Two peaks present in the Teflon sample, m/z = 133 and 99, were also present in the spectrum of exposed alizarin. The high mass fragments, m/z = 257, 239 (cellulose), and 229 (Teflon) correspond to products of MW = 256, 238, and 228, respectively. The product of MW = 256 may be a trihydroxyanthraquinone (several possible isomers). Indeed, m/z = 257 was the base peak in the CI spectrum we recorded of an authentic sample of the 1,2,4 isomer, i.e., purpurin (8). The product of MW = 238 may be the 1,2-quinone:

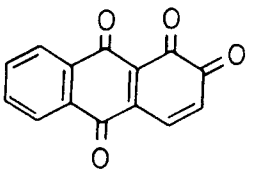

The product of MW = 228, tentatively dihydroxy xanthone, may result from oxidation of the 4-hydroxy xanthone present as impurity:

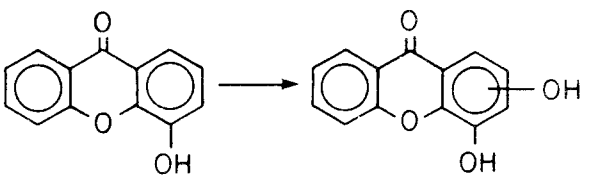

in a manner analogous to the oxidation of alizarin to purpurin reported in the synthetic dye literature (12,13).

Literature Review of Ozone-Quinone Reactions

The mechanism of the reaction of ozone with aromatic compounds is complex and as yet not fully understood even for simple molecules such as benzene and phenol (14). Much of the considerable amount of literature available consists of studies

carried out in the liquid phase, where solvent effects and oxidative workup for product analysis introduce additional difficulties in the interpretation of reaction mechanisms (14). However, the major features of the aromatic compound-ozone reaction are now reasonably well understood and are summarized below for the simplest aromatic hydrocarbon, benzene.

It is generally accepted that the initial step is analogous to that involved in ozone-olefin reactions, i.e., addition to form an 1,2,3 trioxolane followed by ring opening involving C-C bond scission in the corresponding Criegee biradical (14-17):

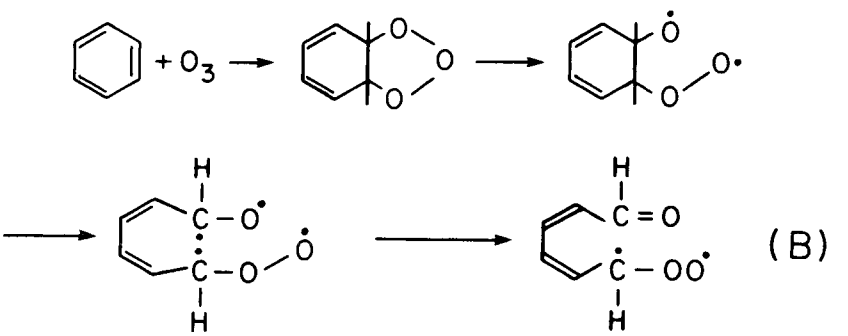

The energy-rich peroxy biradical (B) may undergo several reactions including decarboxylation (loss of CO_2) and rearrangement to form the corresponding acid, COOH-CH=CH-CH=CH-CHO. This unsaturated product reacts rapidly with ozone (much faster than benzene does) to yield dicarboxyl products, e.g., CHO-CHO, CHO-COOH, etc. There is still substantial debate concerning the mode of initial ozone attack, i.e., bond attack (shown above) versus atom attack:

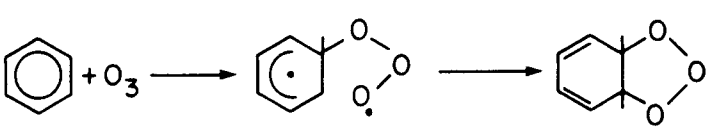

Atom attack, while leading to the same products in the case of benzene, will yield different products for substituted aromatics. Thus, for phenol:

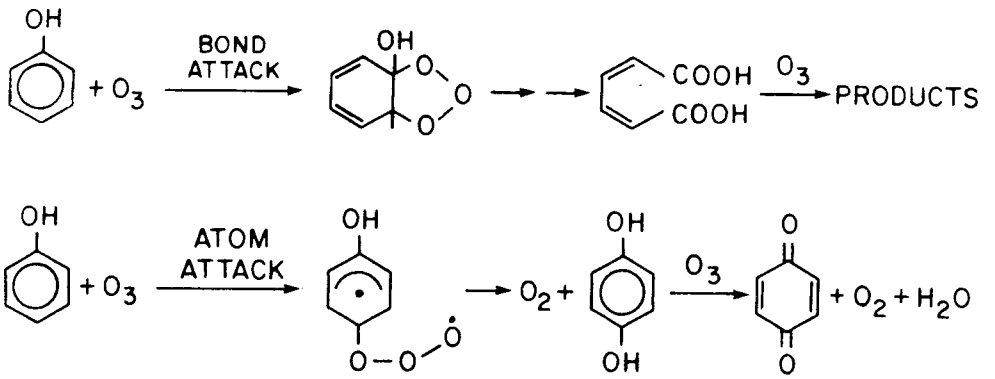

Fused-ring aromatics (polycyclic hydrocarbons) may react with ozone to yield both bond-attack products (ring opening) and atom-attack products (ring substitution, i.e., phenols and quinones). The relative importance of the two reaction modes has been extensively studied for most polycyclic hydrocarbons (14), but little information is available for quinones. A probable reaction sequence is as follows:

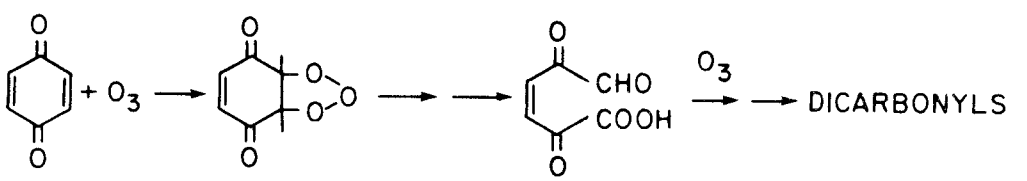

A comprehensive review of the literature concerning oxidation of polycyclic aromatic hydrocarbons (PAH) in the bulk liquid phase and in gas-solid (heterogeneous) systems, including the voluminous environmental sciences literature concerning reactions of ozone and other oxidants with substrate-deposited PAH (18-22), was undertaken and

yielded only limited information regarding the products and mechanisms of the ozone-quinone reaction. Moriconi et al. (23,24) reported on the reaction of ozone with benzo(a)pyrene and of 3-methylcholanthrene in CH_2Cl_2 and CH_2Cl_2-MeOH and on the reaction of the corresponding quinones with ozone to yield ring-opening products including phthalic acid (Figure 4.3). Kortum and Braun (25) studied the photooxidation of anthraquinone on silica gel and alumina and identified 1,4-dihydroxyanthraquinone as a major reaction product:

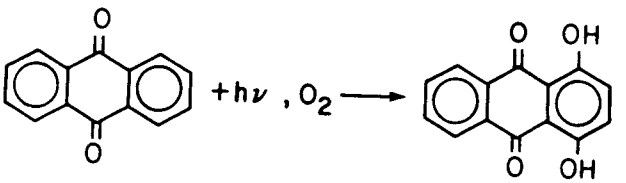

and Luebs (12) reports on the oxidation of alizarin to 1,2,4-trihydroxyanthraquinone (purpurin):

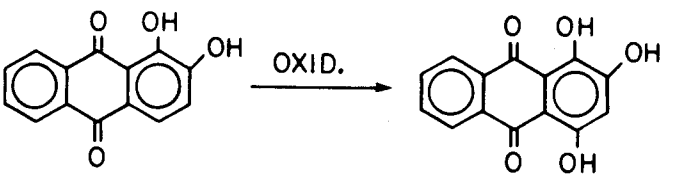

From the studies cited above, quinone oxidation may involve both ring opening (bond attack) and ring substitution products (atom attack).

Ozone-Quinone Reaction Mechanism Applied to Alizarin: Lack of Agreement with Experimental Data

A tentative scheme for the alizarin-ozone reaction is given in Figure 4.4. This scheme takes into account the polyfunctional character of alizarin and includes the corresponding features of ozone reaction with PAH (bond attack major, as in naphthalene but *not* anthracene), phenols (ortho-para orientation effect of the 2-

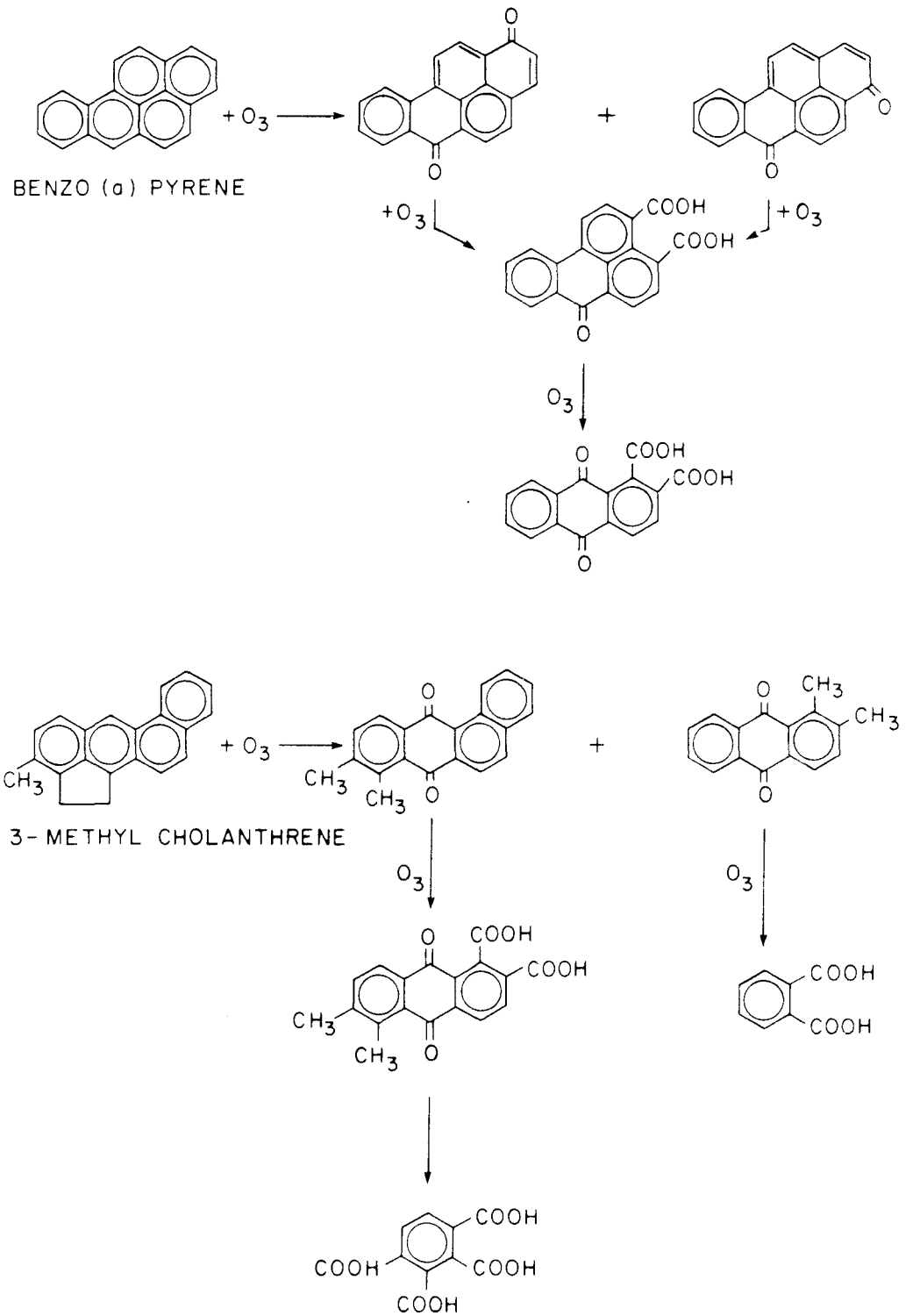

Figure 4.3 Ozone-quinone reaction products. Adapted from Moriconi et al. (23,24).

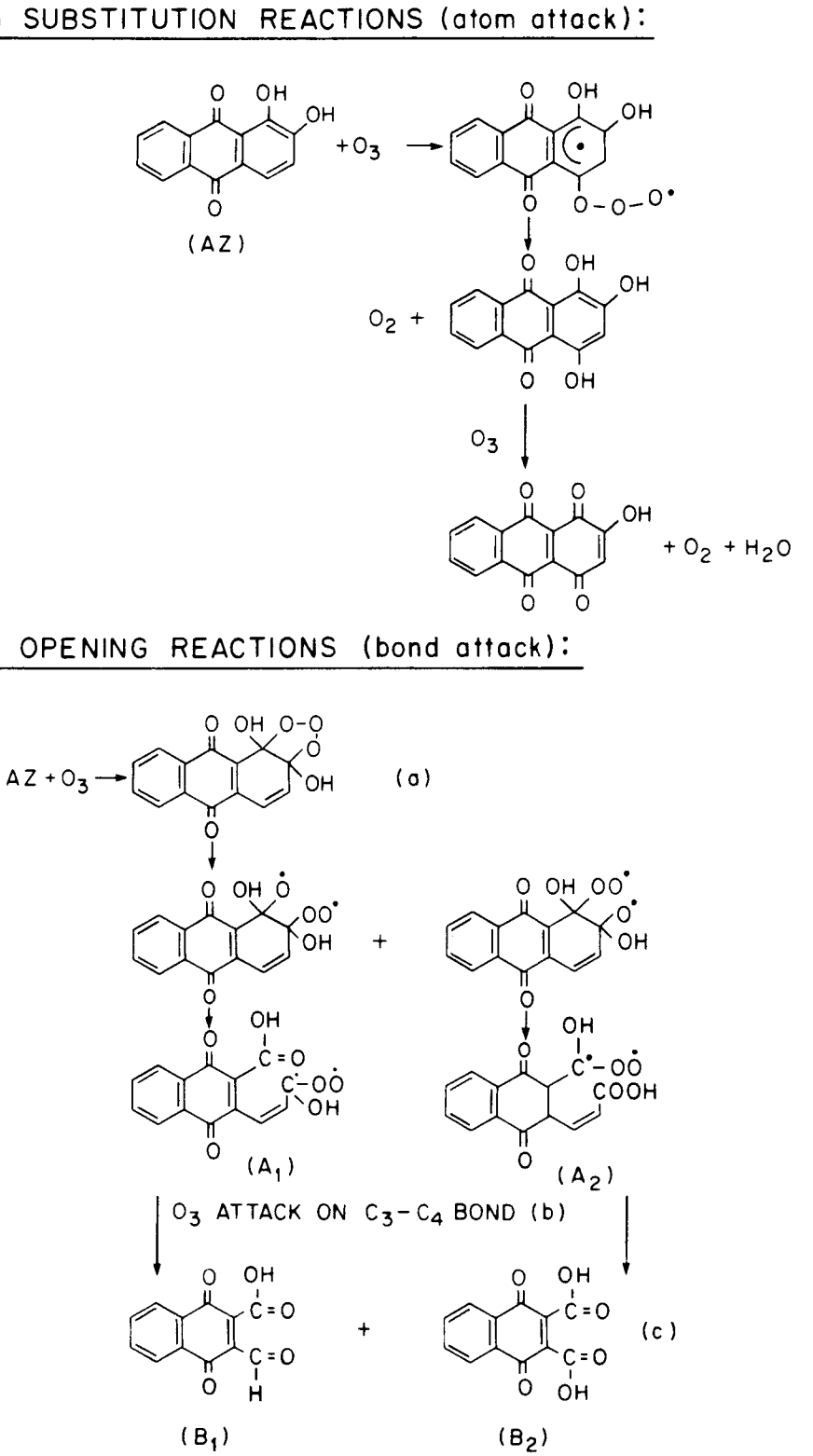

Figure 4.4 Alizarin-ozone reaction mechanism. Footnotes in pathway 2, ring opening reactions: (a) initial ozone attack is shown on C_1–C_2 bond. Ozone attack on C_3–C_4 bond, not shown for clarity, yields the same products; (b) initial ozone addition and reactions of the peroxy biradicals omitted for clarity, see text for details; (c) the peroxy biradicals A_1 and A_2 give the same two products B_1 and B_2.

3. REACTIONS OF B_1 and B_2 (shown for B_2)

3a. bond attack on quinone ring:

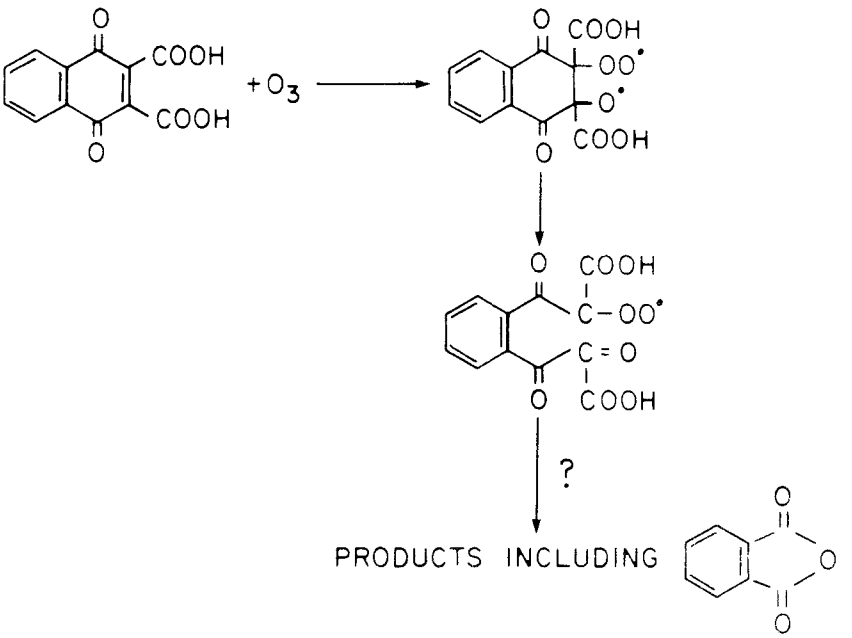

3b. attack on aromatic ring:

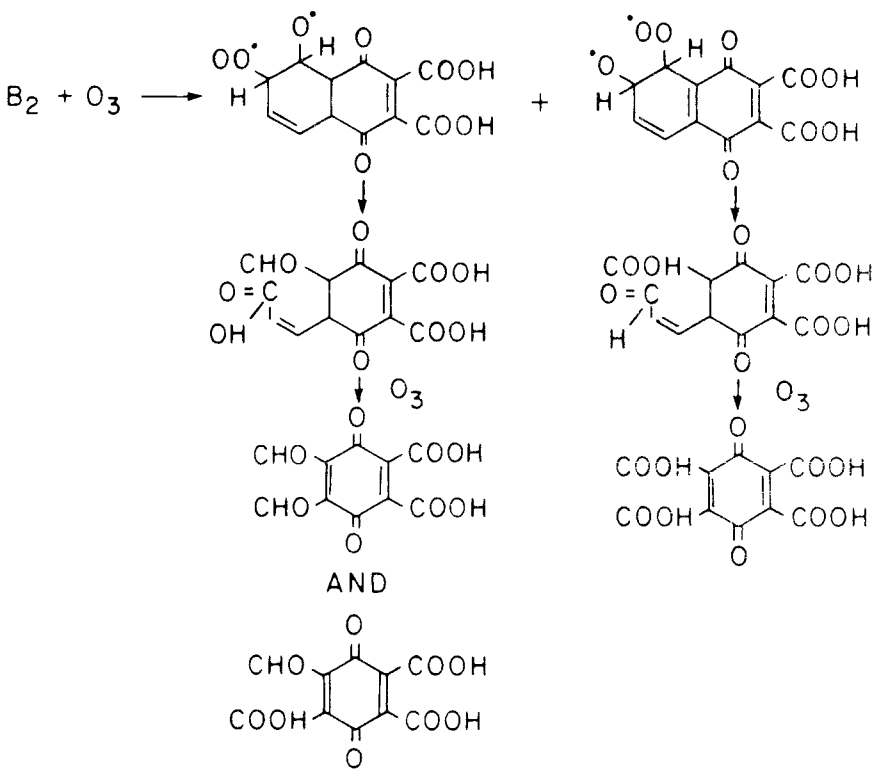

Figure 4.4 (continued)

hydroxyl groups), and quinones (the aromatic ring bearing the two OH groups is oxidized first). The proposed scheme, while making use of well-accepted oxidation steps, gives no satisfactory agreement with our experimental data: the "first generation" products (A and B in Figure 4.4) were not observed, and their further oxidation to phthalic anhydride (acid), the major product in our experiments, would require several untested (and perhaps unlikely) reaction steps. Furthermore, this scheme does not account for the observed substrate effects (no reaction on Teflon and cellulose versus nearly complete oxidation on silica gel) and offers no clue regarding the observed reactivity sequence, i.e., Alizarin Crimson > alizarin > anthraquinone. The alternate mechanism described below is more consistent with experimental observations.

An Alternate Mechanism for the Ozone-Alizarin Reaction

This mechanism is summarized in Figure 4.5 and involves the reaction of ozone with the 9,10-dihydroxy tautomeric form of alizarin:

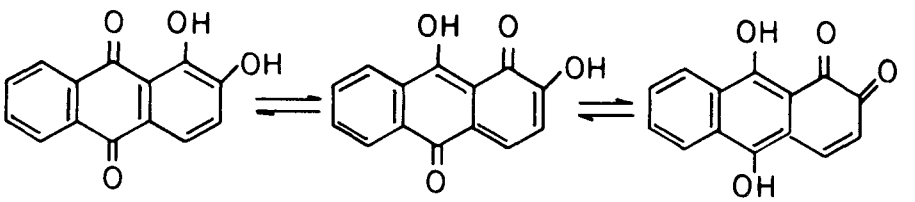

in which the carbon-carbon bonds including the 9-carbon and 10-carbon atoms, respectively, have a partially unsaturated character. Since ozone reacts with olefinic bonds much faster than with aromatic bonds, facile formation of phthalic acid, as is shown in Figure 4.5, is expected in this case.

Perkins (26) has described the 9-hydroxy tautomeric form of alizarin, which is consistent with strong hydrogen bonding between the 1-hydroxyl and 9-carboxyl groups:

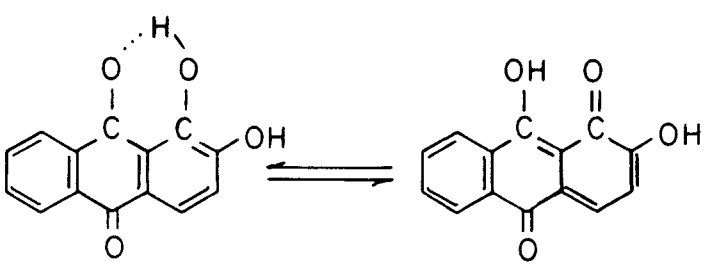

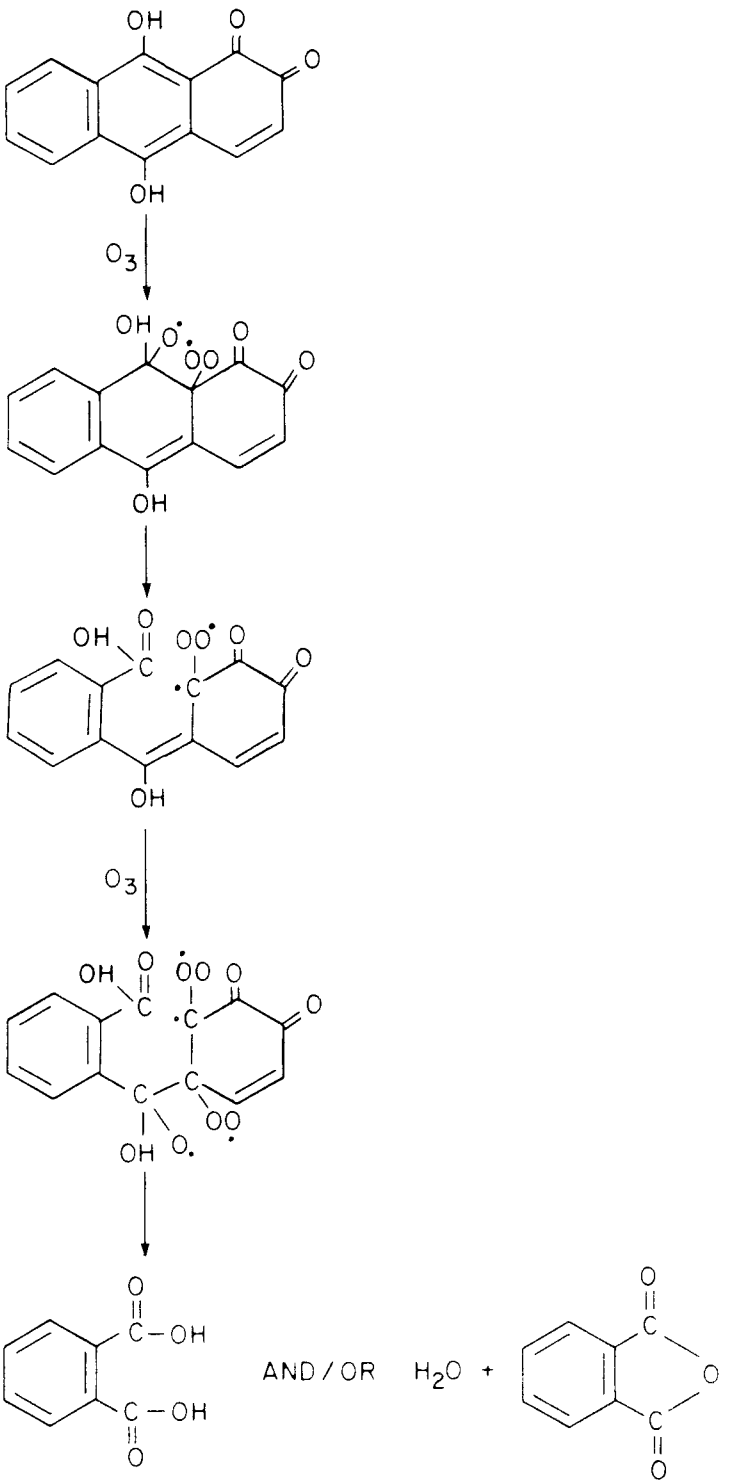

Figure 4.5 Reaction of ozone with the 9,10-dihydroxy tautomeric form of alizarin.

Evidence for hydrogen bonding can be found in infrared data, as well as in OH dissociation constants data (27). In addition, the 2-hydroxyl and 10-carboxyl groups are conjugated, and the 9,10 dihydroxy tautomeric form is expected to be stabilized by resonance of the ionic form, e.g.:

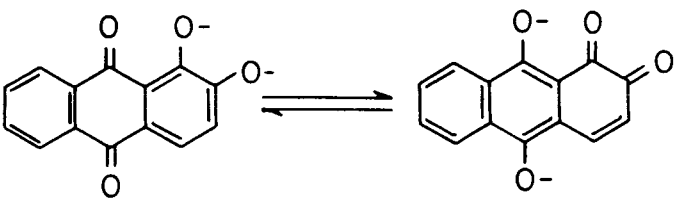

In Alizarin Crimson, the carbon bonds have indeed a pronounced unsaturated character (see Figure 4.1), in agreement with the observed facile ozonation irrespective of the substrate. In alizarin, a shift towards the ozone-reactive tautomeric structure would result from bonding to the silica gel silanol and siloxane groups. This type of bonding has been well documented for a number of polycyclic aromatic compounds (28-30) and would provide a rationale for our observations of substantial reaction with ozone on silica gel but not on Teflon. In the same way, no reactive tautomeric form can exist for anthraquinone, and no reaction was observed irrespective of substrate.

Finally, the proposed mechanism not only provides a rationale for our observations, but may also give clues to the reactivity of other alizarin derivatives towards ozone. For example, the dialkylamino anthraquinones are expected to react readily with ozone and to yield phthalic acid because of the following resonance structure:

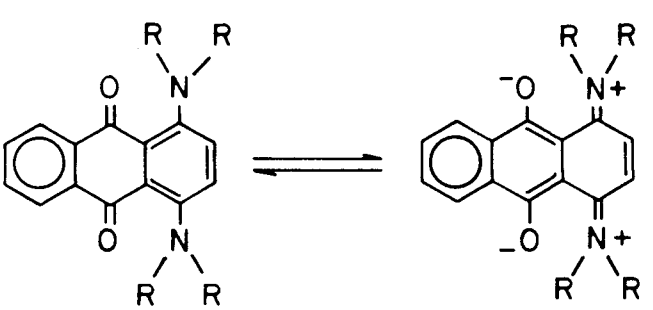

Indeed, many dyes of this type are ozone-fugitive (31-33). Like alizarin, many of the 1,4- and 1,5-dihydroxy, dialkylamino, or hydroxyalkylamino substituted anthraquinones are expected to be ozone-fugitive on substrates such as silica gel that promote or facilitate hydrogen bonding. Most alizarin lakes, as well as lakes of other disubstituted anthraquinones, are expected to be ozone-fugitive irrespective of the substrate. In fact, a number of red alizarin lake pigments are ozone-fugitive when tested on watercolor paper (1,2), as are modern "indigo" pigments that are formulated from blends that contain an alizarin lake (2). These considerations could be taken into account in the formulation of substitute pigments and dyes less susceptible to fading by atmospheric ozone.

REFERENCES FOR CHAPTER 4

1. Shaver, C.L.; Cass, G.R.; Druzik, J.R. *Environ. Sci. Technol. 1983, 17,* 748-52.

2. Drisko, K.; Cass, G.R.; Whitmore, P.M.; Druzik, J.R. "Fading of Artists' Pigments due to Atmospheric Ozone" in *Wiener Berichte über Naturwissenschaft in der Kunst, Doppelband 2/3;* Vendl, A.; Pichler, B.; Weber, J. Eds; Verlag ORAC: Vienna, 1985/86.

3. Whitmore, P.M.; Cass, G.R.; Druzik, J.R. *J. American Institute for Conservation 1987, 26,* 45-58.

4. Salvin, V.S.; Walker, R.A. *Text. Res. J. 1955, 25,* 571-85.

5. Salvin, V.S. *Text. Chem. Color 1969, 1,* 245-51.

6. Grosjean, D.; Whitmore, P.M.; De Moor, C.P.; Cass, G.R.; Druzik, J.R. Reaction of curcumin, indigo, triphenylmethane and related artists' pigments with ozone. Manuscripts in preparation, California Institute of Technology, 1986.

7. Whitmore, P.M.; Cass, G.R. Reaction of artists' pigments with oxides of nitrogen. Manuscript in preparation, California Institute of Technology, 1986.

8. Grosjean, D.; Sensharma, D.K.; Cass, G.R. Mass spectra of selected artists' organic colorants. Manuscript in preparation, California Institute of Technology, 1986,.

9. "Munsell Book of Color"; Macbeth Division of Kollmorgen Corp.: Baltimore, MD, 1976.

10. "Standard Method of Specifying Color by the Munsell System"; American Society for Testing and Materials: Philadelphia, PA, 1980; ed. D 1535-80.

11. Fales, H.M.; Milne, G.W.A.; Nicholson, R.S. *Anal. Chem. 1971, 43,* 1785- 1785-89.

12. Luebs, H., Ed. "The Chemistry of Synthetic Dyes and Pigments"; Reinhold Pub. Corp.: New York, NY, 1955.

13. Venkatamaran, K., Ed. "The Chemistry of Synthetic Dyes"; Academic Press: New York, 1952; Vol. 2, pp. 818-33.

14. Bailey, P.S. "Ozonation in Organic Chemistry"; Academic Press: New York, 1982; Vol. 2.

15. Toby, S.; Van de Burgt, L.J.; Toby, F.S. *J. Phys. Chem. 1985, 89,* 1982-86.

16. Pryor, W.A.; Gleicher, G.J.; Church, D.F. *J. Org. Chem. 1983, 48,* 4198-4202.

17. Van Vaeck, L.; Van Cauwenburghe, K. *Atmos. Environ. 1984, 18,* 323-28.

18. "Particulate Polycyclic Organic Matter"; National Academy of Sciences, National Academy Press: Washington, D.C., 1972.

19. "Polycyclic Aromatic Hydrocarbons: Evaluation of Sources and Effects"; National Academy of Sciences, National Academy Press: Washington, D.C., 1983.

20. Wu, C.H.; Salmeen, I.; Niki, H. *Environ. Sci. Technol. 1984, 18,* 603-607.

21. Butkovic V. et al. *Environ. Sci. Technol. 1983, 17,* 546-48.

22. Grosjean, D.; Fung, K.; Harrison, J. *Environ. Sci. Technol. 1983, 17,* 673-79.

22. Moriconi, E.J.; Taranko, L.B. *J. Org. Chem. 1963, 28,* 2526-29.

24. Moriconi, E.J.; Rakoczy, B.; O'Connor, W.F. *J. Amer. Chem. Soc. 1961, 83,* 4618-23.

25. von Kortüm, G.; Braun, W. *Justus Liebig Ann. Chem., 632,* 104-115.

26. Perkins, M.A. In "The Chemistry of Synthetic Dyes and Pigments"; Luebs, H.A., Ed.; Reinhold Pub. Corp.: New York, 1955; pp. 335-69.

27. Kiel, E.G.; Heertjes, P.M. *J. Soc. Dyers Colour 1963, (79)*(1), 21-27.

28. Bauer, R.K. et al. *J. Phys. Chem. 1982, 86,* 3781-89.

29. Jäger, T.; Hanus, V. *J. Hyg. Epidemiol. Microbiol. Immunol. 1980, 24,* 1-15.

30. Saucy, D.A.; Cabaniss, G.E.; Linton, R.W. *Anal. Chem. 1985, 57,* 876-79.

31. Saunders, F.M.; Gould, J.P.; Southerland, C.R. *Water Res. 1983, 17,* 1407-19.

32. Couper, M. *Textile. Res. J. 1951, 21,* 720-25.

33. Lebensaft, W.W.; Salvin, V.S. *Text. Chem. Color 1972, 4,* 182-86.

CHAPTER 5

OZONE FADING OF NATURAL ORGANIC COLORANTS: MECHANISMS AND PRODUCTS OF THE REACTION OF OZONE WITH INDIGOS

INTRODUCTION

The results reported in Chapters 2 and 3, as well as previous studies, have shown that many artists' organic colorants fade substantially when exposed to ozone in the dark (1-3). These experiments involved 12-week exposures to air containing 0.3-0.4 parts per million (ppm) of ozone at ambient temperature (21–25°C) and humidity (RH = 46–50%). Examination of data for ambient levels of ozone in urban air, together with investigations of ozone levels inside museums (2,4) and of the corresponding indoor-outdoor relationships (2,5), indicate that the total ozone dose (concentration × duration of exposure) to which the colorants were subjected in those laboratory studies is equivalent to about six years to eight years inside a typical air-conditioned building in Los Angeles.

Organic compounds that were identified as ozone-fugitive in these experiments included modern (synthetic) as well as natural colorants. Many alizarin lakes and madder lakes faded noticeably upon exposure to ozone (2), and in Chapter 4 it was shown that the products of this chemical reaction are consistent with ozone attack on those anthraquinone derivatives that have a pronounced unsaturated character (6). In Chapters 2 and 3, natural indigo was found to be very ozone-fugitive. Although ancient works of art created using natural colorants such as indigo may have "survived" well before the recent introduction of ozone and other anthropogenic pollutants into urban air, the demonstrated ozone fading of these natural colorants has direct implications for current practices in the conservation of museum collections.

This chapter describes the methods and results of a study focusing on the confirmation that ozone is indeed responsible for the fading of indigo that was observed in the above studies, on the identification of the products of the ozone-indigo reaction, and on the discussion of the corresponding reaction mechanisms that account for the loss of the chromophore, i.e., ozone fading. To test the general applicability of these findings, several indigo derivatives have been investigated as well. These include thioindigo, 6,6'-dibromoindigo, and several colorants containing chlorinated thioindigo. The chemical structures of these colorants are given in Figure 5.1. Thioindigo was included as a simple structural homologue of indigo. Dibromoindigo, the Royal Purple dye of fabrics widely traded by the Phoenicians in the first millenium B.C., has been used as a natural colorant since at least the 13th century B.C. (7,8). The chlorinated thioindigos have found applications as artists' pigments and in the printing ink and paper industries (9). Also included in this study are the results of experiments involving the reaction of ozone with the major products of the ozone-indigo reaction.

EXPERIMENTAL SECTION

Colorants Studied

Indigo (MW = 262, CAS number 482-89-3, CI number 73000) was obtained from Aldrich Chemical Company, Milwaukee, WI, and was used without further purification following verification of its structure by mass spectrometry. A second indigo sample was obtained from Fezandie and Sperrle (F&S). Dibromoindigo (MW = 420, CI number 75800) was obtained from Dr. F. D. Preusser of the Getty Conservation Institute, Marina del Rey, CA, and from the Forbes collection (sample 7.01.8, Tyrian purple, murex) maintained at the Fogg Museum, Harvard University, Cambridge, MA. Thioindigo (MW = 296), Vat Red 41, was obtained as a liquid emulsion and as a "press cake" from Hoechst. Thioindigoid Violet (Binney and Smith

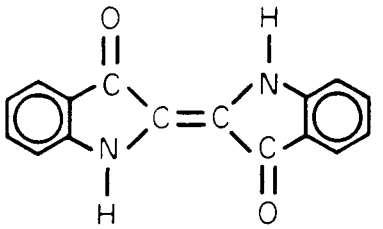

INDIGO

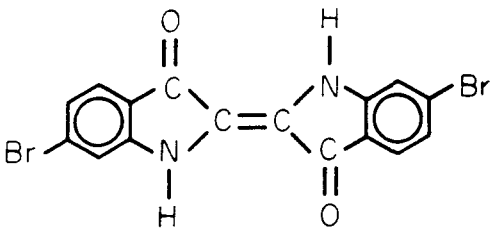

6, 6′ – DIBROMOINDIGO

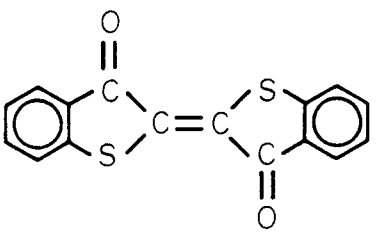

THIOINDIGO

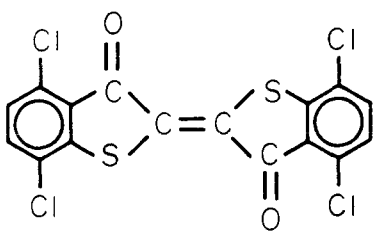

4, 4′, 7, 7′ – TETRACHLOROTHIOINDIGO

Figure 5.1. Structure of indigo and related compounds.

PR 88 MRS, CI 73312) and Thioindigo Red (BASF PR 88, CI 73312) were shown by mass spectrometry to be mixtures containing tetrachlorothioindigo (as expected) along with alkyl-substituted and chlorinated thioindigo(s), (e.g., tentatively dichlorothioindigo and dimethyl dichlorothioindigo).

Ozone Exposure Protocol

Approximately 10 mg of each colorant were deposited on a 47 mm diameter, 0.5 micron pore size, Teflon membrane filter (Ghia-Membrana Corp., CA) of the type employed for sampling of airborne pollutants by filtration. Teflon is a chemically resistant substrate, does not react with ozone under the conditions of our study, and has negligible absorption characteristics. Teflon filters were thus selected so as to minimize any spurious substrate-mediated (artifact) reactions between ozone and the colorants of interest. Filters with deposited colorants were mounted in an in-line, all-Teflon holder and exposed to purified air containing ~10 ppm of ozone as measured, following dynamic dilution, by ultraviolet photometry using a Dasibi Corp. (Glendale, CA) model 1003-AH ozone analyzer. The matrix air was purified by passing through Purafil and activated carbon beds which remove air contaminants including ozone, hydrocarbons, oxides of nitrogen and sulfur dioxide, followed by an in-line particle filter. Ozone was produced downstream of the beds using a Pen-ray ultraviolet lamp. Each colorant was exposed for 4 days (96 hours) to air containing ~10 ppm ozone at a flow rate of 1 liter per minute. All exposures were carried out in the dark at room temperature (T = 24°C) and low relative humidity (RH $\leq$ 5%). Control samples consisting of colorants deposited on Teflon filters but not exposed to ozone were included for each colorant studied.

Mass Spectrometry Analysis

Control and ozone-exposed samples were obtained simply by scraping the deposits off the Teflon filters. All samples were stored in the dark in glass vials

with Teflon-lined caps prior to analysis.

Mass spectrometry analyses were carried out by direct insertion probe with electron impact (probe-EI) and chemical ionization (probe-CI), the latter using methane as reagent gas. Experimental conditions were as follows:

(a) probe-EI: Kratos Scientific Instruments Model MS-25 hexapole, double focusing magnetic sector mass spectrometer, electron energy 70 eV, probe temperature 250°C, source temperature 200°C, and acceleration potential 2 kV.

(b) probe-CI: MS-25 mass spectrometer, reagent gas (methane) pressure ~0.1 torr, reagent gas flow rate 30 mL min^{-1}, electron energy 100 eV, probe temperature 200-300°C, source temperature 320°C, and acceleration potential 2 kV.

RESULTS AND DISCUSSION

Mass Spectra of Reactants

The EI and CI spectra of indigo, dibromoindigo, thioindigo, and the thioindigoid samples (in fact containing chlorinated indigo compounds) were recorded, and their fragmentation patterns are discussed in detail elsewhere (10). Of the two indigo samples, the Aldrich sample contained no detectable impurity, while the F&S sample contained minor amounts of aniline and of a compound containing the indoxyl group (Figure 5.2). The higher-purity Aldrich sample was thus selected for exposure to ozone. Structure confirmation was obtained by mass spectrometry for the two dibromoindigo and the two thioindigo samples, for which no literature data are available. All high mass fragments in the spectrum of the dibromoindigo sample obtained from the Getty Conservation Institute could be accounted for on the basis of the structure given in Figure 5.1, with the exception of a triplet (isotopic distribution of ^{79}Br and ^{81}Br, 2 bromine atoms per molecule) at m/z = 420, 422, and

INDIGO:

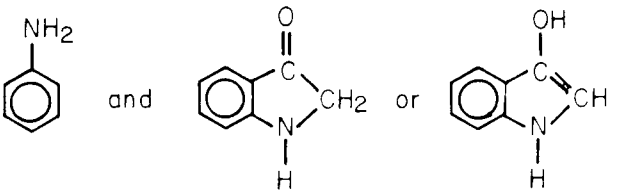

DIBROMOINDIGO:

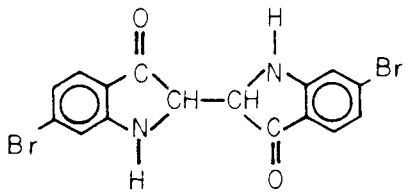

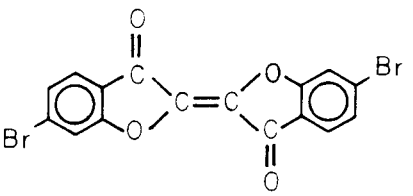

THIOINDIGO:

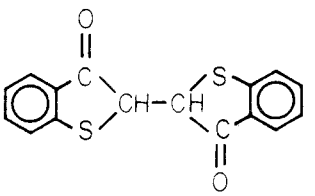

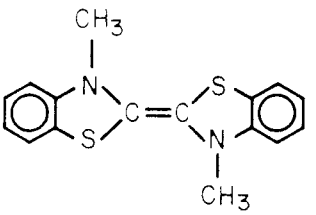

TETRACHLOROTHIOINDIGO:

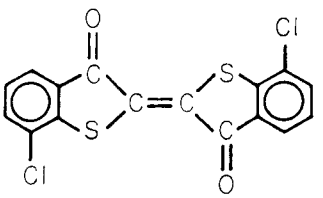

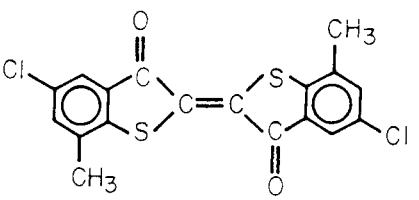

Figure 5.2. Probable impurities in samples of indigo and derivatives.

424 atomic mass units (amu). This triplet was first attributed to the saturated homologue of 6,6'-dibromoindigo, as is shown in Figure 5.2, but may originate from an isobaric unsaturated compound, an example of which is also shown in Figure 5.2. The latter appears more likely since the m/z = 420-422-424 amu triplet was absent from the spectrum after exposure to ozone, as would be expected for an unsaturated compound. The Forbes collection dibromoindigo sample contained larger amounts of the same impurity. The thioindigo samples contained substantial amounts of an impurity at m/z = MW + 2, where MW is the molecular weight of thioindigo. By analogy with dibromoindigo as discussed above, we suggest saturated and isobaric unsaturated compounds as possible impurities (see Figure 5.2). Upon exposure to ozone, little, if any, of this impurity was consumed, thus suggesting that the impurity may be the saturated compound shown in Figure 5.2 (unsaturated compounds such as the benzothiazole shown in Figure 5.2 are expected to be ozone-fugitive). Finally, the spectra of the two thioindigoid samples were complex and indicated (a) the presence of tetrachlorothioindigo, (b) the absence of thioindigo, (c) the presence of other chlorinated thioindigos (e.g., dichloro and dimethyl-dichloro, see Figure 5.2), (d) extensive thermal decomposition in the mass spectrometer source even at lower probe temperature, and (e) substantial amounts of unknown impurities. To our knowledge, 4,4',7,7'-tetrachloroindigo is not commercially available in pure form, and its synthesis was beyond the scope of this project.

Products Identification: Definitions and Limitations

Reaction products that could go undetected in our conditions include:

- compounds of molecular weight higher than 517, the upper limit of our spectrometer mass scan (e.g., polymeric reaction products),

- compounds of very low vapor pressure, no detectable amount of which could be introduced into the spectrometer source at the maximum probe temperature,
- volatile products that were no longer present on the Teflon filters at the completion of the 4-day ozone exposure experiment,
- products formed in very low yields of $\leq 0.1\%$, since the mass spectrometer does not record mass fragments whose intensity is less than 0.1% of that of the most abundant ion (base peak).

Within these constraints, product identification was deemed *positive* when the sample mass spectrum was identical to that of an authentic sample recorded under the same conditions (e.g., isatin), *probable* when no authentic sample was available but mass spectral data were available for structural homologues, and *possible* when no authentic sample was available and the structure of the product was derived solely from interpretation of its CI and EI mass spectra.

Indigo

Comparison of the spectra of the control and ozone-exposed samples indicated that all of the indigo had been consumed at the end of the 4-day exposure. The CI spectrum of indigo (10) includes the high mass fragments at m/z = 291,277 (indigo-reagent gas adducts), 264 (contribution of ^{13}C to MH ion), 263 (MH ion, base peak) 262 (M), 247-249 (loss of N and NH), and 234-236 (loss of CO). All these fragments are absent in the spectrum of the ozone-exposed sample. The initial amount of indigo was ~10 mg; the amount of ozone flowing through the Teflon filter was ~108 mg, i.e., ~50 times more than needed to consume indigo in a bimolecular reaction. These results are consistent with those obtained in Chapters 2 and 3 with lower ozone levels (~0.4 ppm vs 10 ppm), longer exposure times (12 weeks vs 4 days), a different substrate (watercolor paper and silk cloth vs Teflon membrane),

and higher relative humidity (~50% vs $\leq$ 5%). These results are also consistent with those obtained in the liquid phase, where indigo has been shown to react readily with ozone in water (11); in fact, the reaction of indigo (as soluble sulfonate salts) with ozone in water serves as the basis for a spectrochemical method for the determination of ozone in aqueous environmental samples (11).

Major mass fragments in the CI spectrum of the ozone-exposed indigo sample included m/z = 148 and m/z = 164, which correspond to compounds of molecular weight 147 and 163, respectively. Interpretation of the sample spectrum suggested isatin and isatoic anhydride as possible products (see structures in Figure 5.3). Authentic samples of isatin (Aldrich, MW = 147, purity = 98%) and of isatoic anhydride (Aldrich, MW = 163, purity = 96%) were obtained, and their spectra were recorded (Table 5.1). These spectra gave an excellent match with that of the ozone-exposed sample, thus allowing positive identification of isatin and isatoic anhydride as the only detectable products of the indigo-ozone reaction under our conditions.

A tentative mechanism consistent with the experimental findings is given in Figure 5.3. This mechanism involves electrophilic addition of ozone onto the unsaturated carbon-carbon bond, which is far more reactive toward ozone than any other reaction center within the indigo molecule. The addition step is assumed to be identical to the well-documented addition of ozone onto the C=C bond of simple olefins (12). The initial addition step thus involves the formation of an ozone adduct (1,2,3-trioxolane) followed by scission of the carbon-carbon bond and rearrangement of the two resulting Criegee biradicals into isatin and isatoic anhydride, respectively.

The fate of the two products of the indigo-ozone reaction was investigated in experiments involving direct exposure of authentic samples of isatin and isatoic anhydride, respectively, to ozone under conditions identical to those employed for

Table 5.1. Chemical ionization mass spectra of indigo-ozone reaction products

Isatin[a], MW = 147			Isatoic anhydride[a], MW = 163		
m/z	Abundance % of base peak	Fragment structure	m/z	Abundance % of base peak	Fragment structure
176	0.3	M + 29[b]	178	1	M + 15[b]
162	1.8	M + 15[b]	165	3	(c)
149	9.7	(c)	164	34	MH
148	100 (BP)	MH	163	3	M
147	6.4	M	149	5	MH - NH
134	3.0	MH - N	148	18	M - NH, MH - O
133	1.0	MH - NH			
132	2.6	M - NH	147	10	(c)
120	3.6	MH - CO	146	100 (BP)	MH - H_2O, MH - OH
119	11.9	MH - HCO, M - CO	120	6	MH - CO_2
92	2.6	MH - 2CO	119	15	M - CO_2, MH - CO_2H
91	1.2	MH - (HCO + CO), M - 2CO	104	2	C_6H_4CO
63	1.6	$C_5H_3^+$ [d]			

(a) See structures in Figure 5.3.

(b) Reagent gas adducts, these minor fragments have diagnostic value.

(c) ^{13}C isotope contribution to MH ion. This fragment has diagnostic value.

(d) Characteristic of aromatic ring scission.

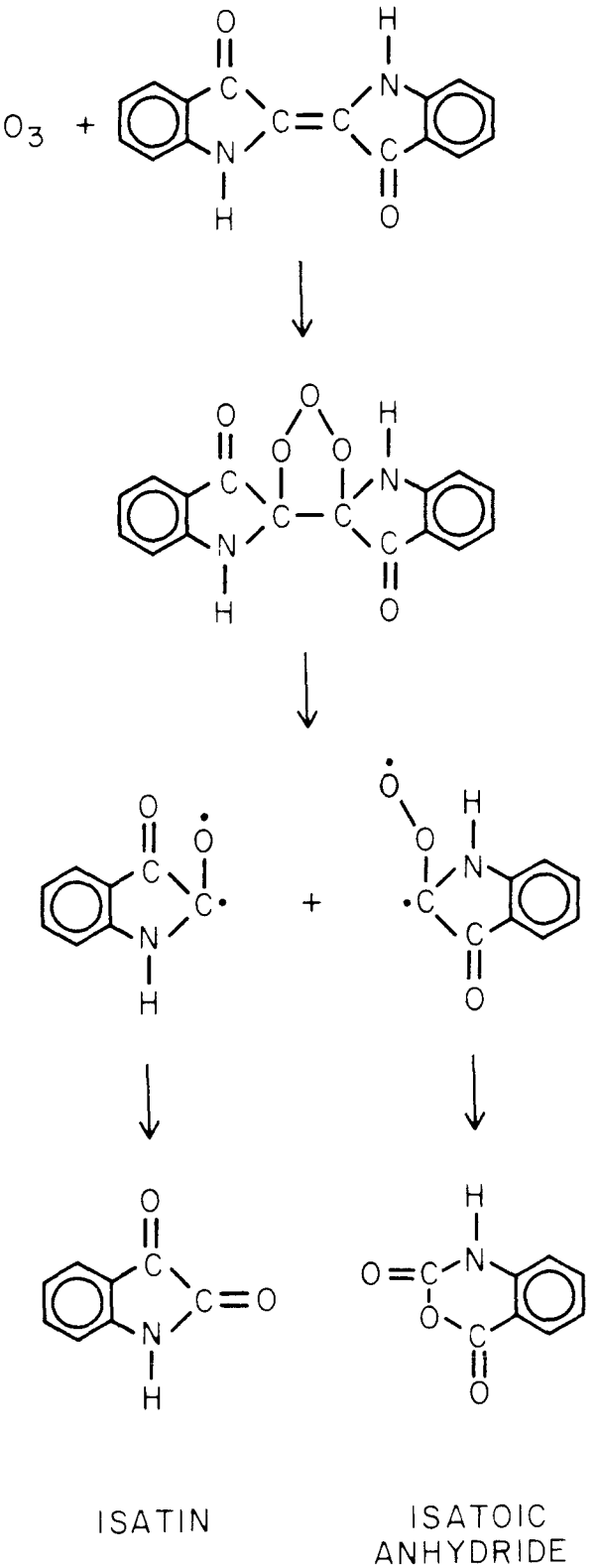

Figure 5.3. Mechanism of the ozone-indigo reaction.

the indigo-ozone reaction. Mass spectra of samples before and after exposure to ozone were identical, i.e., isatin and isatoic anhydride were not ozone-fugitive under our conditions.

Dibromoindigo

As for indigo, dibromoindigo was entirely consumed by ozone under the conditions of our study. The CI spectrum of dibromoindigo, discussed in detail elsewhere (10), contained major high mass fragments at m/z = 419, 421, 423 (MH ions, triplet due to ^{79}Br and ^{81}Br, 2 bromine atoms per molecule), 405 (loss of NH), 340 and 342 (loss of Br), 325-329 (loss of NH and Br), 261-264 (loss of 2 Br), and so on. All these fragments are absent from the spectrum of the ozone-exposed sample, whose prominent ion fragments include m/z = 244 (11% of base peak), 242 (13% of base peak), 228 (84.6%), 226 (base peak, 100%), 224 (26%), and so on. Thus, the spectrum of the ozone-exposed sample can be accounted for (in terms of both fragment m/z values *and* their relative abundance including ^{79}Br, ^{81}Br, and ^{13}C isotopes) by two reaction products, namely bromoisatin and bromoisatoic anhydride (Table 5.2, see structures in Figure 5.4). While no authentic samples were available for comparison, the identification of these two products is deemed probable in view of the close similarity of the recorded spectra to those of the indigo-ozone system, for which positive identification could be made using authentic samples of isatin and isatoic anhydride.

A mechanism consistent with experimental findings is given in Figure 5.4. As for indigo, this mechanism involves ozone addition onto the unsaturated carbon-carbon bond, followed by unimolecular decomposition of the trioxolane adduct to form two Criegee biradicals, whose rearrangement yields bromoisatin and bromoisatoic anhydride, respectively. It should be noted here that the mechanism of the dark reaction between ozone and dibromoindigo is substantially different from that involving its photooxidation, i.e., exposure to sunlight in air: photooxidation

Table 5.2. Contribution of bromoisatin and bromoisatoic anhydride to the CI spectrum of the ozone-exposed dibromoindigo sample

	Bromoisatoic Anhydride[a]		Bromoisatin[a]		Ozone-Exposed Dibromoindigo
	^{79}Br	^{81}Br	^{79}Br	^{81}Br	Sample
m/z	(MW = 241)	(MW = 243)	(MW = 225)	(MW = 227)	(% of Base Peak)
245	—	MH (^{13}C)	—	—	1.5
244	—	**MH**	—	—	**10.6**
243	MH(^{13}C)	M	—	—	2.7
242	**MH**	—	—	—	**12.8**
241	M	—	—	—	1.0
230	—	MH - N	—	—	10.0
229	—	MH - NH	—	MH (^{13}C)	15.0
228	MH - N	M - NH, MH - O	—	**MH** [b]	**84.6**
227	MH - NH	—	MH (^{13}C)	M	22.4
226	M - NH, MH - O	MH - H_2O [c]	**MH** [b]	—	**100** (BP)
225	—		M	—	8.8
224	MH - H_2O [c]				25.9
214	—	—	—	MH - N	10.1
213	—	—	—	MH - NH	10.0
212	—	—	MH - N	M - NH	46.5
211	—	—	MH - NH	—	11.0
210	—	—	M - NH	—	43.7

(a) See structures in Figure 5.4. The relative abundance of ^{79}Br and ^{81}Br is 50.54/49.46, i.e., $\simeq$ 1:1.

(b) MH is base peak in isatin; see Table 5.1.

(c) MH - H_2O is base peak in isatoic anhydride; see Table 5.1.

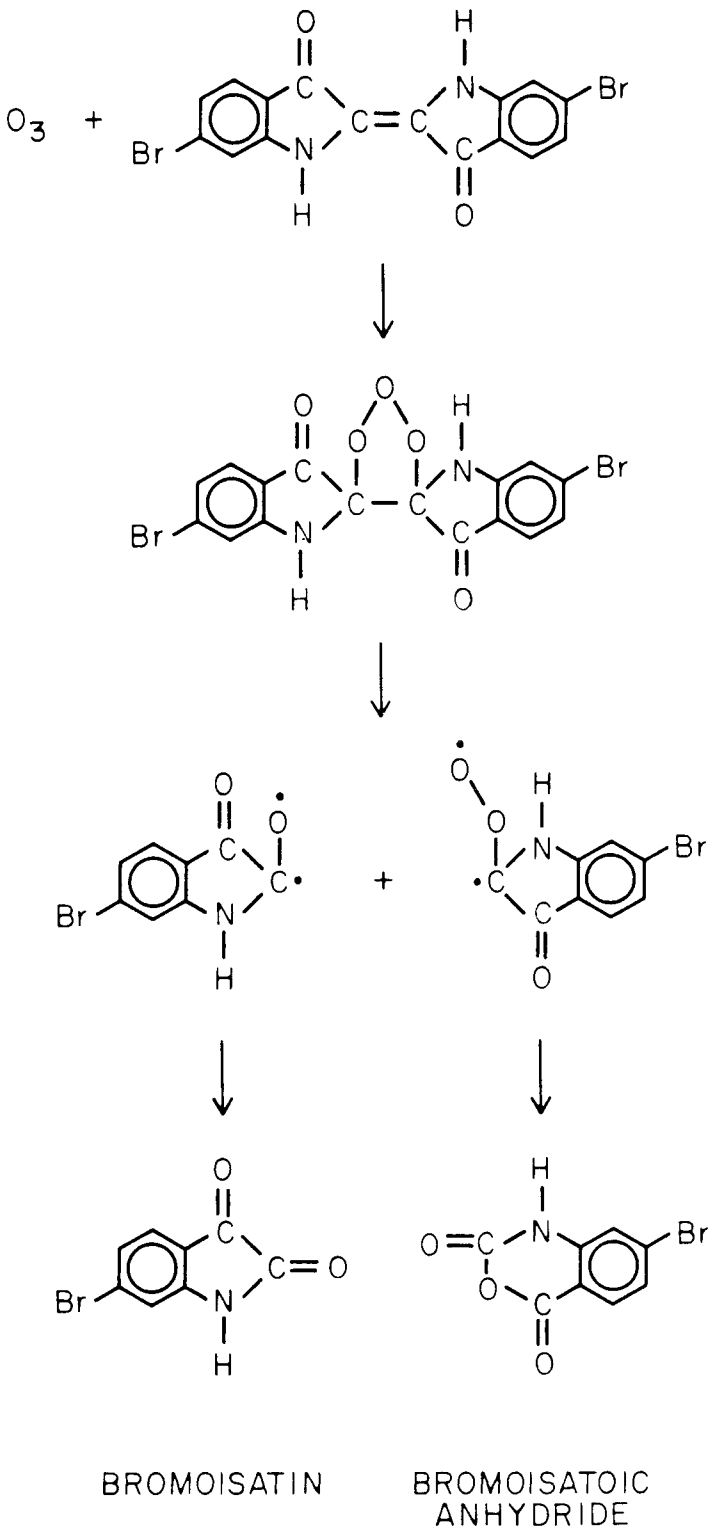

Figure 5.4. Tentative mechanism for the ozone-dibromoindigo reaction.

involves loss of bromine atoms and the formation of indigo as a reaction product (7); the opposite is true of the ozone reaction, which involves the breaking of the indigo carbon skeleton and the retention of bromine atoms in the major products.

No attempts were made to isolate or synthesize bromoisatin and bromoisatoic anhydride in order to study their stability toward ozone. The dibromoindigo sample, initially a deep violet, faded to a light gray after exposure to ozone. Whether the final color of the sample is attributable to bromoisatin, bromoisatoic anhydride, or to one or more of their ozone reactions products is not known at this time.

Thioindigo

The sample of thioindigo tested was significantly less reactive toward ozone than indigo and dibromoindigo. The exposed sample, while distinctly faded, still retained much of its original violet color. The mass spectrum of the exposed sample indicated a substantial amount of unreacted thioindigo. A comparison of the relative abundance of mass fragments of thioindigo and of those of the saturated impurity (which presumably did not react with ozone) indicates that only ~20-30% of the thioindigo had reacted with ozone after 4 days of exposure. In addition, thioisatin and thioisatoic anhydride, the expected reaction products (see Figure 5.5), were tentatively identified in the mass spectrum of the exposed sample but accounted for only ~5-10% of the initial thioindigo. No other product could be detected, but some products may have escaped detection if their mass fragments coincided with those of unreacted thioindigo and/or sample impurities unreactive toward ozone.

Thus, it appears that thioindigo is less ozone-fugitive than the nitrogen-containing indigos, but this conclusion should be verified by carrying out more detailed studies with colorant samples of higher purity.

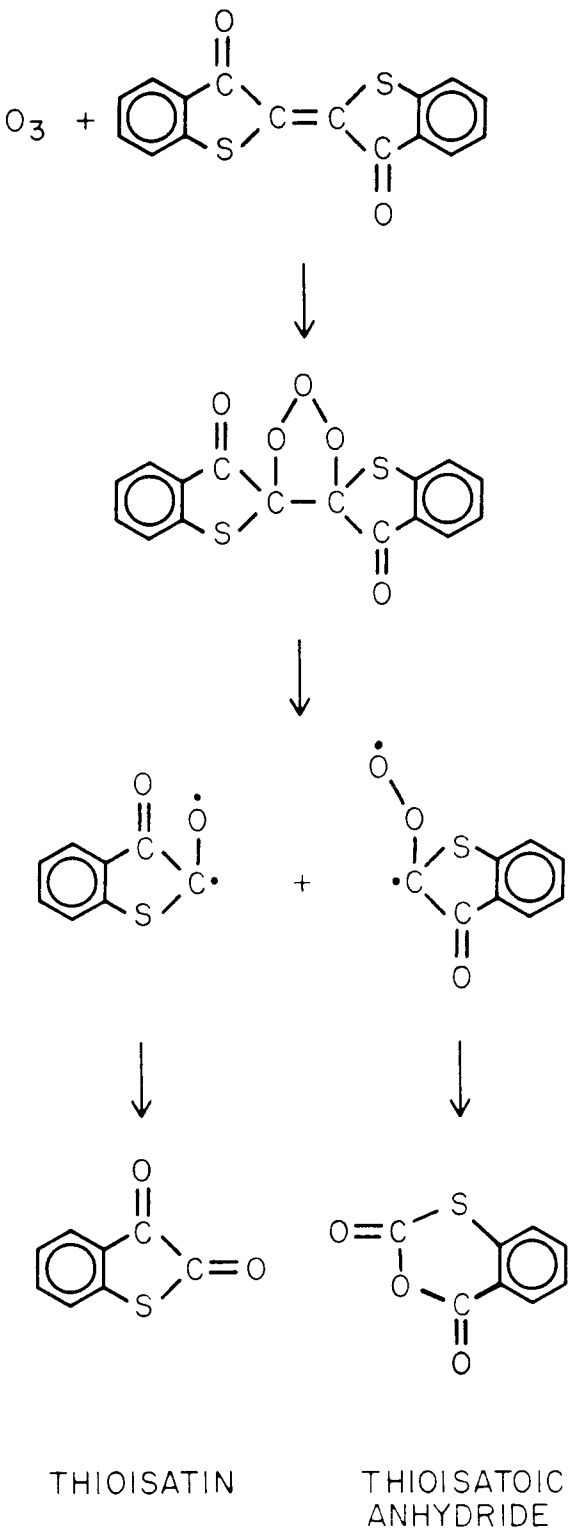

Figure 5.5. Tentative mechanism for the ozone-thioindigo reaction.

Tetrachlorothioindigo

The behavior of the colorants containing tetrachlorothioindigo was similar to that discussed above for thioindigo, i.e., lower reactivity toward ozone than the nitrogen-containing homologues, spectra obscured by large amounts of unreacted materials and of impurities, with the added complexity of extensive thermal decomposition of the samples when subjected to mass spectrometry analysis. The expected reaction products (Figure 5.6), dichloroisatin and dichloroisatoic anhydride, were tentatively identified in low yields, along with chloroisatin (presumably from the dichlorothioindigo impurity) and methyl chloroisatin (presumably from the dimethyl dichlorothioindigo impurity).

Relationship Between Color and Ozone Reactivity for the Indigoid Colorants

The exact nature of the chromophore in colorants having the indigoid structure has been determined (13). The fundamental chromogen in such structures is the so-called "H-chromophore", the central arrangement of carbonyl-olefin-amine (or thioether) groups. This chromophore can be considered as a pair of extended donor (amine)-acceptor (carbonyl) chromogens linked by a common olefinic bond. It is the sharing of the central olefinic linkage that gives the molecule its low $\Pi\Pi^*$ excitation energy.

Since this chromophore is of a donor-acceptor type, the resulting color is very sensitive to the electron donating/accepting abilities of the component functional groups. Thus, the replacement of the amine by the thioether in going from indigo to thioindigo leads to an increase in the $\Pi\Pi^*$ excitation energy (and a shift in color from blue to red) because sulfur is a poorer electron donor than nitrogen. Other indigo derivatives, obtained by replacing the amine group with other heteroatoms, show similar shifts in color directly related to the electron donating ability of these groups.

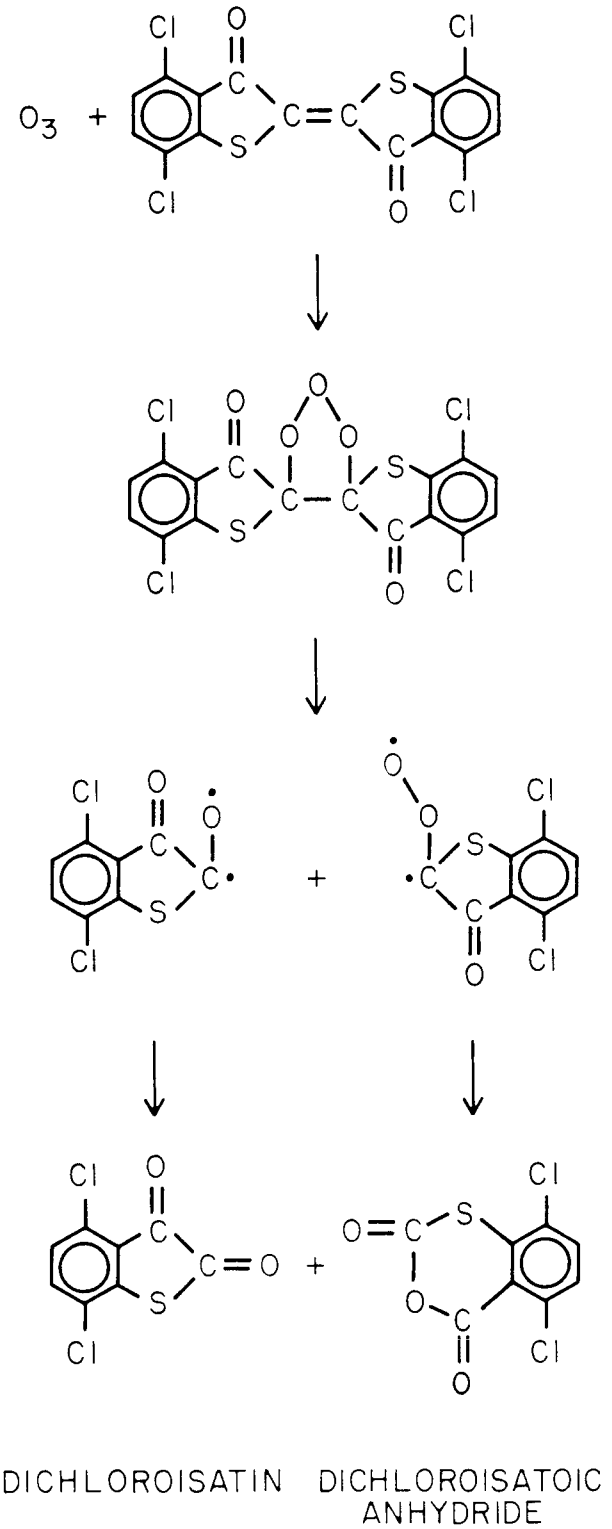

Figure 5.6. Tentative mechanism for the ozone-tetrachlorothioindigo reaction.

It has been found that the benzene rings attached on either side of this "H-chromophore" have only a secondary influence on the color of the molecule. Substituents on these rings, such as the halogen atoms in the 6,6'dibromoindigo and the 4,4',7,7'tetrachlorothioindigo, seem to have an effect on the color only insofar as they alter the electron donating/accepting of the groups of the central chomophore, either through mesomeric (through-bond) or steric (through space) interactions. For example, the bromine atoms in 6,6'dibromoindigo are *para* to the carbonyl groups in the central chromophore, and thus reduce the electron accepting ability of those carbonyls. The shift in $\Pi\Pi^*$ excitation to slightly higher energies accounts for the shift in color from the blue indigo to the violet dibromoindigo (Tyrian purple).

Since the apparent colors of indigo and its derivatives are such a sensitive measure of the electron donating/accepting of the groups adjacent to the central olefinic bond, it is not surprising that the reaction of these compounds with ozone, which proceeds by electrophilic addition onto the olefinic bond, should also show a wide range of apparent rates. It is well known that, in both liquid-phase and vapor-phase ozonolyses (12) the rate of reaction of ozone with substituted olefins *increases* if the substituent is *electron-donating,* and decreases if the substituent is *electron-withdrawing.* This trend seems to be in evidence in the ozone reaction of the indigoid colorants studied here. The observed products are consistent with an electrophilic addition of ozone to the olefinic bond, and the reaction rate seems to be greatest for those colorants having the greatest electron-donating capability adjacent to that double bond, i.e. indigo and dibromoindigo. In contrast, substitution of the amine by a sulfur atom decreases the electron-donating ability in thioindigo and tetrachlorothioindigo, and the corresponding ozone reaction rates are reduced. Just as the color of these compounds indicated this large change in electron-donating ability near the olefinic bond, the very slight shift in color upon

halogenation (indigo to dibromoindigo, thioindigo to tetrachlorothioindigo) indicates a minor change in electron-donating capability in the chromophore; consequently, the ozone reactivities of the compound and of its halogenated analogs are very similar. These conclusions have diagnostic value for the selection of less ozone-fugitive indigo colorants.

Comparison of Indigo Fading by Exposure to Ozone and by Exposure to Sunlight

In museum settings, indigo colorants may fade due to exposure to ozone and/or to sunlight. The poor lightfastness of indigos has long been documented in the textile industry (14,15). When exposed to light (including sunlight) in air, i.e., photooxidation, indigo colorants undergo dehalogenation (loss of bromine and chlorine substituents) as well as oxidation (e.g., indigo $\rightarrow$ isatin). Dehalogenation was not observed (and is not expected) in our experiments with ozone in the dark. Thus, the chemical characterization of the products in an art object containing faded indigo colorants may have diagnostic value for the implementation of mitigation measures, i.e., removal of ozone or protection from light.

CONCLUSIONS

Several indigo colorants deposited on Teflon filters were exposed in the dark to purified air containing 10 parts per million of ozone. These exposures were carried out for four days at ambient temperature (24°C) and low relative humidity (RH $\leq$ 5%). Mass spectrometry analysis of the exposed samples indicated that indigo and dibromoindigo were entirely consumed, that the major reaction products of the ozone-indigo reaction were isatin and isatoic anhydride, and that the major products of the ozone-dibromoindigo reaction were bromoisatin and bromoisatoic anhydride. Under the same conditions, thioindigo and colorants containing tetrachloroindigo and/or other chlorinated indigos also reacted with ozone, though at a

slower rate; the corresponding isatins and anhydrides were tentatively identified as reaction products.

The reaction products identified can be explained in terms of electrophilic addition of ozone onto the unsaturated carbon-carbon bond of the indigo molecule. This mechanism adequately accounts for the loss of chromophore for all indigos studied and for the lower reactivity of thioindigo and its derivatives as compared to indigo and its derivatives. The dose of ozone employed in our experiments, 10 ppm for 4 days, is equivalent to, for example, 0.04 ppm O_3 for 1000 days (2.74 years). Long-term average ozone concentrations of about 0.04 ppm are common in urban air, including indoor air such as in museums, in many urban areas of the world.

REFERENCES FOR CHAPTER 5

1. Shaver, C.L.; Cass, G.R.; Druzik, J.R. *Environmental Science and Technology 1983, 17,* 748-752.

2. Drisko, K.; Cass, G.R.; Whitmore, P.M.; Druzik, J.R. "Fading of artists' pigments due to atmospheric ozone" in *Wiener Berichte über Naturwissenschaft in Der Kunst,* Doppelband 2/3; Vendl, A.; Pichler, B; Weber, J. Eds; Verlag ORAC:Vienna, 1985/86, pp. 66-87.

3. Whitmore, P.M.; Cass, G.R.; Druzik, J.R. *J. Amer. Inst. for Conservation 1987, 26,* 45-58.

4. Davies, T.D.; Ramer, B.; Kaspyzk, G.; Delany, A.C. *J. Air Pollut. Control Assoc. 1984, 31,* 135-137.

5. Nazaroff, W.W.; Cass, G.R. *Environmental Science and Technology 1986, 20,* 924-934.

6. Grosjean, D.; Whitmore, P.M.; De Moor, C.P.; Cass, G.R.; Druzik, J.R. *Environmental Science and Technology 1987, 21,* 635-643.

7. McGovern, P.E.; Michel, R.H. *Anal. Chem. 1985, 57,* 1514A-1522A.

8. Pritchard, J.B. *Recovering Sarepta: A Phoenician City,* Princeton University Press, Princeton, NJ, 1978.

9. Luebs, H.A., ed. *The Chemistry of Synthetic Dyes and Pigments,* American Chemical Society Monograph Series, Reinhold Pub. Corp., New York, NY, 1955.

10. Grosjean, D.; Sensharma, D.K.; Cass, G.R. Chemical ionization mass spectra of artists' pigments and dyes: Indigos, anthraquinones and triphenylmethanes. Manuscript in preparation, California Institute of Technology, 1988.

11. Bader, H.; Hoigne´, J. *Water Research 1981, 15,* 449-456.

12. Bailey, P.S. *Ozonation in Organic Chemistry,* vol. 2. Academic Press, New York, NY, 1982.

13. Griffiths, J. *Color and Constitution of Organic Molecules,* Academic Press, London, 1976.

14. Hibbert, E. *Soc. Dyers and Colourists J. 1927, 43,* 292-294.

15. Weber, A.E. *Amer. Dyestuff Reporter 1933, 22,* 157-161.

CHAPTER 6
OZONE FADING OF ORGANIC COLORANTS: PRODUCTS AND MECHANISM OF THE REACTION OF OZONE WITH CURCUMIN

INTRODUCTION

Studies such as those reported in Chapters 2 and 3 have shown that a number of organic colorants faded substantially when exposed, in the dark, to purified air containing 0.3-0.4 parts per million (ppm) of ozone. The colorants tested included contemporary artists' pigments (1,2) as well as traditional natural colorants (3). Study of the reaction mechanisms involved in the fading of these ozone-fugitive colorants can be used to determine that the fading phenomena observed are indeed caused by reaction with ozone. In Chapters 4 and 5, major products have been identified and reaction pathways proposed for the reaction of ozone with several indigos (4) and with alizarin and related colorants (5). In this chapter, the methods and results of a similar study focusing on curcumin are described. Curcumin is a traditional natural colorant (e.g., the coloring agent in turmeric) whose poor ozone-fastness has been initially suggested in a study involving Japanese woodblock prints (1) and subsequently confirmed in the detailed kinetic study of the ozone fading of natural colorants on watercolor paper that was presented in Chapter 2 (3). Indeed, curcumin is the most ozone-fugitive of all the colorants, organic or inorganic, synthetic or natural, tested to date (1-5).

EXPERIMENTAL METHODS

Compounds Studied

Curcumin, vanillin, vanillic acid and ferulic acid (Table 6.1 and Figure 6.1) were obtained from Aldrich Chemical Co. and were used without further purification.

Table 6.1. Compounds studied.

Name	CAS Registry No.	MW	Purity, %	mp, °C	λ_{max}, nm
Curcumin					
1,7-bis(4-hydroxy-3-methoxyphenyl)-1,6-heptadiene-3,5-dione	458-37-7	368	≥95	—	430
Vanillic acid					
4-hydroxy-3-methoxy benzoic acid	121-34-6	168	97	210	—
Vanillin					
4-hydroxy-3-methoxy benzaldehyde	121-33-5	152	99	113	—
Ferulic acid					
4-hydroxy-3-methoxy cinnamic acid	1135-24-6	194	99		—

CURCUMIN

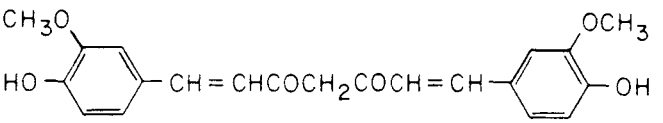

VANILLIN

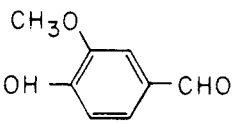

VANILLIC ACID

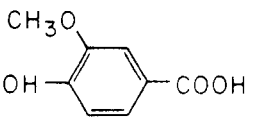

FERULIC ACID

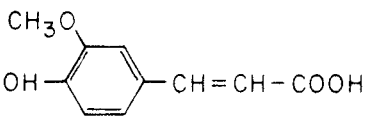

Figure 6.1. Structures of compounds studied.

Ferulic acid was selected as a simple structural homologue of curcumin in order to verify the consistency of mass fragmentation patterns.

Ozone Exposure Protocols

A list of the experiments performed is given in Table 6.2 according to compound studied, mode of exposure, and substrate. The protocols employed in this study for exposure of colorants to ozone and for mass spectrometry analysis of the exposed samples have been described in detail in Chapters 2 and 4; only a brief summary of these protocols is given here.

Two types of experiments were performed, both involving exposure to ozone in purified air in the absence of light. Long-term exposures to low concentrations of ozone (0.36 ± 0.11 ppm for 95 days at T = 25°C and 49.5 ± 1.9% relative humidity, air flow rate 2.5 liters/min) involved ~100 mg of curcumin airbrushed on cellulose and on silica gel thin layer chromatography (TLC) plates. Samples prepared in an identical manner but with a lighter loading on cellulose, on silica gel and on watercolor paper were also exposed in the same conditions (see "optical measurements" below). These conditions are similar to those employed in Chapter 2 in which curcumin was exposed to ozone on watercolor paper (3). In addition, short-term exposures to higher levels of ozone (~10 ppm for 4 days at T = 24°C and RH $\leq$ 20%, air flow rate = 1.0 liter/min) were carried out with 10 mg of colorant deposited on a Teflon membrane filter. Control samples, prepared in an identical manner but not exposed to ozone, were included for each type of exposure experiment.

Mass Spectrometry Analysis

After exposure to ozone, the cellulose and silica gel TLC plate samples were extracted with either methanol or methylene chloride, and the solvent extracts were concentrated prior to analysis. The Teflon filter samples were analyzed directly without solvent extraction.

Table 6.2. Summary of exposure experiments.

	Curcumin	Vanillin	Vanillic Acid	Ferulic Acid
Ozone exposure mode				
long term to low O_3	+			
short term to high O_3	+	+	+	+
Substrate (a)				
silica gel	+			
cellulose	+			
Teflon filter	+	+	+	+
Sample extraction				
methylene chloride	+			
methanol	+			
none (direct MS analysis)	+	+	+	+
Mass spectrometry analysis (b)				
probe-electron impact (EI)	+			
probe-chemical ionization (CI)	+	+	+	+

(a) Curcumin was also exposed to ozone on watercolor paper (see reference 2) and as a colorant on a Japanese woodblock print (see reference 1). Reflectance spectra were recorded on both substrates but chemical analyses of reaction products were not performed.

(b) Includes for all compounds, the analysis of control (unexposed) samples and of all appropriate solvent and substrate blanks.

Mass spectrometry analyses were carried out using a Kratos Scientific Instruments Model MS-25 hexapole, double focusing magnetic sector instrument. All samples were analyzed by direct insertion probe with two ionization modes, electron impact (EI) or chemical ionization (CI) with methane as reagent gas. The conditions are identical to those described earlier in Chapter 4 (5). The conventions adopted in Chapter 4 will be followed here for structural information on reactants and products to be deemed positive, probable, or tentative (5), depending upon the availability of reference compounds for comparison. Reaction products that could go undetected in our conditions include (a) volatile products that were no longer present on the substrate at the completion of the ozone exposure experiments, (b) products formed in very low yields (<0.1%), (c) products with very low vapor pressure, no detectable amount of which could reach the instrument's ionization source, and (d) compounds of molecular weight higher than 517, the upper limit of the spectrometer mass scan.

Optical Measurements

In order to associate color changes in the samples with the consumption of the colorant by chemical reaction, reflectance spectra were recorded for both control and exposed samples. Of the two types of samples on TLC plates subjected to ozone exposure, those heavily loaded (~100 mg of colorant per TLC plate) were dedicated to chemical analysis (these will be called "analytical" samples), while those with a lighter wash of colorant on silica gel, cellulose and watercolor paper were used for optical measurements (and will be referred to as "optical" samples). The color of the ozone-exposed and control samples was specified using the Munsell system of color notation (6). Munsell matches were made by a human observer using the illumination provided by a Macbeth Spectra Light booth under the daylight setting in accordance with ASTM standard methods (7). The tristimulus values of each sample were calculated from reflectance spectra recorded using a Diano

Matchscan II reflectance spectrophotometer. The total color difference ΔE between exposed and control samples was computed using the CIE 1976 L*a*b* formula.

RESULTS AND DISCUSSION

Mass Spectra of Reactants and Products

The EI and CI spectra we recorded are consistent with the structure of curcumin given in Figure 6.1. As expected, the EI spectrum was of limited diagnostic value due to extensive fragmentation. The most abundant large fragment was m/z = 177, i.e., 4–OH–3–CH_3O–C_6H_3CH=$CHCO^+$. In contrast, the CI spectrum included all large diagnostic fragments at m/z = 369 (MH, molecular weight of curcumin = 368), 351 (MH-H_2O), and so on (Table 6.3). CI spectra of methylene chloride extracts of control samples of curcumin on cellulose and on silica gel TLC plates matched well those of the pure (solid) compound, thus indicating reasonable recovery with our solvent extraction protocol. As an aid to the elucidation of the fragmentation pattern of curcumin, the CI spectrum of its simple structural homologue, ferulic acid, was also recorded. The CI spectra of ferulic acid, vanillin and vanillic acid are summarized in Table 6.4.

Color Changes due to Exposure to Ozone

Color changes in the curcumin samples due to the low-level (0.36 ppm) O_3 exposure for 95 days are quantified in Table 6.5. Curcumin fades rapidly in the presence of ozone on all of the substrates tested. As seen in Table 6.5, curcumin, when applied on either watercolor paper or as a thin coating on a cellulose TLC plate, is yellow-red in color. After the 95 day ozone exposure, Figure 6.2ab shows that the strong absorption of curcumin at wavelengths between 380-500 nm has been noticeably reduced (the sample has faded and reflectance has increased), but the samples still are clearly yellow in color. In contrast, the curcumin optical sam-

Table 6.3. Methane chemical ionization mass spectrum of curcumin (MW = 368).

m/z	Abundance, % of base peak	Fragment
397	1	M+29[a]
383	1	M+15[a]
370	5.5	MH, ^{13}C[b]
369	25	MH
351	2	MH–H_2O
350	6	M–H_2O
339	5	MH–H_2CO, M-HCO
285	4	—
245	3	XCH=CHCOCH$_2$COCH=CH[c]
233	4	MH-XCH
232	2	XCH=CHCOCH$_2$COCH
219	13	XCH=CHCOCH$_2$CO
205	4	233-CO
193	7	—
191	7	XCH=CHCOCH$_2$
190	9	XCH=CHCOCH
177	100(BP)	XCH=CHCO
151	12	BP-(CH=CH)
147	17	BP-H_2CO
137	26	XCH$_2$
136	3	XCH
124	2	XH
123	2	X
107	7	XH-OH, X-O
91	5	C_6H_3O (phenoxy)

(a) Reagent gas adducts.

(b) ^{13}C isotope contribution of MH.

(c) X = guaiacyl group, 4-OH-3CH_3O–C_6H_3–

Table 6.4. Methane chemical ionization mass spectra of vanillin, vanillic acid and ferulic acid.

Vanillin, MW = 152			Vanillic acid, MW = 168		
m/z	Abundance, % of base peak (BP)	Fragment structure	m/z	Abundance, % of base peak (BP)	Fragment structure
181	0.5	M + 29[a]	197	0.5	M + 29[a]
167	1	M + 15[a]	183	3	M + 15[a]
154	8	MH, ^{13}C[b]	170	8	MH, ^{13}C[b]
153	100 (BP)	MH	169	100 (BP)	MH
152	48	M	168	34	M
151	17	MH - 2, M - 1[c]	153	11	MH - O, M - CH_3
138	4	MH - CH_3	151	21	MH - H_2O
125	35	MH - CO	125	37	MH - CO_2
121	6	MH - O_2	121	10	C_6H_3COOH, H^+
109	5	MH - CO_2	97	7	MH - (CO_2 + CO)
93	19	C_6H_3OH, H^+	93	15	C_6H_3OH, H^+
81	9				

Ferulic acid, MW = 194		
m/z	Abundance, % of base peak (BP)	Fragment structure
196	6	MH, ^{13}C[b]
195	56	MH
194	63	M
180	10	MH - CH_3
179	8	MH - O, M - CH_3
178	12	BP, ^{13}C[b]
177	100 (BP)	MH - H_2O
163	10	loss of OCH_3
153	11	—
151	26	MH - CO_2
150	28	MH - COOH
137	10	MH - CHCOOH
136	9	MH - CH_2COOH
119	17	$C_6H_3(OCH_3)CH$
91	9	C_6H_3O

(a) Reagent gas adducts.
(b) Contribution of ^{13}C isotope to MH and/or BP.
(c) Typical for aldehydes.

Table 6.5. Observed color change in curcumin samples as a function of substrate after exposure to 0.36 ppm O_3 at 49.5% RH for 95 days in the absence of light.

COLORANT AND SUBSTRATE	Munsell Notation[a]		Tristimulus Value[b]						Color Difference[c]
	Control	O_3 Exposed	Control			O_3 Exposed			
			X	Y	Z	X	Y	Z	ΔE
Curcumin									
Watercolor Paper[d]	9.5YR 8.4/12.8	3.5Y 8.7/8.8	66.06	62.27	12.34	71.93	75.53	32.44	29.85
Cellulose TLC Plate (Optical)[e]	9.0YR 8/14.4	6.25Y 9.1/9.2	64.44	58.41	8.66	72.97	78.84	34.60	41.86
Cellulose TLC Plate (Analytical)[e]	5.0YR 7.3/13.6	7.5YR 7.5/13.6							
Silica Gel TLC Plate (Optical)	4.0Y 7.9/8.4	N8.75/(PB 0.5)	52.11	53.90	22.55	71.59	73.21	86.65	48.82
Silica Gel TLC Plate (Analytical)	4.5YR 6/13.6	10.5Y 8.7/0.8							
Blanks									
Blank Watercolor Paper			85.13	87.16	97.47	86.62	88.65	100.69	1.15
Blank Cellulose TLC Plate			88.05	90.15	101.36	89.41	91.49	104.71	1.26
Blank Silica Gel TLC Plate			71.67	73.33	86.55	72.77	74.37	88.45	0.69

(a) Munsell matches are by a human observer using a Macbeth Spectra Light Booth under the daylight setting according to ASTM standards.

(b) Tristimulus values (X,Y,Z) are reported for CIE Illuminant C.

(c) Color differences between the control and exposed samples are calculated for CIE Illuminant C using the CIE 1976 $L^*a^*b^*$ formula.

(d) Included for relevance to artists; no chemistry.

(e) For distinction between optical versus analytical samples; see text.

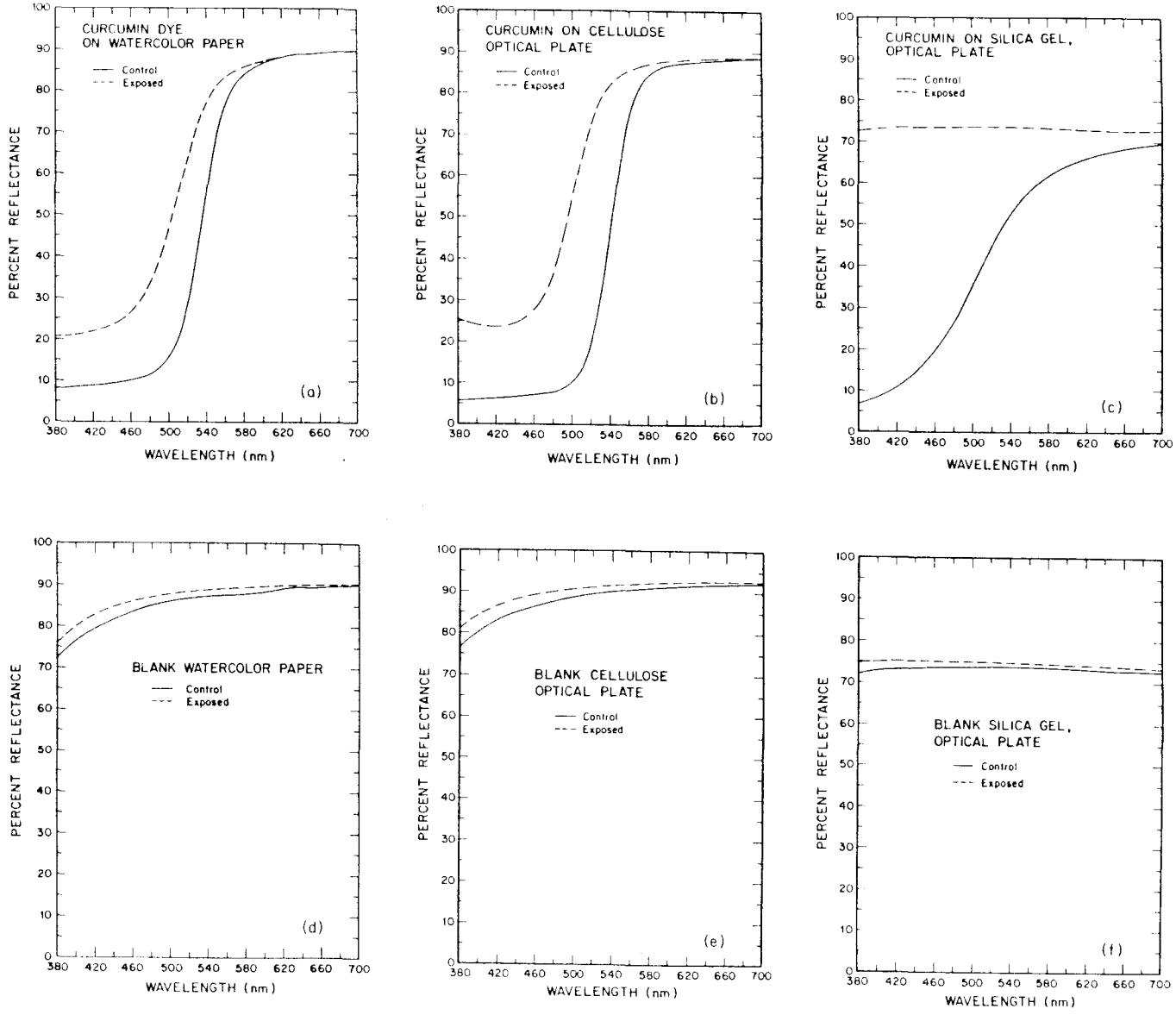

Figure 6.2. Reflectance spectra of ozone-exposed curcumin on watercolor paper, and on cellulose and silica gel TLC plates.

ple on silica gel has faded from yellow to a neutral shade (Table 6.5), and comparison of the reflectance spectrum of the curcumin sample on silica gel after the ozone exposure (Figure 6.2c) to the reflectance spectrum of a blank silica gel TLC plate (Figure 6.2f) suggests that virtually all of the curcumin initially present on the silica gel has reacted to form other nearly colorless products.

Reaction Products

Upon exposure to ozone, curcumin yielded 4-hydroxy-3-methoxy benzaldehyde (vanillin) and 4-hydroxy-3-methoxy benzoic acid (vanillic acid) as major products. These two products were positively identified by comparison to the mass spectra of authentic samples, see Table 6.4, and are consistent with the unusual fragrance of the samples that was noted at the end of the exposure experiment. Tentatively identified as reaction products were the three aliphatic dicarbonyls $R_1COCH_2COR_2$ with R_1=R_2=CHO, R_1=CHO and R_2=COOH, and R_1=R_2=COOH, the latter possibly as the anhydride since diacids and their anhydrides give very similar mass spectra (5).

Reaction Mechanism

A tentative scheme summarizing the ozone-curcumin reaction mechanism is given in Figures 6.3 and 6.4. As for other ozone-olefin reactions (8,9) the initial ozone attack is expected to proceed by electrophilic addition on the unsaturated carbon-carbon bonds (Figure 6.3) to form an 1,2,3-trioxolane and the corresponding Criegee biradicals, whose unimolecular decomposition in turn yields two aldehydes and two carboxylic acids. Uncertainties in the proposed reaction sequence include (a) the relative abundance of the two Criegee biradicals from each initial trioxolane adduct and (b) the amount of carboxylic acid formed by rearrangement of the R$\dot{C}$(H)O$\dot{O}$ Criegee biradicals. While the size of the substituents would favor thermal stabilization of the carboxylic acids, decarboxylation and other fragmentation path-

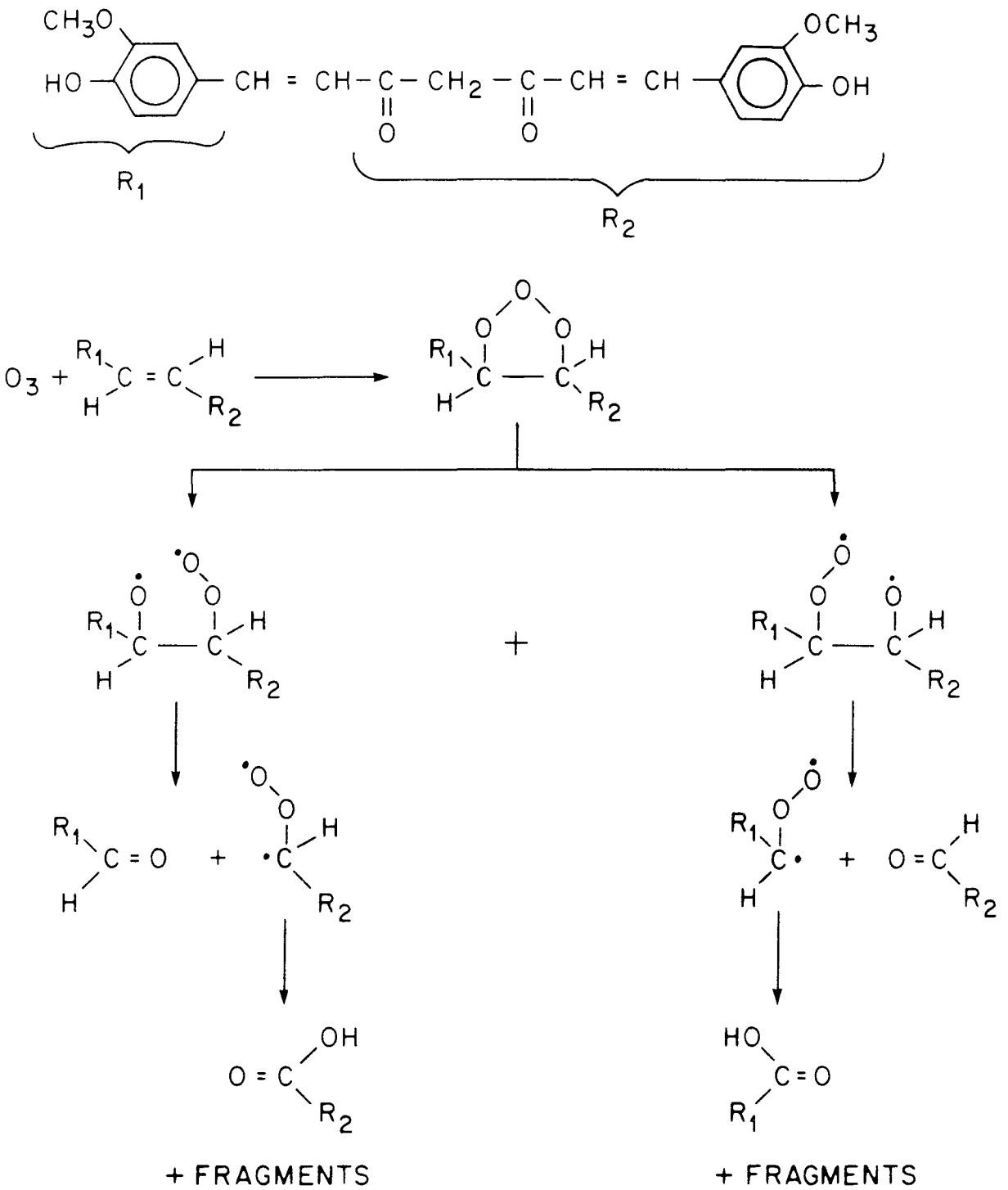

Figure 6.3. Tentative mechanism for the ozone-curcumin reaction.

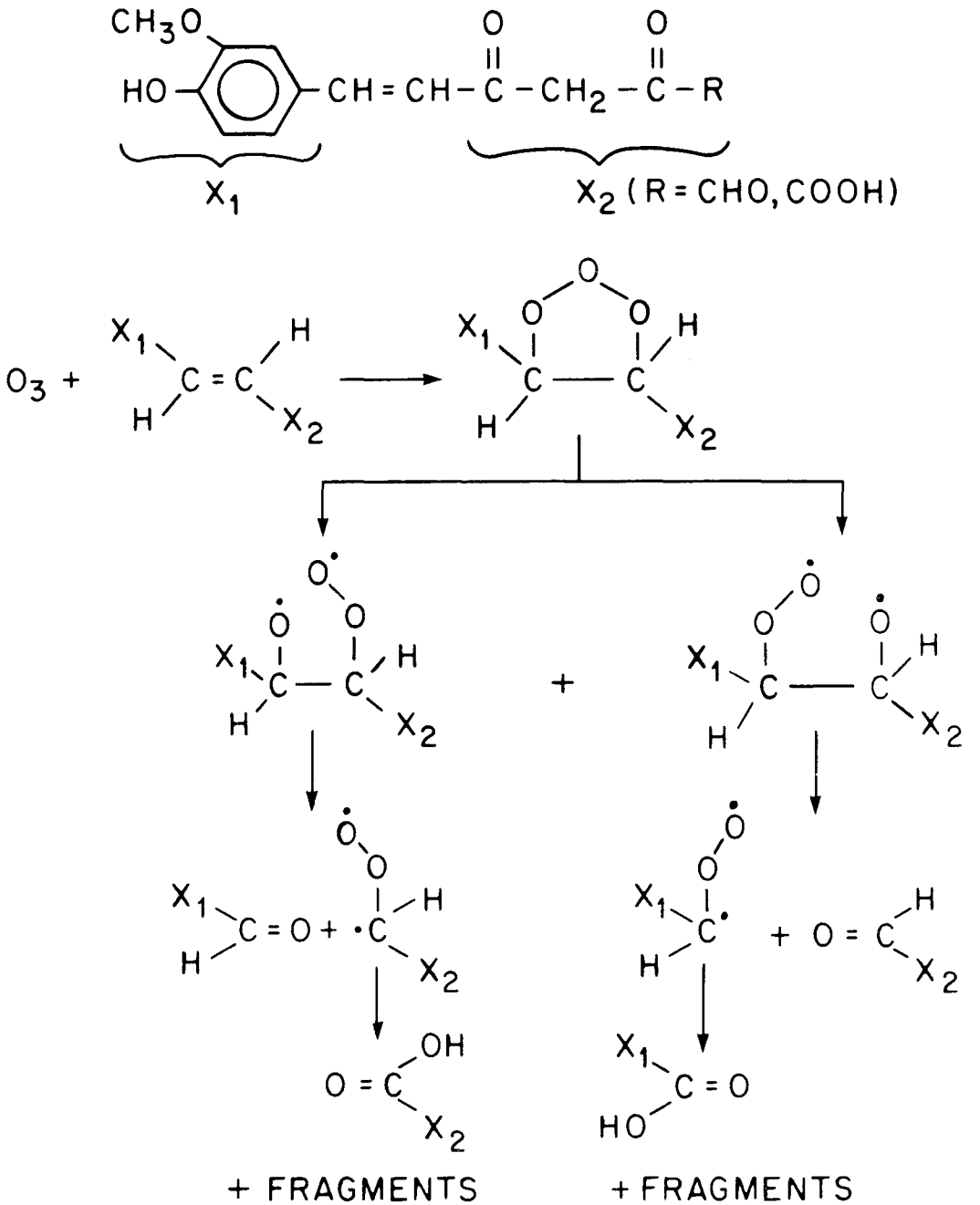

Figure 6.4. Reaction of ozone with "first generation" products of the curcumin-ozone reaction.

ways may compete with acid formation.

The saturated compounds predicted to form in this initial sequence, namely vanillin and vanillic acid, were indeed identified as reaction products. The corresponding unsaturated compounds, which were not seen as reaction products, are in turn expected to react with ozone according to a sequence identical to that described above for curcumin. The expected products are again vanillin and vanillic acid, along with aliphatic dicarbonyls (Figure 6.4) which were tentatively identified (no reference compounds were available) on the basis of CI mass spectral data. Thus, experimental findings appear to be consistent with a simple reaction mechanism involving electrophilic addition of ozone onto the curcumin unsaturated carbon-carbon bonds.

While there is no mention in the literature of any previous studies of the oxidation of curcumin, vanillin has been reported to form in high yields (~25%) in the alkaline oxidation of lignin. Lignin contains sulfonate derivatives of coniferyl alcohol, a compound structurally related to curcumin (10):

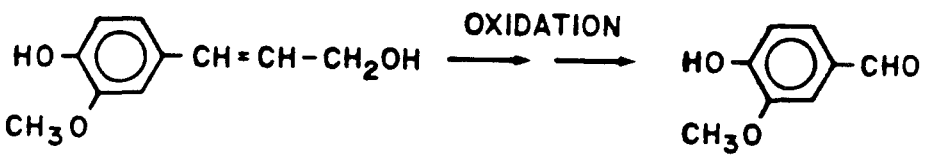

Since few structural homologues of curcumin are commercially available, we could not test the general applicability of the proposed ozone-curcumin reaction mechanism. Exposure of ferulic acid to ozone also yielded vanillin and vanillic acid as reaction products. Because of the electron-withdrawing carboxylic acid substituent, the reactivity of ferulic acid toward ozone is expected to be substantially lower than that of curcumin. Indeed, vanillic acid and vanillin were only formed in small amounts in the ferulic acid-ozone reaction (~5% estimated from the CI spectrum of the ozone-exposed sample). Thus, for the single structural homologue tested, the nature and yields of the ozone reaction products appear to be consistent

with those predicted from the proposed mechanism.

Substrate-Mediated Effects

In the investigation of alizarin and related compounds reported in Chapter 4, it was found that alizarin was unreactive towards ozone when deposited on Teflon and cellulose substrates, but was consumed rapidly upon exposure to ozone on silica gel (4). In this work, curcumin was found to react with ozone on all three substrates (silica gel, cellulose and Teflon) as well as on watercolor paper (2) and as a colorant on a woodblock print (1). Identified reaction products were the same on all three substrates, thus indicating no major substrate-mediated effect on the overall reaction mechanism. However, color change observations, together with *estimates* of reaction products and unreacted curcumin concentrations (based on fragment abundances in mass spectra of control and exposed samples) indicate marked differences in the extent of reaction on different substrates. Less than 30% of the initial curcumin had reacted in the short-term exposure to high levels of ozone on Teflon, and 20-30% had reacted in the long term exposure to lower levels of ozone on cellulose. In contrast, essentially all ($\geq$90%) of the curcumin had been consumed on silica gel, with the corresponding methanol extracts changing from an intense bright orange to a pale yellow. The exposures on Teflon and cellulose are difficult to compare in view of the different conditions employed. Those on cellulose and silica gel, however, were carried out under identical conditions. The enhanced reactivity of curcumin towards ozone on silica gel may reflect complex heterogeneous effects, including hydrogen bonding to the silica gel silanol and siloxane groups.

Reactivity of "First Generation" Products Toward Ozone

Vanillin and vanillic acid were also exposed to ozone on Teflon filters (~10 ppm ozone for 96 hours, T = 76°F, RH < 20%, flow rate 1 liter/minute). Comparison

of the CI spectra of exposed and control samples gave no evidence of reaction for either compound. Possible reactions include oxidation of vanillin to vanillic acid and, for both compounds, opening of the guaiacyl (4-hydroxy-3-methoxyphenyl) aromatic ring to yield small oxygenated aliphatic compounds. These reactions, while possibly occurring under more "severe" ozonolysis conditions, were not observed to take place under the present experimental conditions.

CONCLUSIONS

The natural colorant curcumin, which has been shown in Chapter 2 to be extremely ozone-fugitive, was exposed to ppm levels of ozone in purified air in the dark. These exposures were carried out on silica gel, cellulose and Teflon substrates, and the reaction products were identified by mass spectrometry. The major products, vanillin and vanillic acid, are consistent with a reaction mechanism involving electrophilic addition of ozone onto the unsaturated carbon-carbon bonds of curcumin. Results obtained for one structural homologue of curcumin, ferulic acid, are also consistent with the proposed mechanism and support its general applicability to other compounds, including colorants, of similar structures. The ozone-curcumin reaction products, vanillin and vanillic acid, were not ozone-fugitive under the conditions of our study.

REFERENCES FOR CHAPTER 6

1. Shaver, C.L.; Cass, G.R.; Druzik, J.R. *Environmental Science and Technology 1983, 17,* 748-752.

2. Drisko, K.; Cass, G.R.; Whitmore, P.M.; Druzik, J.R. "Fading of artists' pigments due to atmospheric ozone" in *Wiener Berichte über Naturwissenschaft in der Kunst,* Doppelband 2/3; Vendl, A.; Pichler, B.; Weber, J. Eds.; Verlag ORAC:Vienna, 1985/86, pp. 66-87.

3. Whitmore, P.M.; Cass, G.R.; Druzik, J.R. *J. Amer. Inst. for Conservation 1987, 26,* 45-58.

4. Grosjean, D.; Whitmore, P.M., Cass, G.R.; Druzik, J.R. *Environmental Science and Technology 1988, 22,* 292-298.

5. Grosjean, D.; Whitmore, P.M.; De Moor, C.P.; Cass, G.R.; Druzik, J.R. *Environmental Science and Technology 1987, 21,* 635-642.

6. *Munsell Book of Color,* Macbeth Division of Kollmorgen, Baltimore, MD, 1976.

7. *Standard Method of Specifying Color by the Munsell System,* American Society for Testing and Materials, Philadelphia, PA, 1980, D1535-1580.

8. Bailey, P.S. *Ozonation in Organic Chemistry,* vol. 2, Academic Press, New York, 1982.

9. Atkinson, R.; Carter, W.L.P. *Chem. Reviews 1984, 84,* 437-470.

10. Pearl, I.A. *The Chemistry of Lignin,* Marcel Dekker, New York, 1967.

CHAPTER 7
OZONE FADING OF TRIPHENYLMETHANE COLORANTS: REACTION PRODUCTS AND MECHANISMS

INTRODUCTION

The studies reported in Chapters 4, 5 and 6 have focused on the reaction mechanisms involved in the ozone fading of organic colorants (1,2). These studies were prompted by observations that a number of colorants, natural and synthetic, used in the formulation of artists' pigments, faded substantially when exposed, in the dark, to air containing ozone levels comparable to those actually recorded in urban air including indoor museum settings (3-5). Since the potential for damage to works of art is of obvious concern to the art conservation community, it is important, with regard to mitigation measures, to develop a better understanding of the relationship between ozone damage and colorant structure.

The colorants previously shown to be among the most ozone-fugitive (3-5) included a commercial watercolor, Winsor and Newton 030 Mauve, which reportedly contained copper phthalocyanine (CP) and a lake of the triphenylmethane colorant Basic Violet 14. For this watercolor sample, fading was accompanied by a shift in color towards that of CP alone. In addition, a number of green CP watercolors and a blend of CP with a substituted alizarin lake did not fade under the same conditions (4). This suggested that triphenylmethane colorants may be particularly susceptible to ozone attack, and prompted an exploration of the mechanism of their reaction with ozone. In this chapter, the watercolor 030 Mauve will be investigated, along with its reported component Basic Violet 14.

Basic Violet 14 is a typical member of an important group of colorants, the triphenylmethane cationic dyes. Other members of this group include malachite green, crystal violet, fuchsin and rosaniline. These dyes are structurally derived from the corresponding triphenylmethane and triphenylcarbinols (Figure 7.1), with

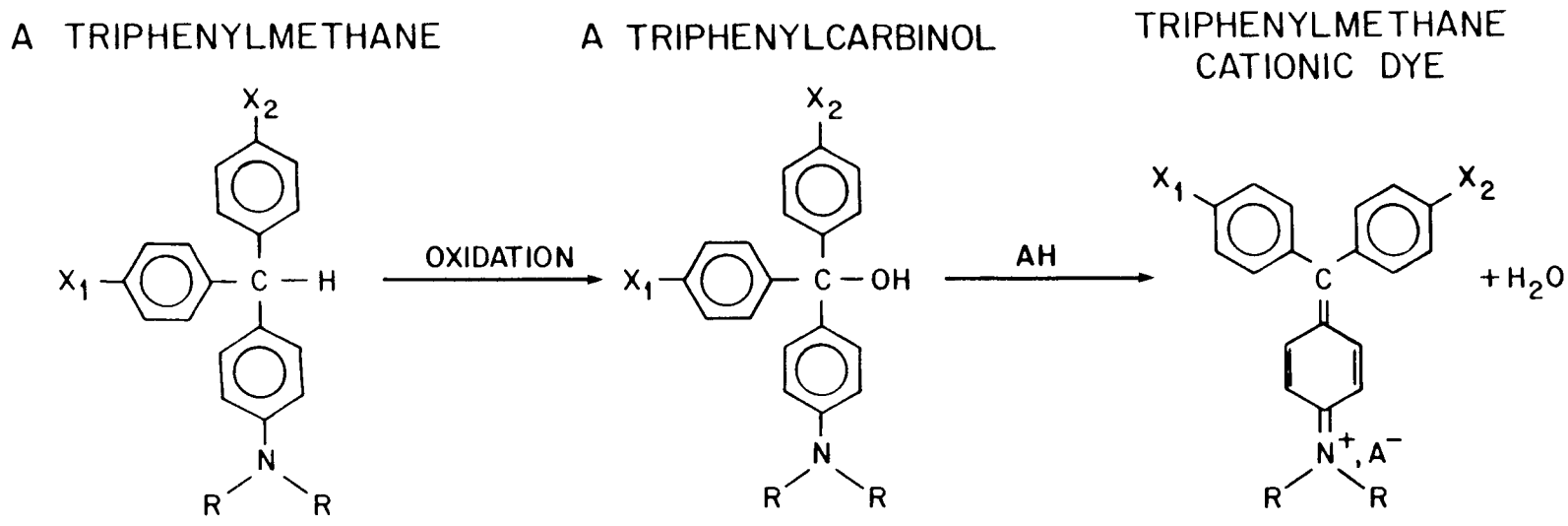

DYE	CI NUMBER	R	X_1	X_2	A^-
MALACHITE GREEN	42000	$-CH_3$	$-H$	$-N(CH_3)_2$	$C_2O_4H^-$
BRILLIANT GREEN	42040	$-CH_2CH_3$	$-H$	$-N(CH_2CH_3)_2$	HSO_4^-
CRYSTAL VIOLET	42555	$-CH_3$	$-N(CH_3)_2$	$-N(CH_3)_2$	Cl^-

Figure 7.1. Structures of some triphenylmethane dyes.

the chromophore associated to *para*-substitution with amino groups (6,7). One triphenylmethane and one carbinol are included in this study as an aid to the interpretation of the reactivity of Basic Violet 14 towards ozone. The poor light fastness of triphenylmethane-based inks (8) and dyes (9-11) has been known for some time. With the exception of one study of malachite green at high reactants concentrations in methanol (12) the reactivity of triphenylmethane colorants towards ozone has not been previously investigated.

EXPERIMENTAL METHODS

Compounds Studied

Basic Violet 14, pararosaniline base and triphenylmethane were obtained from commercial sources and were used without further purification. The Winsor and Newton 030 Mauve colorant was available from a previous study (3). In order to facilitate the identification of reaction products and the interpretation of mass spectra fragmentation patterns, mass spectra also were recorded for a number of benzoic acids and benzophenones. Relevant information regarding these compounds is given in Table 7.1. The corresponding structures are shown in Figure 7.2.

Ozone Exposure Protocols

A list of the experiments performed is given in Table 7.2 according to compound studied, mode of exposure, and substrate. The protocols for ozone exposure and for mass spectrometry analysis have been described in detail in Chapters 2 and 4. Only a summary of these protocols is given below.

The 030 Mauve watercolor sample was airbrushed on cellulose and silica gel thin layer chromagraphy plates. Samples containing ~100 mg colorant per plate were employed for mass spectrometry analysis. Samples were exposed in the dark to purified air containing 0.36 ± 0.11 ppm of ozone. The exposure was carried out

Table 7.1. Compounds studied.

Name(s)	MW	CAS Registry No.	CI No.	mp(°C)	Purity, percent	λ_{max}, nm
Basic Violet 14[a] (basic fuchsin, rosaniline)	337.9	632-99-5	42510	250(dec.)	-	-
Pararosaniline base[a]	305.4	25620-78-4	42500	205(dec.)	~95	544
Triphenylmethane[a]	244.3	519-73-3	-	92-94	97	-
030 Mauve	unknown[b]	-	-	-	-	(c)
Benzoic acid	122.1	65-85-0	-	122-123	99	-
Phthalic acid	166.1	88-99-3	-	210(dec.)	99	-
4-amino benzoic acid	137.1	150-13-0	-	188	99	-
4-amino-3-methyl-benzoic acid[a]	151.2	2486-70-6	-	169-171	98	-
Benzophenone	182.2	119-61-9	-	49-51	99	-
4-aminobenzophenone[a]	197.2	1137-41-3	-	121-124	98	-

[a]See structures in Figure 7.2.

[b]Reportedly a blend of Basic Violet 14 lake and copper phthalocyanine (MW = 576, CAS 147-14-8, CI 74160).

[c]See 400-700 nm reflectance spectrum in ref. 3.

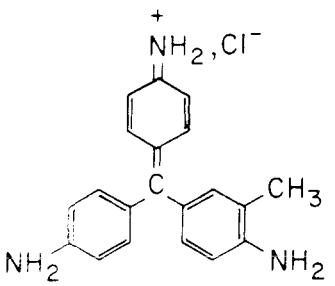

BASIC VIOLET 14

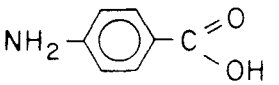

4-AMINO-BENZOIC ACID

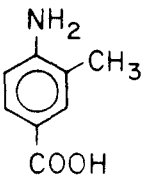

4 AMINO-3-METHYL BENZOIC ACID

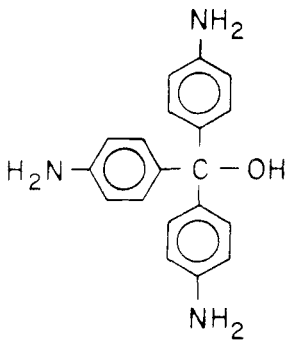

PARAROSANILIN BASE

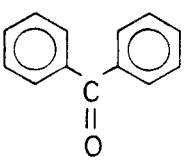

BENZOPHENONE

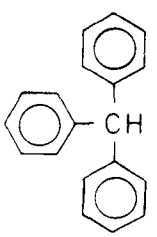

TRIPHENYLMETHANE

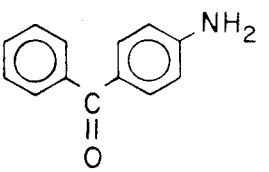

4-AMINO-BENZOPHENONE

Figure 7.2. Structures of compounds studied.

Table 7.2. Summary of experimental conditions.

	030 Mauve	Triphenyl-methane	Pararosani-line base	Basic Violet 14
Ozone exposure mode				
long term to low O_3 (95 days x 0.36 ppm)	+			
short term to high O_3 (96 hours x 10 ppm)		+	+	+
Substrate				
silica gel	+			
cellulose	+			
Teflon		+	+	+
watercolor paper[a]	+			
Sample extraction				
methanol	+			
methylene chloride	+			
none (direct MS analysis)		+	+	+
Mass spectrometry analysis[b]				
methane chemical ionization	+	+	+	+
electron impact		+	+	

[a]Reference 3, see text.

[b]Includes, for all compounds, the analysis of the corresponding control samples and substrate and solvent blanks.

for 95 days with an air flow rate of 2.5 liters per minute at constant temperature (24°C) and humidity (RH = 49.5 ± 1.9%). This protocol is identical to that employed earlier to study the 030 Mauve sample deposited on another substrate, watercolor paper (3) and to study the ozone-fastness of alizarin compounds (1) and of indigo derivatives on silica gel, cellulose and watercolor paper (2,4).

Triphenylmethane, pararosaniline base and Basic Violet 14 were deposited on Teflon filters (~10 mg per filter) and exposed in the dark to air containing higher levels of ozone (~10 ppm). These exposures were of shorter duration (96 hours) than those described above, and were carried out at the same temperature (24°C), lower air flow rate (1.0 liter per minute) and lower humidity (RH $\leq$ 20%). Control samples (not exposed to ozone) were included for each colorant and each mode of exposure.

Mass Spectrometry Analysis

After exposure, the 030 Mauve samples were extracted in methanol and were analyzed by mass spectrometry (MS) as concentrated solvent extracts. The Teflon filter samples were analyzed directly by probe insertion MS. The MS analyses were carried out using a Kratos Scientific Instruments model MS-25 hexapole, double focusing magnetic sector instrument. All samples were analyzed in the chemical ionization (CI) mode with methane as the reagent gas. Operating conditions have been described in detail in Chapter 4, which also specifies the convention for structural information on reactants and products to be deemed positive, probable or tentative. Reaction products that could go undetected include (a) those too volatile to remain on the substrate at the completion of the exposure experiment, (b) those formed in yields of less than 0.1%, (c) those with a molecular weight higher than 517, the upper limit of our mass scans, and (d) those with very low vapor pressure, no detectable amount of which could reach the spectrometer's ionization source.

RESULTS AND DISCUSSION

Mass Spectra of Reactants and Other Reference Compounds

Methane chemical ionization mass spectra were recorded for all compounds listed in Table 7.1. The spectra of the three triphenylmethanes of interest were consistent with the structures given in Figure 7.2. The CI spectrum of Basic Violet 14, which was successfully recorded in spite of the ionic character of the compound, exhibited clusters of four fragments (m/z = x, x+1, x+2, x+3) as expected from the isotopic distribution of ^{35}Cl and ^{37}Cl. Details of this spectrum are discussed elsewhere (13) along with those of the spectrum of pararosaniline base. No impurities could be detected from examination of the spectrum of Basic Violet 14. That of pararosaniline base suggested diaminobenzophenone as a minor (~5%) impurity. The CI spectrum of benzoic acid was recorded and matched well earlier literature data (14). The EI and CI spectra of phthalic acid have been discussed previously (1). Those of triphenylmethane and of the other aromatic compounds are summarized in Table 7.3. The spectra of the substituted benzoic acids included MH (base peak), MH-H_2O and MH-CO_2 as major fragments. Those of the benzophenones exhibited major MH and XC_6H_4CO fragments (X = H, NH_2). Attempts to obtain a CI spectrum of the 030 Mauve sample, either directly or as a solution in methanol and methylene chloride were not successful.

Ozone-Triphenylmethane Reaction: Products and Tentative Mechanism

The mass spectra of control and ozone-exposed samples of triphenylmethane were identical, i.e., there was no evidence for reaction between ozone and triphenylmethane or for any other triphenylmethane loss process in our exposure protocol. In particular, there was no evidence for even minor oxidation of triphenylmethane to triphenylcarbinol. In the same way, pararosaniline base did not react measurably with ozone under the conditions of our study: the CI spectrum of the exposed sam-

Table 7.3. Methane chemical ionization mass spectra of triphenylmethane and relevant aromatic compounds.

Triphenylmethane (MW = 244)			4-amino benzoic acid (MW = 137)		
m/z	Abundance, % of base peak (BP)	Fragment structure	m/z	Abundance % of base peak (BP)	Fragment structure
245	3	MH	138	100(BP)	MH
244	15	M	137	41	M
243	3	$(Ph)_3C$, $Ph=C_6H_5$	123	11	MH - $NH^{(b)}$
168	14	^{13}C contribution to $BP^{(a)}$	122	6	M - $NH^{(b)}$
167	100(BP)	$(Ph)_2CH$	120	43	MH - $H_2O^{(c)}$
166	7	$(Ph)_2C$	94	44	MH - $CO_2^{(c)}$
165	9	-	92	8	$C_6H_4NH_2$
91	6	PhCH, H^+			
79	2	PhH, H^+			
78	2	PhH			
77	4	$C_4H_3^+$ (aromatic)			

4-amino-3-methyl benzoic acid (MW = 151)			Benzophenone (MW = 182)		
m/z	Abundance, % of base peak (BP)	Fragment structure	m/z	Abundance % of base peak (BP)	Fragment structure
152	100(BP)	MH	183	56	MH
151	57	M	182	18	M
134	42	MH - $H_2O^{(b)}$	106	7	^{13}C contribution to $BP^{(a)}$
108	55	MH - $CO_2^{(b)}$	105	100(BP)	C_6H_5CO
107	16	M - CO_2, MH - COOH	77	22	C_6H_5
106	15	$CH_3C_6H_3NH_2$			

4-aminobenzophenone (MW = 197)		
m/z	Abundance, % of base peak (BP)	Fragment structure
198	100(BP)	MH
197	35	M
121	5.4	^{13}C of $120^{(a)}$
120	70	$NH_2C_6H_4CO$
105	63	C_6H_5CO
92	9	$NH_2C_6H_4$
77	10	C_6H_5

[a] These fragments have diagnostic value.

[b] And/or benzoic acid (MW = 122) as a minor impurity.

[c] Typical of all benzoic acids.

ple was identical to that of the control sample, with the exception of minor fragments (corresponding to less than 2% yields) at m/z = 107 and 109 which possibly correspond to benzaldehyde (MW = 106) and benzoquinone (MW = 108), respectively. These products may also have formed by oxidation of the diamino benzophenone impurity. There was no discernable change in the deep violet color of pararosaniline base after exposure to ozone.

In contrast, Basic Violet 14 yielded a number of products including substituted benzophenones and aromatic compounds (Table 7.4). Major products included diamino- and methyldiamino benzophenone, benzoquinone, benzoic acid and a product of molecular weight 147 (MH = 148) whose mass fragmentation pattern matches that of phthalimide. Comparison of the CI spectra of control and exposed samples also indicated that a substantial amount of Basic Violet 14 was still present at the completion of the 96 hour exposure experiment.

Ozone attack on triphenylmethane compounds may involve several reaction sites: (a) the carbon-carbon unsaturated bond, (b) the carbon-nitrogen unsaturated bond, (c) the aromatic rings, (d) the amino group nitrogen atoms, and (e) the saturated aliphatic carbon atoms. Of these, reaction centers (a) and (b) are specific to Basic Violet 14, reaction center (c) is absent in Basic Violet 14, and reaction center (d) is absent in triphenylmethane.

In the liquid phase (15) ozone reacts rapidly with unsaturated carbon-carbon bonds by 1,3 dipolar addition (see details of mechanism below); the electrophilic addition of ozone to the nitrogen atom in aromatic amines yields nitroaromatic and aromatic ring oxidation products, e.g., nitrobenzene and benzoquinone from aniline; the addition of ozone to C=N bonds yields epoxides, e.g. $C_6H_5CH\overset{O}{\diagdown\!\diagup}NCH_3$ from $C_6H_5CH{=}NCH_3$; and the reaction of ozone with aromatic rings may involve atom and bond attack to form phenols and ring-opening carbonyls, respectively (15).

Table 7.4. Products of the reaction between gas phase ozone and Teflon-deposited Basic Violet 14.

Reaction product	MW	MH[a]	Identification
Benzophenones			
$NH_2-C_6H_4-CO--C_6H_3(COOH)NH_2$[c]	256	257	tentative[b]
$NH_2-C_6H_4-CO-C_6H_3(CH_2OH)NH_2$[c]	242	243	tentative
$NH_2-C_6H_4-CO-C_6H_3(OH)NH_2$[c]	228	229	tentative
$NH_2-C_6H_4-CO-C_6H_3(CH_3)NH_2$[d]	226	227	probable
$NH_2-C_6H_4-CO-C_6H_4-NH_2$[d]	212	213	positive
Substituted benzenes			
phthalimide[d]	147	148	tentative
amino benzoic acid[c]	137	138	positive
benzoic acid[d]	122	123	positive
benzoquinone[d]	108	109	positive
benzaldehyde[c]	106	107	probable
phenol	94	95	positive

[a]Reagent adduct MH peak in methane chemical ionization mass spectrum.

[b]See Experimental Section and reference (1) for definitions of tentative, probable and positive identification.

[c]Minor product.

[d]Major product.

The relative reactivity of these reaction centers towards ozone in the liquid phase decreases according to the sequence:

>C=C< > amino > >C=N- > aromatic ring > saturated aliphatic

A similar sequence of reactivity towards ozone is observed in the gas phase as well (16). The results of the present study for the heterogeneous reaction between gaseous ozone and substrate-deposited triphenylmethane also appear to be consistent with this reactivity sequence. Thus, triphenylmethane and pararosaniline base, which lack the more reactive >C=C< reaction center, were unreactive towards ozone under the conditions of our study. Of the two reaction centers specific to Basic Violet 14, one, the C=N bond, is even less reactive towards ozone than the amino groups of pararosaniline; the corresponding epoxide products were not observed. This leaves only the C=C bond as the initial site of ozone attack.

A tentative mechanism for the ozone-Basic Violet 14 reaction, consistent with the above discussion and with currently accepted mechanisms for ozone addition to the C=C bond in substituted olefins (15-17, and references therein), is outlined in Figure 7.3. The mechanism involves the steps of 1,3 dipolar addition, formation of the Criegee biradicals from the initial 1,2,3-trioxolane adduct, and carbon-carbon bond scission to yield the carbonyl products, in this case methyldiaminobenzophenone. Examination of resonance hybrid forms suggests diaminobenzophenone as another product of the same reaction sequence. Benzophenone products have also been identified in the oxidation of other triphenylmethane dyes by ozone in methanol (12), by hydrogen peroxide in the presence of light, both with dye powders and in solution (10), and by photooxidation of the dyes as powders, on cellulose and in aqueous solution (9-11). The one-ring oxidation products listed in Table 7.4 are structurally consistent with further oxidation of the parent dye and of the benzophenone products.

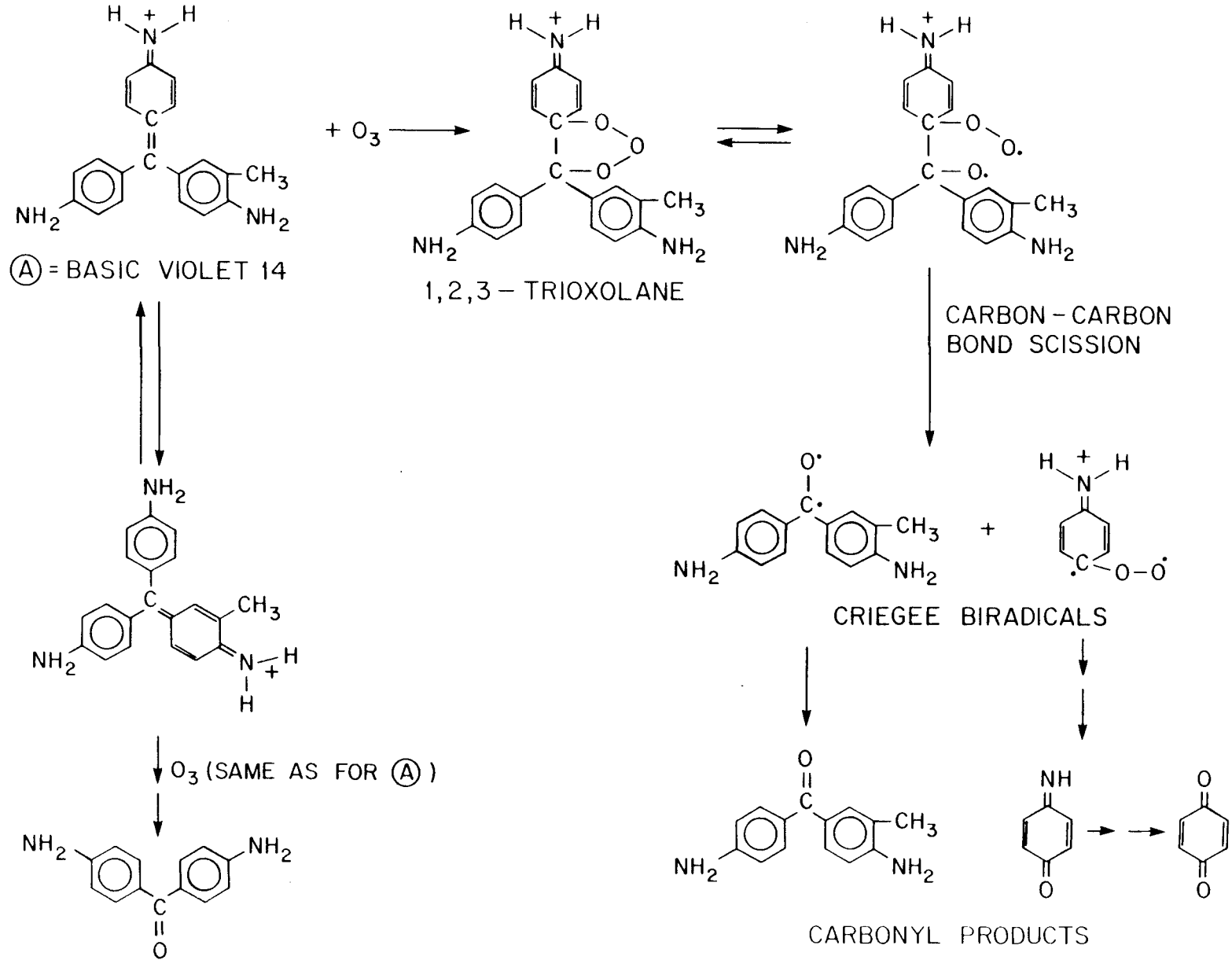

Figure 7.3. Tentative mechanism for the ozone-Basic Violet 14 reaction.

Ozone-030 Mauve Reaction Products

While the 030 Mauve watercolor faded substantially upon exposure to ozone, both on cellulose and on silica gel, the identified reaction products were not consistent with the reported colorant composition. Mass spectra of methanol extracts of the control (unexposed) samples yielded no information, the only observed fragments being those corresponding to benzoic acid as a minor impurity (MH = 123, MH-H_2O = 105, MH-CO_2 = 79). Methanol extracts of the ozone-exposed sample on cellulose yielded, along with the benzoic acid initially present, acetic acid (major) and methyl acetate (minor) as the only products. These products result from oxidation of cellulose acetate and acetic acid esterification in the methanol solvent, respectively. Upon exposure on silica gel, large amounts of phthalic acid (MW = 148, base peak m/z = 149), and benzoic acid (MW = 122, base peak m/z = 123) were formed, along with smaller amounts of phthalimide (MW = 147, base peak m/z = 148).

Reflectance spectra of control and ozone-exposed samples of the 030 Mauve (3,4) suggest that the copper phthalocyanine component did not react appreciably towards ozone. Phthalocyanines are reported to be quite resistant to oxidation, including photooxidation (6,7,18), and to catalyze the air oxidation of aromatic compounds such as that of benzaldehyde to benzoic acid (6). Phthalocyanines may nevertheless react with strong oxidants, e.g., nitric acid (color shifts to purple) or ceric sulfate, to yield phthalimide (18). The small amount of phthalamide we found in the exposed Mauve sample may indicate some decomposition of the copper phthalocyanine upon exposure to ozone on silica gel.

With respect to the other component of the Mauve, the nature of the oxidation products (phthalic and benzoic acids) is not consistent with the reaction products of authentic samples of Basic Violet 14. Further investigation is warranted to determine whether the unexpected reaction products are due to substrate-mediated

effects, changes in chemical structure that occur during the laking process, or to the presence of a colorant other than a Basic Violet 14 lake.

Ozone-Fastness of Triphenylmethane Dyes

While substituent effects, lake composition, substrate and other factors may have significant effects on the ozone fastness of triphenylmethane colorants, the results of our study suggest that members of this group containing unsaturated carbon-carbon bonds may fade upon exposure to ozone. Triphenylmethane colorants that are expected to be ozone-fugitive include the amino substituted cationic dyes Malachite Green, Brilliant Green, Crystal Violet, Basic Fuchsin (see structures in Figure 7.1) and Methyl Green, among others. Acid triphenylmethane dyes (e.g., Acid Fuchsin, CI 42685), hydroxy-substituted members of the rosolic acid series (e.g., Aurin, CI 43800) and members of the xanthene chromophore group such as the Rhodamines (e.g., Basic Red 1, CI 45160) are also expected to fade upon exposure to ozone.

REFERENCES FOR CHAPTER 7

1. Grosjean, D.; Whitmore, P.M.; De Moor, P.C.; Cass, G.R.; Druzik, J.R. *Environ. Sci. Technol. 1987, 21,* 635-643.

2. Grosjean, D.; Whitmore, P.M.; Cass, G.R.; Druzik, J.R. *Environ. Sci. Technol. 1988, 22,* 292-298.

3. Shaver, C.L.; Cass, G.R.; Druzik, J.R. *Environ. Sci. Technol. 1983, 17,* 748-752.

4. Drisko, K.; Cass, G.R.; Whitmore, P.M.; Druzik, J.R. In *Wiener Berichte über Naturwissenschaft in der Kunst, Doppelband 2/3;* Vendl, A.; Pichler, B.; Weber, J. Eds; Verlag ORAC: Vienna, 1985/86.

5. Whitmore, P.M.; Cass, G.R.; Druzik, J.R. *J. Am. Inst. Conserv. 1987, 26,* 45-58.

6. *The Chemistry of Synthetic Dyes;* Venkatamaran, K., Ed.; Academic Press: New York, 1952; Vol. 2, pp. 705-739.

7. *The Chemistry of Synthetic Dyes;* Venkatamaran, K., Ed.; Academic Press: New York, 1971; Vol. 4, pp. 103-157.

8. Arney, J.S.; Jacobs, A.J.; Newman, R.J.; *J. Amer. Inst. Conserv. 1979, 18,* 108-117.

9. Iwamoto, K. *Bull. Chem. Soc. Japan 1935, 10,* 420-425.

10. Desai, C.M.; Vaidya, B.K. *J. Indian Chem. Soc. 1954, 31,* 261-264.

11. Porter, J.J.; Spears, S.B., Jr. *Textile Chem. Colorist 1970, 2,* 191-195.

12. Matsui, M.; Takase, Y. *Senryo to Yakuhin (Dyes and Chemicals) 1982, 27,* 10-17.

13. Grosjean, D.; Sensharma, D.K.; Cass, G.R. "Chemical Ionization Mass Spectra of Artists' Pigments and Dyes: Indigos, Anthraquinones and Triphenylmethanes"; manuscript in preparation, California Institute of Technology, 1988.

14. Hichikawa, H.; Harrison, A.G. *Organic Mass Spectrom. 1978, 13,* 389-396.

15. Bailey, P.S. *Ozonation in Organic Chemistry;* Academic Press: New York, 1982; Vol. 2.

16. Atkinson, R.; Carter, W.L.P. *Chem. Reviews 1984, 84,* 437-470.

17. Martinez, R.L.; Herron, J.T. *J. Phys. Chem. 1987, 91,* 946-953.

18. *The Chemistry of Synthetic Dyes and Pigments;* Luebs, H., Ed.; Reinhold Pub. Corp.: New York, NY, 1955.

CHAPTER 8
THE FADING OF ARTISTS' COLORANTS BY EXPOSURE TO ATMOSPHERIC NITROGEN DIOXIDE

INTRODUCTION

It is widely accepted that control of temperature, humidity, lighting levels and air quality are essential to the preservation of objects housed in museum and archival facilities (1-3). One of the major threats to the air quality in these environments is the intrusion of gaseous pollutants from the outdoor atmosphere, a problem of increasing concern in modern urban areas. The available technologies for reducing indoor particulate matter, ozone (O_3), nitrogen oxides (NO_x), gaseous organics and sulfur dioxide (SO_2) concentrations vary greatly from pollutant to pollutant, both in their physical implementation and in their likelihood of success (3). The exact chemical identity of both the damaging pollutants and sensitive artists' materials must be known if conservators, architects and engineers are to select the most effective measures for protecting a particular collection.

In Chapters 2-7 of this report an experimental program to explore the damage to artists' colorants caused by exposure to atmospheric ozone was described. The color stability of a number of modern watercolors (4,5), natural organic colorants (6), and traditional Japanese colorants (7), has been measured during exposure to air containing ozone, a highly oxidizing air pollutant present in low concentration even in remote atmospheres and, in high concentrations, in photochemical smog. The ozone level in these tests was 0.3 to 0.4 parts per million (ppm), concentrations which are encountered occasionally outdoors during heavy smog episodes. The total amount of ozone administered to the samples in these experiments is roughly equivalent to the accumulated ozone dose during less than ten years in a typical air-conditioned museum environment. The results of these tests indicate that a large number of natural organic colorants, both pigments on paper and dyes on

textiles, and a few synthetic lake pigments, are quite sensitive to ozone exposure, and would probably suffer some color change in a relatively short time if left unprotected in a museum.

Besides ozone, a number of other oxidizing gases are present in the atmospheres of populated areas. A variety of nitrogen oxides commonly occur due to the emissions from combustion sources, and prolonged exposure to atmospheres containing these pollutants has been demonstrated to cause deterioration of certain textiles and textile dyes (8-10). Nitrogen oxides may also promote the acidification of paper, corrosion of metals, and deterioration of stone and photographic film (1-3,9-11).

In most outdoor exposure studies involving nitrogen oxides, the exact identity of the damaging agent has been left undetermined, although nitrogen dioxide (NO_2), among all the nitrogen oxides, has been implicated most strongly. This uncertainty arises because the nitrogeneous pollutants in urban air always occur as a mixture of various oxides of nitrogen: nitric oxide (NO), nitrogen dioxide (NO_2), organic nitrates (e.g. peroxyacetyl nitrate), aerosol nitrates (e.g. NH_4NO_3), and even nitric and nitrous acids. This uncertainty as to the relative hazard of the various nitrogeneous pollutants which coexist in polluted air complicates selection of protective measures because the affinity of the sorbent materials used in air purification systems differs between the various nitrogen oxides species. Nitric acid, for example, can be removed from air rather easily while removal of NO and NO_2 from building atmospheres or protecting objects individually can be very expensive, and, in practice, some museum and library NO_2 removal systems have proven to be largely ineffective (3,12). As NO_2 removal is difficult and expensive, it is very important to know the precise hazard posed by NO_2 in order to set rational objectives for indoor NO_2 concentrations that are commensurate with the risk of damage that NO_2 may pose to a particular museum or archival collection.

This chapter reports the results of a chamber experiment in which the color stability of a variety of artists' materials was evaluated during exposure to air containing nitrogen dioxide in the absence of light. The samples tested were analogous to those examined in the ozone exposure studies: a selection of natural and synthetic colorants applied to paper with little or no binder, and a number of silk cloths dyed with natural dyes. These materials were exposed to a flow of purified air into which a small amount of NO_2 had been added. Nitric acid was specifically removed from the air stream, and the level of the milder oxidant NO was monitored to ensure that it was present only in trace quantities. The observed changes in the color of the samples can thus be attributed to the exposure to nitrogen dioxide, although the detailed chemistry of the deterioration may not be limited to simple NO_2 attack. The nitrogen dioxide dose administered in this test could be accumulated during a few years' exposure in an urban setting: this experiment, then, identifies colorant systems which exhibit extreme sensitivity towards nitrogen dioxide, and provides some measure of the risk faced by objects in museums and archives.

EXPERIMENTAL

Natural organic colorants were obtained from various museum collections, artists' suppliers, and chemical supply houses. These materials, listed in Table 8.1, had been authenticated previously as part of an ozone exposure experiment (6). A selection of synthetic organic and inorganic colorants in current use also was included in this NO_2 exposure test. These dry pigments and watercolors, shown in Table 8.2, were chosen so that a variety of chemical classes were represented, and a few of these modern materials had demonstrated a sensitivity towards ozone (5) or to high concentrations of nitric acid (13). With the exception of the mineral pigments orpiment and realgar, the compositions of the products shown in Table 8.2

Table 8.1. Natural organic colorants tested.

Weld Lake	Natural Yellow 2
Curcumin	Natural Yellow 3
Saffron	Natural Yellow 6
Quercitron Lake	Natural Yellow 9
Persian Berries Lake	Natural Yellow 14
Gamboge	Natural Yellow 24
Cochineal Lake	Natural Red 4
Madder Lake	Natural Red 9
Lac Lake	Natural Red 25
Litmus	Natural Red 28
Dragon's Blood	Natural Red 31
Indigo	Natural Blue 1
Van Dyke Brown	Natural Brown 8
Sepia	Natural Brown 9
Bitumen	Natural Black 6
Indian Yellow	—
Aigami	—

Table 8.2. Synthetic organic and inorganic colorants tested.

Colorant Name	Manufacturer	Composition
Synthetic Organic Colorants		
Arylide Yellow G	Binney & Smith	Monoazo (PY1)
Arylide Yellow 10G	Binney & Smith	Monoazo (PY3)
Paliogen Yellow	BASF	Anthraquinone (PY108)
Toluidine Red	BASF	Naphthol (PR3)
Bright Red (watercolor)	Winsor & Newton	Monoazo (PY1) + Naphthol (PR4)
Scarlet Lake (watercolor)	Winsor & Newton	Monoazo (PR10)
Rose Carthame (watercolor)	Winsor & Newton	Monoazo (PR10) + Xanthene (PR90)
Alizarin Crimson	Winsor & Newton	Anthraquinone (PR83)
Thioindigo Violet	BASF	Thioindigoid (PR88)
Naphthol	Binney & Smith	Naphthol (PR188)
Permanent Magenta (watercolor)	Winsor & Newton	Quinacridone (PV19)
Dioxazine Purple	BASF	Dioxazine (PV23)
Mauve (watercolor)	Winsor & Newton	Triphenylmethane lake (of BV14) + phthalocyanine (PB15)
Phthalo Blue	Binney & Smith	Phthalocyanine (PB15)
Prussian Blue	Binney & Smith	Ferric ferrocyanide (PB27)
Paliogen Blue	BASF	Indanthrone (PB60)
Phthalocyanine Green	Binney & Smith	Phthalocyanine (PG7)
Aniline Black	BASF	Azine (PBk1)
Inorganic		
Chrome Yellow (watercolor)	Winsor & Newton	Lead chromate (PY34)
Aureolin (watercolor)	Winsor & Newton	Potassium cobaltinitrite (PY40)
Cadmium Yellow Medium	Binney & Smith	Cadmium sulfide (PY37)
Manganese Violet	Binney & Smith	Manganese ammonium pyrophosphate (PV16)
Vermilion (watercolor)	Winsor & Newton	Mercuric sulfide (PR106)
Orpiment	Forbes Collection	Arsenic trisulfide (PY39, CI 77086)
Realgar	Ransome Collection	Arsenic disulfide (PY39, CI 77085)

were provided by the manufacturers' literature. The arsenic sulfides, orpiment (As_2S_3) and realgar (As_2S_2), were obtained from the Forbes pigment collection at the Fogg Museum and the Ransome mineral collection at the California Institute of Technology, respectively, and were identified using x-ray diffraction. As described earlier (6), the samples were prepared by airbrushing methanol suspensions/solutions of the colorants (or methanol/water washes of the water-colors) onto 2.5cm x 5cm pieces of hot-pressed watercolor paper.

Iron inks, widely used prior to the 20th century, were prepared according to two standard formulations, one containing a ferrous salt ($FeSO_4 \cdot 7H_2O$) with gallic and tannic acids (Fed. Spec. No. TT-I-563), and the other combining this ferrous compound with gallic and tartaric acids (Fed. Spec. No. TT-I-563b) (14). These recipes also included a blue organic dye to make legible the initial application of the otherwise clear solutions, but this dye was omitted from the inks prepared for this study. The inks were applied to hot-pressed watercolor paper with a pen, and the samples were aged for several months to develop the dark color. In addition to these freshly prepared inks, authentic samples of 19th century inks were also tested in the form of document fragments, obtained from the Huntington Library. No analysis of the chemical composition of these manuscript inks was attempted.

The textiles tested in this NO_2 exposure were silk cloths dyed using traditional colorants and techniques. The dyes and mordants, listed in Table 8.3, were specified by the dyer, and no further analyses were performed. Square swatches of the cloths (2.5cm x 2.5cm) were sewn to pieces of watercolor paper for convenient handling. In addition, a sample of AATCC NO_2 fading standard No. 1 (Disperse Blue 3 on cellulose acetate) was included in the NO_2 exposure experiment.

Color changes were used to indicate the damage caused by the exposure of the colorant systems to nitrogen dioxide. With the exception of the document fragments, the color of the samples was followed throughout the test by periodically

Table 8.3. Natural colorant/mordant combinations for silk cloths tested.

Color	Natural Dye	Mordant
Yellow	*Enju* (Japanese pagoda tree)	Al
	Kariyasu (Miscanthus)	Al
	Kariyasu (Miscanthus)	Cu
	Kihada (Japanese yellow wood)	Al
	Kuchi nashi (Jasmine)	Al
	Ukon (Turmeric)	Al
	Ukon (Turmeric)	Acetic acid
	Woren (*Coptis japonica*)	None
	Yamahaji (Japanese sumac)	Al
	Yama-momo (*Myrica rubia*)	Al
	Zumi (Mustard)	Al
	Shiō (Orpiment, As_2S_3)	None
Red	*Seiyo akane* (Western madder)	Al
	Akane (Japanese madder)	Al
	Enji (Cochineal)	Sn
	Shiko (Lac)	Al
	Suo (Sappanwood)	Al
	Beni (Safflower)	None
Blue	*Ai* (Indigo)	None
Green	*Ai* + *enju*	Al
	Ai + *kariyasu*	Al
	Ai + *kihada*	Al
Violet	*Shikon* (Lithospermum)	Al

measuring the diffuse reflectance spectra, using a Diano Matchscan II spectrophotometer with its beam size limited to 7mm in diameter. This instrument was calibrated with standard reflectance white tiles (which had been referenced to an NBS standard), and a reference white tile was also used as a backing for all the samples during the color measurements. Tristimulus values (X, Y, Z) and color differences (ΔE, from the CIE 1976 L*a*b* formula) were calculated for CIE Illuminant C, and Munsell notations were subsequently computed from these tristimulus values. The precision of the reflectance measurements was a few percent, producing uncertainty in ΔE of about 1 unit: color changes could thus only be detected when the calculated color difference ΔE exceeded this value. The value of ΔE gives the magnitude of a color change and provides a basis for comparing the effect of NO_2 exposure on the colorant systems. The Munsell notation breaks this color change down into changes in the visual perception of hue, value, and chroma, which occur after exposure of the colorant systems.

For the document fragments, color changes were qualitatively evaluated visually (as the line width of the inscriptions was too narrow to allow color measurements using the spectrophotometer). Manuscript samples were cut in half, one portion being exposed to NO_2 while the other was kept sealed and in the dark. At the conclusion of the test, the two halves were compared under simulated daylight in a Macbeth Spectralight color matching booth to determine if the exposure had caused a perceptible color change.

A schematic diagram of the NO_2 exposure apparatus is illustrated in Figure 8.1. Air was pumped, first through packed beds of Purafil (potassium permanganate-impregnated alumina pellets), activated carbon, and Drierite, to remove existing pollutants and moisture, then through a cellulose fiber filter to remove airborne particulate matter. The purified, dried air stream was divided into two metered flows, with one part being humidified by passage through a distilled water bubbler. NO_2

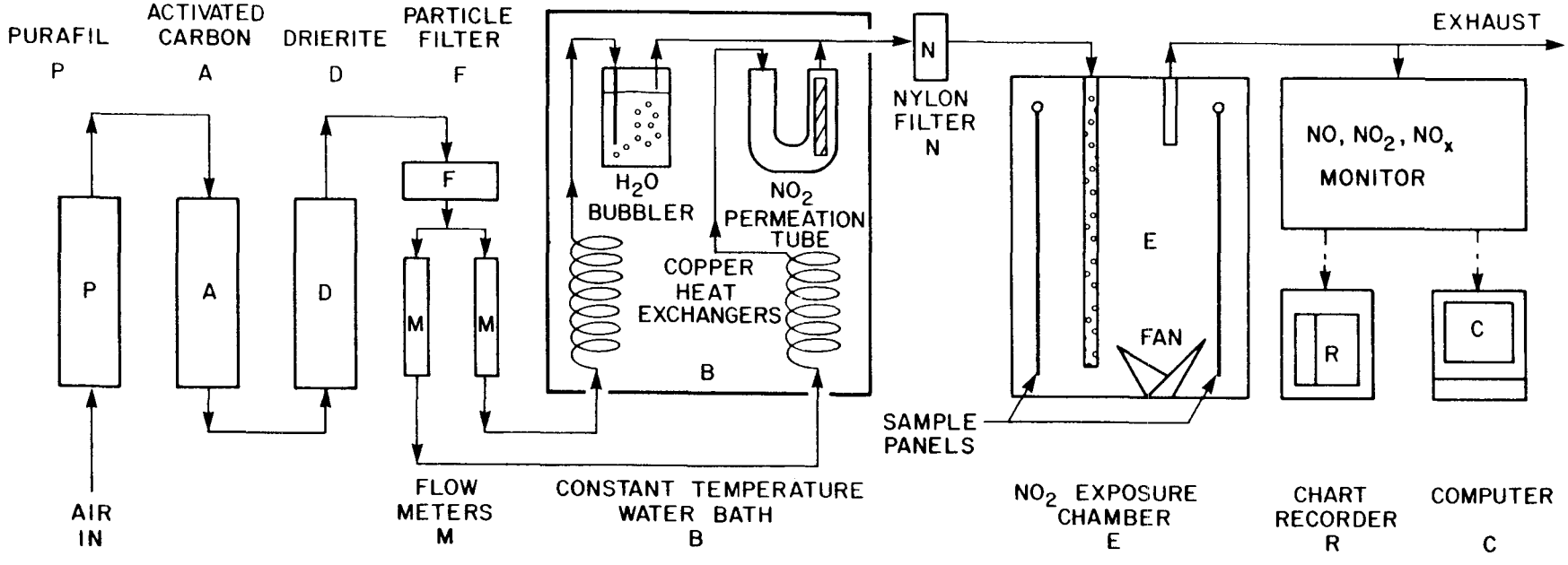

Figure 8.1. Experimental apparatus.

was introduced into the second part of the divided air stream by flowing over a permeation tube (VICI Metronics), a sealed Teflon tube filled with liquid NO_2. Gaseous NO_2 permeates through the wall of this tube at a rate determined by the temperature of the tube and its surroundings, and this temperature was regulated by immersion of the permeation tube holder in a constant temperature water bath. The NO_2-polluted air flow was recombined with the humidified air, and the air stream was passed through a nylon membrane filter (Nylasorb filter, Membrana Corp.) to remove any residual nitric acid before introduction into the exposure chamber through a perforated Teflon tube. Control of the air flow rates and the water bath temperature allowed the maintenance of the desired humidity and pollutant concentration in the exposure chamber.

The exposure chamber was constructed of stainless steel and glass, with the glass walls kept masked to exclude light. The samples were mounted along the interior walls of the chamber, facing the center, on anodized aluminum holders. The air in the box was stirred by a fan blade powered by a magnetically coupled external motor. The temperature and humidity inside the chamber were measured with a thermohygrometer (Pastorelli and Rapkin), and NO_2 and NO concentrations were determined continuously with a chemiluminescent nitrogen oxides monitor (Thermoelectron Corp. Model 14 B/E). Pollutant levels were recorded on a strip chart, and hourly average NO_2 concentrations were automatically calculated and stored by a computer.

In this study, the samples were exposed for 12 weeks at 24°C and 50% RH, in the absence of light. Air flowed through the sample chamber at a rate of 1.0 liter per minute. The concentration of NO_2 during the test was 0.50 ± 0.01 parts per million (ppm), while the NO level was more than an order of magnitude smaller than this (about 0.04 ± 0.01 ppm). Color measurements were performed after 1, 2, 3, 4, 6, 8, and 12 weeks of exposure.

RESULTS

The color measurements of the samples before and after the 12 week exposure to NO_2 are shown in Tables 8.4-8.9. The tristimulus values for CIE Illuminant C are calculated from the reflectance spectra, and color differences and Munsell notations have been calculated from these to indicate the magnitude and nature of the color changes effected by the exposure.

AATCC Standard of Fading

A sample of the AATCC NO_2 fading test ribbon was included in this experiment in order to provide a quantitative measure that anchors the results of this experiment to the large body of work that is presently referenced to that standard. Exposure to the NO_2 concentrations in this test caused a large color change in the AATCC NO_2 fading standard test cloth as indicated in Table 8.4 by the ΔE value of 26.3 after 12 weeks. The calculated Munsell notation for the unexposed and exposed cloth show that (under CIE Standard Illuminant C) the color change takes the form of a large hue shift, from blue toward red, and a decrease in chroma. This is manifested visually as a dramatic reddening and dulling of the originally bright blue cloth, when viewed under ordinary incandescent lights.

Qualitatively, the nature of the color change can be understood by examining the visible reflectance spectrum, the actual experimental observable, before and after the sample has been exposed to the pollutant. Figure 8.2 shows the reflectance spectra for the unexposed and exposed fading standard. The color change is indicated by the change in the spectrum: reflectance values for blue light (about 450nm) decrease and those in the red (about 620nm) increase upon exposure to NO_2. The chroma of the sample color is roughly measured by the steepness of the slopes of the peaks and valleys in the reflectance spectrum. The spectrum of the unexposed sample has reflectance maxima and minima with relatively steep edges: the unexposed sample has a high chroma. Nitrogen dioxide reaction lowers

Table 8.4. Response of AATCC NO_2 fading standard (Disperse Blue 3 on cellulose acetate) to 0.50 ppm NO_2 for 12 weeks.

Weeks of Exposure	Tristimulus X	Y	Z	Munsell	ΔE
0	28.25	26.90	85.80	5.52PB 5.72/12.52	—
12	33.02	30.17	59.49	9.86PB 6.01/6.82	26.34

Table 8.5. Changes observed in natural organic colorants on paper exposed to 0.50 ppm NO_2 for 12 weeks.

Sample	Weeks of Exposure	Tristimulus X	Y	Z	Munsell	ΔE
Paper	0	87.85	89.85	98.03		
	12	88.92	91.08	98.72		0.7
Weld Lake	0	82.51	85.04	83.21		
	12	83.39	85.88	85.16		0.9
Curcumin	0	74.85	80.39	35.95	6.4Y 9.1/6.8	
	12	75.13	79.42	47.88	5.6Y 9.0/4.8	14.5
Saffron	0	76.12	80.24	55.15	5.8Y 9.1/3.9	
	12	75.66	79.35	57.17	5.3Y 9.0/3.6	2.7
Quercitron Lake	0	75.01	79.01	58.83	6.3Y 9.0/3.3	
	12	73.54	76.86	59.98	5.3Y 8.9/3.0	3.2
Persian Berries Lake	0	74.84	80.81	55.15	9.8Y 9.1/3.9	
	12	75.79	81.08	58.80	9.0Y 9.1/3.5	3.5
Gamboge	0	75.04	79.67	56.71	7.2Y 9.0/3.6	
	12	76.43	80.93	62.70	7.8Y 9.1/3.0	4.4
Cochineal Lake	0	58.67	48.87	53.42	8.4RP 7.4/6.8	
	12	59.83	50.87	53.13	0.1R 7.5/6.2	3.7
Madder Lake	0	74.73	70.06	74.09	4.1R 8.6/3.4	
	12	74.89	70.37	75.14	3.7R 8.6/3.4	0.7
Lac Lake	0	60.36	55.33	63.38	7.6RP 7.8/4.0	
	12	62.46	58.74	63.81	2.6R 8.0/3.2	4.9
Litmus	0	79.94	81.79	90.40		
	12	79.45	81.35	88.47		1.0
Dragon's Blood	0	61.79	54.76	36.46	2.6YR 7.7/6.3	
	12	62.03	58.00	38.92	5.8YR 7.9/5.4	7.6
Indigo	0	38.67	40.40	51.16	6.8B 6.8/1.2	
	12	40.08	42.10	50.77	8.1BG 6.9/0.8	2.8
Van Dyke Brown	0	48.85	48.49	42.20		
	12	49.34	48.99	42.35		0.5
Sepia	0	36.79	36.87	32.87	0.1Y 6.5/1.9	
	12	38.49	38.54	33.88	0.1Y 6.7/2.1	1.5
Bitumen	0	54.86	55.30	47.42		
	12	53.92	54.45	46.38		0.6
Indian Yellow	0	77.32	80.58	51.59		
	12	78.52	81.81	52.32		0.6
Aigami	0	54.11	56.86	69.22	0.3B 7.9/0.9	
	12	58.03	60.70	67.97	9.9GY 8.1/0.6	5.2

Table 8.6. Changes observed in modern synthetic organic colorants on paper exposed to 0.50 ppm NO_2 for 12 weeks.

Sample	Weeks of Exposure	Tristimulus X	Y	Z	Munsell	ΔE
Arylide Yellow G	0	76.48	82.75	45.55		
	12	76.01	82.29	45.16		0.2
Arylide Yellow 10G	0	74.48	83.27	45.19		
	12	75.10	83.95	45.49		0.4
Paliogen Yellow	0	76.80	83.30	49.81		
	12	76.11	82.52	49.17		0.4
Toluidine Red	0	57.06	46.32	36.19		
	12	56.48	45.81	35.23		0.7
Bright Red	0	62.20	52.49	30.55		
	12	62.01	52.41	30.30		0.4
Scarlet Lake	0	62.16	47.31	38.80		
	12	61.70	47.07	38.17		0.7
Rose Carthame	0	66.47	53.71	48.44		
	12	67.46	54.67	48.57		1.0
Alizarin Crimson	0	62.72	55.23	56.56	2.1R 7.8/5.3	
	12	64.35	57.68	57.86	3.8R 7.9/4.8	2.9
Thioindigo Violet	0	47.04	38.41	52.90		
	12	46.93	38.38	52.15		0.7
Naphthol	0	59.01	45.47	32.84		
	12	58.81	45.36	32.37		0.5
Permanent Magenta	0	55.67	48.80	66.83		
	12	55.24	48.50	65.59		0.8
Dioxazine Purple	0	36.90	31.64	58.30	4.7P 6.1/7.2	
	12	37.45	32.35	58.01	4.9P 6.2/6.8	1.6
Mauve	0	46.42	40.17	71.30	5.1P 6.8/7.3	
	12	46.72	41.62	70.08	4.9P 6.9/6.3	4.6
Phthalocyanine Blue	0	50.00	53.49	82.18		
	12	49.72	53.22	80.35		1.1
Prussian Blue	0	41.92	46.28	73.16		
	12	41.58	46.05	71.72		1.0
Paliogen Blue	0	42.56	43.79	71.81	4.1PB 7.0/4.8	
	12	42.60	44.20	69.39	3.2PB 7.1/4.2	2.6
Phthalocyanine Green	0	48.01	59.10	63.81		
	12	47.53	58.52	62.77		0.5
Aniline Black	0	29.51	30.25	34.34		
	12	29.32	30.03	33.76		0.5

Table 8.7. Changes observed in inorganic pigments on paper exposed to 0.50 ppm NO_2 for 12 weeks.

Sample	Weeks of Exposure	Tristimulus X	Y	Z	Munsell	ΔE
Chrome Yellow	0	77.09	81.92	39.57		
	12	78.14	83.12	40.30		0.6
Aureolin	0	76.78	84.42	46.90		
	12	77.28	85.01	47.12		0.3
Cadmium Yellow Medium	0	73.97	79.41	30.42		
	12	73.31	78.74	29.83		0.4
Manganese Violet	0	47.17	39.42	61.56		
	12	46.90	39.25	60.52		0.8
Vermilion	0	64.66	56.60	41.15		
	12	64.17	56.25	40.57		0.5
Orpiment	0	75.75	79.43	56.54	5.2Y 9.0/3.7	
	12	77.33	81.36	64.62	6.8Y 9.1/2.8	5.7
Realgar	0	74.95	75.27	52.12	0.9Y 8.8/4.2	
	12	78.81	80.64	67.99	2.4Y 9.1/2.6	10.6

Table 8.8. Changes observed in iron ink samples on paper exposed to 0.50 ppm NO_2 for 12 weeks.

Sample	Weeks of Exposure	Tristimulus X	Y	Z	Munsell	ΔE
Iron Ink I	0	19.77	19.42	25.11	5.6P 5.0/1.2	
	12	21.84	21.82	24.90	7.9R 5.2/0.5	5.8
Iron Ink II	0	24.88	24.47	31.44	5.9P 5.5/1.3	
	12	29.68	29.65	33.51	9.7R 6.0/0.6	7.4

Table 8.9. Color changes observed in Japanese dyed silk cloths exposed to 0.50 ppm NO_2 for 12 weeks.

Sample	Weeks of Exposure	Tristimulus X	Y	Z	Munsell	ΔE
Seiyo akane/Al	0	21.23	15.31	8.35		
	12	21.80	15.76	8.42		1.0
Akane	0	34.33	27.60	14.04	1.3YR 5.8/7.9	
	12	36.15	29.27	14.56	1.7YR 5.9/8.0	2.1
Suo/Al	0	17.84	12.01	8.89	3.6R 4.0/8.3	
	12	17.98	12.34	8.93	4.0R 4.0/7.9	1.8
Shiko/Al	0	17.24	11.25	10.77	0.2R 3.9/8.6	
	12	18.16	11.96	11.11	0.6R 4.0/8.6	1.6
Enji/Al	0	18.98	11.36	10.70		
	12	19.34	11.59	10.72		0.7
Beni	0	30.79	22.62	11.73		
	12	31.38	23.06	12.05		0.5
Ukon/Al	0	47.36	46.24	11.18	2,1Y 7.2/9.5	
	12	46.58	45.49	11.36	2.0Y 7.2/9.3	1.4
Ukon/acetic acid	0	48.01	47.01	11.23	2.2Y 7.3/9.6	
	12	46.85	45.68	10.96	2.0Y 7.2/9.5	1.2
Kariyasu/Cu	0	30.71	31.09	10.50	3.6Y 6.1/6.6	
	12	30.88	31.13	11.03	3.4Y 6.1/6.4	1.5
Kariyasu/Al	0	45.93	47.95	22.37		
	12	46.68	48.65	22.65		0.6
Enju/Al	0	44.06	45.78	11.28	4.7Y 7.2/8.8	
	12	40.51	41.66	12.19	4.3Y 6.9/7.9	7.8
Kihada/Al	0	45.72	46.85	17.91		
	12	45.88	46.87	17.87		0.4
Kuchi nashi/Al	0	32.19	29.60	5.68	0.2Y 6.0/9.4	
	12	31.99	29.22	6.12	9.8Y 5.9/9.2	2.5
Yamahaji/Al	0	47.47	47.82	27.31	2.4Y 7.3/4.9	
	12	45.80	45.75	25.89	1.8Y 7.2/5.0	1.7
Woren	0	51.09	50.47	15.84	2.2Y 7.5/8.4	
	12	52.32	51.63	15.96	2.2Y 7.6/8.6	1.2
Yama-momo/Al	0	30.65	30.51	19.14	1.5Y 6.0/3.8	
	12	30.00	29.07	17.89	9.7YR 5.9/4.1	3.2
Zumi/Al	0	40.67	40.93	17.61	2.9Y 6.8/6.1	
	12	38.70	38.76	17.60	2.6Y 6.7/5.8	3.1
Shiō	0	57.79	59.52	23.05	3.9Y 8.0/7.4	
	12	59.05	60.75	25.77	3.7Y 8.1/7.0	3.3
Ai	0	35.79	39.69	57.71	5.7B 6.8/3.5	
	12	36.69	40.79	57.24	4.2B 6.8/3.2	2.0
Ai + *enju*/Al	0	29.77	35.55	13.63	3.2GY 6.4/6.6	
	12	32.06	37.07	14.68	1.8GY 6.6/6.3	3.6
Ai + *kariyasu*/Al	0	9.31	11.14	12.00	7.3G 3.9/2.5	
	12	9.91	11.79	12.62	6.8G 4.0/2.4	1.1
Ai + *kihada*/Al	0	12.33	14.87	8.39	5.5GY 4.4/4.0	
	12	12.93	15.34	9.15	5.3GY 4.5/3.7	1.9
Shikon/Al	0	9.35	8.14	12.75	7.7P 3.3/2.7	
	12	9.83	8.55	12.58	9.8P 3.4/2.6	2.0

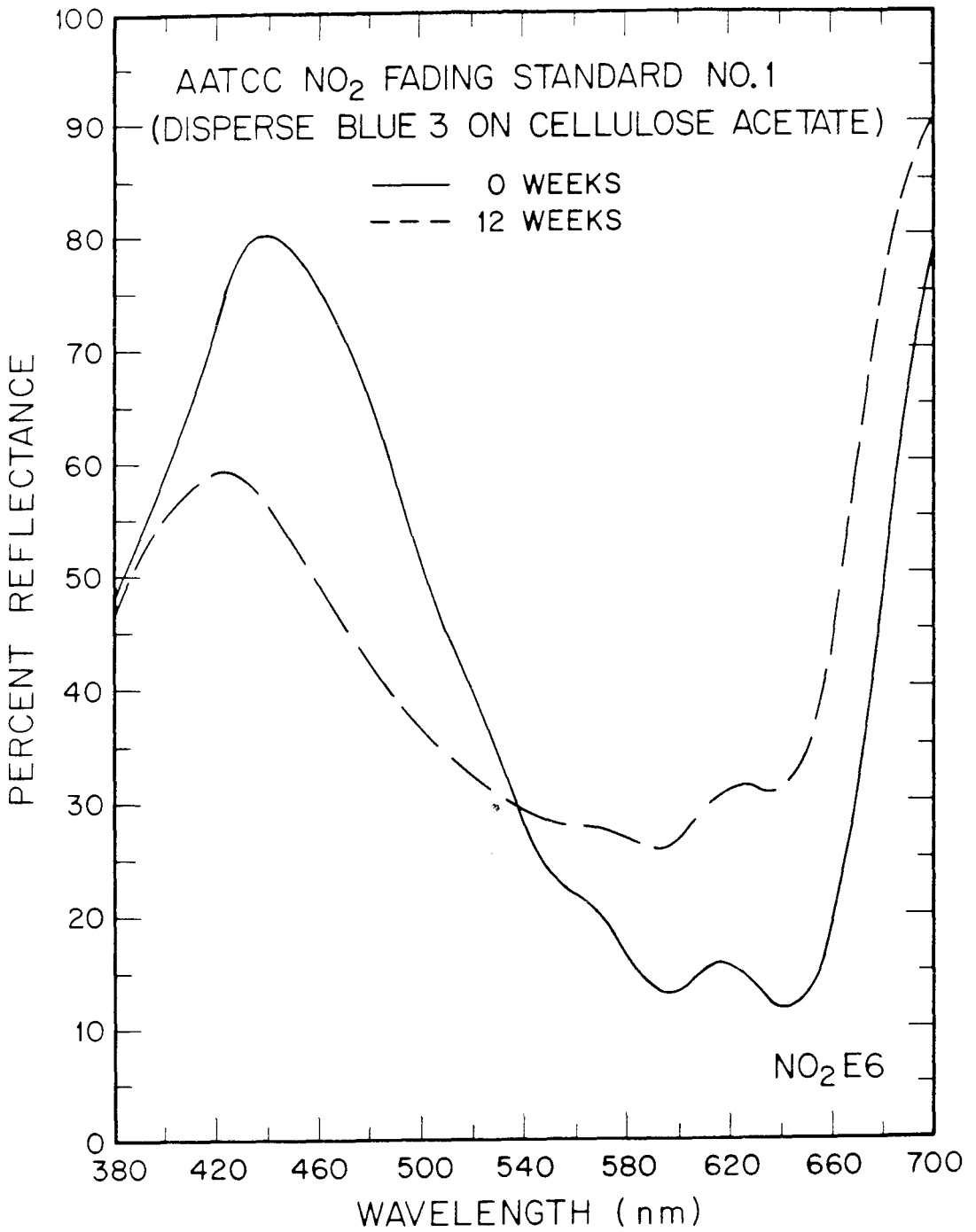

Figure 8.2. Reflectance spectrum of the AATCC NO_2 fading test ribbon (Disperse Blue 3 on cellulose acetate) before and after exposure to 0.50 ppm NO_2 at 24°C, 50% RH for 12 weeks in the absence of light.

the peak and raises the valley, and a much less sharp transition between them results: the chroma has been reduced. The average level of the reflectance is about 40% for both spectra, so the Munsell value is roughly unchanged after the exposure.

Colorants on Paper

The effect of exposure to 0.5 ppm NO_2 for 12 weeks on a variety of colorants on paper is given in Tables 8.5-8.8. These colorant samples on paper were applied as uniformly as possible in an attempt to produce samples of identical depth of shade, which would permit a direct comparison of the relative vulnerability of these colorant systems towards NO_2. Exposure of plain paper to this pollutant produced a slight yellowing (Table 8.5) although the measurement of a color change this small is difficult, and whether this results from degradation of the paper or absorption of nitrogen dioxide is unknown.

Many of the natural colorant systems showed color changes much larger than that of the plain paper: curcumin, dragon's blood, *aigami* (dayflower blue), lac lake, gamboge, cochineal lake, Persian berries lake, quercitron lake, indigo, and saffron, each showed evidence of reactivity towards NO_2. The changes in the reflectance spectra for many of these samples show a slight yellowing (decrease in the reflectance of blue light) in addition to an increase in the minimum of the reflectance spectrum (which suggests a decrease in the concentration of the original colorant). The change in the reflectance spectrum is illustrated in Figure 8.3 for the sample of cochineal lake on paper.

When the samples are considered on the basis of chemical structure, the diaroyl methane, curcumin, seems to be the most fugitive. Pigments derived from flavonoid plant dyes (e.g., quercitron and Persian berries lake) seem to be sensitive to NO_2 exposure, and two of the colorants which contain anthraquinone compounds, cochineal and lac lake, also experience a color change upon NO_2 exposure. However, the madder lake sample tested here, a third natural colorant containing

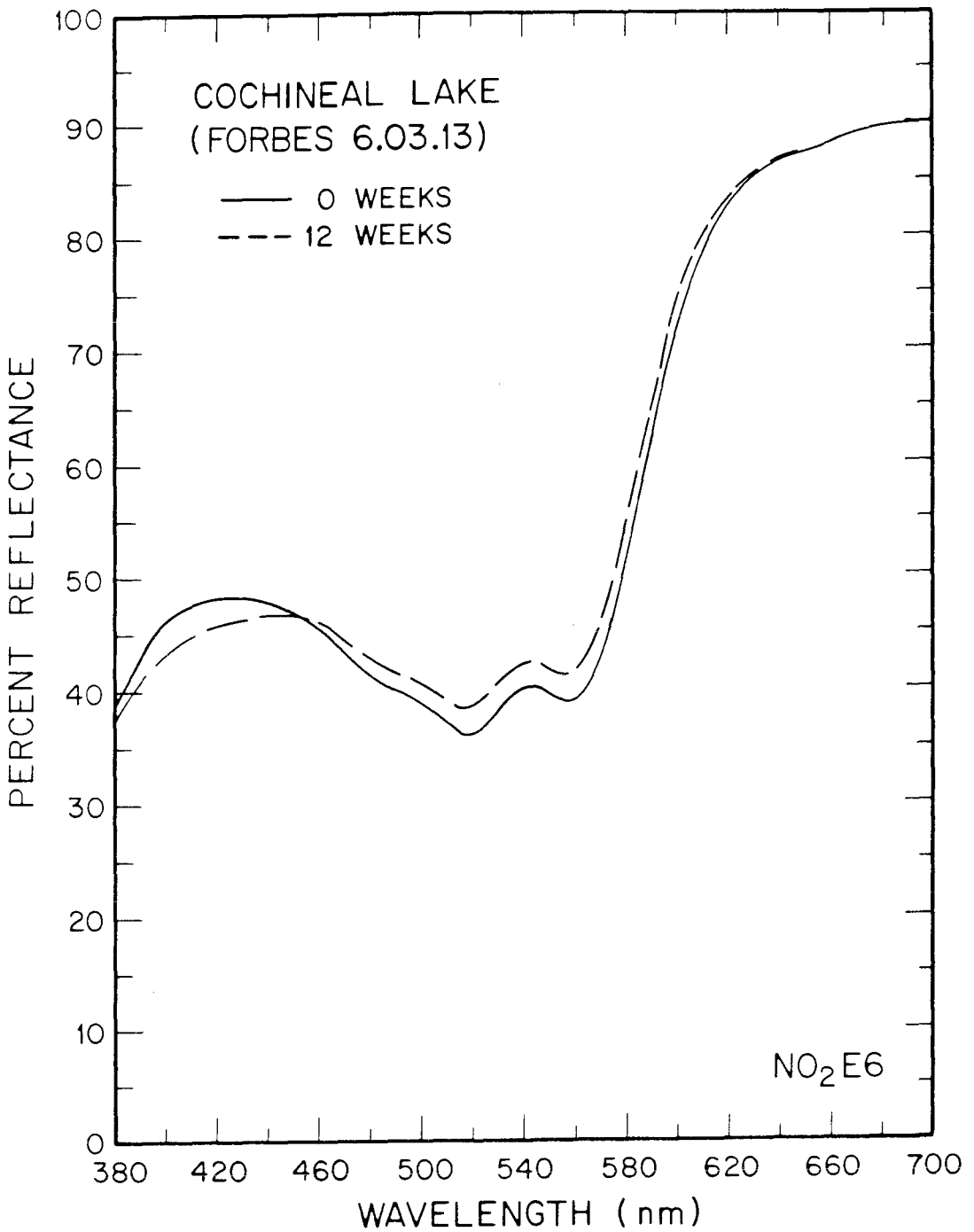

Figure 8.3. Reflectance spectrum of Cochineal Lake dry pigment on watercolor paper before and after exposure to 0.50 ppm NO_2 at 24°C, 50% RH for 12 weeks in the absence of light.

predominantly anthraquinone-type colorant molecules, is apparently unreactive to this NO_2 dose. Similarly, the weld lake, derived from a mixture of flavonoid dyes, also seems unchanged by this NO_2 exposure. Despite this difference in the rate of color change, NO_2 does affect a broad spectrum of natural colorants on paper.

Of the synthetic organic colorants tested on paper, four showed measurable color changes after the 12 week NO_2 exposure. Alizarin crimson (PR83), a calcium-aluminum lake of alizarin, the major anthraquinone dye found in madder root, showed a rather mild sensitivity, as did dioxazine purple (PV23) and Paliogen blue (PB60), a blue aminoanthraquinone-based colorant. A fourth colorant mixture, the Winsor and Newton "Mauve" watercolor, which reportedly contains a phthalocyanine blue and a lake of a triphenyl methane dye, showed a somewhat larger color change after the exposure. All of the observed color changes involve a shift in hue, a decrease in chroma, and a very slight increase in value. A slight yellowing (indicated by a decrease in reflectance of blue light) contributes to the hue shift produced in these samples.

Only two of the inorganic colorants on paper showed evidence of a color change after exposure to NO_2. The arsenic sulfides, orpiment and realgar, faded considerably during the experiment. These sulfides applied to paper with no binder, have been observed to fade over time even in the absence of light and pollutants. The orpiment and realgar both oxidize naturally to form the more stable arsenic oxide (arsenolite), and this transformation was observed to proceed more rapidly in the presence of ozone (7). In the present case, however, the fading occurred more slowly than in the ozone exposure test, and it is not clear whether the color change accompanying natural oxidation of these colorants has been accelerated by the presence of NO_2.

Finally, the two samples of iron ink on paper, one an iron gallotannate (Ink I), and the other an iron tannate (Ink II), both experienced a color change in this test.

The dark blue-violet colors of these inks developed slowly after the application of the originally clear ink solution. After the oxidation of the iron salt upon exposure to air for two months, the color had stabilized, and the exposure test was begun. Twelve weeks of exposure to 0.50 ppm NO_2 caused a fading as well as a slight yellowing of the ink/paper samples. By contrast, visual comparison of exposed and unexposed old manuscript samples showed no perceptible change in the ink or paper upon exposure to NO_2.

Natural Colorants on Silk

The textile materials (other than the AATCC fading standard) tested in this experiment were silk cloths dyed with natural colorants that have been used traditionally in Japan. As seen in Table 8.9, some color changes were produced in these cloths by the NO_2 exposure, but in most cases these changes were quite small. The largest color change occurred for the sample of *enju* (from the Japanese pagoda tree), and this example is also notable because the sample has darkened (i.e., the value has decreased) upon NO_2 exposure. At this point, the color changes noted are specific to the entire system studied: dyes/mordant/silk cloth substrate. Examples of undyed mordanted material were unavailable, so the effect of the NO_2 exposure on the silk substrate alone could not be studied. Also, the available samples were not dyed to the same depth of shade. Therefore, the color changes observed are indicators of whether or not each colorant system is sensitive to NO_2, but cannot be used to precisely rank the NO_2 sensitivities of the colorant systems. Nevertheless, the fact remains that a number of these materials show some degree of color instability in an environment containing NO_2.

DISCUSSION

There are several chemical mechanisms by which gaseous nitrogen dioxide is capable of degrading artists' materials. NO_2 is a mild oxidant, causing the oxidation

of materials which are not readily affected by exposure to atmospheric oxygen. Unsaturated organic compounds (i.e., molecules which contain carbon-carbon double bonds) are particularly vulnerable to oxidation reaction, and this reaction will often cause breakdown of a polymer (such as cellulose) or decolorization of a colorant. In addition to oxidation reactions, NO_2 can cause the formation of nitro- ($-NO_2$) or nitroso ($-ONO_2$) groups by addition to organic molecules. These products tend to have a yellow color derived from the $-NO_2$ chromophore. Finally, the gaseous NO_2 can react to form acidic species – nitric acid, nitrous acid, and nitrate salts – by oxidation in the air or on surfaces of materials. These compounds would tend to affect materials which are acid sensitive (paper, textiles, and many colorants, for example) or subject to electrochemical corrosion processes (10).

Although very few mechanistic studies have been performed on systems which experience damage from exposure to NO_2, a pattern of the NO_2 attack emerges which is consistent with the known chemical pathways for NO_2 reaction. The so-called "reddening" of the blue aminoanthraquinone textile dyes (such as the Disperse Blue 3 used in the AATCC test cloth for NO_2 exposure) has been attributed to the oxidation of the amine groups ($-NH_2$), to the nitro groups ($-NO_2$) (15), and the fading of other textile dyes may be a result of the oxidation of their chromophoric carbon-carbon double bonds. Some textile fibers themselves, as well as additives, show pronounced yellowing from exposure to NO_2 (16). These sensitive compounds contain amine groups which are presumably oxidized to form the yellow nitro- or nitroso-containing products. Cotton and nylon fibers show a loss of tensile strength upon NO_2 exposure, probably from hydrolytic breakdown of the polymer structure of the fiber (17). Finally, the accelerated corrosion and stress cracking of some metals has been linked to the deposition of hygroscopic nitrate salts on their surfaces (18).

Visual evidence of material damage observed in this experiment suggests that

similar NO_2 chemistry is operative in the exposure of colorants on paper. The apparent yellowing of the paper could result from the formation of yellow nitro or nitroso compounds in either the cellulose fibers or possibly in the gelatin sizing of the paper. Fading of the organic colorants is probably due to oxidation of the chromophores in those molecules, but in those cases where the hue is also changed (as is the case for the iron inks) nitration of the organic molecules is possible. A more complete chemical analysis of the products of these NO_2 reactions is beyond the scope of the present work. For now, the exact nature of the attacking species and the mechanism of the damage is undetermined, but at this point the changes which have occurred are a result of exposure only to NO_2, as precautions were taken to exclude the other oxides of nitrogen from the present exposure experiment.

In light of the results of this test, the risk posed to museum collections by prolonged exposure to indoor atmospheres containing NO_2 can be assessed. The NO_2 dose accumulated by the samples is roughly equivalent to that which would be encountered during two years of exposure inside an unprotected museum in downtown Los Angeles or during 5 to 6 years of exposure to the atmosphere in many other urban settings. Although no colorant systems showed the extreme sensitivity of the AATCC fading cloth, there were several colorant systems – notably the *enju* on silk, curcumin, dragon's blood, and the iron inks on paper – which suffered noticeable color changes in this test. The yellowing of the rag paper and/or gelatin sizing suggests that perhaps the degradation of the structural integrity of supports may be as serious a problem as the discoloration of pigments and dyes. In any event, the damage incurred by a few of these samples should probably be viewed as unacceptable, especially since they are cumulative effects which will become more severe with longer exposures or higher pollutant levels.

REFERENCES FOR CHAPTER 8

1. Thomson, G., *The Museum Environment,* Butterworths, London, 1978.

2. Baer, N.S. and Banks, P.N., "Indoor Air Pollution: Effects on Cultural and Historic Materials," *Int. J. Museum Manage. Curatorship 4,* 1985, 9-20.

3. Committee on Preservation of Historical Records, *Preservation of Historical Records,* National Academy Press, Washington, D.C., 1986, Chapter 3.

4. Shaver, C.L., Cass, G.R., and Druzik, J.R., "Ozone and the Deterioration of Works of Art," *Environmental Science and Technology 17,* 1983, 748-752.

5. Drisko, K., Cass, G.R., Whitmore, P.M., and Druzik, J.R., "Fading of Artists' Pigments due to Atmospheric Ozone," in *Wiener Berichte über Naturwissenschaft in der Kunst,* Bd. 2/3, 1985/86, ed. A. Vendl, B. Pichler and J. Weber. Vienna:Verlag ORAC.

6. Whitmore, P.M., Cass, G.R., and Druzik, J.R., "The Ozone Fading of Traditional Natural Organic Colorants on Paper," *J. Amer. Inst. Cons., 26,* 1987, 45-58.

7. Whitmore, P.M., and Cass, G.R., "The Ozone Fading of Traditional Japanese Colorants," *Studies in Conservation, 33,* 1988, 29-40.

8. Rowe, F.M. and Chamberlain, K.A., "Fading of Dyes on Cellulose Acetate Rayon," *J. Soc. Dyers Colour., 53,* 1937, 268-278.

9. Graedel, T.E. and McGill, R., "Degradation of Materials in the Atmosphere," *Environ. Sci. Technol. 20,* 1986, 1093-1100.

10. *Air Quality Criteria for Oxides of Nitrogen,* EPA Report EPA 600/8-82-026, U.S. Environmental Protection Agency, Washington, D.C., 1982, 13-1–13-29.

11. Yocom, J.E., Baer, N.S., Robinson, E., "Air Pollution Effects on Physical and Economic Systems," in *Air Pollution,* ed. A.C. Stern, Vol. VI, New York, Academic Press, 1986.

12. Hughes, E.E. and Myers, R., "Measurement of the Concentration of Sulphur Dioxide, Nitrogen Oxides, and Ozone in the National Archives Building," NBSIR 83-2767, National Bureau of Standards, Washington, D.C.

13. Whitmore, P.M., and Cass, G.R., unpublished results.

14. Kirk, R.E., and Othmer, D.F., eds., *Encyclopedia of Chemical Technology,* Vol. 7, Interscience Encyclopedia, Inc., New York, 1951, 870.

15. Couper, M., "Fading of a Dye on Cellulose Acetate by Light and by Gas Fumes," *Textile Res. J. 21,* 1951, 1720-725.

16. Salvin, V.S., "Yellowing of White Fabrics due to Air Pollutants," in *Collected Papers of the American Association of Textile Chemists and Colorists,* National Technical Conference, New Orleans, 1974, 40-51.

17. Morris, M.A., "Effect of Weathering on Cotton Fabrics," California Agricultural Experiment Station Bulletin 823, Davis, CA, 1966.

18. Hermance, H.W., Russell, C.A., Bauer, E.J., Egan, T.F., and Wadlow, H.V., "Relation of Airborne Nitrate to Telephone Equipment Damage," *Environ. Sci. Technol. 5,* 1971, 781-789.

CHAPTER 9
MATHEMATICAL MODELING OF CHEMICALLY REACTIVE POLLUTANTS IN INDOOR AIR

INTRODUCTION

The existence of a fading hazard to works of art posed by photochemical oxidants depends in part on whether or not the high ozone and NO_2 concentrations found in outdoor urban air are transferred to the indoor atmospheres of museums. In this chapter, a computer-based mathematical model is developed and tested for predicting the indoor concentrations of photochemically-related air pollutants. The model is designed for subsequent use as a tool for diagnosing the causes of the high indoor pollutant levels that are found in certain buildings. The model also may be used by architects and engineers to test the likely performannce of building air handling and purification systems in advance of their construction.

Considerable progress has been made recently in developing mathematical models for predicting pollutant concentrations in outdoor ambient air. In modeling urban air basins, state-of-the-art approaches utilize a spatially resolved grid with explicit treatment of advective transport, photochemical reactions, deposition to the earth's surface, and pollutant emissions (1,2). Regional models, used in the study of acid deposition, incorporate many of the above features plus transformation processes involving pollutant reaction within aqueous droplets (3).

By comparison, most approaches to modeling pollutant concentrations in indoor air have been relatively primitive, treating pollutant species as chemically independent and assuming the building interior to be a single, well mixed volume (e.g., see ref. 4-7). Extended developments have included 1) multichamber formulations (8-10), 2) a model for predicting radon progeny concentrations which incorporated a description of natural convection (11), and 3) explicit treatment of the kinetics of the primary photolytic cycle (9). To date, however, there has not been

an indoor air pollution model with the capability of explicitly treating an arbitrary chemical kinetic mechanism.

Despite the moderate success of the models cited above, there are many reasons which argue for development of a model for indoor air pollution that explicitly incorporates reactive chemistry. Data on indoor pollutant concentrations suggest that chemical reactions may proceed at rates comparable to, or even much greater than, the ventilation rate (for example, $NO + O_3$ and $NO_2 + O_3$). A major element of the mass-balance models cited above—the "reactivity" (5) or "indoor sinks" (4) —is not well understood, and there are discrepancies between the wall-loss rates determined in chamber studies and field experiments (12,13). Some secondary pollutants produced, for example, in photochemical smog may not be well determined by the simple mass-balance approach. And finally, it is becoming increasingly apparent that many indoor environments are as complex in their constitution—if not more so—than polluted outdoor environments (e.g., see ref. 14). It is reasonable to expect, given the wide range of pollutants which may be emitted directly indoors, the introduction of pollutants from outdoor air via the ventilation system, and the wide range of indoor lighting levels (and hence photolytic reaction rates), that there are numerous circumstances in which a chemically explicit model is needed to accurately predict indoor pollutant concentrations.

In this chapter, a general mathematical model is formulated that describes the time dependence of indoor air pollutants in a chemically reacting system. An important contribution of this formulation over previous work is the explicit treatment of gas-phase photolytic and thermal reactions. The model is formulated to also compute for each species the production rates associated with ventilation, chemical reaction, and direct emission, and the removal rates associated with ventilation, chemical reaction, filtration, and wall loss. As a partial validation of the model, a case is simulated in which outdoor air, containing photochemically reactive

air pollutants, is introduced into a museum gallery. The simulated indoor concentrations of ozone, nitric oxide and NO_x-NO are compared with measured data during a 2-day period in November 1984. Several interesting perturbations from this base case are considered to study the likely effects of pollutant sources and altered building materials on indoor air chemistry.

MODEL FORMULATION

Two fundamental postulates form the basis of the model:

1. The building can be represented as a set of chambers, with the air flow rate from each chamber to all others known as a function of time. Each chamber is visualized as a room or group of rooms. The core of each chamber is considered to be well mixed and separated from the building surfaces by a thin concentration boundary layer. The details of the boundary layer affect the rate of pollutant removal at fixed surfaces, but may otherwise be neglected in determining pollutant concentrations.

2. Within each chamber, the rate of change of the concentration of each chemical species may be described by an equation of the form

$$\frac{dC}{dt} = S - LC \tag{9.1}$$

where S represents the sum of all sources: direct emission, advective transport from other chambers (including the mechanical ventilation system and outdoors), and production by chemical reaction; L represents the sum of all sinks: loss by homogeneous chemical reaction, transformation and removal processes occurring on surfaces, and removal by transport from the chamber. S and L are, in general, functions of time and of the concentrations of all pollutant species in all chambers.

The following subsections present details of the manner in which the various elements of the problem are treated in the model.

Ventilation

The treatment of ventilation is an extension of the formulation of Shair and Heitner (4) to incorporate an arbitrary number of chambers. A schematic illustration of the approach is presented in Figure 9.1. For each chamber, air may enter directly from outside (infiltration), from the mechanical ventilation system (supply), and from each of the other chambers (cross-ventilation). Air may be removed to the outside (exfiltration or exhaust), to the mechanical ventilation system (return), and to each of the other chambers. The mechanical ventilation system is treated as a special chamber having zero volume. In addition to the return air from each chamber, air from outdoors (makeup) may be supplied directly to the mechanical ventilation system. Pollutant removal devices ("filters") may be specified for each return-air line and for the makeup air line. Also, within each chamber, air may be recirculated through a filter. For each pollutant species, the filtration efficiency may be specified by the user.

Mathematically, if we consider a chemically inert compound, the effects of the ventilation system may be represented as follows:

$$\frac{dC_i}{dt} = \sum_{j=0}^{n} \left[\frac{f_{ji}C_j - f_{ij}C_i}{V_i} \right] + \left[\frac{f_{xi}C_x - f_{ix}C_i}{V_i} \right] - \frac{\eta_{ii} f_{ii} C_i}{V_i} \tag{9.2}$$

and

$$C_x = \frac{\sum_{j=0}^{n} (1 - \eta_{jx}) f_{jx} C_j}{\sum_{j=0}^{n} f_{xj}} \tag{9.3}$$

where C_i = the concentration of the compound in chamber i, V_i = the volume of chamber i, f_{ij} = the volume flow rate from chamber i to chamber j, η_{ij} = the

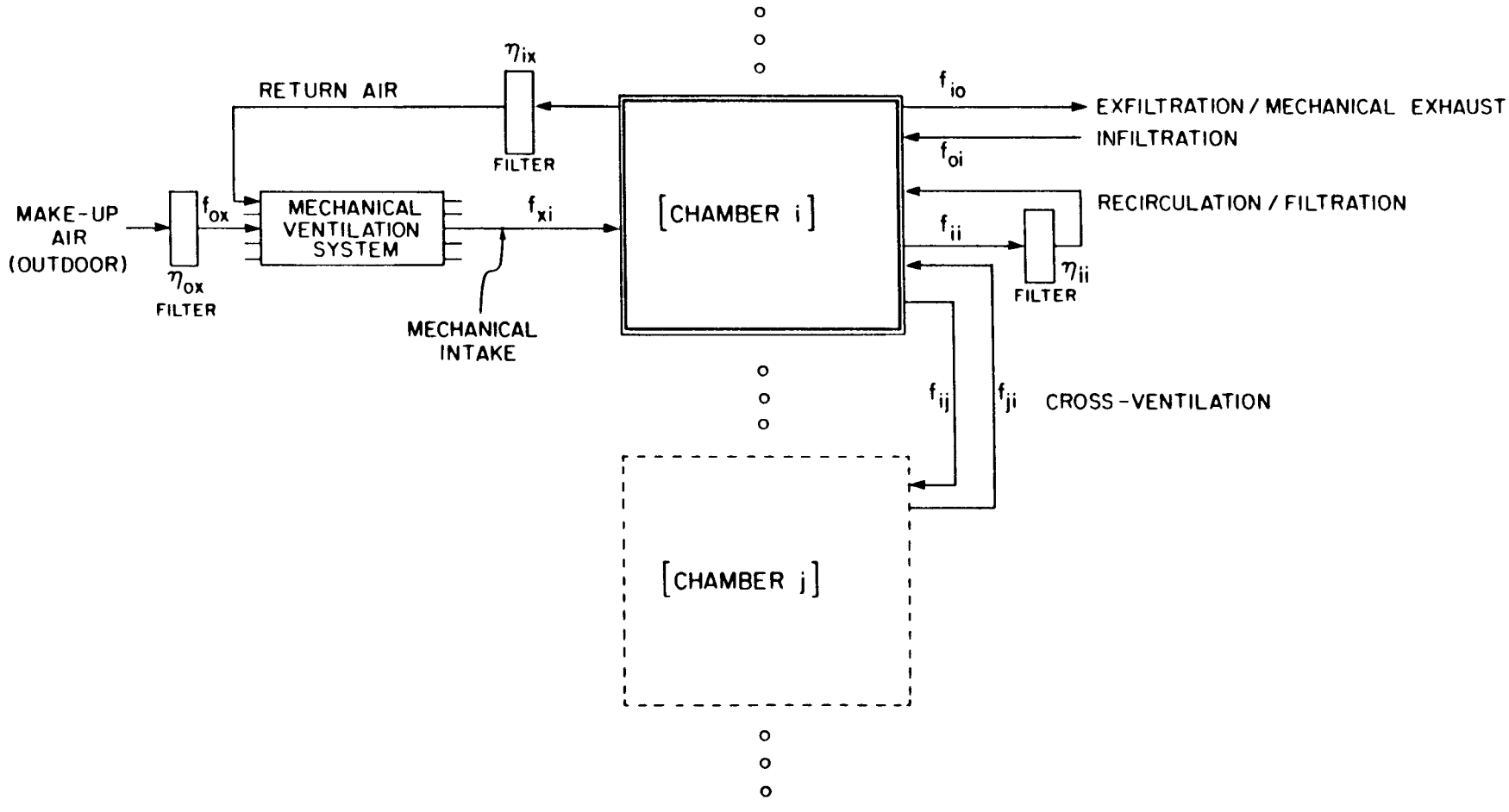

Figure 9.1. Schematic representation of the ventilation components of the multichamber indoor air quality model.

efficiency of removal of the compound by the filter located in the air stream connecting chamber i to chamber j, and subscripts x and 0 refer, respectively, to the mechanical ventilation system and to outdoor air. Equation 9.2 can readily be converted into the form of Equation 9.1.

Ventilation data for a specific building can be obtained in several ways. Tracer gas experiments may be used to determine flow rates between pairs of chambers (15). Under the uniform-mixing assumption, flow rate measurements in ventilation system ducts may be used to provide the necessary data. In buildings without mechanical ventilation systems, such as many residences, simple models may be used to predict infiltration (16).

Chemical Kinetics

The model can be adapted to incorporate any of the kinetic mechanisms commonly employed in outdoor photochemical air quality models and can be modified to explicitly treat special problems occurring from the indoor emission of unusual chemical substances. For the examples illustrated in the present chapter, a modified version of the Falls and Seinfeld chemical mechanism is employed (1,2,17-20). More than 50 simultaneous chemical reactions are considered. Because the current form of the mechanism is not available in a single reference, it is presented in Table 9.1 of this chapter.

Photolysis Rates

A number of important atmospheric chemical reactions are photolytic in nature. Rates of such reactions depend on the spherically integrated photon flux and are commonly expressed as

$$k_p = \int_0^\infty \sigma[\lambda]\phi[\lambda]I[\lambda,t]\mathrm{d}\lambda \tag{9.4}$$

Table 9.1. Kinetic Mechanism (1, 2, 20-22)

	Reaction	Rate Constant (ppm min K units)
1	$NO_2 + h\nu \rightarrow NO + O(3P)$	a
2	$O(3P) + O_2 + M \rightarrow O_3 + M$	$0.346\ T^{-2} \exp(510/T)$
3	$O_3 + NO \rightarrow NO_2 + O_2$	$9.245 \times 10^5\ T^{-1} \exp(-1450/T)$
4	$NO_2 + O(3P) \rightarrow NO + O_2$	$3.99 \times 10^6\ T^{-1}$
5	$NO + O(3P) \rightarrow NO_2$	$1.67 \times 10^5\ T^{-1} \exp(584/T)$
6	$NO_2 + O(3P) \rightarrow NO_3$	$8.81 \times 10^5\ T^{-1}$
7	$O_3 + NO_2 \rightarrow NO_3 + O_2$	$5.19 \times 10^4\ T^{-1} \exp(-2450/T)$
8	$NO_3 + NO \rightarrow 2\ NO_2$	$8.81 \times 10^6\ T^{-1}$
9	$NO + OH \rightarrow HNO_2$	$5.07 \times 10^6\ T^{-1}$
10	$HNO_2 + h\nu \rightarrow NO + OH$	a
11	$HO_2 + NO_2 \rightarrow HNO_2 + O_2$	$17.3\ T^{-1} \exp(1006/T)$
12	$HNO_2 + OH \rightarrow H_2O + NO_2$	$2.91 \times 10^6\ T^{-1}$
13	$NO_2 + HO_2 \rightarrow HNO_4$	$1.73 \times 10^4\ T^{-1} \exp(1006/T)$
14	$HNO_4 \rightarrow HO_2 + NO_2$	$1.80 \times 10^{15} \exp(-9950/T)$
15	$HO_2 + NO \rightarrow NO_2 + OH$	$3.58 \times 10^6\ T^{-1}$
16	$RO_2 + NO \rightarrow NO_2 + RO$	$3.58 \times 10^6\ T^{-1}$
17	$RCO_3 + NO \rightarrow NO_2 + RO_2 + CO_2$	$1.13 \times 10^6\ T^{-1}$
18	$NO_2 + OH \rightarrow HNO_3$	$4.401 \times 10^{17}\ T^{-1}\ (280/T)^{1/2}\ 10^{-(11.6T/(17.4+T))}$
19	$CO + OH\ (+ O_2) \rightarrow HO_2 + CO_2$	$1.31 \times 10^5\ T^{-1}$
20	$O_3 + h\nu \rightarrow O(3P) + O_2$	a
21	$HCHO + h\nu\ (+ 2\ O_2) \rightarrow 2\ HO_2 + CO$	a
22	$HCHO + h\nu \rightarrow H_2 + CO$	a
23	$HCHO + OH\ (+ O_2) \rightarrow HO_2 + H_2O + CO$	13890
24	$RCHO + h\nu \rightarrow HO_2 + RO_2 + CO$	a
25	$RCHO + OH\ (+ O_2) \rightarrow RCO_3 + H_2O$	25680
26	$C_2H_4 + OH \rightarrow RO_2$	11660
27	$C_2H_4 + O(3P) \rightarrow HO_2 + RO_2$	1219
28	$OLE + OH \rightarrow RO_2$	89142
29	$OLE + O(3P) \rightarrow RO_2 + RCO_3$	22118
30	$OLE + O_3 \rightarrow 0.5\ RCHO + 0.5\ HCHO + 0.3\ HO_2 + 0.31\ RO_2 + 0.14\ OH + 0.03\ RO$	0.136
31	$ALK + OH \rightarrow RO_2$	4700

Table 9.1. (Cont.)

Reaction		Rate Constant (ppm min K units)
32	ALK + O(3P) → RO_2 + OH	99.8
33	ARO + OH → RO_2 + RCHO	16112
34	RO → HO_2 + 0.5 HCHO + RCHO	2.0×10^5
35	RONO + hν → RO + NO	a
36	RO + NO → RONO	4.38×10^6 T^{-1}
37	RO + NO_2 → RNO_3	2.19×10^6 T^{-1}
38	RO + NO_2 → RCHO + HNO_2	1.91×10^5 T^{-1}
39	NO_2 + RO_2 → RNO_4	1.64×10^6 T^{-1}
40	b	
41	RNO_4 → NO_2 + RO_2	1.80×10^{15} exp(-9950/T)
42	RCO_3 + NO_2 → PAN	6.17×10^5 T^{-1}
43	PAN → RCO_3 + NO_2	4.77×10^{16} exp(-12516/T)
44	NO_2 + NO_3 → N_2O_5	7.48×10^5 T^{-1}
45	N_2O_5 → NO_2 + NO_3	4.07×10^{16} exp(-11080/T)
46	H_2O + N_2O_5 → 2 HNO_3	5.66×10^{-4} T^{-1}
47	O_3 + OH → HO_2 + O_2	6.62×10^5 T^{-1} exp(-1000/T)
48	O_3 + HO_2 → OH + 2 O_2	4.85×10^3 T^{-1} exp(-580/T)
49	NO_3 + hν → NO + O_2	a
50	HO_2 + HO_2 → H_2O_2 + O_2	3.4×104 T^{-1} exp(1100/T) + 5.8×10^{-5} T^{-2} exp(5800/T) [H_2O] [c]
51	H_2O_2 + hν → 2 OH	a
52	RO_2 + RO_2 → 2 RO + O_2	2.04×104 T^{-1} exp(223/T)
53	NO_3 + HCHO (+ O_2) → HNO_3 + HO_2 + CO	0.86
54	NO_3 + RCHO (+ O_2) → HNO_3 + RCO_3	3.6
55	NO_3 + hν → NO_2 + O(3P)	a
56	NO_3 + OLE → RPN[d]	3288 T^{-1}
57	NO_2 + NO_3 → NO_2 + NO + O_2	175 T^{-1}

[a] Rate depends on photon flux; see Table 9.2.

[b] Reaction in earlier mechanisms that was subsequently eliminated.

[c] [H_2O] is water vapor concentration in ppm.

[d] Nitroxyperoxyalkyl nitrates and dinitrates, not considered to participate in further chemistry.

where $\sigma[\lambda]$ is the absorption cross-section of the molecule (cm^2), $\phi[\lambda]$ is the quantum yield, $I[\lambda,t]$ is the photon flux density (photons cm^{-3} s^{-1}), and λ is the wavelength of light (cm).

The most accurate calculation of photolysis rates within a given building requires data on the spectral, spatial, and temporal distribution of the ambient lighting, and the model is capable of handling information provided at that level of detail. However, in many cases lighting levels indoors are so much lower than those outdoors that many otherwise important photolytic reactions proceed at small or even negligible rates. For such cases an approximate approach is provided.

In the approximate case, light is treated as having two components, ultraviolet (300—400 nm) and visible (400—760 nm). Within each component, the spectral distribution is assumed to be flat. Consequently,

$$k_p = h_{uv} I_{uv} + h_{vis} I_{vis} \tag{9.5}$$

$$h_{uv} = (100\ \text{nm})^{-1} \int_{300\text{nm}}^{400\text{nm}} \sigma\phi \, d\lambda \tag{9.6}$$

$$h_{vis} = (360\ \text{nm})^{-1} \int_{400\text{nm}}^{760\text{nm}} \sigma\phi \, d\lambda \tag{9.7}$$

In Equation 9.5, I_{uv} and I_{vis} represent the spherically integrated (spatially averaged) photon flux (photons cm^{-2} s^{-1}) in the ultraviolet and visible bands, respectively. The constants h_{uv} and h_{vis} are determined from published data (21,22) and are presented in Table 9.2.

In the model, the ultraviolet and visible fluxes are each assumed to have two components, one due to artificial lighting, the other due to sunlight entering through windows or skylights. For the former, hourly values of the photon flux are specified in each band. For the latter, hourly values of ultraviolet and visible attenuation factors are specified. These factors are then applied to the outdoor

Table 9.2. Coefficients Used to Determine Photolysis Rates (21, 22)

Reaction		h_{uv} (10^{-20} cm^2)	h_{vis} (10^{-20} cm^2)
1	$NO_2 + h\nu \rightarrow NO + O(3P)$	39.4	0.95
10	$HNO_2 + h\nu \rightarrow NO + OH$	8.1	0
20	$O_3 + h\nu \rightarrow O(3P) + O_2$	0.16	0.21
21	$HCHO + h\nu (+ 2\ O_2) \rightarrow 2\ HO_2 + CO$		0.58 0
22	$HCHO + h\nu \rightarrow H_2 + CO$	0.43	0
24	$RCHO + h\nu \rightarrow HO_2 + RO_2 + CO$	0.56	0
35	$RONO + h\nu \rightarrow RO + NO$	8.7	0.21
49	$NO_3 + h\nu \rightarrow NO + O_2$	0	11.5
51	$H_2O_2 + h\nu \rightarrow 2\ OH$	0.13	0
55	$NO_3 + h\nu \rightarrow NO_2 + O(3P)$	0	99.1

photon fluxes determined using a solar simulator (22).

For calculations of outdoor radical concentrations, outdoor photolysis rates are required. Here, the approach of McRae et al. (22) is followed without modification.

Data on indoor light levels sufficient to exercise the model for a specific building may be obtained with a radiometer and ultraviolet light meter (23,24) as described in a later section of this paper. Ultraviolet photon flux also may be inferred by measuring the photolysis rate of NO_2 (25).

Treatment of Highly Reactive Species

In the indoor model calculations, the pseudo-steady-state approximation (PSSA) (26) is applied for O, OH, and RO. The PSSA is also employed to determine the outdoor concentrations of these three species and HNO_4, HO_2, NO_3, N_2O_5, RCO_3, RNO_4, and RO_2 as has been done in simulating outdoor air pollution (27).

Heterogeneous Reactions

In addition to photolytic and thermal reactions occurring in the gas phase, important processes may occur on fixed surfaces such as the floor, walls, and ceiling, and on or within airborne particles. Considerable evidence demonstrates that such processes have substantial impact on both outdoor (e.g., see ref. 20) and indoor (e.g., see ref. 4) pollutant concentrations.

In previous indoor air pollution models, these processes have been lumped into a first-order decomposition rate, k_s, often assumed to take place entirely on fixed surfaces. An alternative, but nearly equivalent, formulation is in terms of deposition velocity, v_d, which is defined as the ratio of the pollutant flux to a surface to the free-stream concentration. The rate of change of pollutant concentration due to this process alone is then given by

$$\frac{dC}{dt} = -k_s C = -v_g \left(\frac{A}{V}\right) C \tag{9.8}$$

where A/V represents the superficial surface-to-volume ratio of the room.

This approach is far from ideal. Processes such as the catalytic conversion of one pollutant species to another and adsorption followed a substantial time later by desorption are not accommodated by this approach. Yet recent evidence suggests that NO_2 may be converted to NO on walls (6) and that, in the presence of NO_2, nitrous acid is formed at substantial rates by heterogeneous reaction (28,29). At present too little is known to incorporate an explicit description of important surface reactions other than unimolecular decomposition and irreversible adsorption.

Measurements of heterogeneous reaction rate or deposition velocity have been reported for several species, as summarized in Table 9.3.

The loss rate depends, in general, on not only the combined reactivity of the compound and the surface, but also on the degree of air movement. Since direct evidence on surface-loss rates of some highly reactive species in the model do not exist (e.g., for HNO_3), it is appropriate that evidence pertaining to the transport-limited deposition velocity be considered.

Although seldom realized in rooms, the case of perfectly still air represents the lower bound on the transport-limited deposition velocity. Here, the deposition velocity is of the order of 10^{-3}cm s^{-1}, determined by the molecular diffusion coefficient divided by a characteristic dimension of the room.

For rooms in which the air is not still, the analogy between heat and mass transfer can be used to obtain estimates of the transport-limited deposition velocity. Gadgil (30) developed a model to predict the rate of heat transfer from room walls due to natural convection. In simulating a $3 \times 3 \times 3$ m enclosure with one wall maintained at 4.5°C higher than the other surfaces, he found an average Nusselt number of 145 for the hot wall. For a compound with a diffusion coefficient

Table 9.3. Measurements of Indoor Deposition Velocity

Species	Dep. Vel. (cm s^{-1})	Notes
O_3	0.036±0.021	24 measurements in 13 buildings; one excluded due to suspected NO source (4).
	0.02-0.07	inferred from measurements of ozone loss rate in a single residence (12).
	0.001-0.11 (New) 0.0005-0.015 (Aged)	for various materials exposed in a chamber study (12).
	0.027[a] (Aluminum) 0.015 (Stainless Steel) 0.036 (Office) 0.061 (Bedroom)	inferred from measurements of ozone loss rate in experimental chambers and rooms (44).
	0.001-0.20	for various typical indoor materials exposed in a test room (45).
NO	-0.0001±0.001	decay rate in a house of emissions from gas-fired range; assumed A/V = 2 m^{-1} (46).
	0.0008	decay rate in a house of emissions from gas-fired range; assumed A/V = 2 m^{-1} (47).
	0.0017±0.0014	analysis of data from gas-stove emissions experiment using simplified kinetic model; assumed A/V = 2 m-1 (9).
	0.0000-0.003	for various indoor surface materials, measured in test chamber; 20-26 C, 40-60% RH (48).
NO_2	0.018±0.009	concentration decay rate from gas-stove emission experiment in test room; 11 runs; includes homogeneous reactions; assumed A/V = 2 m^{-1} (5).
	0.011	decay rate in a house of emissions from gas-fired range; assumed A/V = 2 m-1 (47).
	0.006 (50% RH) 0.011 (60% RH) 0.017 (70% RH)	analysis of decay rates from emissions due to gas- and kerosene-fired unvented heaters; attempt to exclude homogeneous reactions (6).
	0.0003-0.12	for various indoor surface materials, measured in test chamber; 20-26 C, 40-60% RH (48).
HCHO	0.005±0.003	analysis of concentration decay rate from gas-stove emission experiment in test room; 5 runs; includes homogeneous reactions; assumed A/V = 2 m^{-1} (5).

[a] Data show strong positive correlation with relative humidity, varying from 0.0007 cm/s at 5% RH to 0.028 cm/s at 87% RH.

of 0.2 $cm^2\ s^{-1}$, the transport-limited deposition velocity to this wall would be 0.1 $cm\ s^{-1}$. This compares well to the deposition velocity of 0.13 $cm\ s^{-1}$, obtained by applying the Von Karman integral momentum balance to a 3-m long, vertically oriented plate, heated to 4.5°C above the free-stream air (31). Wilson (32) measured the relaxation time for air temperature in a suddenly cooled room. His results suggest a transport-limited deposition velocity of 0.07 $cm\ s^{-1}$ for natural convection and 0.18 $cm\ s^{-1}$ for stirred air, again assuming a diffusion coefficient of 0.2 $cm^2\ s^{-1}$.

Somewhat higher values are indicated by experimental studies of the behavior of unattached decay products of radon in rooms. The deposition velocity for these species, which are believed to be removed at surfaces at the transport-limited rate, have been found to be 0.06—0.6 $cm\ s^{-1}$, with the consensus value of 0.2 $cm\ s^{-1}$ (33). The diffusion coefficient of these species is approximately 0.05 $cm^2\ s^{-1}$, smaller than that for gaseous pollutants with lower molecular weights.

The results from Wilson and from the theoretical heat-transfer studies suggest that for circumstances in which room air is not highly stirred, the average transport-limited deposition velocity is within 50% of 0.07 $cm\ s^{-1}$. Further research is needed to resolve the discrepancy with studies of radon decay-product removal at surfaces.

Outdoor Concentrations

With the current chemical mechanism the model requires as input the hourly averaged outdoor concentration of 15 species or groups of species. These data may be obtained by direct outdoor measurement or from a photochemical air quality model that describes the chemical evolution of the outdoor air over time (1,20). For the application reported in this paper, an approach was used which combines outdoor monitoring data with inferences based on detailed experimental and modeling studies.

Initial Conditions

The initial indoor pollutant concentrations are treated in the same way as the outdoor concentrations: concentrations of 15 species are specified and the remaining 10 are computed assuming that steady-state conditions prevail. For most buildings, simulation results are relatively insensitive to changes in the initial conditions: the limiting characteristic time associated with a perturbed initial condition is given by the inverse air-exchange rate which in many cases is less than 1 h.

Direct Emissions

The model accepts as input the direct indoor emission of any species other than O, OH, and RO. As currently formulated, hourly averaged values are specified, and linear-interpolation is used to obtain the emission rate at any instant during the simulation. This rate is added directly to the source term S in Equation 9.1.

Numerical Solution Technique

The procedure used for solving the system of coupled differential equations that constitutes the model is known as the asymptotic integration method (34). The implementation used in the present model was slightly modified from that established by McRae et al. (27). The program is written in Vax-11 Fortran and is run on a Vax-11/750. A 24-h simulation of a single chamber with an average integration time step of 10 s requires approximately 8 min of CPU time.

MODEL APPLICATION: VIRGINIA STEELE SCOTT GALLERY

Introduction

Control of indoor pollutants is sought not only to prevent adverse health effects but also to limit the rate of materials damage. Some of the most stringent standards for indoor air quality are specified for museums, archives, and rare book

libraries. Since these collections must be preserved indefinitely, even very slow rates of deterioration could lead to unacceptable accumulated damage. Recommended objectives for indoor SO_2, NO_x, and O_3 concentrations in such facilities are a few parts per billion (35). Strong acids (e.g., HCl), organic acids (e.g., acetic acid) and formaldehyde are to be controlled to the lowest possible levels (36).

Analytical tools are needed both to predict the levels of chemically complex mixtures that will occur in new buildings prior to their construction, and to diagnose the source of pollutants present in existing facilities. Surface loss of pollutants is particularly important in museums as it indicates the dose delivered to the collection. In the present chapter, simulations are conducted of pollutant levels in a newly constructed museum, based on data taken for this purpose at the Virginia Steele Scott Gallery on the Huntington Library grounds in San Marino, CA. First, the model is exercised to verify that it correctly represents indoor pollutant levels in this building as it was constructed. Next, the effect of a series of hypothetical perturbations on that building's design are analyzed. These cases illustrate circumstances in which homogeneous chemistry in indoor air assumes added significance in determining the concentrations of photochemically reactive pollutants.

Description of the Site

Figure 9.2 shows a floor plan of the west gallery at the Scott building and the ventilation flow rates, taken from the architectural plans and engineering specifications. The conditioned volume of the west gallery is 2530 m^3 and the superficial surface area is 3060 m^2. In the gallery areas, rooms 101 and 102, which constitute 86% of the conditioned volume, the floors are oak plank, and the walls are painted plaster and plywood. The ceiling consists of plaster-veneer coffered beams and plastic diffusers. Above room 101 are skylights; fluorescent lamps behind the diffusers provide background lighting to room 102. The lighting in both

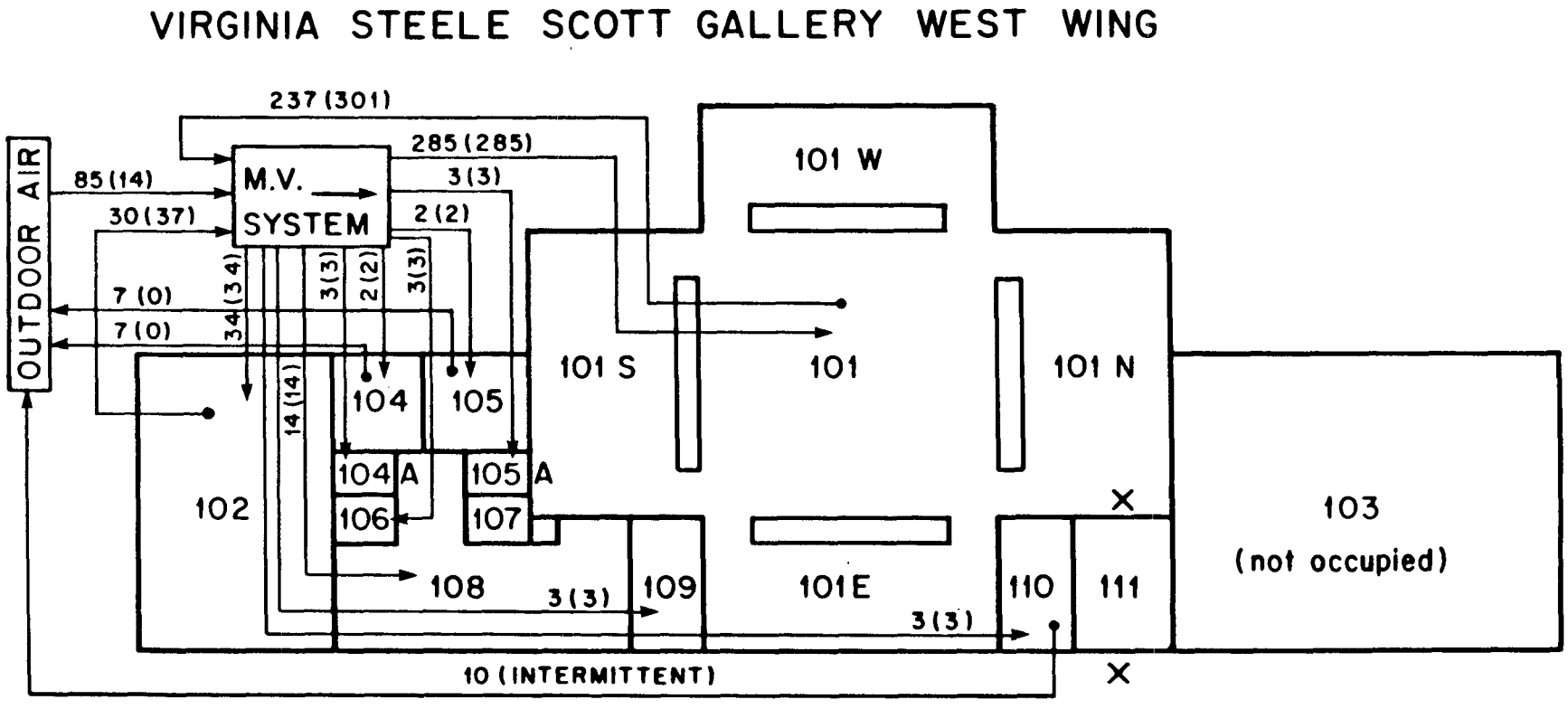

Figure 9.2. Floor plan of the west wing of the Virginia Steele Scott Gallery, San Marino, California. Daytime (nighttime) ventilation flow rates are given in units of $m^3\ min^{-1}$. Air sampling locations for the validation experiment are indicated by "x".

rooms is supplemented by track lamps. Floor coverings in the other rooms are granite or ceramic tile, or linoleum-type flooring. Walls and ceilings are, for the most part, gypsum dry-wall.

The ventilation system is designed to maintain a temperature of 70±1°F and a relative humidity of 50±3% in the galleries. The only pollutant removal devices in the ventilation system at the time of our tests are strainer mat-type filters (U.L. Class 2, Farr 30/30), designed to remove coarse particulate matter. When the internal recirculation fan is on, the total air flow rate through the mechanical ventilation system is 345 $m^3\ min^{-1}$. The outdoor makeup air flow rate assumes two values: 85 $m^3\ min^{-1}$ during the day and 14 $m^3\ min^{-1}$ at night. The daytime setting was maintained from approximately 7 a.m. to 6 p.m. during the study period. In each room, supply and return registers are located on the ceiling raising the possibility of ventilation "short-circuiting" which would lead to a smaller effective ventilation rate than suggested by the flow rate data. However, the relatively low outdoor-air exchange rate (0.3—2.0 h^{-1}) and the absence of rapid fluctuations in monitored pollutant concentrations, combined with the relatively large recirculation rate (8 h^{-1}), suggests that convection was sufficient to effect rapid mixing during the daytime. On the other hand, the indoor data show fluctuations in pollutant concentrations at night that could be due to incomplete mixing.

Monitoring Experiment

For a 10-day period beginning on 30 October 1984, O_3, NO, and NO_2 concentrations were monitored inside and outside the Scott Gallery. Ozone concentrations were measured with a pair of UV photometric ozone monitors (Dasibi models 1003-AH and 1003-PC). A pair of chemiluminescent NO_x monitors (Thermo Electron Corporation, model 14 B/E) was used to measure NO and NO_2. NO_2 values measured by this method include contributions from other nitrogen-containing species such as HNO_3 and PAN (37). The symbol NO_2* will be used to signify measurement data for

this group of species, determined as NO_x-NO by the monitors. The NO_x monitors were calibrated daily against zero air and a known supply of 0.4 ppm NO in nitrogen. Data from all instruments were continuously registered on strip-chart recorders. Pollutant concentration values averaged over 12-min intervals throughout the experiment were extracted from the strip-chart records.

On two days during the monitoring period, 4 and 5 November, peak outdoor O_3 concentrations exceeded 120 ppb in the presence of NO_x levels in excess of 200 ppb. Because of the relatively high pollution levels, model validation efforts were focused on these days.

Input Data for the Validation

Because of the large recirculation rate and the large fractional volume in room 101, the Scott Gallery was initially modeled as a single chamber. Ventilation rates were those indicated in the architectural specifications, as the building had been balanced recently against those specifications. Filter efficiency was assumed to be zero for all gaseous species.

Ultraviolet and visible photon fluxes were computed from data taken both in room 101 and outdoors with a radiometer equipped with a UV cutoff filter (Eppley model PSP; filter GG 395) and a spot meter (UVC meter) designed to measure the ratio of radiance in the ultraviolet to the total illuminance (23,24). From these measurements the skylights were estimated to transfer a photon flux equal to 0.7% of the visible light and 0.15% of the ultraviolet light falling on the roof of the building outdoors. Artificial lighting was estimated to contribute flux densities of 0.7×10^{15} and 2.3×10^{13} photons $cm^{-2}\,s^{-1}$ in the visible and ultraviolet, respectively, between 9 a.m. and 6 p.m.

For the "base case" simulation, deposition velocities reported in the literature for NO, NO_2, O_3, and HCHO have been used (see Table 9.4). Higher aldehydes were

Table 9.4. Simulation Input Parameters

Base Case

Deposition Vel.(cm s-1):	O3	0.036
	NO2	0.006
	HCHO,RCHO	0.005
	PAN	0.035
	HNO2, HNO3, HNO4, HO2, H2O2, NO3, N2O5, RCO3, RNO4, RONO, RO2	0.07
	NO, ALK, ARO, CO, C2H4, OLE	0.0

All other input parameters discussed in text.

Low NO2 Wall Loss (WL)

Same as base case except deposition velocity for NO2 changed to 0.0.

No Explicit Chemistry (No Chem)

Same as base case except rates of all reactions in kinetic mechanism set to 0.0.

Multichamber Case

Same as base case except building treated as four chambers:

Chamber 1 - Rooms 101, 101E, 101W, 101N, 101S
Chamber 2 - Room 102
Chamber 3 - Rooms 104, 104A, 105, 105A, 106, 107, 108, 109
Chamber 4 - Rooms 110, 111

Mechanical ventilation rates determined from architectural specifications (see Figure 9.2). Cross-ventilation flow rates taken as minimum necessary to balance air flows. Artificial lighting assumed same for each chamber. Daylighting only in chamber 1.

Indoor Hydrocarbon Source (HC Source)

Same as base case with added continuous indoor emission of hydrocarbons at following rates (ppb min^{-1}):

Alkanes	46.7
Aromatics	9.6
Olefins	9.6

This corresponds approximately to evaporation of 10 cm^3 h^{-1} of gasoline (22) and is taken as a model either of the use of a naptha-based solvent as may occur in a preservation lab, or of the presence of an underground garage.

Indoor Oxides of Nitrogen Source (NOx Source)

Same as base case with added emission of combustion-generated pollutants during the hours 0700-1300 at following rates (ppb min^{-1})

Nitrogen dioxide	2.5
Nitric oxide	2.5
Carbon monoxide	64.4
Formaldehyde	0.6

Simulates the emissions due to gas-fired cooking equipment such as might be present in a cafeteria. Emissions data from Traynor et al (5). Assumes 10 range-top burners and 5 ovens (residential sized) on continuously during 6-hour cooking period. Range hoods assumed to reduce emissions into the main volume to 40% of the total (49).

Glass-Walled Building (Glass-Walled)

Changes from base case: 1) all deposition velocities reduced to 5% of base case values (based on chamber measurements of deposition rates on glass surfaces, 12,48); 2) indoor photolysis rates computed assuming indoor photon flux in visible range is 50% of that outdoors and that ultraviolet light is further attenuated according to the transmissivity data for window glass given in Summer (50).

assumed to have the same surface removal characteristics as formaldehyde. Removal of highly reactive species (H_2O_2, PAN, HNO_2, RNO_2, RNO_4, HNO_3, N_2O_5, NO_3, HO_2, RO_2, HNO_4, and RCO_3) was taken to proceed at a transport-limited rate, based principally on Wilson's experiments. Other species (e.g., CO) are assumed to be sufficiently inert that their removal rates at building surfaces are negligible.

Data on outdoor concentrations of the 15 pollutants required by the model were specified by the following approach.

The outdoor monitoring data on O_3, NO, and NO_2* collected on-site were used. Based on the results of monitoring studies (38,39) outdoor HNO_3 and PAN concentrations in ppb were estimated as 10% and 5%, respectively, of the outdoor ozone concentration in ppb. The concentrations of HNO_3 and PAN were subtracted from the measured NO_x-NO concentration to correct for interference in determining the NO_2 values used in the validation study (37).

The outdoor data taken at the Scott Gallery were compared with NO, NO_x-NO, and O_3 measurements reported for the same time interval by the South Coast Air Quality Management District's (SCAQMD) monitoring station in Pasadena, located within 1.5 km of the Scott Gallery. Good agreement between these two data sets was found. Having established the close correspondence between these two monitoring sites, data for CO from the Pasadena station of the SCAQMD were used.

Hourly data on total hydrocarbons are measured by the SCAQMD at Azusa, CA. These total hydrocarbon data were subdivided into formaldehyde, higher aldehydes, olefins, alkanes, aromatics and ethylene using the splitting factors determined by Russell and Cass (40) on the basis of detailed analysis of the composition of morning air in Los Angeles reported by Grosjean and Fung (41).

Input data for concentrations of the remaining species in outdoor air (H_2O_2, HNO_2, and RNO_2) were determined from general experience in modeling ambient air pollution in the Los Angeles basin (42). The hydrogen peroxide concentration was

assumed to be 5% of the outdoor ozone concentration. Nitrous acid concentration was assumed to peak at 1.5 ppb during the hour after sunrise, falling to zero linearly over an hour on either side of the peak. The outdoor concentration of RNO_2 was assumed to be zero.

The initial indoor concentrations of NO, NO_2 and O_3 were specified based on values measured inside the Scott Gallery. For all other species, the initial concentration was computed by bringing the model to its steady-state value based on the initial outdoor concentration, the air-exchange rate, the wall loss rate, and assuming no homogeneous chemical reaction. Since there are no known direct emissions of pollutants within the Scott gallery, indoor pollutant source strengths were set to zero for the base case model calculations.

Perturbations of the Model Parameters

Six simulations in addition to the base case were run to examine the response of the model to changes in some of the input parameters (see Table 9.4). Three of these cases were run to examine the sensitivity of the results to assumptions about the input data. In particular, the "low NO_2 wall loss" case was run because indoor and outdoor monitoring data showed that the average total NO_x levels inside the Scott Gallery were very close to those outside. The case with "no explicit chemistry" was run to compare the predictions of previous model formulations with the present work. The "multichamber" case addresses the magnitude of errors resulting from assuming that this building may be represented as a single well mixed chamber.

The three remaining cases were selected to examine how changes in building design or operation could influence indoor pollutant concentrations through chemical reaction. The case with an "indoor hydrocarbon source" could represent a situation in which fumes from an underground parking garage enter the building, or a case in which solvents are used within the building. The "indoor oxides of nitrogen

source" considers the effect of operating combustion appliances. The "glass-walled building" case considers the effects of increased photolytic reaction rates and reduced wall loss rates associated with glass.

Results

A comparison of measured and simulated ozone concentrations is presented in Figure 9.3. Model results are shown for both the base case and the no-chemistry case. The full kinetic model is slightly better in predicting indoor ozone concentrations, particularly during the morning hours when the presence of a significant nitric oxide concentration constitutes a substantial sink for ozone by reaction 3. As indicated in Table 9.5, the heterogeneous wall loss rate is the dominant factor in accounting for the difference between indoor and outdoor ozone concentrations within this particular building. Chemical reaction is, however, a significant net sink.

Comparisons between measurements and simulations for oxides of nitrogen are presented in Figure 9.4. At most times the measured NO_x and NO_2* concentrations are seen to lie between the results for the base case and "low NO_2 wall loss" simulations. The nitric oxide concentration, on the other hand, is underpredicted at most times by both simulations, supporting Yamanaka's inference that NO_2 is converted to NO at indoor surfaces (6). The "low NO_2 wall loss" case predicts a total NO_x concentration that is closer to the measured value (5% high) than is the result for the base case simulation (14% low).

Tables 9.5 and 9.6 summarize the simulation results, giving average source and sink rates and average concentrations, respectively. Figure 9.5 presents average concentrations for selected species. Several of the findings are noteworthy.

Comparing the average concentrations for the base case and no chemistry simulations, we see that several nitrogen-containing species—HNO_2, HNO_3, HNO_4, NO_3 and N_2O_5—are produced at substantial net rates by chemical reaction indoors.

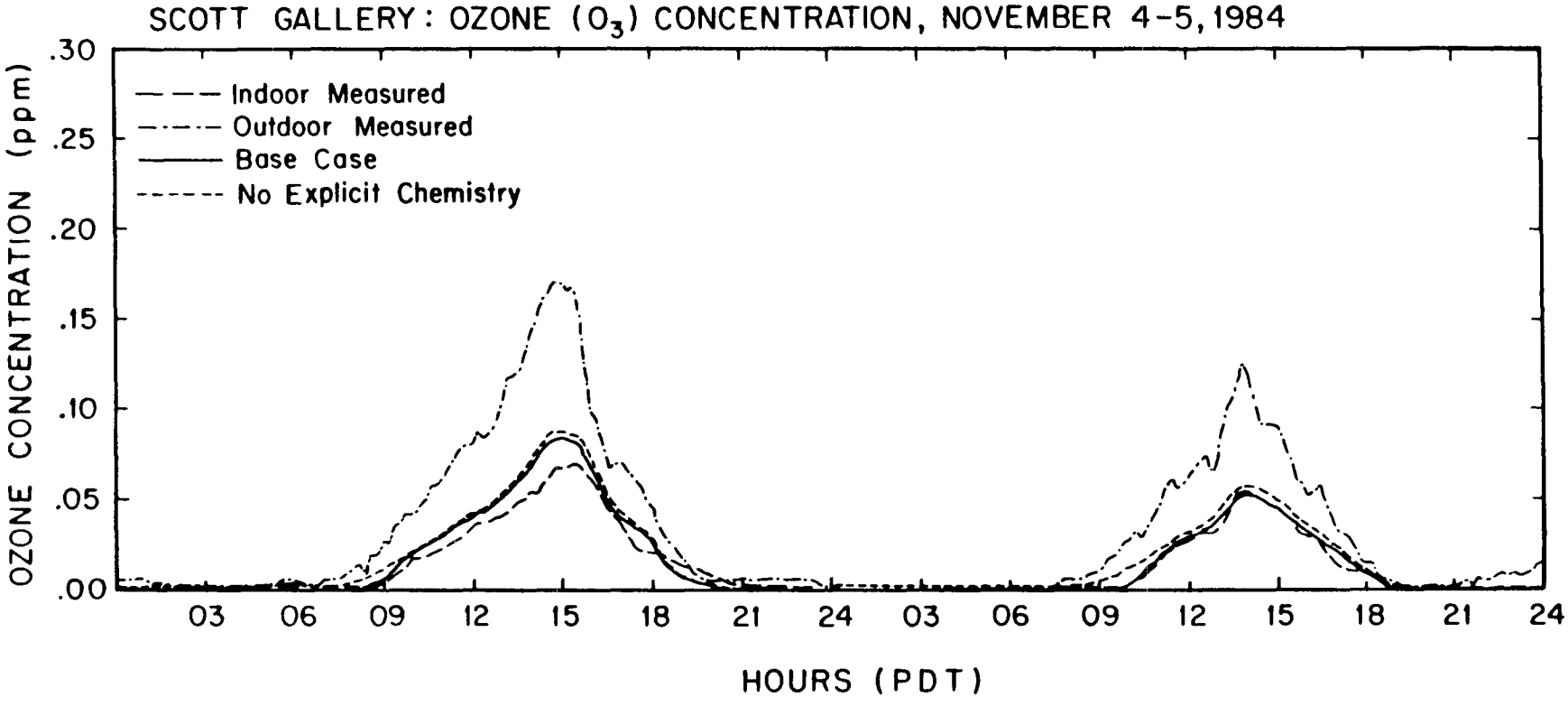

Figure 9.3. Comparison of modeled and measured ozone concentrations for a two-day period.

Table 9.5. Source and Sink Rates (ppb h^{-1}) in Scott Gallery for Selected Species and Simulations: Average for November 4 and 5, 1984

Simulation:		Base Case		HC Source		NOx Source		Glass-Walled Bldg.	
Species	Process	Source	Sink	Source	Sink	Source	Sink	Source	Sink
NO	Ventilation	17.6	15.0	17.6	8.6	17.6	36.2	17.6	16.6
	Chemical Rxn	1.6	5.7	1.4	11.8	3.4	24.1	129	131
	Emission	0		0		38		0	
	Wall Loss		0		0		0		0
NO2	Ventilation	69	58	69	54	69	99	69	67
	Chemical Rxn	172	172	666	666	154	136	418	418
	Emission	0		0		38		0	
	Wall Loss		12		13		19		1
O3	Ventilation	58	29	58	20	58	21	58	65
	Chemical Rxn	2	8	1	25	3	23	131	123
	Emission	0		0		0		0	
	Wall Loss		23		15		17		3
HNO2	Ventilation	0.029	0.025	0.029	0.064	0.029	0.046	0.029	0.134
	Chemical Rxn	0.051	0.0001	0.161	0.0004	0.104	0.0003	0.175	0.049
	Emission	0		0		0		0	
	Wall Loss		0.055		0.125		0.086		0.019
HNO3	Ventilation	5.8	2.6	5.8	2.4	5.8	2.7	5.8	7.4
	Chemical Rxn	0.8	0	0.4	0	1.1	0	2.4	0
	Emission	0		0		0		0	
	Wall Loss		4.1		3.8		4.3		0.8
NO3	Ventilation	0.007	0.008	0.007	0.004	0.007	0.005	0.007	0.007
	Chemical Rxn	29.6	29.6	12.8	12.8	24.7	24.7	43.1	43.1
	Emission	0		0		0		0	
	Wall Loss		0.013		0.007		0.009		0.001
N2O5	Ventilation	0.4	0.5	0.4	0.2	0.4	0.4	0.4	0.5
	Chemical Rxn	29.1	28.1	12.2	12.1	23.8	23.1	38.8	38.6
	Emission	0		0		0		0	
	Wall Loss		0.8		0.4		0.7		0.1
PAN	Ventilation	2.9	1.6	2.9	1.7	2.9	1.6	2.9	3.4
	Chemical Rxn	0.8	0.8	0.9	0.8	0.8	0.8	2.6	1.9
	Emission	0		0		0		0	
	Wall Loss		1.3		1.3		1.3		0.1
HCHO	Ventilation	14.3	13.1	14.3	23.9	14.3	21.2	14.3	18.1
	Chemical Rxn	1.0	0.03	13.7	0.06	1.1	0.1	4.3	0.5
	Emission	0		0		8.9		0	
	Wall Loss		2.2		4.0		3.1		0.2

Table 9.5. (Cont.)

Simulation:		Base Case		HC Source		NOx Source		Glass-Walled Bldg.	
Species	Process	Source	Sink	Source	Sink	Source	Sink	Source	Sink
RCHO	Ventilation	12.8	12.0	12.8	25.6	12.8	12.7	12.8	20.6
	Chemical Rxn	1.3	0.05	17.5	0.1	2.0	0.1	8.8	0.9
	Emission	0		0		0		0	
	Wall Loss		2.0		4.5		2.1		0.2
H2O2	Ventilation	2.9	1.2	2.9	2.0	2.9	1.1	2.9	2.9
	Chemical Rxn	0.1	0.0001	2.2	0.0002	0.1	0.0001	0.2	0.003
	Emission	0		0		0		0	
	Wall Loss		1.9		3.1		1.8		0.2

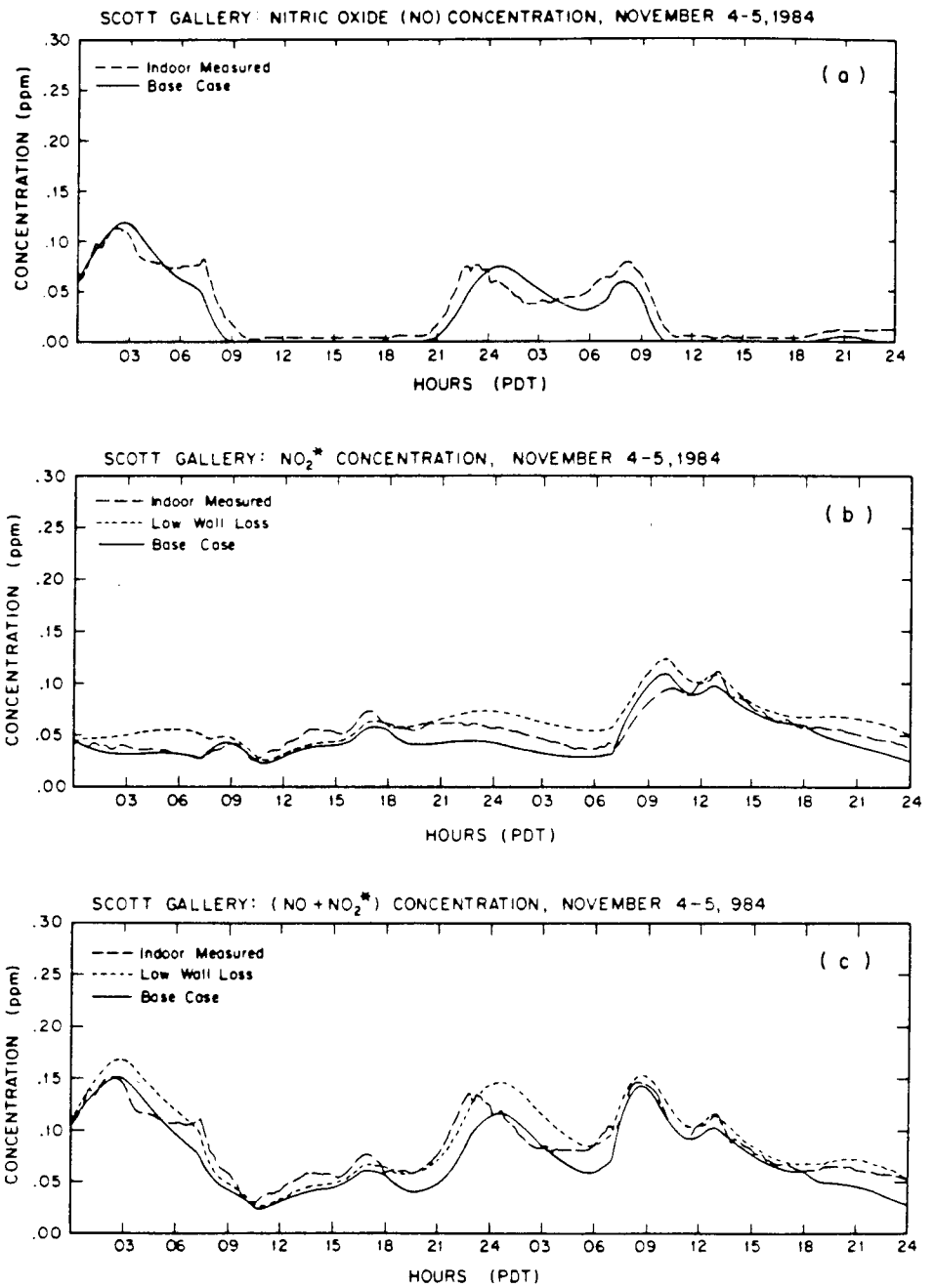

Figure 9.4. Comparison of modeled and measured concentrations of a) nitric oxide, b) nitrogen dioxide (NO_2*, measured as NO_x-NO), and c) total oxides of nitrogen for a two-day period. In the case of nitric oxide, the "base case" and "low (NO_2) wall loss" simulations produce essentially equivalent results.

Table 9.6. Species Concentrations (ppb) in Scott Gallery: Average for November 4 and 5, 1984

Spec.	Outdoor: Meas/Sim.[a]	Indoor: Measured	Indoor Simulations: Base Case	Low NO_2 WL	No Chem	Multichamber[b]	HC Source	NOx Source	Glass–Walled
NO	31.8	32.3	27.2	27.5	30.7	27.2	15.2	38.1	26.0
NO2	59.8 [c]	52.4 [c]	45.9	61.6	45.0	46.5	48.5	70.4	61.0
O3	31.2	14.0	15.1	14.9	16.8	15.5	9.8	11.1	34.1
HNO2	0.063		0.018	0.018	0.007	0.019	0.041	0.028	0.124
HNO3	3.12		1.35	1.36	1.17	1.43	1.25	1.39	4.96
HNO4	0.343		0.176	0.181	0.133	0.184	0.646	0.135	0.304
NO3	0.0035		0.0042	0.0041	0.0014	0.0044	0.0022	0.0029	0.0046
N2O5	0.181		0.258	0.285	0.072	0.277	0.110	0.211	0.350
PAN	1.56		0.86	0.86	0.85	0.89	0.87	0.85	1.96
RNO4	0.87		0.44	0.44	0.34	0.47	2.21	0.34	0.78
RONO	0.0		0.00007	0.00006	0.0	0.00007	0.00205	0.00043	0.00107
HCHO	13.2		10.3	10.3	9.8	10.4	18.3	14.5	15.1
RCHO	11.7		9.5	9.5	8.8	9.6	21.0	9.8	16.3
HO2	0.0151		0.0079	0.0072	0.0060	0.0082	0.0400	0.0049	0.0123
H2O2	1.56		0.61	0.60	0.59	0.64	1.02	0.59	1.69
O	1.31 E-06		6.21 E-09	6.92 E-09	0.0	6.24 E-09	5.10 E-09	12.0 E-09	4.62 E-07
OH	2.80 E-03		0.22 E-05	0.21 E-05	0.0	0.23 E-05	0.22 E-05	0.40 E-05	2.41 E-05
RCO3	0.00042		0.00017	0.00015	0.00016	0.00018	0.00030	0.00011	0.00043
RO	6.03 E-07		0.37 E-07	0.35 E-07	0.0	0.38 E-07	4.62 E-07	1.08 E-07	5.10 E-07
RO2	0.0146		0.0071	0.0063	0.0058	0.0074	0.0584	0.0044	0.0104

[a] Outdoor average concentrations for species not listed: ALK - 241 ppb, ARO - 63 ppb, CO - 3.04 ppm, C2H4 - 22 ppb, OLE - 15 ppb.
[b] Volume-weighted average for four chambers.
[c] Quantitative interference from HNO3 and PAN assumed and subtracted from measured NOx-NO. For indoor value, results from base case simulation used.

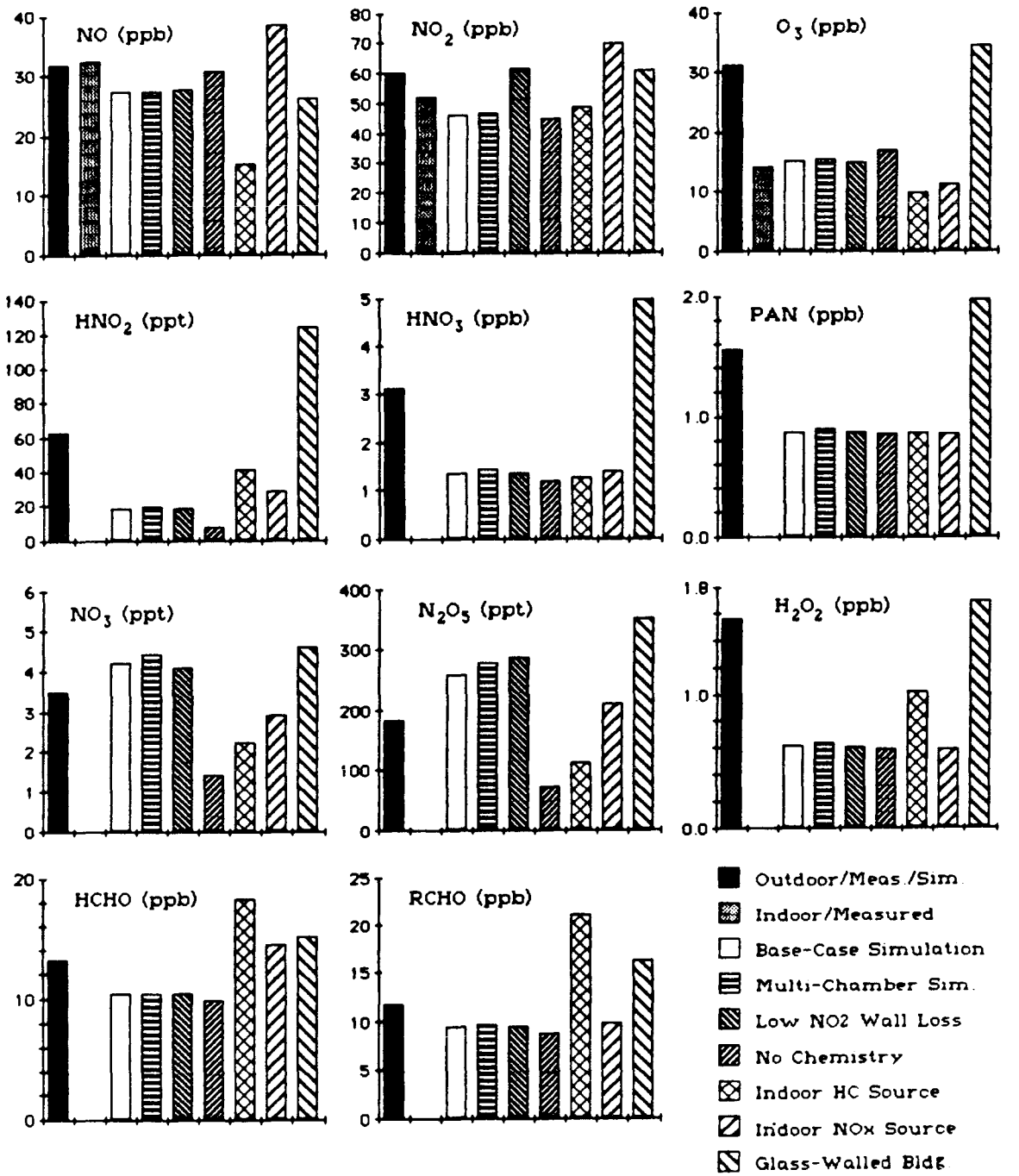

Figure 9.5. Average measured and modeled pollutant concentrations for the Scott Gallery, November 4-5, 1984.

For the latter two species, indoor concentrations exceed those outdoors. In a conventionally lit building, formation of these species may occur indoors during the day by reaction pathways normally associated with nighttime chemistry outdoors (20). N_2O_5 recently has been implicated in the production of mutagenic compounds in outdoor air (43); the possibility that N_2O_5 is present at elevated levels indoors should be further studied.

Pitts et al. (28) experimentally demonstrated the production of nitrous acid in an indoor environment with elevated levels of NO_2, and inferred from their data a steady-state average ratio of HNO_2 to NO_2 of 15×10^{-3}. The base case indoor simulation also indicates that HNO_2 is formed indoors, but the HNO_2 to NO_2 ratio due to homogeneous gas-phase chemistry alone is lower, 0.4×10^{-3}. This discrepancy supports the hypothesis that heterogeneous reactions (e.g., on building surfaces) may play an important role in nitrous acid production.

Information on the flux of reactive species to interior surfaces may be useful in assessing the potential for damage to materials displayed in museums. Under the assumptions of the base case simulation, the average fluxes of O_3 and HNO_3 to the walls during this 2-day period were 38.4 and 8.8 $\mu g\ m^{-2}\ h^{-1}$, respectively.

The results of the multichamber simulation indicate that the treatment of this building as a single chamber is a reasonable approximation. Concentration variations among chambers are approximately 10% or less, due to the relatively high rate of recirculation through the mechanical ventilation system.

The two cases for which an indoor pollutant source is postulated show that such sources may either increase or decrease the concentration of species not directly emitted. For example, the hydrocarbon source leads to substantial reduction in the indoor concentration of O_3 and NO, but markedly increased concentrations of HNO_2, HNO_4, HCHO, and H_2O_2, among others. The indoor combustion source likewise leads to a consumption of O_3, but increased production of HNO_2,

and HNO_3.

In the case of the glass-walled building, indoor concentrations of several key species—including O_3, HNO_2, HNO_3, PAN, and H_2O_2—are increased markedly over the base case values, and in fact are seen to exceed the outdoor levels. In this case, homogeneous chemical reactions are greatly enhanced by the combined effects of increased lighting, leading to higher photolysis rates, and reduced wall loss, leading to higher concentrations of reactive species.

Discussion

The results of this study identify those cases where homogeneous chemistry is important as a pollutant transformation process in indoor atmospheres. Concentrations of many species (e.g., O_3) are significantly perturbed by chemical reaction, especially when outdoor air pollutants are combined with direct indoor emissions. For other species (e.g., N_2O_5) an accounting of the effect of homogeneous chemical reactions is essential because the rates of chemical production in indoor air dominate other source terms.

The results of the present work—the reasonable agreement between measured and simulated pollutant concentrations, and the minor effect of treating the Scott Gallery as a four-chamber rather than a one-chamber building—indicate that the assumption that each chamber in the model is well mixed did not interfere with obtaining accurate results. Additional work to relax the uniform mixing hypothesis is warranted. Efforts to determine the rates of mixing in indoor air and to examine the effect of poor mixing on the apparent rates of chemical reaction are recommended. One approach to relaxing the uniform-mixing assumption is to use the atmospheric diffusion equation (26) in place of Equation 9.1 to describe the time-rate-of-change of pollutant concentrations. To solve the problem using this approach, one requires information on localized indoor air velocities and eddy diffusivities. The basis for describing indoor air motion is partially established in

numerical codes for natural convection in enclosures (30). A model that employs an explicit description of air motion at scales smaller than the dimension of the rooms would be considerably more difficult to validate and costly to apply than the present approach. Nevertheless, it could prove quite useful in examining the validity of the uniformly mixed model, and in treating the mass-transport aspects of surface reaction on a more fundamental basis.

The present model is also restricted in the scope of the transformation processes considered. The explicit description is limited to gaseous pollutants and gas-phase chemistry. The approach taken to account for pollutant interactions at fixed surfaces is a simplified one and possible interactions of gaseous pollutants with suspended particulate matter are not considered at all. The results reported here indicate that a dominant route for removal of highly reactive pollutants is deposition on walls (see Table 9.5). Also, as discussed above, there are indications that nitrogen-containing species may be chemically transformed rather than simply removed at surfaces. Further research is needed to improve the understanding of these heterogeneous processes. Such work should include carefully designed experiments that account for both mass transport and surface-reaction kinetics.

The model as presently formulated has a number of important applications in addition to those discussed in this paper. It may be used to assess the effects of filtration of selected compounds, to design indoor air quality control strategies based on ventilation scheduling, and to simulate specialized cases where unusual chemicals are present. The model is formulated to be a general tool for studying chemically reactive air pollution systems. Within limits, one can specify an arbitrary chemical mechanism, modify the computer code in a straightforward manner, and simulate an indoor environment in which homogeneous chemical reactions play an important role in determining pollutant concentrations.

REFERENCES FOR CHAPTER 9

1. McRae, G.J., Goodin, W.R., and Seinfeld, J.H., "Development of a Second-Generation Mathematical Model for Urban Air Pollution — I. Model Formulation," *Atmos. Environ. 16,* 1982, 679-696.

2. McRae, G.J., and Seinfeld, J.H., "Development of a Second-Generation Mathematical Model for Urban Air Pollution — II. Evaluation of Model Performance," *Atmos. Environ. 17,* 1983, 501-522.

3. Ruff, R.E., Nitz, K.C., Ludwig, F.L., Bhumralkar, C.M., Shannon, J.D., Sheih, C.M., Lee, I.Y., Kumar, R., and McNaughton, D.J., "Evaluation of Three Regional Air Quality Models," *Atmos. Environ. 19,* 1985, 1103-1115.

4. Shair, F.H., and Heitner, K.L., "Theoretical Model for Relating Indoor Pollutant Concentrations to Those Outside," *Environ. Sci. Technol. 8,* 1974, 444-451.

5. Traynor, G.W., Anthon, D.W., and Hollowell, C.D., "Technique for Determining Pollutant Emissions from a Gas-Fired Range," *Atmos. Environ. 16,* 1982, 2979-2987.

6. Yamanaka, S., "Decay Rates of Nitrogen Dioxide in a Typical Japanese Living Room," *Environ. Sci. Technol. 18,* 1984, 566-570.

7. Fisk, W.J., "Ventilation for Control of Indoor Air Quality," in *Indoor Air: Buildings Ventilation and Thermal Climate,* Berglund, B., Lindvall, T., and Sundell, J., Eds., Swedish Council for Building Research, Stockholm, 1984, Vol. 5, 187-192.

8. Hernandez, T.L., and Ring, J.W., "Indoor Radon Source Fluxes: Experimental Tests of a Two-Chamber Model," *Environ. Int. 8,* 1982, 45-57.

9. Özkaynak, H., Ryan, P.B., Allen, G.A., and Turner, W.A., "Indoor Air Quality Modeling: Compartmental Approach with Reactive Chemistry," *Environ. Int. 8,* 1982, 461-471.

10. Davidson, C.I., Osborn, J.F., and Fortmann, R.C., "Modeling and Measurement of Pollutants Inside Houses in Pittsburg, Pennsylvania," in *Indoor Air: Chemical Characterization and Personal Exposure,* Berglund, B., Lindvall, T., and Sundell, J., Eds., Swedish Council for Building Research, Stockholm, 1984, Vol. 4, 69-74.

11. Schiller, G.E., "A Theoretical Convective-Transport Model of Indoor Radon Decay Products," Ph.D. Thesis, University of California, Berkeley, 1984.

12. Sabersky, R.H., Sinema, D.A., and Shair, F.H., "Concentrations, Decay Rates and Removal of Ozone and Their Relation to Establishing Clean Indoor Air," *Environ. Sci. Technol. 7,* 1973, 347-353.

13. Shair, F.H., "Relating Indoor Pollutant Concentrations of Ozone and Sulfur Dioxide to those Outside: Economic Reduction of Indoor Ozone Through Selective Filtration of the Makeup Air," ASHRAE Trans. 1981, 87 (Part I), 116-139.

14. Berglund, B., Lindvall, T., and Sundell, J., Eds., *Indoor Air,* Swedish Council for Building Research, Stockholm, 1984; 5 vol.

15. Sinden, F.W., "Multichamber Theory of Air Infiltration," *Building and Environ. 13,* 1978, 21-28.

16. Sherman, M.H., "Air Infiltration in Buildings," Ph.D. Thesis, University of California, Berkeley, 1980.

17. Hecht, T.A., and Seinfeld, J.H., "Development and Validation of a Generalized Mechanism for Photochemical Smog," *Environ. Sci. Technol. 6,* 1972, 47-57.

18. Hecht, T.A., Seinfeld, J.H., and Dodge, M.C., "Further Development of Generalized Kinetic Mechanism for Photochemical Smog," *Environ. Sci. Technol. 8,* 1974, 327-339.

19. Falls, A.H., and Seinfeld, J.H., "Continued Development of a Kinetic Mechanism for Photochemical Smog," *Environ. Sci. Technol. 12,* 1978, 1398-1406.

20. Russell, A.G., McRae, G.J., and Cass, G.R., "The Dynamics of Nitric Acid Production and the Fate of Nitrogen Oxides," *Atmos. Environ. 19,* 1985, 893-903.

21. Baulch, D.L., Cox, R.A., Crutzen, P.J., Hampson, R.F., Jr., Kerr, J.A., Troe, J., and Watson, R.T., "Evaluated Kinetic and Photochemical Data for Atmospheric Chemistry: Supplement 1," *J. Phys. Chem. Ref. Data 11,* 1982, 327-496.

22. McRae, G.J., "Mathematical Modeling of Photochemical Air Pollution," Ph.D. Thesis, California Institute of Technology, Pasadena, 1982.

23. Hall, E.T., "Design of a UV Light Meter," in *London Conference on Museum Climatology,* International Institute for Conservation, London, 1967, 151-157.

24. Thomson, G., "Calibration and Use of a UV Monitor," in *London Conference on Museum Climatology,* International Institute for Conservation, London, 1967.

25. Jackson, J.O., Stedman, D.H., Smith, R.G., Hecker, L.H., and Warner, P.O., "Direct NO_2 Photolysis Rate Monitor," *Rev. Sci. Instrum. 46,* 1975, 376-378.

26. Seinfeld, J.H., *Atmospheric Chemistry and Physics of Air Pollution,* J.Wiley and Sons, New York, 1986.

27. McRae, G.J., Goodin, W.R., and Seinfeld, J.H., "Numerical Solution of the Atmospheric Diffusion Equation for Chemically Reacting Flows," *J. Comp. Phys. 45,* 1982, 1-42.

28. Pitts, J.N., Jr., Wallington, T.J., Biermann, H.W., and Winer, A.M., "Identification and Measurement of Nitrous Acid in an Indoor Environment," *Atmos. Environ. 19,* 1985, 763-767.

29. Besemer, A.C., and Nieboer, H., "The Wall as a Source of Hydroxyl Radicals in Smog Chambers," *Atmos. Environ. 19,* 1985, 507-513.

30. Gadgil, A. J., "On Convective Heat Transfer in Building Energy Analysis," Ph.D. Thesis, University of California, Berkeley, 1980.

31. Eckert, E.R.G., and Drake, R.M., Jr., *Analysis of Heat and Mass Transfer,* McGraw-Hill, New York, 1972, 528.

32. Wilson, M.J.G., "Indoor Air Pollution," *Proc. Roy. Soc. London A307,* 1968, 215-221.

33. Knutson, E.O., "Modeling Indoor Concentrations of Radon and its Decay Products," in *Radon and Its Decay Products in Indoor Air,* Nazaroff, W.W., and Nero, A.V., Eds., Wiley, New York, 1988.

34. Young, T.R., and Boris, J.P., "A Numerical Technique for Solving Stiff Ordinary Differential Equations Associated with the Chemical Kinetics of Reactive-Flow Problems," *J. Phys. Chem. 81,* 1977, 2424-2427.

35. Baer, N.S., and Banks, P.N., "Indoor Air Pollution: Effects on Cultural and Historic Materials," *Int. J. of Museum Management and Curatorship 4,* 1985, 9-20.

36. Mathey, R.G., Faison, T.K., Silberstein, S., Woods, J.E., Johnson, W.B., Lull, W.P., Madson, C.A., Turk, A., Westlin, K.L., and Banks, P.N. *Air Quality Criteria for Storage of Paper-Based Archival Records,* National Bureau of Standards, Washington, D.C., 1983, NBSIR 83-2795.

37. Winer, A.M., Peters, J.W., Smith, J.P., and Pitts, J.N., Jr., "Response of Commercial Chemiluminescent NO–NO_2 Analyzers to Other Nitrogen-Containing Compounds," *Environ. Sci. Technol. 8,* 1974,1118-1121.

38. Hanst, P.L., Wong, N.W., and Bragin, J., "A Long-Path Infra-Red Study of Los Angeles Smog," *Atmos. Environ. 16,* 1982, 969-981.

39. Tuazon, E.C., Winer, A.M., and Pitts, J.N., Jr., "Trace Pollutant Concentrations in a Multiday Smog Episode in the California South Coast Air Basin by Long Path Length Fourier Transform Infrared Spectroscopy," *Environ. Sci. Technol. 15,* 1981, 1232-1237.

40. Russell, A.G., and Cass, G.R., "Verification of a Mathematical Model for Aerosol Nitrate and Nitric Acid Formation and its Use for Control Measure Evaluation," *Atmos. Environ. 20,* 1986, 2011-2025.

41. Grosjean, D., and Fung, K., "Hydrocarbons and Carbonyls in Los Angeles Air," *J. Air Pollut. Contr. Assoc. 34,* 1984, 537-543.

42. Russell, A.G., Carnegie-Mellon University, personal communication, 1985.

43. Pitts, J.N., Jr., Sweetman, J.A., Zielinska, B., Atkinson, R., Winer, A.M., and Harger, W.P., "Formation of Nitroarenes from the Reaction of Polycyclic Aromatic Hydrocarbons with Dinitrogen Pentoxide," *Environ. Sci. Technol. 19,* 1985, 1115-1121.

44. Mueller, F.X., Loeb, L., and Mapes, W.H., "Decomposition Rates of Ozone in Living Areas," *Environ. Sci. Technol. 7,* 1973, 342-346.

45. Sutton, D.J., Nodolf, K.M., and Makino, K.K., "Predicting Ozone Concentrations in Residential Structures," *ASHRAE J. 18(9),* 1976, 21-26.

46. Traynor, G.W., Apte, M.G., Dillworth, J.F., Hollowell, C.D., and Sterling, E.M., "The Effects of Ventilation on Residential Air Pollution Due to Emissions from a Gas-Fired Range," *Environ. Int. 8,* 1982, 447-452.

47. Wade, W.A., III, Cote, W.A., and Yocum, J.E., "A Study of Indoor Air Quality," *J. Air Pollut. Contr. Ass. 25,* 1975, 933-939.

48. Miyazaki, T., "Adsorption Characteristics of NO_x by Several Kinds of Interior Materials," in *Indoor Air: Chemical Characterization and Personal Exposure,* Berglund, B., Lindvall, T., and Sundell, J., Eds., Swedish Council for Building Research, Stockholm, 1984, Vol. 4, 103-110.

49. Revzan, K.L., "Effectiveness of Local Ventilation in Removing Simulated Pollution from Point Sources," in *Indoor Air: Building Ventilation and Thermal Climate,* Berglund, B., Lindvall, T., and Sundell, J., Eds., Swedish Council for Building Research, Stockholm, 1984, Vol. 5, 65-72.

50. Summer, W. *Ultraviolet and Infra-Red Engineering,* Interscience Publishers, New York, 1962, 60.

CHAPTER 10

THE MEASUREMENT AND MODEL PREDICTIONS OF INDOOR OZONE CONCENTRATIONS IN ART MUSEUMS

INTRODUCTION

Until the early 1970's, very little was known about the ozone concentrations encountered inside buildings. Even at present, the data base on this subject is not large and a wide range of indoor/outdoor ozone concentration relationships can be found in the technical literature. In a major critical review, Yocum (1) noted that indoor/outdoor O_3 concentration ratios generally fall in the range from 0.1 to 0.7 and concludes, "In summary, one can say with assurance that indoor concentrations of O_3, will almost invariably be significantly less than those outdoors, and that the indoor environment will be an efficient refuge from outdoor exposure to O_3." Thomson (2) drawing upon the work of Derwent (3) and Mueller et al. (4) concluded similarly that ozone levels inside museums and galleries must be low due to the high reactivity of ozone with indoor surfaces. But while indoor O_3 levels are expected to be below those outdoors, Shair and Heitner (5), Sabersky et al. (6) and Hales et al. (7) have reported ozone concentrations within buildings at the California Institute of Technology that ranged up to 70% of the outside levels at times when the outdoor O_3 concentrations were quite high. The question remains, is ozone found within museums at concentrations high enough to pose a risk of damage to the collections?

Previous studies of the ozone concentrations within buildings housing cultural properties have shown that there is great variability between buildings. In Southern California in 1982, Shaver et al. (8) measured ozone concentrations in an art gallery that lacked an ozone removal system and in two museums with activated carbon air filtration systems. The unprotected gallery showed indoor ozone at concentrations slightly higher than 50% of the ozone concentration outdoors, while the

museums with activated carbon air filtration systems showed very low ozone levels. A 1983 report on the atmosphere within the U.S. National Archives (9) found undetectably low ozone levels within that building in the winter. Lastly, Davies et al. (10) reported ozone concentrations at 70% ± 10% of the outside ozone levels within a contemporary art gallery in rural eastern England. The wide variety of indoor/outdoor ozone concentration relationships reported in the technical literature provides little guidance to museum conservators who may be called upon to estimate whether or not high indoor O_3 concentrations are likely to pose a problem for the preservation of collections in their particular facility.

The purpose of the present study is to characterize indoor/outdoor ozone relationships in museums and to illuminate the causes for the differences observed between buildings. The study will be based on measurements made in a significant number of buildings which differ in size and in the types of air conditioning, ventilation and heating systems that they possess. From these data, indoor air quality models (5,11) can be tested for their accuracy in describing the ozone levels inside buildings housing works of historic and artistic value. The ozone concentration relationships characteristic of various types of building ventilation systems will be compared, and a systematic basis will be established for estimating the ozone levels inside buildings that have not yet been tested based on the structural nature of building ventilation systems plus the outdoor O_3 levels reported by governmental air pollutant monitoring agencies. These indoor ozone levels then can be compared to the ozone levels recommended for storage conditions in museums, libraries and archives (12,13), and corrective actions can be taken where necessary.

MEASUREMENT PLAN

During the summers of 1984 and 1985, two matched ultraviolet photometric ozone monitors (Dasibi Corp., Models 1003-AH and 1003-PC) with strip chart

recorders were used to take simultaneous indoor/oudoor ozone measurements at eleven institutions housing cultural properties over a period totaling thirty-eight days. These sites were picked to represent a wide range of building types in the Los Angeles area and 100 miles to the south in San Diego, California. Represented within this group were six art museums, two historical society houses, a museum library, and two college art galleries (Table 10.1). The blueprints of each facility were examined to determine the volume, surface area, and materials of construction used in each building. Each building's ventilation system was documented. Whenever possible, the senior building engineer was consulted to determine the air exchange rates at which he was actually running the building's air handling system. A hot wire anemometer was used to measure air flow into and out of ventilation ducts, doors and windows at each site. In stagnant areas, air exchange rates were evaluated from standard engineering estimates for air infiltration (14). From this information, the air exchange rates and retention times for ozone destruction by reaction with building surfaces could be determined. The physical dimensions, air exchange rates, and interior surface characteristics of those buildings not equipped with activated carbon ozone removal systems at the time of this study are given in Table 10.2.

RESULTS

Each of these sites fell into one of three distinct groups: not air conditioned (Pasadena Historical, Southwest, Lang, Villa Montezuma, and Serra); air conditioned but without an activated carbon air filtration system (Scott and Montgomery); and air conditioned with activated carbon filters (Southwest Museum Library, Huntington Art Gallery, Los Angeles County Museum of Art, and the J. Paul Getty Museum).

Buildings that operate without conventional air conditioning are arrayed in a distribution between two extremes: those with rapid infiltration of outdoor air and

Table 10.1. Indoor/outdoor ozone measurement sites.

Site	Use	HVAC Type	Date	Comments
Pasadena Historical Society, Pasadena	1	1	7/3 to 7/5 1984	a
Southwest Museum, Los Angeles	2	1	7/11 to 7/12 1984	b
Southwest Museum Library, Los Angeles	3	3	7/13 to 7/15 1984	c
Virginia Steele Scott Gallery, San Marino	4	2	7/25 to 7/26 1984	d
Huntington Art Gallery, San Marino	4	3	7/27 to 7/29 1984	e
Montgomery Gallery, Claremont	5	2	7/30 to 7/31 1984	
Lang Gallery, Claremont	5	1	8/1 to 8/2 1984	a
Villa Montezuma, San Diego	1	1	8/7 to 8/8 1984	f
Junipero Serra Museum, San Diego	2	1	8/9 to 8/10 1984	f
Los Angeles County Museum of Art, Los Angeles	4	3	6/28 to 6/30 1985	
J. Paul Getty Museum, Malibu	4	3	7/2 to 7/15 1985	g

Use:

1) Historical society
2) Archeological museum
3) Museum library
4) Art museum
5) College art gallery

Heating, ventilation and air conditioning (HVAC) system type:

1) Not air conditioned. The Southwest Museum has a partial forced ventilation system (see text).
2) Modern heating, ventilation and air conditioning plant without activated carbon filtration. The Scott Gallery was retrofitted with an activated carbon filtration system following the completion of the present study.
3) Modern air conditioned plant with activated carbon filtration.

Comments:

a) Observed during worst and best case situations and during normal operations.
b) Normal operation.
c) Normal operation, and with the building "buttoned up".
d) New structure completed within the year prior to this study.
e) Old structure retrofitted for complete environmental control.
f) Sites outside of Los Angeles County.
g) Located near the ocean and northwest of downtown Los Angeles. Usually assumed to be "upwind" of major air pollution sources.

Table 10.2. Building characteristics of selected museums and galleries in Southern California.

Institution	Surface Area[a] (ft^2)	Surface Area[a] (m^2)	Building Volume (ft^3)	Building Volume (m^3)	Surface to Volume Ratio (ft^{-1})	Surface to Volume Ratio (m^{-1})	Outdoor Air Exchange Rate (hr^{-1})
Southwest Museum upper floor galleries in direct line with exhaust fans	22,399	2,081	101,915	2,886	0.22	0.72	5.5[b]
Serra Museum	12,922	1,200	43,000	1,218	0.30	0.98	--[c]
Pasadena Historical Museum	30,272	2,812	105,285	2,981	0.29	0.94	0.06[d]-2.2[e][f]
Lang Gallery	13,062	1,213	42,405	1,201	0.31	1.01	0.0[d]-0.99[e]
Villa Montezuma	16,608	1,543	34,282	971	0.48	1.59	1.8-2.6
Scott Gallery east wing + west wing	43,033	3,998	177,343	5,022	0.24	0.80	1.6
Montgomery Gallery	23,964	2,226	83,475	2,364	0.29	0.94	1.6

(a) Estimated surface area includes area of walls, floors, and ceilings.

(b) Based on measured exhaust rate divided into the volume of those upper floor galleries that are in a direct line between the open windows and the exhaust fans. This is a realistic ventilation estimate for the location of our ozone monitor. For purposes of comparison, the estimated air exchange rate is about 3.2 hr^{-1} if the exhaust air flow is divided by the volume of the entire building.

(c) Not possible to measure flow as many open windows are far above ground level.

(d) When building is closed. The value 0.0 indicates that the air exchange rate through building openings was too small to measure with a hot wire anemometer.

(e) With doors and windows open. This condition is normal during the daytime in the summer at the Lang Gallery.

(f) Under "normal operating conditions", the air exchange rate at the Pasadena Historical Museum is about 0.5 air exchanges per hour.

those with little air exchange with the outdoors. Rapid air exchange can be achieved, as at the Southwest Museum, if forced exhaust fans induce a once-through flow of outdoor air. At the other extreme, community galleries operating in converted private mansions with the doors and windows kept closed often experience very slow air exchange rates with the outdoors.

The Southwest Museum and the Serra Museum are examples of buildings with rapid air exchange but no air conditioning:

(1) Southwest Museum — This facility is a multi-story poured concrete building with an attached tower, built in the early 1900's. High-power fans installed in a former window force about 9400 cubic feet of air per minute (266.2 m^3/min) out of the building and initiate convection throughout the main portion of the building. Two exhibit rooms are largely unaffected by this continuous flow. Many open windows and doors allow large amounts of circulatory air to pass through the building. A complete air exchange with the outdoors occurs about 3.2 to 5.5 times per hour under the operating conditions followed during the period of our tests. The slower air exchange rate is computed on the basis of the volume of the entire building, while the faster air exchange rate is based on the volume of that portion of the upper floor of the building that is directly aligned with the flow from the open windows to the exhaust fans. The faster air exchange rate applies in the zone where our ozone monitor was located.

(2) Serra Museum — Like the Southwest Museum, the Serra Museum is a poured concrete Spanish-style building with an attached tower. Open doors and windows, generally large in size and few in number, provide for ventilation at this facility. One open door facing the ocean is subjected to a steady breeze.

Ozone concentrations observed inside these buildings are generally quite high, on the order of 70 to 80% of the ozone level in the outdoor air that is brought into the building, as seen in Table 10.3 and in Figure 10.1.

Table 10.3. Indoor/outdoor ozone concentration relationships in buildings with a high air exchange rate, but no air conditioning.

Site	Date	Indoor Max. O_3 (ppm)	Outdoor Max. O_3 (ppm)	Indoor O_3 as Percentage of Outdoor O_3
Southwest	7/11/84	0.090	0.132	69%
Southwest	7/12/84	0.143	0.173	84%
Serra	8/09/84	0.034	0.049	69%
Serra	8/10/84	0.022	0.028	79%

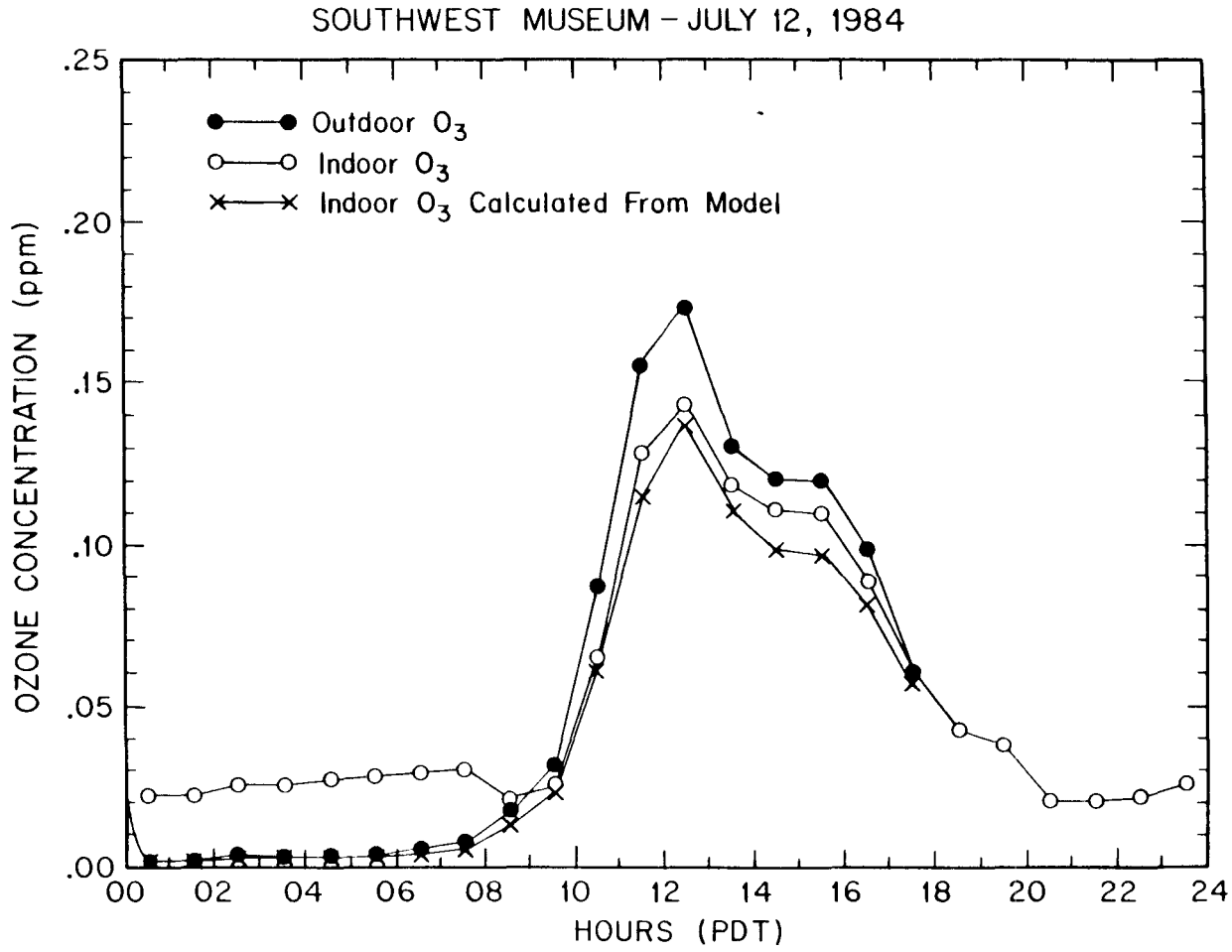

Figure 10.1. Indoor/outdoor ozone concentration relationships in the upper floor main gallery of the Southwest Museum, July 12, 1984. Model results show indoor O_3 concentrations predicted from equations 10.1 and 10.2 using measured outdoor O_3 concentrations, an outdoor air exchange rate of 5.5 exchanges per hour, building surface and volume values in the galleries of interest from Table 10.2, and an ozone deposition velocity at surfaces of 0.051 cm sec^{-1} (0.10 ft^3/ft^2-min).

In contrast, museums that lack air conditioning and that have very low air infiltration rates show some of the lowest indoor O_3 levels observed:

(1) Pasadena Historical Museum — This building is a former private mansion converted for use as a museum. A few open windows, mostly on the second floor, provide poor ventilation. Under normal operating conditions with the front door closed, the building is reasonably well sealed, and outdoor air enters the building at a very slow rate, with an air exchange occurring about once every two hours. An exception occurs when the site is used for luncheons or meetings, and the large front door is left open for the duration of the meeting. Under those conditions, the air exchange rate is once every 27 minutes.

(2) Lang Gallery — This college art gallery occupies a portion of a modern institutional building. One open window and one door open during public hours provide the ventilation at this site. Under those conditions, the air exchange rate with the outdoors is slightly less than once per hour. The door is shut when the staff leaves for lunch or in the evening. When the building is closed, very little outside air is permitted to enter the facility. One or two fans circulate the air within the facility, but these fans do not force exchange with the air outdoors.

As seen in Table 10.4, with the exception of the case at the Pasadena Historical Society where the doors and windows were left wide open, indoor ozone levels in the above facilities are very low, on the order of 10% to 20% of the outdoor O_3 level. This can be attributed to the very low air exchange rates (circa once every 1 to 2 hours) which yield long retention times for ozone depletion by reaction with indoor surfaces (5). Concentrations much lower than this cannot be expected in the absence of a deliberate pollutant removal system. Work at Lawrence Berkeley Laboratory (1) has shown that even for complete weatherization (i.e., storm doors, and indoor insulation and weatherstripping) indoor/oudoor O_3 ratios range

Table 10.4. Indoor/outdoor ozone concentration relationships in buildings with no air conditioning and with a low air exchange rate.

Site	Date	Indoor Max. O_3 (ppm)	Outdoor Max. O_3 (ppm)	Indoor O_3 as Percentage of Outdoor O_3	Comment
Pasadena Historical Society Museum	7/3/84	0.098	0.166	59%	1
Pasadena Historical Society Museum	7/4/84	0.025	0.155	16%	2
Pasadena Historical Society Museum	7/5/84	0.019	0.133	14%	3
Lang	8/1/84	0.030	0.140	20%	4
Lang	8/2/84	0.017	0.168	10%	5

Comment:

1) Worst case. Luncheon held with front door open during peak ozone hours.

2) Building sealed for holiday.

3) Normal operations.

4) Front door open in morning and late afternoon; closed otherwise.

5) Building closed. This is the best case and is observed only when the building is sealed.

between 0.10 and 0.25, close to those values found for the Pasadena Historical Society mansion when closed over the 4th of July holiday and at the Lang Gallery when it is closed.

Conditions at the Villa Montezuma represent an intermediate condition between the rapidly ventilated vs. stagnant non-air conditioned galleries. Villa Montezuma is a Victorian era mansion of shingled wood frame construction. It is unique in that it is the only building tested in which air circulation is driven by natural convection. A dozen or so open windows and a door provide ventilation, while numerous fans circulate the air within the facility. An up-draft can be felt in the stairwells of this largely vertical building as the warm interior air rises to be replaced at the ground level. Consequently, many of the first floor doors and windows serve as air inlets. The ozone monitor was placed within the main sitting room located on the first floor since many of the major artifacts were located in this area, and ozone concentrations at that location were 33% to 49% of those outside as shown in Table 10.5. The surface to volume ratio for this house was very large (0.48 ft^2/ft^3; 1.59 m^2/m^3), resulting from its design which incorporates many small rooms and corridors.

A summary of peak ozone concentrations observed inside museums with conventional air conditioning but without activated carbon air filtration is shown in Table 10.6. Both the Scott Gallery and Montgomery Gallery are modern buildings built specifically as art museums. Ozone levels in these buildings are reduced relative to the experience at the Southwest Museum because air is recirculated through the cooling zone of the building air conditioning system many times before being exhausted from the building, thus increasing the retention time for ozone loss by reaction with building surfaces. Based on these experiments, one can expect that a museum with a typical conventional air conditioning system will experience ozone levels inside the building that are 30 to 40% of those observed outside, with the

Table 10.5. Indoor/outdoor ozone concentration relationships in a building with a natural convection-induced air exchange system.

Site	Date	Indoor Max. O_3 (ppm)	Outdoor Max. O_3 (ppm)	Indoor O_3 as Percentage of Outdoor O_3	Comment
Villa Montezuma	8/7/84	0.014	0.042	33%	1
Villa Montezuma	8/8/84	0.022	0.045	49%	2

Comment:

1) Normal operations.

2) More windows open than on previous day.

Table 10.6. Indoor/outdoor ozone concentration relationships in buildings with a conventional air conditioning system but with no activated carbon air filtration.

Site	Date	Indoor Max. O_3 (ppm)	Outdoor Max. O_3 (ppm)	Indoor O_3 as Percentage of Outdoor O_3
Scott	7/25/84	0.043	0.179	24%
Scott	7/26/84	0.065	0.221	29%
Montgomery	7/30/84	0.060	0.150	40%
Montgomery	7/31/84	0.067	0.171	39%

peak concentration indoors lagging that outdoors by about one half hour.

Ozone concentrations within museums fitted with activated carbon air filtration units were generally quite low. Typical O_3 removal efficiencies greater than 90% were observed, and indoor O_3 levels usually were found to be at or below 0.01 ppm, as shown in Table 10.7. A typical example of O_3 removal performance by the activated carbon system at the Huntington Art Gallery is attached as Figure 10.2. Exceptions to this rule were found in certain portions of the J. Paul Getty Museum in Malibu, where the intrusion of untreated outdoor air was observed in ground floor galleries that were operated with doors left open to the outdoors, and in administrative areas of the museum that are connected to these ground floor galleries via the building's air recirculation system.

MODEL PREDICTIONS

Having acquired the indoor and outdoor ozone concentration data and data on ventilation system design in a variety of buildings, it becomes possible to explain how the indoor concentrations depend on outdoor ozone levels and on various building parameters. The indoor/outdoor ozone air quality modeling computer code developed in Chapter 9 of this study will be used (11). In the absence of chemical reaction, the calculation reduces to a form equivalent to that of Shair and Heitner (5) which is the simplest model available that incorporates most of the key features of the problem at hand. This model takes into account factors such as building volume, total surface area, re-circulated air flow, make-up air, ozone filtration efficiency (if applicable), and the ozone removal rates at the surface of the various materials found inside the building. For a building that can be treated as a single well mixed volume with the typical ventilation system shown schematically in Figure 10.3, the starting equation is:

Table 10.7. Indoor/outdoor ozone concentration relationships in buildings with an activated carbon air filtration system.

Site	Date	Indoor Max. O_3 (ppm)	Outdoor Max. O_3 (ppm)	Indoor O_3 as Percentage of Outdoor O_3	Comment
Southwest Museum Library	7/13/84	0.026	0.149	17%	
	7/14/84	0.008	0.174	5%	
	7/15/84	0.003	0.116	3%	
Huntington Art Gallery	7/27/84	0.004	0.110	4%	
	7/28/84	0.010	0.172	6%	
Los Angeles County Museum of Art	7/1/85	0.010	0.165	6%	
J. Paul Getty Museum	7/2/85	0.022	0.104	21%	1
	7/8/85	0.009	0.095	9%	2
	7/15/85	0.028	0.075	37%	3

Comments:

1) In the administrative area of the museum. Infiltration of untreated outdoor air into the ground floor galleries also affects the administrative area of this museum.

2) Second floor, room 203.

3) Ground floor, room 117. Ground floor galleries generally have open doors through which untreated outdoor air may enter.

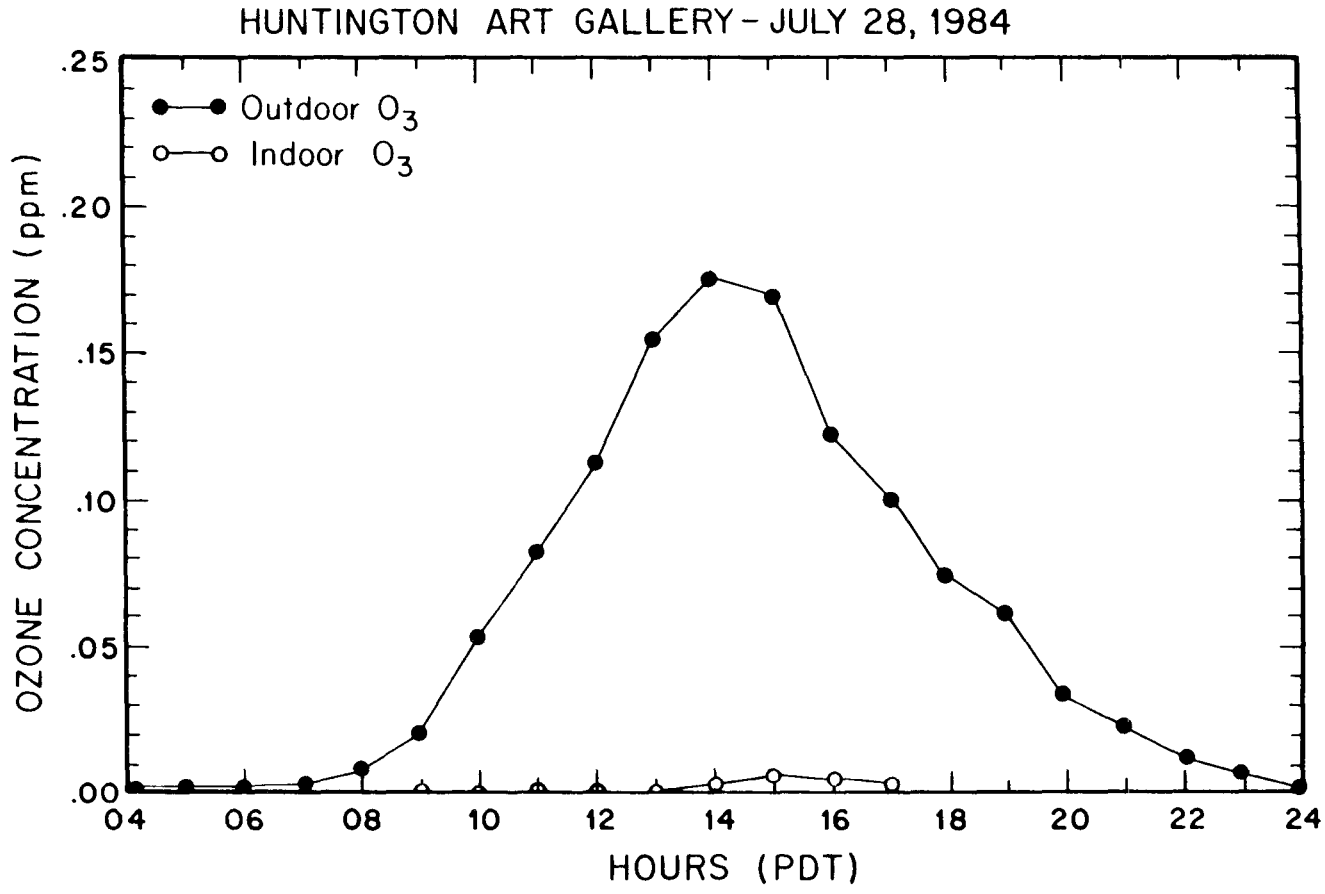

Figure 10.2. O_3 removal performance achieved by the activated carbon air filtration system at the Huntington Art Gallery.

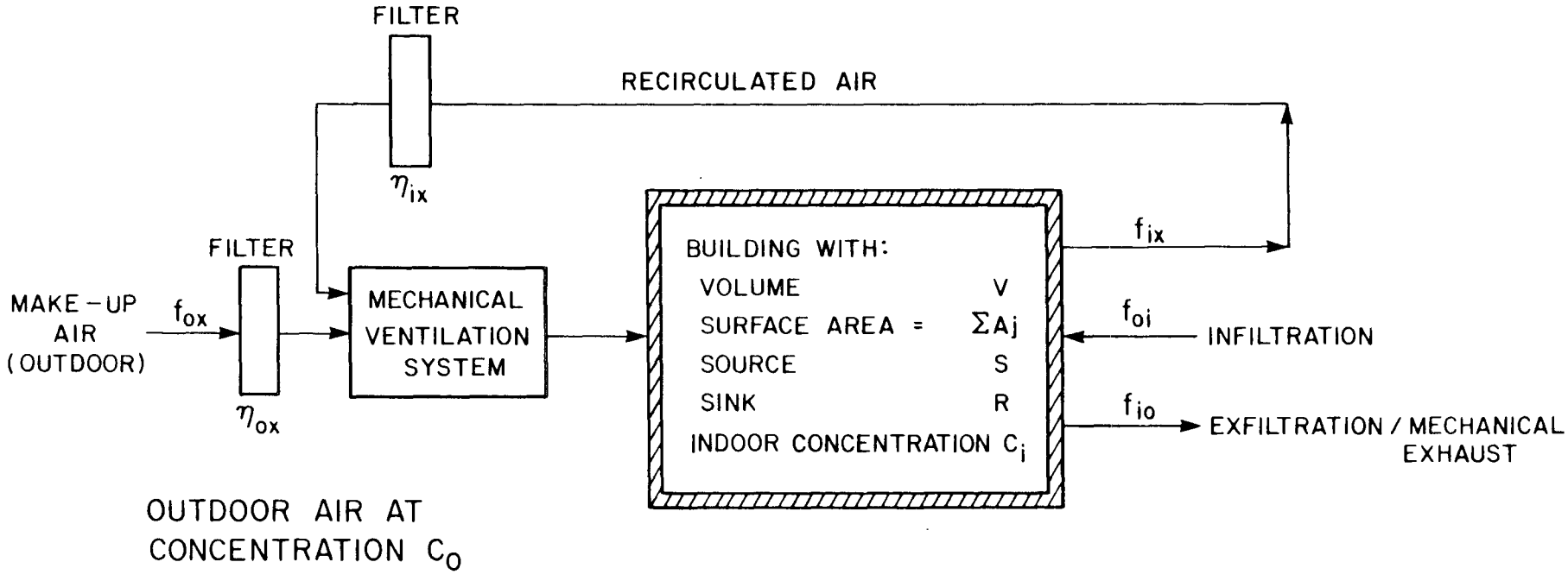

Figure 10.3. Schematic of typical ventilation system.

$$V\frac{dC_i}{dt}=(1-\eta_{ox})\,f_{ox}C_o+(1-\eta_{ix})\,f_{ix}C_i+f_{oi}C_o-f_{io}C_i+s-R \qquad (10.1)$$

where f_{ox}, f_{ix}, f_{oi} and f_{io} represent make-up air, recirculated air, infiltration air, and exfiltration plus exhaust air, respectively. C_0 and C_i are the outdoor and indoor pollutant concentrations. The filtration efficiencies for pollutant removal are given at the make-up air supply (η_{ox}) and at the recirculated air supply (η_{ix}). The quantity (s - R) represents the internal pollutant sources less pollutant loss mechanisms internal to the building. In the absence of indoor sources, the term (s - R) for the ozone modeling cases studied here reduces to R alone, which is computed as the product of the surface removal rate constant (deposition velocity) for ozone at each surface times the area of that surface times the indoor ozone concentration, C_i, summed over all interior surfaces. That is:

$$R=\sum_j v_{g_j}A_jC_i \qquad (10.2)$$

where v_{g_j} is the ozone deposition velocity at the j-th surface with the area A_j. Hales et al. (7) used an ozone deposition velocity, v_{g_j}, of 0.051 cm sec^{-1} (0.10 ft^3/ft^2-min) as an average value for modeling purposes, and that value will be used in the present study. A brief literature review on the variation of ozone removal rates between surfaces of different types is given in references (5-7) and (11).

The museum data acquired during the summer field studies were supplied to the model (11) to determine if measured indoor ozone levels were consistent with the ozone levels found in the outside air that supplies the buildings. Model predictions for the Southwest Museum are shown in Figure 10.1. Figure 10.4 shows results for the Montgomery Gallery with its modern conventional air conditioning system. Generally good agreement between model calculations and indoor measurements also was obtained at sites where unassisted slow air infiltration predominated, as shown for the Pasadena Historical Society in Figure 10.5. The generally

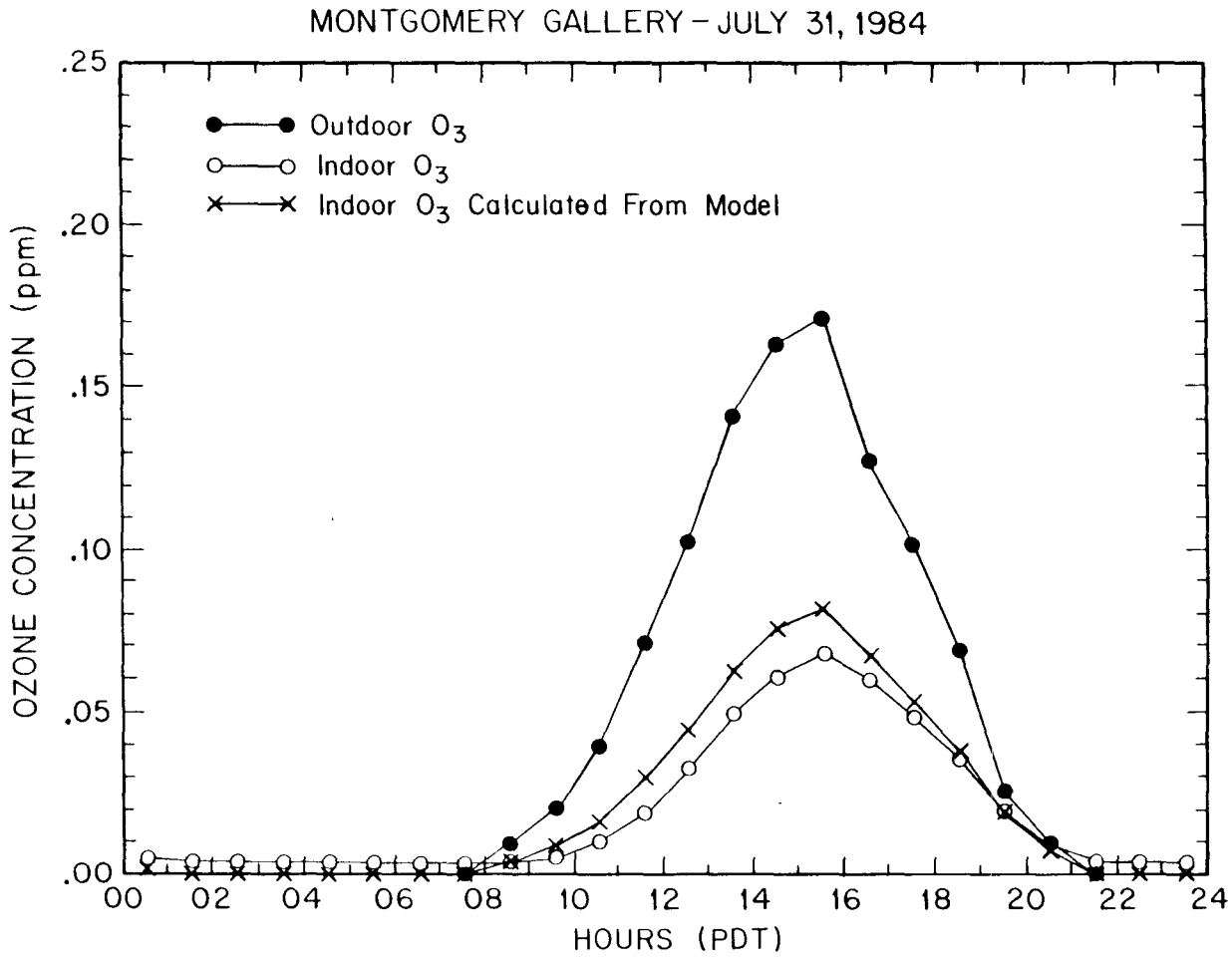

Figure 10.4. Indoor/outdoor ozone concentration relationships in the Montgomery Gallery, which has a modern conventional air conditioning system. Model results show indoor O_3 concentrations predicted from equations 10.1 and 10.2 using measured outdoor O_3 concentrations, an outdoor air exchange rate of 1.62 exchanges per hour, an internal air recirculation rate of 4.9 exchanges per hour, building surface and volume values from Table 10.2, and an ozone deposition velocity at surfaces of 0.051 cm sec^{-1} (0.10 ft^3/ft^2-min).

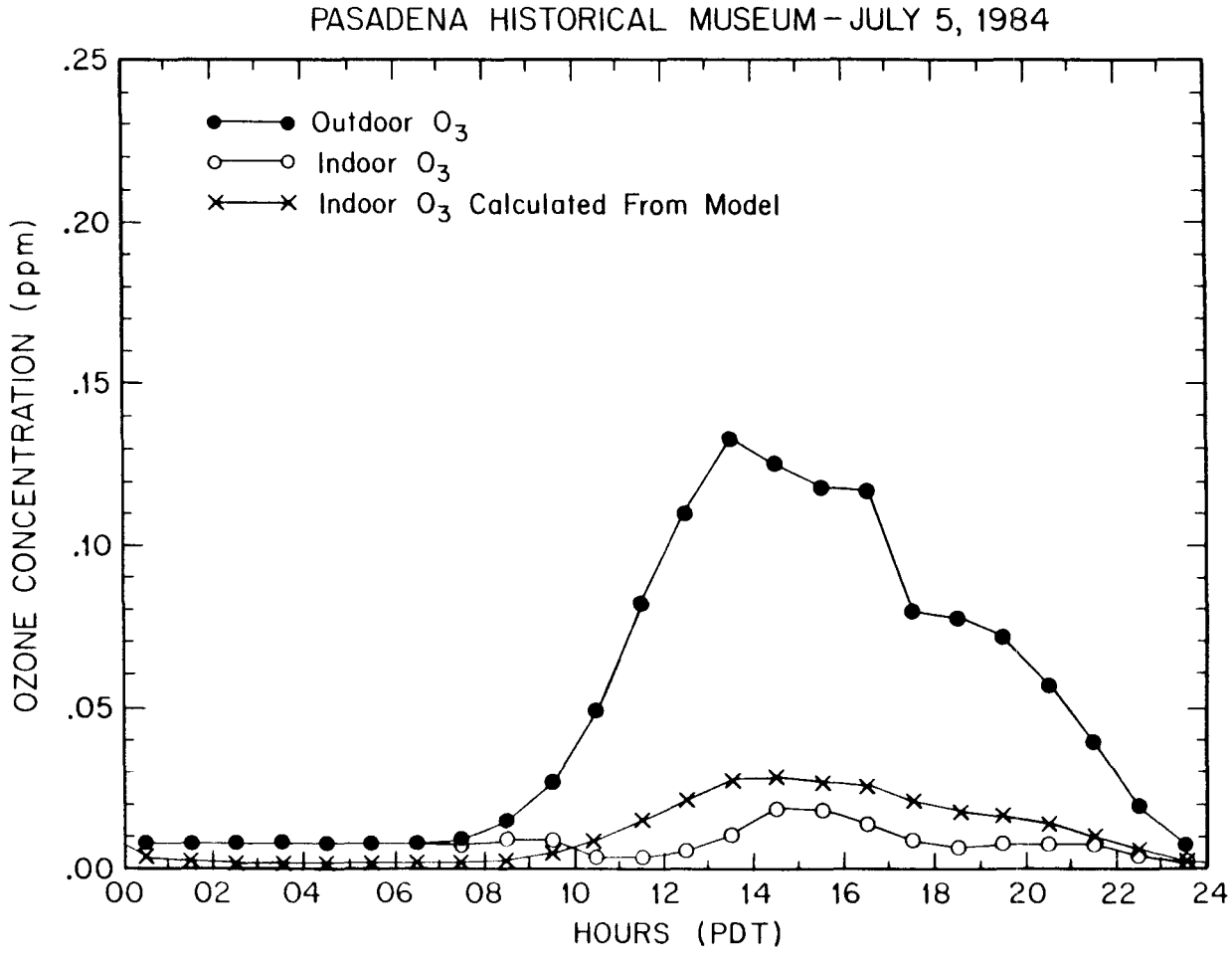

Figure 10.5. Indoor/outdoor ozone concentration relationships in the Pasadena Historical Society Museum, which has no air conditioning system and which has a slow air exchange rate. Model results show indoor O_3 concentrations predicted from equations 10.1 and 10.2 using measured outdoor O_3 concentrations, an outdoor air exchange rate of 0.5 exchanges per hour, building surface and volume values from Table 10.2, and an ozone deposition velocity at surfaces of 0.051 cm sec^{-1} (0.10 ft^3/ft^2-min).

good agreement between model predictions and observations confirms that the major contributors to the variability of indoor/outdoor ozone relationships between museums can be explained by the combined influence of air exchange rates, building surface and volume, and pollutant removal mechanisms. The best comparisons between theory and observation were obtained for buildings such as the Southwest Museum with rapid air exchange but no air conditioning or pollutant removal systems. Model calculations for buildings with a ducted ventilation system typically over-predict indoor concentrations and this might be due to the fact that large volumes of air are recirculated through ducts, particulate filtration and air handlers resulting in some loss of O_3 to surfaces within the ventilation system that are not represented within the present calculations. Reaction of O_3 with the oxides of nitrogen present in polluted urban air may also act to reduce indoor O_3 concentrations, but the effect of indoor chemical reactions cannot be evaluated here because data on the co-occurring oxides of nitrogen concentrations were not available during these experiments. In cases where high concentrations of NO or olefinic hydrocarbons are present in indoor or outdoor air, the air quality model computer code used here can explicitly treat O_3 removal by chemical reaction as explained in reference (11).

CONCLUSION

The distribution of ozone concentrations within museums in Southern California has been documented. Buildings with high rates of air exchange with the outdoor atmosphere but with no pollutant removal system show peak indoor concentrations greater than two-thirds as high as those outdoors. Buildings with conventional air conditioning systems show peak ozone levels inside about 30 to 40% of those outside. Museums with no forced ventilation system where slow air infiltration provides the only means for air exchange show lower ozone levels, typi-

cally 10% to 20% of those outdoors. Museums with well-maintained activated carbon air filtration systems and no air infiltration through open doors show low indoor ozone levels, usually below 0.01 ppm O_3, often as low as 0.003 to 0.004 ppm O_3, with indoor O_3 levels typically less than 10% of those experienced outdoors.

Indoor ozone levels generally can be predicted from data on building design and air exchange rates if ozone levels outside the facility are known. Using building parameters obtained from building superintendents and blueprints, the ozone level in many types of buildings can be computed with a reasonable degree of accuracy using existing indoor air quality models (5,11). This approach can be used to make estimates of the indoor exposure of works of art to O_3 concentrations on a year-round basis given the outdoor O_3 data routinely collected by governmental pollution control agencies. These predicted indoor O_3 levels can be compared to the levels recommended for storage conditions in museums, libraries and archives (12,13). Recommended indoor ozone levels range from 13 ppb to less than 1 ppb, with the most recent recommendations in the vicinity of 1 ppb O_3. If necessary, corrective actions then can be taken, as outlined in Chapter 12 of this study.

REFERENCES FOR CHAPTER 10

1. Yocum, J.E., 'Indoor-outdoor air quality relationships: A critical review', *J. Air Pollut. Control Assoc.*, **32** (1982) 500-520.

2. Thompson, G., *The Museum Environment*, Butterworths, London (1978).

3. Derwent, R.G., 'Ozone measurement in an art gallery,' Warren Spring Laboratory CR810(AP), (1973, unpublished) from Thomson, G., *The Museum Environment*, Butterworths, London (1978).

4. Mueller, F.X., Loeb, L., and Mapes, W.H., 'Decomposition rates of ozone in living areas', *Environ. Sci. Technol.*, **7** (1973) 342-346.

5. Shair, F.H., and Heitner, K.L., 'Theoretical model for relating indoor pollutant concentrations to those outside', *Environ. Sci. Technol.*, **8** (1974) 444-451.

6. Sabersky, R.H., Sinema, D.A., and Shair, F.H., 'Concentration, decay rates, and removal of ozone and their relation to established clean indoor air', *Environ. Sci. Technol.*, **7** (1973) 345-353.

7. Hales, C.H., Rollinson, A.M., and Shair, F.H., 'Experimental verification of linear combination model for relating indoor-outdoor pollutant concentrations', *Environ. Sci. Technol.*, **8** (1974) 452-453.

8. Shaver, C.L., Cass, G.R., and Druzik, J.R., 'Ozone and the deterioration of works of art', *Environ. Sci. Technol.*, **17** (1983) 748-752.

9. Hughes, E.E., and Myers, R., 'Measurement of the concentration of sulfur dioxide, nitrogen oxides, and ozone in the National Archives building', U.S. Department of Commerce/National Bureau of Standards, NBSIR 83-2767, Washington, D.C. (1983).

10. Davies, T.D., Ramer, B., Kaspyzok, G., and Delany, A.C., 'Indoor/outdoor ozone concentrations at a contemporary art gallery', *J. Air Pollut. Control Assoc.*, **31** (1984) 135-137.

11. Nazaroff, W.W., and Cass, G.R., 'Mathematical modeling of chemically-reactive pollutants to indoor air', *Environ. Sci. Technol.*, **20** (1986) 924-934.

12. Baer, N.S., and Banks, P.N., 'Indoor air pollution: Effects on cultural and historic materials', *Int. J. Museum Manage. Curatorship*, **4** (1985) 9-20.

13. Committee on Preservation of Historical Records, *Preservation of Historical Records*, National Research Council, National Academy Press, Washington, D.C. (1986).

14. Jennings, B.H., and Lewis, S.R., *Air Conditioning and Refrigeration*, International Textbook Co., Scranton, PA (1965).

CHAPTER 11

THE OZONE FADING OF ARTISTS' PIGMENTS: AN EVALUATION OF THE EFFECT OF BINDERS AND COATINGS

INTRODUCTION

Experiments described earlier in this report have shown that ozone, a common air pollutant, is capable of causing many artists' pigments to fade significantly upon prolonged exposure. These exposure studies, carried out in the absence of light, tested a variety of synthetic and natural organic colorants, including those found in modern watercolor paints, those used traditionally in western pictorial art, and traditional Japanese colorants (1-4). The results of these experiments indicate that, of the pigments studied, the alizarin lakes (including their natural counterpart, the madder lakes), curcumin, dragon's blood, indigo and orpiment are among the most ozone-sensitive. Subsequent studies focused on the chemical reactions occurring between ozone and alizarin lakes, indigos, curcumin, and triphenylmethane colorants to verify that ozone attack was indeed responsible for the rapid color loss observed during these experiments (5-8).

In these previous experiments the colorants tested were applied with either a very light binder (in the case of the watercolors) or no binder at all. However, in traditional pictorial and decorative arts the pigments are often applied as paints in a heavy binder (commonly oils, proteins, or more recently, synthetic polymers), frequently with a final varnish coating both for protection of the paint from dirt and abrasion and for optical saturation of the colors. It is natural to ask how these pigment plus binder plus coating systems react toward ambient ozone. Does the binder of the paint or the varnish coating act as a diffusion barrier, preventing or slowing the penetration of ozone into the paint to contact the pigment particles? Does the binding medium itself react with ozone, thereby scavenging the ozone but possibly breaking down to produce substances which can then attack the colorants?

Does the medium react so quickly that chalking of the paint rather than fading of the pigment becomes the more serious problem?

Although there is to our knowledge no documented instance of ozone damage to an easel painting, there is evidence which suggests that the potential for such attack is present. The vulnerability of many colorants to ozone fading has already been established, both in our work on artists' materials and in the extensive studies of dyes on textiles. A comprehensive review of the literature on textile dyes is beyond the scope of the present paper, but the reader is referred to reference (9) for a review of the subject. Investigations into the mechanism of the ozone reaction with artists' colorants indicate predominantly electrophilic attack at unsaturated carbon-carbon double bonds of the chromophore in the colorant molecules, the subsequent cleavage at these sites causing irreversible color loss (5-8).

Although it is the most visually obvious result of ozone damage, destruction of the colorant may not be the only consequence of ozone exposure of a paint. The polymers and other large organic molecules which constitute the paint medium or varnish layer may also suffer. The most rapid, and consequently the most studied ozone-polymer reaction is the deterioration of natural rubber, an elastomer having a large number of unsaturated carbon-carbon double bonds. Rapid ozone attack at these sites and subsequent chain scission leads to a loss of elasticity and mechanical strength. In fact, some of the earliest methods for monitoring ambient ozone concentrations were based on observation of the disintegration of a standard piece of rubber (10). Polymers composed of saturated hydrocarbons are less vulnerable to ozone damage than rubber, but ozone reaction with nylon (11) and polystyrene (12) has been observed, and the chalking and erosion of some modern house and industrial paints (particularly an "acrylic" coating of unspecified composition) also has been reported (13).

In addition to chain scission reactions, in which the average molecular weight

of the polymer decreases with a concomitant degradation of mechanical properties, ozone reaction with saturated hydrocarbon polymers also can generate free radicals or peroxides which can lead to cross-linking and the loss of solubility (14). The same chemistry occurs when such materials are exposed to oxygen or light, leading eventually to brittleness and insolubility in polymers, particularly those used as picture varnishes. These degradation processes are clearly of major importance to conservators, and it has been reported (although no comparative data have been given) that the ozone-induced cross-linking reactions are even more rapid than the thermal or light-induced chemistry (15).

Research into ways to protect polymers from ozone attack has in the past focused on the protection of the most vulnerable polymer, rubber. Modification of the rubber by substituting chlorine atoms near the carbon-carbon double bonds (forming neoprene rubber) reduces the polymer's reactivity towards ozone. (An analogous stabilization of the site for ozone reaction makes the thioindigo colorants much less ozone-sensitive than indigo (6); see Chapter 5.) The addition of anti-ozonants to a formulation can protect in the same ways as anti-oxidants or ultraviolet stabilizers (16,17), either by reacting more quickly with the ozone than the polymer, or, once the polymer has reacted with ozone, by scavenging the radicals which are formed and limiting the extent of the cross-linking reactions. Similar mechanisms occur in the anti-ozonant protection of colorants (18).

Protective coatings also have been used on polymers. Waxes added to rubber formulations will bloom on the surface, forming a coating which, unless damaged, is relatively impermeable to ozone (19). (This may also be the mechanism by which wax additives to ketone resin varnishes slow gradual oxidative cross-linking (20).) Passivation of the polymer surface by partial oxidation with chemicals or light also can slow the penetration of ozone to the bulk material (19), but such measures would not seem widely practical. The permeability of these coatings is of

paramount importance for their protective ability, and this quality is an additional characteristic by which to judge the adequacy of a picture varnish. Although an undesirable solution in many instances, framing under glass has been found to be quite effective in protecting even very vulnerable materials such as watercolors and pastels, which offer few alternatives for their safeguarding against atmospheric ozone (21).

The large number of different artists' paints and varnishes and the probable complexity of the ozone attack on a composite formed of pigment plus binders and coatings encouraged us to begin the study of this phenomenon with a carefully constructed model system. The work reported here focuses on systems containing Alizarin Crimson, one of the most ozone sensitive pigments currently used in artists' paints (1,2,5). Its fading rate as a dry pigment on paper and as a watercolor has been demonstrated in previous experiments, and its sensitivity as a dry pigment applied on a painted substrate was measured for comparison to the other systems in this study. The Alizarin Crimson is used here as a sensitive colorimetric detector of the penetration of ozone or its reaction products through the binder and coating systems tested. A variety of paints were obtained/prepared and tested, each containing Alizarin Crimson in a different binding medium. These paint vehicles included those used most commonly by artists (linseed oil, egg tempera, casein, beeswax, damar, alkyd enamel, and acrylic polymer emulsions) as well as those often used by conservators (solvent-based acrylics). Assuming that the ozone reactivity of the Alizarin Crimson pigment itself is relatively constant from one manufacturer to another (which in our experience has been the case), this part of the experiment allows comparison of the effect of the paint media on the ozone fading of the pigment. Similarly, a series of varnishes was tested (including damar, acrylics, and several commercial products of proprietary composition), as coatings for both Alizarin Crimson dry pigment with no binder, and for the Alizarin Crimson

paints of the first half of the study. Thus the protection afforded to the paints by the application of these coatings can be assessed and compared.

As in our previous exposure tests, the samples in this experiment were exposed to 0.40 parts per million (ppm) ozone at ambient temperature (22°C) and at 52% relative humidity (RH) for a period of twelve weeks. This ozone dose is roughly equivalent to that of a six to eight year exposure in a typical air-conditioned building in Los Angeles (1-3,22). Instrumental color measurements taken periodically during the exposure were used to determine the colorfastness of the various samples. Other changes in the appearance of the surface of the samples were evaluated visually but were not quantified. In those instances where a color loss was observed, the determination of the chemical mechanism for the ozone fading was beyond the scope of this survey experiment and has been left to be the subject of future work.

EXPERIMENTAL

The list of binders and coatings tested, and their manufacturers, is given in Table 11.1. Each of the samples tested in this experiment was prepared on a glass slide backing (5cm x 7.6cm), so that the backing would be inert towards the ozone and to ensure no ozone penetration from the underside of the paints being tested. The samples consist of a titanium white paint background layer, followed by additional layers of Alizarin Crimson paint or dry pigment, with or without a subsequent coating layer. The underpaint containing titanium white was used so that the translucence of the test paint and the color of the glass substrate would have a minimum effect on the measured color of the sample. A single layer of the titanium white background paint with dimensions 2.5cm wide by 5cm long first was "drawn down" over the glass slide using a razor blade, with a single strip of cellophane tape used as a thickness guide on either side of the paint film. Additional layers contain-

Table 11.1. The binders, coatings, and dry pigments used in this experiment. Listed also are the manufacturers of these materials.

BINDERS	Acrylic Color (Winsor & Newton)
	Acryloid B-72--Ethyl methacrylate copolymer (Conservation Materials Ltd.)
	Alkyd Color (Winsor & Newton)
	Beeswax (Conservation Materials Ltd.)
	Casein Color (Shiva, Inc.)
	Damar Varnish (Winsor & Newton)
	Egg Tempera (Rowney)
	Hyplar Acrylic Color (Grumbacher)
	Oil Color (Winsor & Newton)
	Magna Acrylic Resin (Bocour)
	Maimeri Restauro--restoring color
	Soluvar Varnish (Liquitex--Binney & Smith)
COATINGS	Aquatec Acrylic Polymer Emulsion Varnish (Bocour)
	Acryloid B-67--Isobutyl methacrylate polymer (Conservation Materials Ltd.)
	Acryloid B-72--Ethyl methacrylate copolymer (Conservation Materials Ltd.)
	Beeswax (Conservation Materials Ltd.)
	Casein Varnish (Shiva, Inc.)
	Damar Varnish (Winsor & Newton)
	Ethulose--Ethylhydroxyethylcellulose (Conservation Materials Ltd.)
	Krylon Crystal Clear Acrylic Spray Coating (Borden, Inc.)
	Magna Varnish (Bocour)
	Shellac (Zehrung Corp.)
	Soluvar Varnish (Binney & Smith)
PIGMENT	Alizarin Crimson--dry ground (Winsor & Newton)

ing Alizarin Crimson paint or coatings, equivalent in thickness to the background layer, were applied by the same method after the underlying layer was dried.

The first series of samples, listed in Table 11.2, tested the ozone sensitivity of Alizarin Crimson pigment in a number of different binding media. Several of these paints (Winsor and Newton Alkyd, Shiva Casein, Rowney Egg Tempera, Grumbacher Hyplar Acrylic, Winsor and Newton Oil, Magna Acrylic, and Maimeri Restauro) were available as tube colors, with the pigments already dispersed in the vehicle. The manufacturers' literature was the only source of information about many of these products--no attempt was made to characterize the identity of the ingredients or the formulation. For these commercial products, Alizarin Crimson paints were blended with the corresponding titanium white paint in the same binder to achieve a uniform color and consistency, with the resultant paint having a diffuse reflectance of approximately 40% at the wavelength of maximum absorption. At this depth of shade the color has been found to be very sensitive to changes in colorant concentration (23). Then, this mixture was applied over the background layer of the dried titanium white paint. Due to the prolonged drying times required for the alkyd and oil paints these two samples were applied without an underpainting. Instead, the Alizarin Crimson alkyd and oil paints were drawn down in layers which were twice as thick as the other Alizarin Crimson paints, making the total thickness of the alkyd and oil samples roughly the same as the others in this series.

Five of the materials tested as binders were not available as commercial paint vehicles, so paints were formulated with dry Alizarin Crimson pigment (Winsor & Newton). Beeswax was prepared as an encaustic paint according to a published recipe (24), with damar, thickened linseed oil, and turpentine (all from Winsor & Newton) added to the melted wax. While still warm, this mixture was mulled with the Alizarin Crimson pigment in a mortar and pestle, then remelted for application as a glaze over its white background layer. Acryloid B-72 (dissolved in toluene),

Table 11.2. Observed color change of Alizarin Crimson paints prepared in various binders upon exposure to 0.40 ppm ozone at 22°C, 52% RH, in the absence of light. CIE tristimulus values (X,Y,Z), chromaticity coordinates (x,y) and calculated Munsell notations (hue, value/chroma) for CIE Illuminant C are reported before and after the 12-week exposure period. Color differences between exposed and unexposed samples are calculated using the CIE 1976 L*a*b* formula.

BINDER	BACKGROUND BINDER	SAMPLE	WEEKS OF EXPOSURE	X	Y	Z	x	y	MUNSELL	ΔE	Category
W&N Acrylic	W&N Acrylic	A	0	56.47	49.78	61.49	0.33662	0.29679	4.13RP 7.44/5.21	--	
			12	60.74	55.11	68.76	0.32900	0.29854	3.26RP 7.77/4.52	4.71	**
		B	0	56.57	49.87	61.58	0.33668	0.29683	4.14RP 7.45/5.21	--	
			12	60.11	54.52	68.02	0.32909	0.29849	3.27RP 7.73/4.52	4.47	**
W&N Alkyd	none	A	0	63.06	55.33	64.40	0.34497	0.30269	6.40RP 7.78/5.43	--	
			12	63.91	56.68	66.36	0.34188	0.30317	6.15RP 7.86/5.14	1.59	*
		B	0	64.07	55.90	64.62	0.34711	0.30284	6.67RP 7.82/5.61	--	
			12	64.88	57.13	66.50	0.34418	0.30307	6.39RP 7.89/5.37	1.42	*
Beeswax	W&N Acrylic	A	0	56.29	48.49	52.16	0.35867	0.30897	9.41RP 7.36/5.75	--	
			12	56.14	48.48	52.12	0.35816	0.30931	9.48RP 7.36/5.68	0.35	
		B	0	62.55	54.41	57.55	0.35845	0.31177	0.21R 7.73/5.65	--	
			12	61.83	53.85	56.40	0.35931	0.31294	0.67R 7.69/5.59	0.65	
Shiva Casein	Shiva Casein	A	0	68.03	61.69	67.95	0.34413	0.31210	9.50RP 8.14/4.45	--	
			12	69.09	62.54	68.92	0.34449	0.31183	9.41RP 8.19/4.52	0.57	
		B	0	69.31	62.88	69.16	0.34423	0.31227	9.59RP 8.21/4.45	--	
			12	68.51	61.97	67.92	0.34533	0.31232	9.69RP 8.16/4.53	0.63	
Damar Varnish	W&N Acrylic	A	0	60.18	51.67	58.94	0.35236	0.30252	7.17RP 7.56/5.96	--	
			12	62.47	54.14	61.73	0.35027	0.30356	7.21RP 7.71/5.75	1.75	*
		B	0	60.51	50.84	56.47	0.36057	0.30292	7.95RP 7.51/6.59	--	
			12	63.26	53.61	59.40	0.35887	0.30412	8.08RP 7.68/6.42	1.83	*
Egg Tempera	Egg Tempera	A	0	59.20	53.21	60.29	0.34279	0.30809	7.91RP 7.66/4.58	---	
			12	60.58	54.48	61.86	0.34243	0.30792	7.77RP 7.73/4.60	0.75	
		B	0	58.49	52.56	59.60	0.34267	0.30801	7.88RP 7.62/4.57	--	
			12	60.18	54.14	61.42	0.34244	0.30807	7.85RP 7.71/4.58	0.93	
Grumbacher Hyplar	Grumbacher Hyplar	A	0	62.65	53.58	63.50	0.34859	0.29811	5.71RP 7.68/6.18	--	
			12	65.28	57.19	68.31	0.34217	0.29976	5.26RP 7.89/5.56	3.66	**
		B	0	61.94	52.83	62.53	0.34936	0.29796	5.77RP 7.63/6.24	--	
			12	65.50	57.48	68.79	0.34157	0.29975	5.16RP 7.91/5.52	4.42	**
W&N Oil	none	A	0	70.66	64.11	74.77	0.33721	0.30596	6.34RP 8.28/4.52	--	
			12	71.88	65.49	76.23	0.33651	0.30660	6.46RP 8.35/4.40	0.88	
		B	0	70.87	64.38	75.50	0.33627	0.30550	6.03RP 8.29/4.50	--	
			12	71.23	65.13	76.30	0.33493	0.30627	6.09RP 8.33/4.30	0.99	
Magna Acrylic	Magna Acrylic	A	0	60.93	51.69	62.40	0.34813	0.29534	5.10RP 7.56/6.38	--	
			12	71.34	67.14	80.96	0.32511	0.30598	4.16RP 8.44/3.45	15.95	***
		B	0	62.50	53.02	64.01	0.34815	0.29532	5.08RP 7.64/6.43	--	
			12	73.30	69.06	83.32	0.32480	0.30601	4.10RP 8.53/3.44	16.28	***
Maimeri Restauro	Maimeri Restauro	A	0	66.66	59.05	71.43	0.33813	0.29954	4.69RP 8.00/5.30	--	
			12	67.14	59.50	71.85	0.33824	0.29977	4.74RP 8.02/5.28	0.26	
		B	0	65.41	57.87	70.62	0.33732	0.29847	4.40RP 7.93/5.32	--	
			12	65.93	58.31	71.01	0.33765	0.29864	4.47RP 7.96/5.34	0.29	
Soluvar Varnish	W&N Acrylic	A	0	43.98	33.76	35.35	0.38889	0.29854	8.86RP 6.31/8.52	--	
			12	45.81	36.11	38.35	0.38091	0.30027	8.74RP 6.49/7.84	3.27	**
		B	0	42.27	30.78	30.24	0.40926	0.29801	9.66RP 6.06/9.77	--	
			12	43.80	32.50	32.42	0.40286	0.29894	9.53RP 6.21/9.40	2.27	*
B-72	W&N Acrylic	A	0	57.44	50.05	54.45	0.35468	0.30908	9.20RP 7.46/5.45	--	
			12	57.71	50.27	54.68	0.35479	0.30904	9.19RP 7.47/5.46	0.16	
		B	0	54.93	47.82	52.63	0.35356	0.30774	8.75RP 7.32/5.40	--	
			12	55.22	48.12	53.14	0.35292	0.30751	8.62RP 7.34/5.38	0.27	

damar (in mineral spirits), and Soluvar varnish were prepared as glazes with Alizarin Crimson pigment in a ball mill, then applied over their respective white underpaintings. The Winsor & Newton Acrylic paint was prepared by milling Alizarin Crimson pigment with the commercial titanium white paint. In each of these samples the Alizarin Crimson pigment was added to achieve the desired depth of shade.

The second set of samples was designed to test the protection afforded to Alizarin Crimson dry pigment by a varnish coating. In these samples, listed in Table 11.3, the pigment, suspended in a volatile solvent, was airbrushed onto the titanium white background paint through a stainless steel mask having two 1-centimeter diameter holes, thereby creating two separate sample spots (A and B) on each glass slide. Each of these Alizarin Crimson dry pigment samples was created with a depth of shade of approximately 40% at the wavelength of maximum absorption. Over this layer of pigment the coating was applied by drawing down with a razor blade (with the exception of the Krylon Crystal Clear, which was applied as two to three heavy coats of the aerosol spray). Most of the coating materials were available as prepared solutions or emulsions. The Acryloid B-67 and B-72 were dissolved in toluene for use as coatings; the Ethulose was used as a solution in water. The beeswax was prepared as an encaustic using the same procedure as described above for the paints. Control samples containing the titanium white background only, and titanium white background plus Alizarin Crimson dry pigment with no binder or coating were created for purposes of comparison, and are listed in Tables 11.4 and 11.5.

The final series of samples were varnished paints, each sample having successively applied single layers of titanium white background, Alizarin Crimson paint, and a coating. These three layers were of approximately equal thickness. The complete list of the various binder plus coating combinations is shown in Table 11.6.

The apparatus used for the ozone exposure is shown in Figure 11.1. A dry air-

Table 11.3. Observed color change of coated Alizarin Crimson dry pigment samples upon exposure to 0.40 ppm ozone at 22°C, 52% RH, in the absence of light. CIE tristimulus values (X,Y,Z), chromaticity coordinates (x,y) and calculated Munsell notations (hue, value/chroma) for CIE Illuminant C are reported before and after the 12-week exposure period. Color differences between exposed and unexposed samples are calculated using the CIE 1976 L*a*b* formula.

COATING	BACKGROUND BINDER	SAMPLE	WEEKS OF EXPOSURE	X	Y	Z	x	y	MUNSELL	ΔE	Category
Aquatec Acrylic Polymer Emulsion	W&N Acrylic	A	0	59.16	51.49	53.67	0.36003	0.31335	0.89R 7.55/5.54	--	
			12	60.05	52.47	54.72	0.35904	0.31376	0.99R 7.61/5.44	0.73	
		B	0	60.03	52.74	54.92	0.35797	0.31453	1.26R 7.63/5.27	--	
			12	60.52	53.08	55.09	0.35876	0.31465	1.34R 7.65/5.34	0.40	
B-67	W&N Acrylic	A	0	58.04	51.87	54.95	0.35207	0.31464	1.16R 7.57/4.70	--	
			12	58.43	52.15	55.50	0.35182	0.31400	0.87R 7.59/4.75	0.36	
		B	0	57.45	51.28	54.23	0.35255	0.31467	1.21R 7.54/4.72	--	
			12	58.24	51.80	55.15	0.35257	0.31357	0.72R 7.57/4.85	0.72	
B-72	W&N Acrylic	A	0	53.89	46.74	49.43	0.35912	0.31148	0.25R 7.25/5.48	--	
			12	53.70	46.40	49.19	0.35971	0.31079	0.05R 7.23/5.59	0.54	
		B	0	55.69	49.26	52.11	0.35457	0.31365	0.86R 7.41/4.95	--	
			12	55.88	49.31	52.39	0.35460	0.31295	0.57R 7.41/5.02	0.40	
Beeswax	W&N Acrylic	A	0	57.27	53.18	53.19	0.34999	0.32498	6.74R 7.65/3.53	--	
			12	60.63	55.90	54.52	0.35448	0.32679	7.19R 7.82/3.85	2.47	
		B	0	60.03	55.14	57.13	0.34842	0.31999	3.83R 7.77/3.90	--	
			12	62.00	56.78	58.27	0.35017	0.32070	4.11R 7.87/4.04	1.23	
Shiva Casein Varnish	Shiva Casein	A	0	51.81	43.33	39.92	0.38361	0.32081	3.77R 7.02/6.57	--	
			12	52.70	44.19	40.16	0.38450	0.32243	4.27R 7.08/6.54	0.94	
		B	0	51.92	43.28	39.54	0.38533	0.32122	3.89R 7.01/6.67	--	
			12	52.27	43.66	39.43	0.38616	0.32257	4.30R 7.04/6.64	0.66	
Damar Varnish	W&N Acrylic	A	0	53.62	44.79	47.34	0.36789	0.30729	9.46RP 7.12/6.57	--	
			12	56.75	47.75	51.34	0.36414	0.30643	9.02RP 7.31/6.45	2.10	
		B	0	55.97	47.04	49.51	0.36697	0.30839	9.68RP 7.27/6.47	--	
			12	56.73	47.58	50.41	0.36665	0.30753	9.43RP 7.30/6.55	0.59	
Ethulose	W&N Acrylic	A	0	56.43	48.80	52.10	0.35866	0.31018	9.77RP 7.38/5.64	--	
			12	57.52	49.71	53.09	0.35880	0.31006	9.73RP 7.44/5.70	0.61	
		B	0	59.38	51.19	53.83	0.36120	0.31137	0.23R 7.53/5.83	--	
			12	60.30	51.87	54.42	0.36196	0.31137	0.25R 7.57/5.92	0.60	
Krylon Crystal Clear	W&N Acrylic	A	0	59.27	51.68	56.07	0.35487	0.30943	9.30RP 7.56/5.48	--	
			12	59.90	52.16	56.71	0.35493	0.30907	9.18RP 7.59/5.54	0.40	
		B	0	61.72	54.45	58.61	0.35315	0.31153	9.88RP 7.73/5.19	--	
			12	62.70	55.30	59.28	0.35367	0.31192	0.04R 7.78/5.22	0.56	
Magna Varnish	Magna Acrylic	A	0	51.47	42.64	49.57	0.35824	0.29678	6.52RP 6.97/6.73	--	
			12	52.13	43.08	50.01	0.35896	0.29664	6.56RP 7.00/6.83	0.52	
		B	0	51.94	43.02	50.40	0.35734	0.29594	6.27RP 7.00/6.77	--	
			12	53.08	43.92	51.48	0.35751	0.29581	6.25RP 7.06/6.83	0.69	
Shellac	W&N Acrylic	A	0	57.53	51.02	48.78	0.36568	0.32430	5.29R 7.52/4.99	--	
			12	57.67	51.21	48.57	0.36628	0.32522	5.63R 7.53/4.96	0.44	
		B	0	56.58	50.07	48.59	0.36445	0.32252	4.63R 7.46/5.01	--	
			12	56.37	49.87	48.21	0.36498	0.32289	4.77R 7.45/5.01	0.22	
Soluvar	W&N Acrylic	A	0	62.24	55.68	59.64	0.35054	0.31359	0.58R 7.80/4.77	--	
			12	66.65	61.80	67.45	0.34022	0.31549	1.09R 8.15/3.72	5.81	**
		B	0	60.48	53.63	57.44	0.35254	0.31262	0.29R 7.68/5.00	--	
			12	66.75	62.29	68.31	0.33823	0.31564	1.16R 8.18/3.52	8.20	**

Table 11.4. Observed color change of titanium white backgrounds upon exposure to 0.40 ppm ozone at 22°C, 52% RH, in the absence of light. CIE tristimulus values (X,Y,Z), chromaticity coordinates (x,y) and calculated Munsell notations (hue, value/chroma) for CIE Illuminant C are reported before and after the 12-week exposure period. Color differences between exposed and unexposed samples are calculated using the CIE 1976 L*a*b* formula.

BACKGROUND BINDER	SAMPLE	WEEKS OF EXPOSURE	X	Y	Z	x	y	MUNSELL	ΔE
W&N Acrylic	A	0	83.69	86.22	100.34	0.30967	0.31903		--
		12	83.12	85.46	100.58	0.30882	0.31750		0.85
	B	0	87.04	89.67	102.35	0.31192	0.32132		--
		12	87.23	89.72	103.43	0.31110	0.32000		0.68
W&N Alkyd	A	0	86.91	89.75	96.70	0.31794	0.32832	0.43GY 9.49/0.65	--
		12	86.95	89.74	96.59	0.31817	0.32836	9.91Y 9.49/0.66	0.11
	B	0	86.38	89.29	96.82	0.31700	0.32768	1.78GY 9.47/0.61	--
		12	86.27	89.11	96.60	0.31719	0.32764	1.20GY 9.46/0.61	0.14
Shiva Casein	A	0	82.58	85.51	87.20	0.32347	0.33495	7.73Y 9.31/1.04	--
		12	83.62	86.39	86.18	0.32641	0.33721	5.90Y 9.35/1.22	1.45
	B	0	83.34	86.23	86.62	0.32531	0.33657	6.73Y 9.34/1.16	--
		12	83.27	85.96	83.75	0.32918	0.33978	5.06Y 9.33/1.41	1.86
Egg Tempera	A	0	79.98	82.75	84.50	0.32351	0.33471	7.37Y 9.19/1.02	--
		12	81.52	84.34	87.28	0.32204	0.33318	8.16Y 9.26/0.93	1.02
	B	0	82.89	85.49	86.28	0.32550	0.33571	5.53Y 9.31/1.15	--
		12	84.12	86.78	88.51	0.32428	0.33452	5.95Y 9.36/1.07	0.81
Grumbacher Hyplar	A	0	89.78	92.18	106.85	0.31087	0.31917		--
		12	92.32	94.77	109.68	0.31109	0.31932		1.05
	B	0	92.74	95.22	109.48	0.31179	0.32013		--
		12	94.05	96.54	110.89	0.31195	0.32023		0.53
W&N Oil	A	0	89.25	91.99	101.65	0.31550	0.32516		--
		12	89.25	91.98	101.11	0.31612	0.32577		0.33
	B	0	88.15	90.87	99.52	0.31647	0.32624	0.74GY 9.54/0.54	--
		12	88.47	91.12	99.41	0.31709	0.32661	9.40Y 9.55/0.57	0.30
Magna Acrylic	A	0	89.53	91.87	106.59	0.31088	0.31901		--
		12	90.57	92.86	108.38	0.31038	0.31821		0.57
	B	0	85.47	87.71	101.97	0.31063	0.31877		--
		12	91.06	93.36	109.10	0.31024	0.31809		2.36(a)
Maimeri Restauro	A	0	91.60	94.22	106.10	0.31379	0.32277		--
		12	91.45	94.09	105.86	0.31383	0.32289		0.08
	B	0	90.69	93.26	104.07	0.31487	0.32380		--
		12	91.84	94.46	105.33	0.31491	0.32391		0.49

Notes:

(a) The actual color change is probably much less than shown. Consecutive color measurements at intervals throughout the 12-week exposure show little change except at the end of the first week. It is possible that the initial measurement at time zero was in error.

Table 11.5. Observed color change of Alizarin Crimson dry pigment samples with no binder or coating upon exposure to 0.40 ppm ozone at 22°C, 52% RH, in the absence of light. CIE tristimulus values (X,Y,Z), chromaticity coordinates (x,y) and calculated Munsell notations (hue, value/chroma) for CIE Illuminant C are reported before and after the 12-week exposure period. Color differences between exposed and unexposed samples are calculated using the CIE 1976 L*a*b* formula.

BACKGROUND BINDER	SAMPLE	WEEKS OF EXPOSURE	X	Y	Z	x	y	MUNSELL	ΔE	Category
W&N Acrylic	A	0	66.01	59.15	64.15	0.34869	0.31245	9.95RP 8.00/4.81	--	
		12	85.07	85.50	97.00	0.31794	0.31953	0.22YR 9.31/0.79	20.69	***
	B	0	67.42	61.08	66.38	0.34595	0.31342	0.22R 8.11/4.47	--	
		12	86.16	86.76	98.33	0.31764	0.31984	1.39YR 9.36/0.70	19.48	***
W&N Alkyd	A	0	60.97	51.83	51.65	0.37075	0.31519	1.77R 7.57/6.31	--	
		12	80.20	78.99	82.78	0.33146	0.32642	1.85YR 9.02/2.02	24.25	***
	B	0	60.62	51.19	50.80	0.37282	0.31479	1.70R 7.53/6.49	--	
		12	81.05	80.15	84.07	0.33044	0.32677	2.65YR 9.07/1.83	26.00	***
Shiva Casein	A	0	58.51	51.67	48.69	0.36831	0.32522	5.52R 7.56/5.16	--	
		12	65.64	60.05	57.05	0.35918	0.32862	7.53R 8.05/4.21	6.36	**
	B	0	60.25	53.32	50.65	0.36690	0.32470	5.34R 7.66/5.13	--	
		12	75.38	73.37	72.33	0.34096	0.33188	2.78YR 8.75/2.50	16.42	***
Magna Acrylic	A	0	66.13	58.33	64.05	0.35081	0.30944	8.97RP 7.96/5.31	--	
		12	80.46	77.29	86.79	0.32902	0.31607	1.25R 8.94/2.73	14.94	***
	B	0	65.29	57.41	63.19	0.35123	0.30886	8.81RP 7.90/5.38	--	
		12	79.22	76.07	85.72	0.32870	0.31563	0.79R 8.88/2.74	15.17	***

Table 11.6. Observed color change of binder and coating systems containing Alizarin Crimson paints upon exposure to 0.40 ppm ozone at 22°C, 52% RH, in the absence of light. CIE tristimulus values (X,Y,Z), chromaticity coordinates (x,y) and calculated Munsell notations (hue, value/chroma) for CIE Illuminant C are reported before and after the 12-week exposure period. Color differences between exposed and unexposed samples are calculated using the CIE 1976 L*a*b* formula.

COATING	BINDER	BACKGROUND BINDER	SAMPLE	WEEKS OF EXPOSURE	X	Y	Z	x	y	MUNSELL	ΔE	Category
Aquatec Acrylic Polymer Emulsion	W&N Acrylic	W&N Acrylic	A	0	49.75	42.28	49.65	0.35115	0.29844	6.19RP 6.95/5.93	--	
				12	50.17	42.71	49.61	0.35208	0.29976	6.57RP 6.98/5.90	0.64	
			B	0	50.73	43.22	52.08	0.34738	0.29595	5.26RP 7.01/5.93	--	
				12	51.23	43.67	52.10	0.34853	0.29705	5.60RP 7.04/5.92	0.59	
	B-72	W&N Acrylic	A	0	56.32	50.93	58.84	0.33910	0.30665	6.97RP 7.52/4.36	--	
				12	56.19	50.77	58.32	0.33997	0.30719	7.28RP 7.51/4.37	0.33	
			B	0	62.41	56.08	62.07	0.34567	0.31058	9.06RP 7.83/4.65	--	
				12	63.06	56.61	62.24	0.34667	0.31119	9.36RP 7.86/4.69	0.51	
	Shiva Casein	Shiva Casein	A	0	63.19	56.73	59.34	0.35251	0.31646	1.96R 7.86/4.68	--	
				12	62.02	55.87	56.00	0.35664	0.32132	4.21R 7.81/4.57	2.34	*
			B	0	63.22	56.67	59.94	0.35156	0.31515	1.30R 7.86/4.73	--	
				12	62.51	56.21	57.56	0.35461	0.31885	3.10R 7.83/4.62	1.77	*
	Egg Tempera	Egg Tempera	A	0	50.71	45.32	44.64	0.36049	0.32217	4.71R 7.15/4.53	--	
				12	50.42	45.20	42.58	0.36483	0.32706	6.59R 7.15/4.49	2.17	*
			B	0	52.31	46.63	47.18	0.35801	0.31911	3.33R 7.24/4.63	--	
				12	51.65	46.12	45.07	0.36157	0.32289	4.98R 7.21/4.59	1.73	*
	Maimeri Restauro	Maimeri Restauro	A	0	60.29	53.06	63.43	0.34106	0.30014	5.25RP 7.65/5.29	--	
				12	60.29	53.09	62.92	0.34197	0.30112	5.64RP 7.65/5.27	0.47	
			B	0	60.50	53.21	63.77	0.34090	0.29978	5.14RP 7.66/5.32	--	
				12	60.60	53.31	63.48	0.34161	0.30054	5.43RP 7.66/5.31	0.37	
B-72	W&N Acrylic	W&N Acrylic	A	0	49.12	42.66	48.85	0.34930	0.30336	7.19RP 6.97/5.30	--	
				12	49.44	42.89	49.13	0.34950	0.30321	7.17RP 6.99/5.34	0.24	
			B	0	48.36	42.03	46.49	0.35327	0.30707	8.60RP 6.93/5.23	--	
				12	48.55	42.16	46.58	0.35364	0.30710	8.63RP 6.94/5.26	0.18	
	B-72	W&N Acrylic	A	0	54.48	48.62	53.44	0.34801	0.31059	9.33RP 7.37/4.65	--	
				12	53.95	48.02	52.88	0.34840	0.31008	9.18RP 7.33/4.72	0.50	
			B	0	56.36	50.12	54.18	0.35082	0.31194	10.00RP 7.47/4.81	--	
				12	56.65	50.25	54.32	0.35140	0.31166	9.92RP 7.47/4.89	0.37	
	Shiva Casein	Shiva Casein	A	0	57.80	51.97	56.76	0.34709	0.31206	9.81RP 7.58/4.51	--	
				12	56.92	51.21	55.30	0.34827	0.31337	0.45R 7.53/4.47	0.76	
			B	0	60.54	54.39	59.43	0.34719	0.31196	9.73RP 7.73/4.60	--	
				12	60.34	54.25	59.12	0.34735	0.31231	9.89RP 7.72/4.58	0.20	
	Egg Tempera	Egg Tempera	A	0	50.31	44.38	48.28	0.35191	0.31040	9.57RP 7.09/4.88	--	
				12	50.90	44.85	48.54	0.35276	0.31085	9.76RP 7.12/4.92	0.46	
			B	0	49.97	44.03	48.24	0.35133	0.30952	9.23RP 7.07/4.90	--	
				12	50.55	44.48	48.59	0.35197	0.30970	9.32RP 7.10/4.96	0.42	
	Maimeri Restauro	Maimeri Restauro	A	0	57.51	51.03	62.02	0.33719	0.29918	4.60RP 7.52/5.02	--	
				12	58.23	51.61	62.60	0.33769	0.29928	4.67RP 7.56/5.06	0.43	
			B	0	57.82	51.25	62.20	0.33761	0.29921	4.65RP 7.54/5.05	--	
				12	58.73	51.99	63.00	0.33809	0.29929	4.71RP 7.58/5.11	0.52	

Table 11.6 Continued. Observed color change of binder and coating systems containing Alizarin Crimson paints upon exposure to 0.40 ppm ozone at 22°C, 52% RH, in the absence of light. CIE tristimulus values (X,Y,Z), chromaticity coordinates (x,y) and calculated Munsell notations (hue, value/chroma) for CIE Illuminant C are reported before and after the 12-week exposure period. Color differences between exposed and unexposed samples are calculated using the CIE 1976 L*a*b* formula.

COATING	BINDER	BACKGROUND BINDER	SAMPLE	WEEKS OF EXPOSURE	X	Y	Z	x	y	MUNSELL	ΔE	Category
Shiva Casein Varnish	Shiva Casein	Shiva Casein	A	0	66.09	59.24	64.96	0.34732	0.31129	9.41RP 8.01/4.80	--	
				12	66.17	59.27	64.67	0.34805	0.31177	9.64RP 8.01/4.83	0.29	
			B	0	66.28	59.36	64.48	0.34861	0.31221	9.85RP 8.01/4.83	--	
				12	65.86	58.98	63.65	0.34942	0.31291	0.18R 7.99/4.83	0.41	
Damar Varnish	W&N Acrylic	W&N Acrylic	A	0	52.31	45.54	54.11	0.34423	0.29969	5.66RP 7.17/5.37	--	
				12	53.79	47.03	55.32	0.34450	0.30122	6.05RP 7.27/5.28	1.16	
			B	0	51.61	44.97	52.99	0.34504	0.30065	6.01RP 7.13/5.31	--	
				12	53.62	46.90	54.74	0.34536	0.30205	6.38RP 7.26/5.26	1.36	
	B-72	W&N Acrylic	A	0	59.65	52.32	57.05	0.35292	0.30953	9.22RP 7.60/5.31	--	
				12	60.67	53.39	57.99	0.35263	0.31033	9.44RP 7.67/5.24	0.76	
			B	0	53.74	46.46	51.53	0.35418	0.30622	8.35RP 7.23/5.56	--	
				12	55.66	48.41	53.89	0.35234	0.30649	8.27RP 7.36/5.45	1.36	
	Shiva Casein	Shiva Casein	A	0	63.40	56.80	61.95	0.34805	0.31182	9.70RP 7.87/4.76	--	
				12	63.79	57.16	62.56	0.34761	0.31148	9.53RP 7.89/4.76	0.27	
			B	0	63.78	57.12	61.82	0.34903	0.31262	0.06R 7.89/4.78	--	
				12	63.71	57.06	61.53	0.34948	0.31302	0.25R 7.88/4.77	0.20	
	Egg Tempera	Egg Tempera	A	0	50.65	44.23	48.52	0.35320	0.30844	8.99RP 7.08/5.18	--	
				12	51.64	45.03	49.82	0.35252	0.30741	8.60RP 7.13/5.25	0.73	
			B	0	50.62	43.98	47.93	0.35517	0.30856	9.15RP 7.06/5.32	--	
				12	52.26	45.26	50.22	0.35371	0.30637	8.37RP 7.15/5.47	1.35	
	Maimeri Restauro	Maimeri Restauro	A	0	57.15	50.13	60.31	0.34102	0.29910	5.05RP 7.487/5.31	--	
				12	58.67	51.73	60.48	0.34332	0.30273	6.26RP 7.57/5.17	1.89	*
			B	0	56.99	50.04	60.40	0.34036	0.29890	4.92RP 7.46/5.28	--	
				12	58.98	51.98	61.36	0.34229	0.30164	5.83RP 7.58/5.20	1.68	*
Magna Varnish	Magna Acrylic	Magna Acrylic	A	0	60.89	51.38	60.44	0.35256	0.29750	6.03RP 7.54/6.51	--	
				12	62.01	52.08	61.58	0.35299	0.29649	5.85RP 7.59/6.69	0.93	
			B	0	61.34	51.80	61.22	0.35180	0.29708	5.86RP 7.57/6.51	--	
				12	61.99	52.11	62.01	0.35199	0.29591	5.63RP 7.59/6.67	0.81	
Soluvar Varnish	W&N Acrylic	W&N Acrylic	A	0	51.49	44.64	53.65	0.34376	0.29803	5.24RP 7.11/5.47	--	
				12	51.67	44.81	54.07	0.34320	0.29762	5.08RP 7.12/5.47	0.24	
			B	0	52.14	45.23	54.61	0.34308	0.29757	5.04RP 7.15/5.48	--	
				12	52.49	45.53	55.17	0.34266	0.29719	4.92RP 7.17/5.50	0.28	
	B-72	W&N Acrylic	A	0	59.06	52.49	58.52	0.34726	0.30862	8.51RP 7.61/4.90	--	
				12	59.04	52.44	58.20	0.34795	0.30904	8.71RP 7.61/4.92	0.26	
			B	0	55.75	49.95	56.98	0.34271	0.30705	7.56RP 7.45/4.60	--	
				12	55.28	49.51	56.43	0.34287	0.30711	7.60RP 7.43/4.60	0.27	
	Shiva Casein	Shiva Casein	A	0	63.90	57.23	61.54	0.34983	0.31328	0.40R 7.89/4.78	--	
				12	63.31	56.76	60.71	0.35020	0.31398	0.72R 7.87/4.73	0.44	
			B	0	63.00	56.36	60.85	0.34957	0.31278	0.16R 7.84/4.79	--	
				12	62.59	56.09	60.01	0.35026	0.31389	0.70R 7.83/4.73	0.55	

Table 11.6 Continued. Observed color change of binder and coating systems containing Alizarin Crimson paints upon exposure to 0.40 ppm ozone at 22°C, 52% RH, in the absence of light. CIE tristimulus values (X,Y,Z), chromaticity coordinates (x,y) and calculated Munsell notations (hue, value/chroma) for CIE Illuminant C are reported before and after the 12-week exposure period. Color differences between exposed and unexposed samples are calculated using the CIE 1976 L*a*b* formula.

COATING	BINDER	BACKGROUND BINDER	SAMPLE	WEEKS OF EXPOSURE	X	Y	Z	x	y	MUNSELL	ΔE	Category
Soluvar Varnish	Egg Tempera	Egg Tempera	A	0	52.01	45.41	50.43	0.35179	0.30711	8.46RP 7.16/5.23	--	
				12	53.72	46.98	52.47	0.35074	0.30670	8.23RP 7.26/5.23	1.05	
			B	0	51.08	44.84	49.35	0.35159	0.30868	8.95RP 7.12/5.04	--	
				12	51.56	45.39	50.00	0.35086	0.30889	8.96RP 7.16/4.97	0.47	
	Maimeri Restauro	Maimeri Restauro	A	0	65.03	58.25	69.58	0.33719	0.30204	5.13RP 7.95/4.90	--	
				12	64.93	58.18	69.49	0.33713	0.30209	5.13RP 7.95/4.89	0.07	
			B	0	64.52	57.59	69.05	0.33754	0.30124	4.98RP 7.91/5.00	--	
				12	64.59	57.72	68.94	0.33771	0.30181	5.15RP 7.92/4.96	0.30	

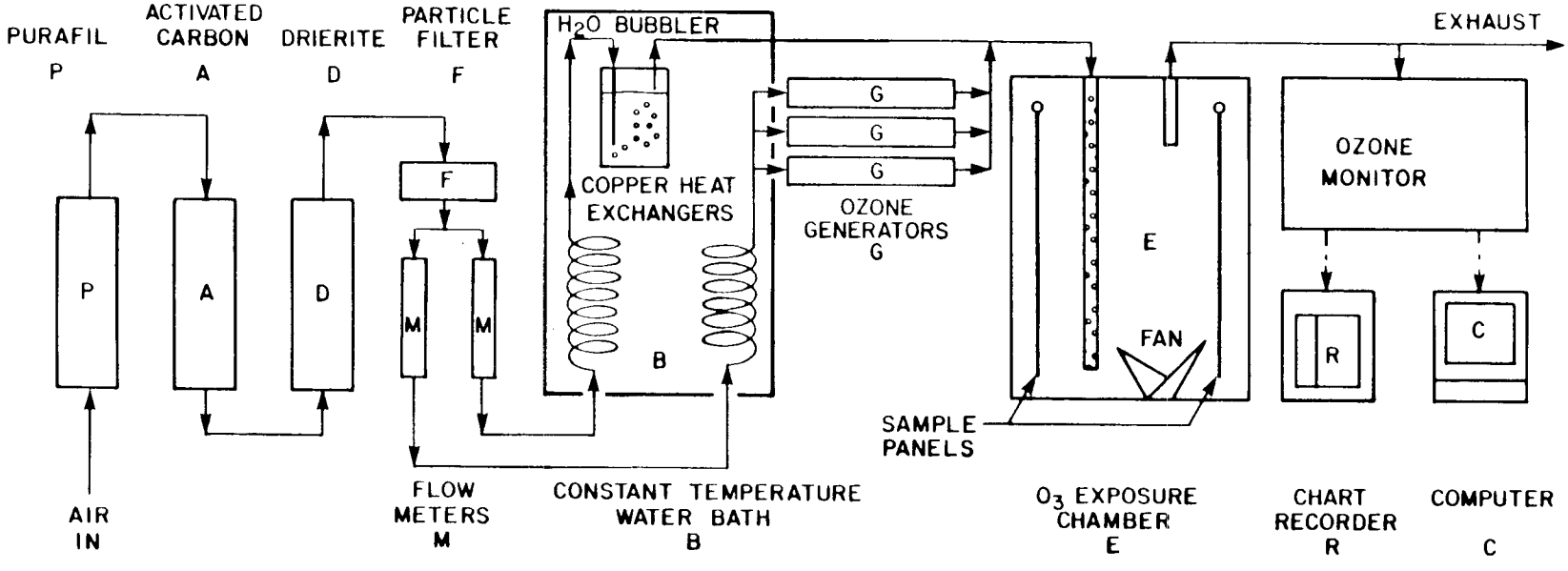

Figure 11.1. Ozone exposure apparatus.

stream at a flow rate of 2.5 lpm was passed through a series of filters to remove pollutants. The flow was then split in half. One stream was saturated with water vapor, while the second dry airstream was irradiated with ultraviolet light to produce ozone. The ozonated and humidified airstreams were mixed and then the air was pumped into a light-tight chamber through a perforated Teflon tube. The colorant samples were mounted on anodized aluminum panels oriented such that the samples faced the interior of the chamber. The ozone concentration was measured continuously with an ultraviolet photometric ozone monitor (Dasibi model 1003-AH), and these data were collected through the use of a computer and averaged hourly. The samples were exposed for a total of twelve weeks to 0.40 parts per million (ppm) ozone at 52% RH and 22°C in the absence of light.

Prior to and periodically during the exposure experiment the diffuse reflectance spectra of the samples were recorded using a Diano MatchScan II spectrophotometer. The instrument was calibrated with a standard white tile which had been referenced to an NBS standard, and the small-area-view option was utilized to limit the measurement to a 7 millimeter diameter area on the sample. Two areas on each sample were measured, and a jig was used to hold the glass slides in a position reproducible from one measurement to the next. Reflectance measurements were made at 2 nanometer (nm) intervals between 380 nm and 700 nm. The results were stored on floppy disk, as well as being printed and plotted. Tristimulus values (X,Y,Z) and chromaticity coordinates (x,y) were calculated from the reflectance data; color differences (ΔE) for CIE Illuminant C were calculated using the CIE 1976 $L^*a^*b^*$ formula (25). Munsell color notations (hue value/chroma) were calculated from the tristimulus values (26). The small viewing area and the variation in sample positioning produced an inherent error in the reflectance spectra of a few percent which translates to an uncertainty in the calculated color difference ΔE of about 1 unit.

RESULTS AND DISCUSSION

The results for the binder and coating systems tested are given in Tables 11.2, 11.3 and 11.6. Data on the control samples consisting of the titanium white background, and white background plus uncoated Alizarin Crimson dry pigment are given in Tables 11.4 and 11.5. The calculated color differences ΔE provide a convenient measure of the total color change that occurred over the course of the ozone exposure experiment. As a color change ΔE of one unit is approximately at the limit of the reproducibility of consecutive measurements in this experiment, and because a ΔE value of less than one is generally considered to be a fairly good color match between samples, only those samples that show a color change ΔE of greater than one unit will be considered to have changed perceptibly under the conditions of this experiment. In an effort to highlight those Alizarin Crimson samples within Tables 11.2-11.6 that did change color perceptibly, asterisks have been placed in the far right column of those tables. Borderline cases with only a slight degree of fading are indicated by one asterisk if a color change in the range ΔE = 1-3 units occurred *and* if both samples of the material show a monotonic increase in reflectance throughout the 12-week ozone exposure. Samples with a larger color change in the range ΔE = 3-8 units receive two asterisks, while very reactive systems with $\Delta E > 9$ units over the 12 week exposure are denoted by three asterisks. The remaining samples have changed by an amount that is too small to be measurable under the conditions of this experiment. It is important to note, however, that the length of exposure used in this experiment is comparatively short (equivalent to only a few years inside a museum) and so only the most reactive materials will show a measurable fading. Samples that changed by less than one ΔE unit may simply deteriorate at a slower rate than the other samples.

The Alizarin Crimson dry pigment samples applied over a white background with no binder or coating faded dramatically, as shown in Table 11.5. The

reflectance spectra of one of these dry pigment samples is given in Figure 11.2, and shows very rapid changes within the first few weeks, with the reflectance spectrum approaching that of the white background alone by the end of 12 weeks (compare Figures 11.2 and 11.3).

Results for the Alizarin Crimson paint samples dispersed in various binders are given in Table 11.2. Obvious color changes occurred in several of the Alizarin Crimson paints, particularly in cases where acrylic media were used as a binder. The changes in reflectance spectra over time for two of these reactive pigment and binder systems are shown in Figures 11.4 and 11.5. These reflectance spectra and the Munsell notations for the samples which exhibited a color change show that this color change is predominantly a fading (increased value or lightness) and decrease in saturation or chroma. A slight shift in hue is also observed, the general trend toward blue in the ozone sensitive paints (Table 11.2) contrasting with the marked yellowing of the ozone-faded dry pigment samples (Table 11.5). It is likely that much of the hue shift in these latter samples is related to the presence of the titanium white underpainting. Color changes observed in the titanium white background samples are given in Table 11.4.

As is seen in Table 11.3, application of most of the coatings tested over the top of an Alizarin Crimson dry pigment sample produced a dramatic reduction in the fading rate when compared to the uncoated dry pigment samples evaluated in Table 11.5. The principal exception to this observation is that the samples coated with Soluvar varnish both faded noticeably. The reflectance spectra of Alizarin Crimson dry pigment samples coated with Soluvar and with B-72 are compared in Figure 11.6. While both of these coatings are acrylic in nature, the B-72 coating was initially prepared in toluene before application, while the commercially distributed Soluvar has a mineral spirits base. Further investigation is needed to determine the possible role of the solvent medium used as it affects the ozone protection afforded

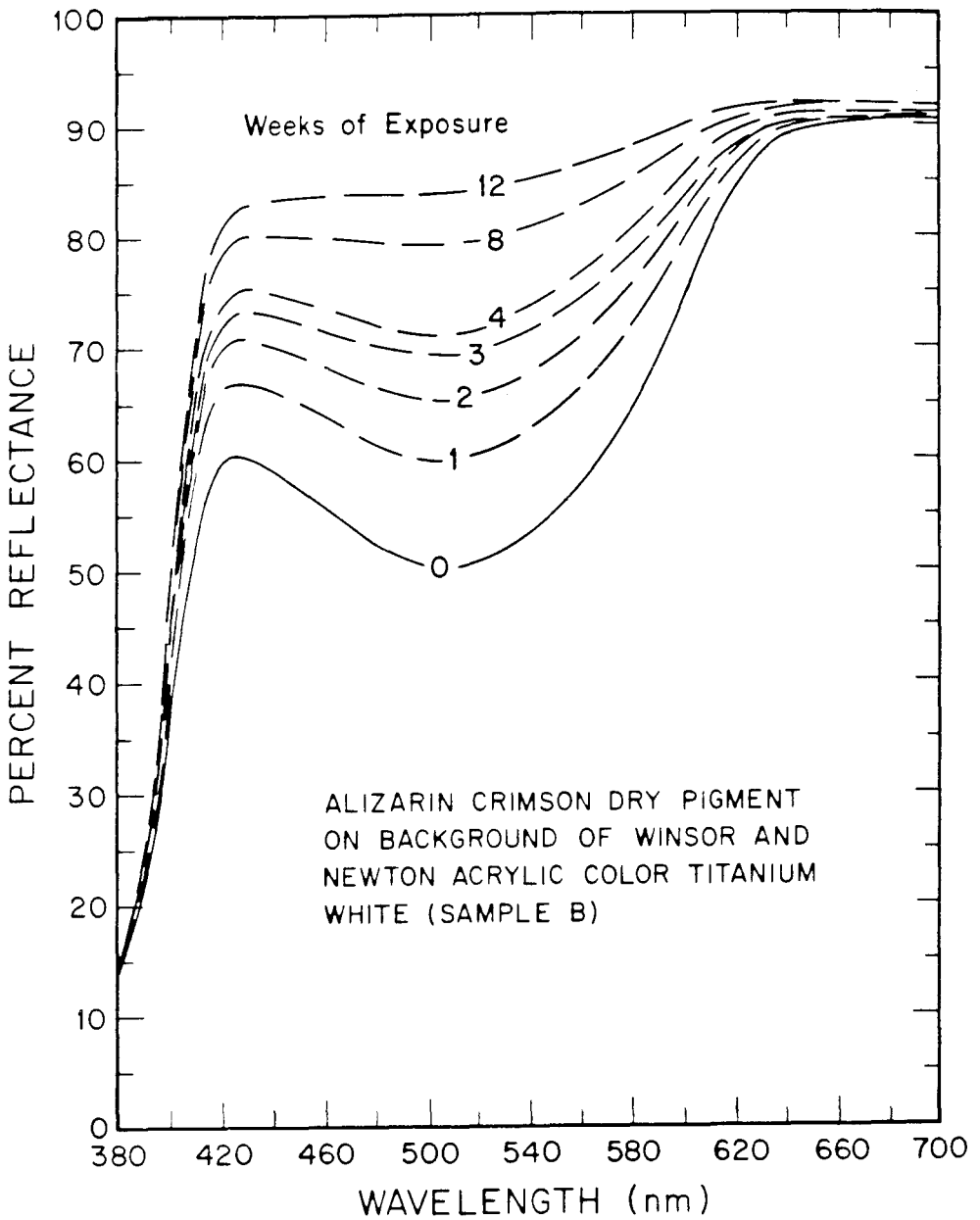

Figure 11.2. Reflectance spectrum of an Alizarin Crimson dry pigment sample with no protective binder or coating at several stages during its exposure to 0.40 ppm ozone at 22°C, 52% RH, in the absence of light.

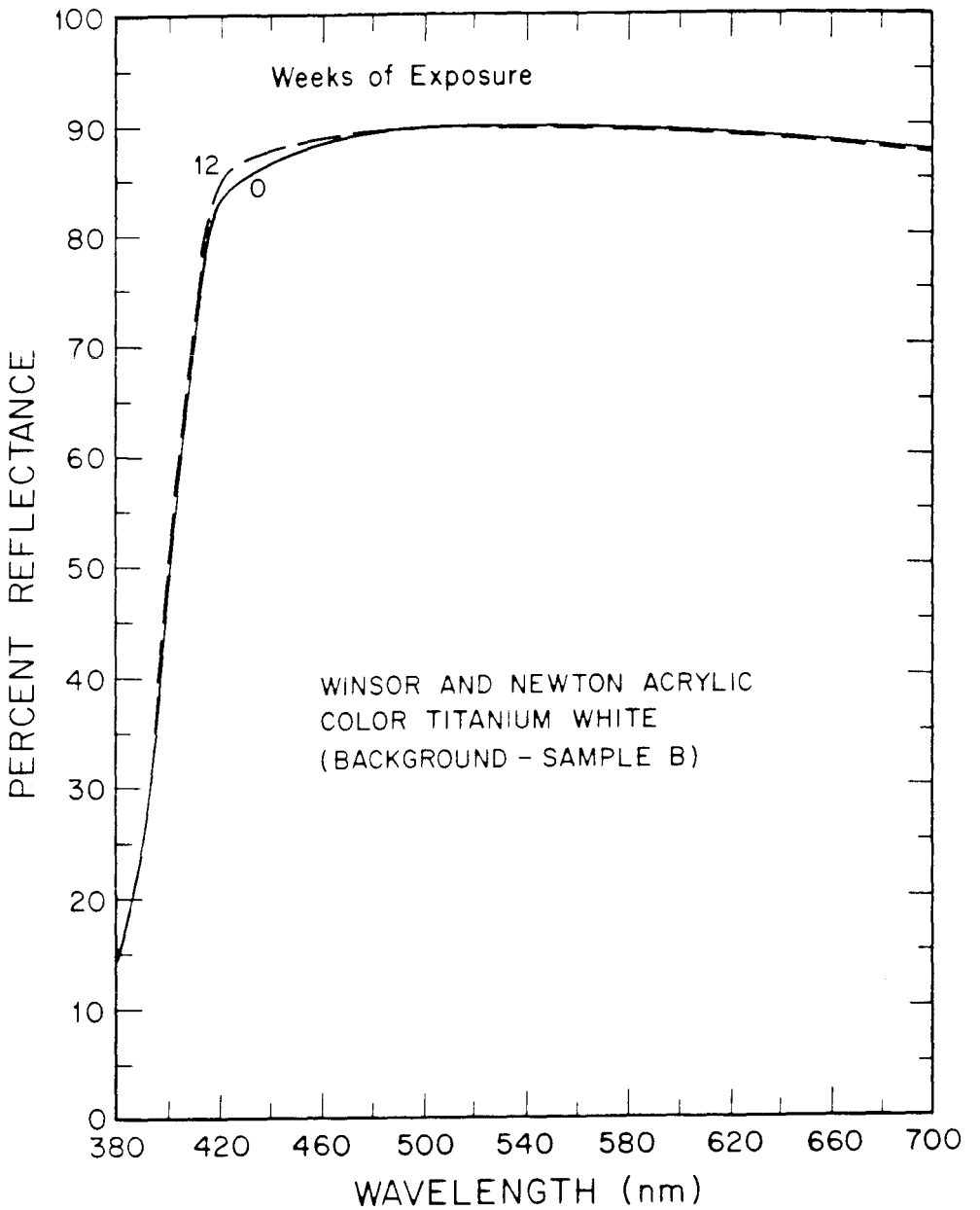

Figure 11.3. Reflectance spectrum of Winsor and Newton acrylic color titanium white paint layer before and after exposure to 0.40 ppm ozone at 22°C, 52% RH in the absence of light for 12 weeks.

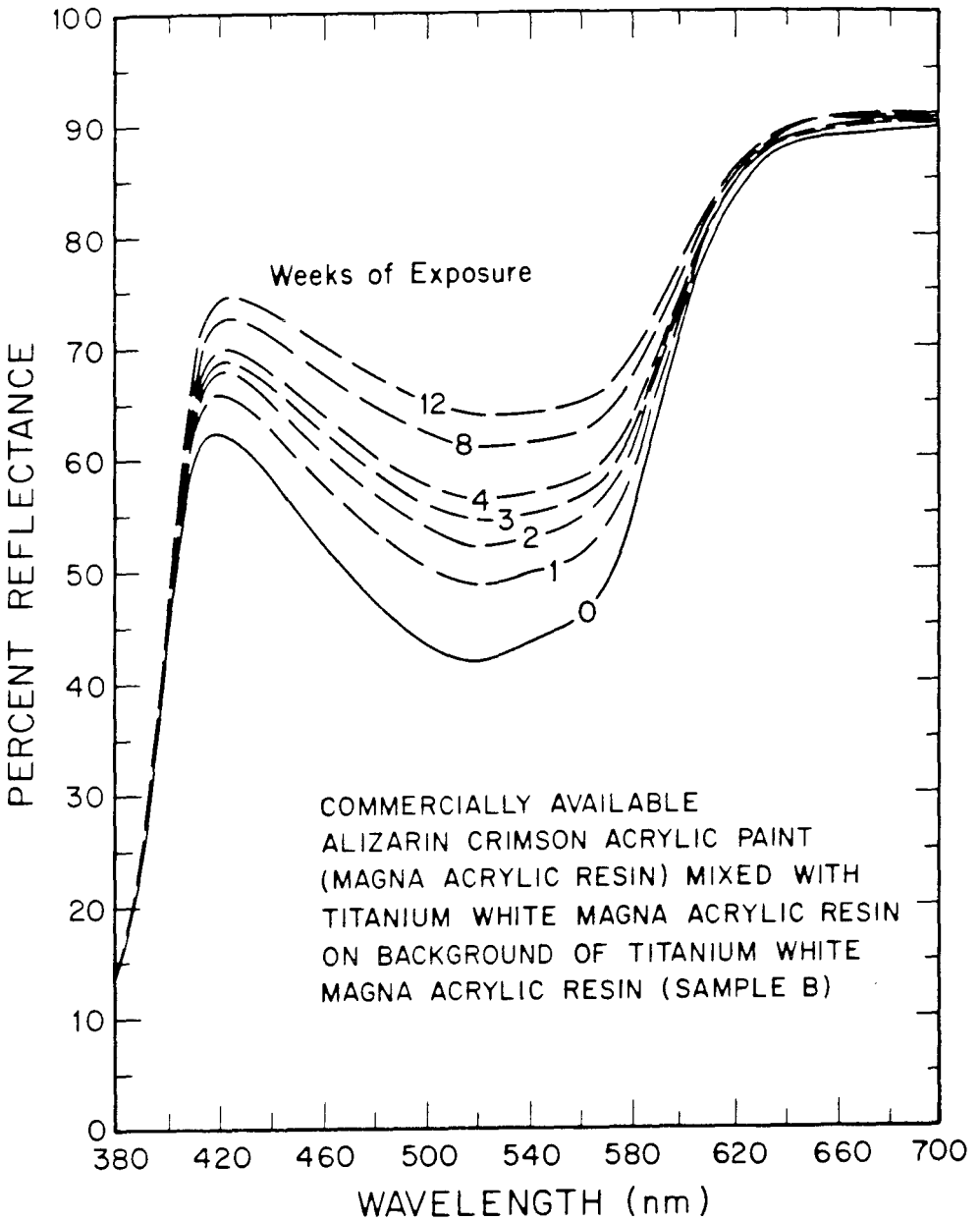

Figure 11.4. The reflectance spectrum of an Alizarin Crimson paint prepared in a binder of Magna Acrylic Resin at varius stages during its exposure to 0.40 ppm ozone, at 22°C, 52% RH, in the absence of light.

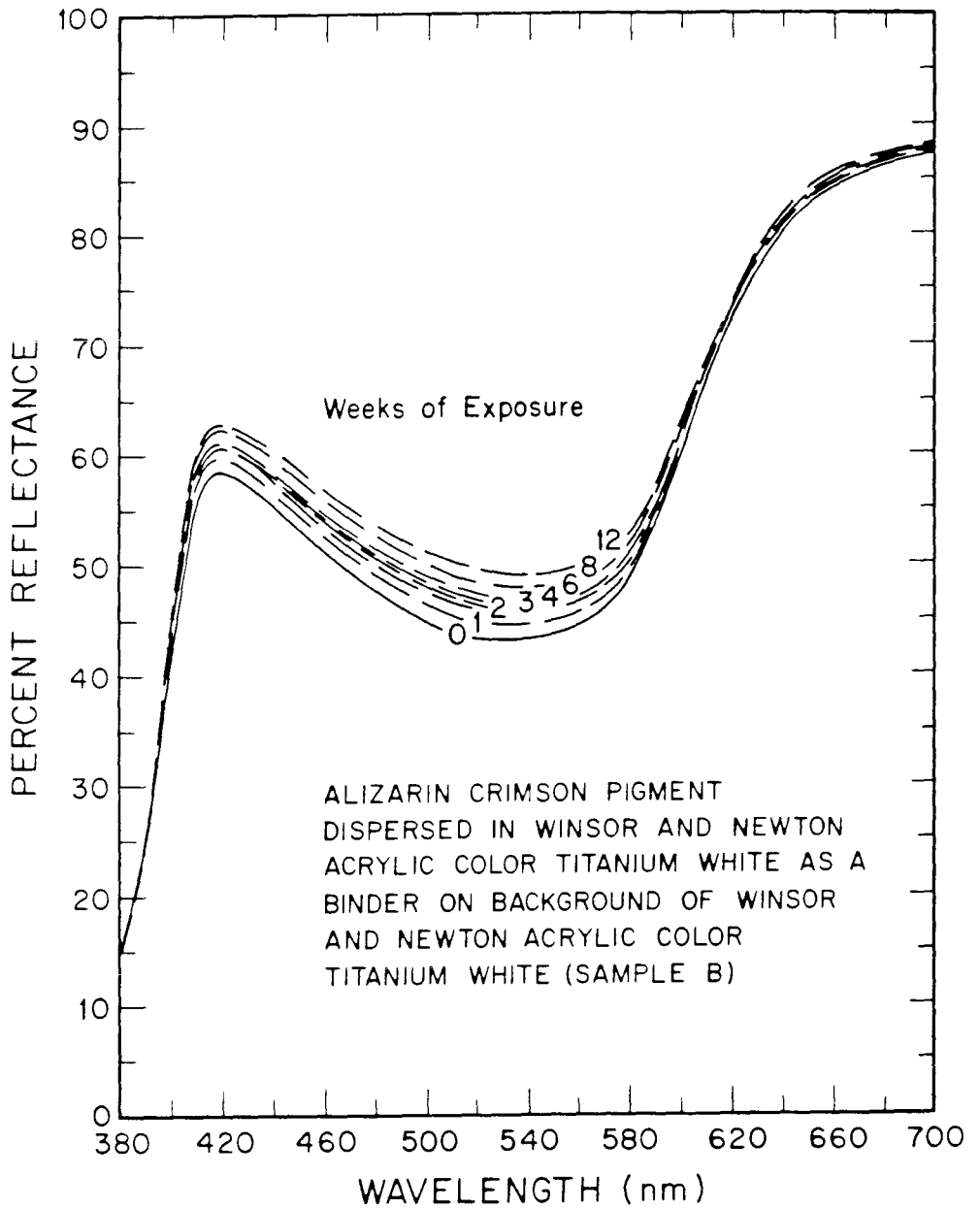

Figure 11.5. The reflectance spectrum of Alizarin Crimson pigment dispersed in Winsor and Newton Acrylic Color titanium white paint at several stages during its exposure to 0.40 ppm ozone at 22°C, 52% RH, in the absence of light.

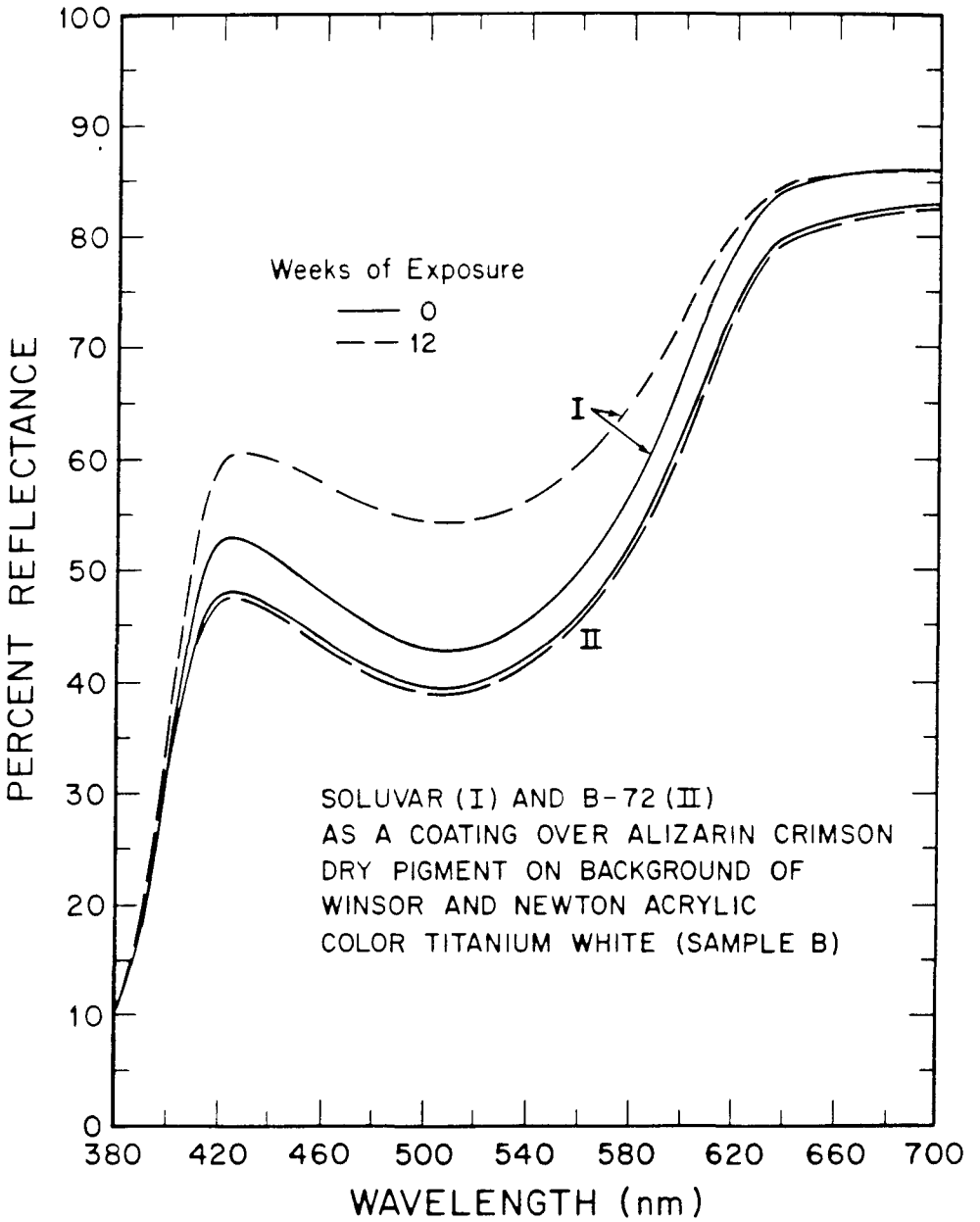

Figure 11.6. The effect of protective coatings on the change in the reflectance spectrum of Aizarin crimson dry pigment on a titanium white background upon exposure to 0.40 ppm ozone at 22°C, 52% RH in the absence of light. Sample I has been coated with Soluvar; Sample II has been coated with B-72.

by such coatings.

The color fastness of compound systems consisting of titanium white backgrounds, an Alizarin Crimson paint layer created using the binders of interest, followed by a coating layer is addressed in Table 11.6. Color changes observed in systems where both a binder and coating are used generally are quite small under the conditions of this experiment. An appropriately chosen coating will protect an ozone-sensitive paint layer, as can be seen by comparing the coated acrylic paint sample shown in Figure 11.7 to its uncoated counterpart in Figure 11.5. It is interesting to note that all of the samples containing damar varnish, which fell in the category of "borderline" materials, had a tendency to become tacky after the exposure to ozone. Presumably this is an indicator of some reaction of the damar itself with ozone. This reactivity could be the reason that Alizarin Crimson is protected by a coating of damar (Table 11.3), which consumes the ozone before reaching the underlying pigment, but not when the pigment is contained in a paint having damar as the binder (Table 11.2). Despite its apparent protection of sensitive paints from ozone fading (Table 11.6), the apparent reaction and change in physical properties of the damar would tend to argue against its general use as a varnish in those cases where protection against ozone damage is sought.

Similarly, the changes in the optical properties, permeability, or solubility of all of these varnishes upon ozone exposure are relevant in assessing their suitability as protective varnishes. Further, the ozone protection afforded by various polymer materials is dependent upon more than merely the chemical constitution of the material. The ability of a polymer to form a continuous, impermeable layer can also depend on the solvent used in the casting of the film from solution and on the surface tension of the layers immediately adjacent to it (27). It is interesting to note that the two paints in this study having polymer emulsion vehicles, which reportedly form very permeable films (28), also provide little protection for the ozone-

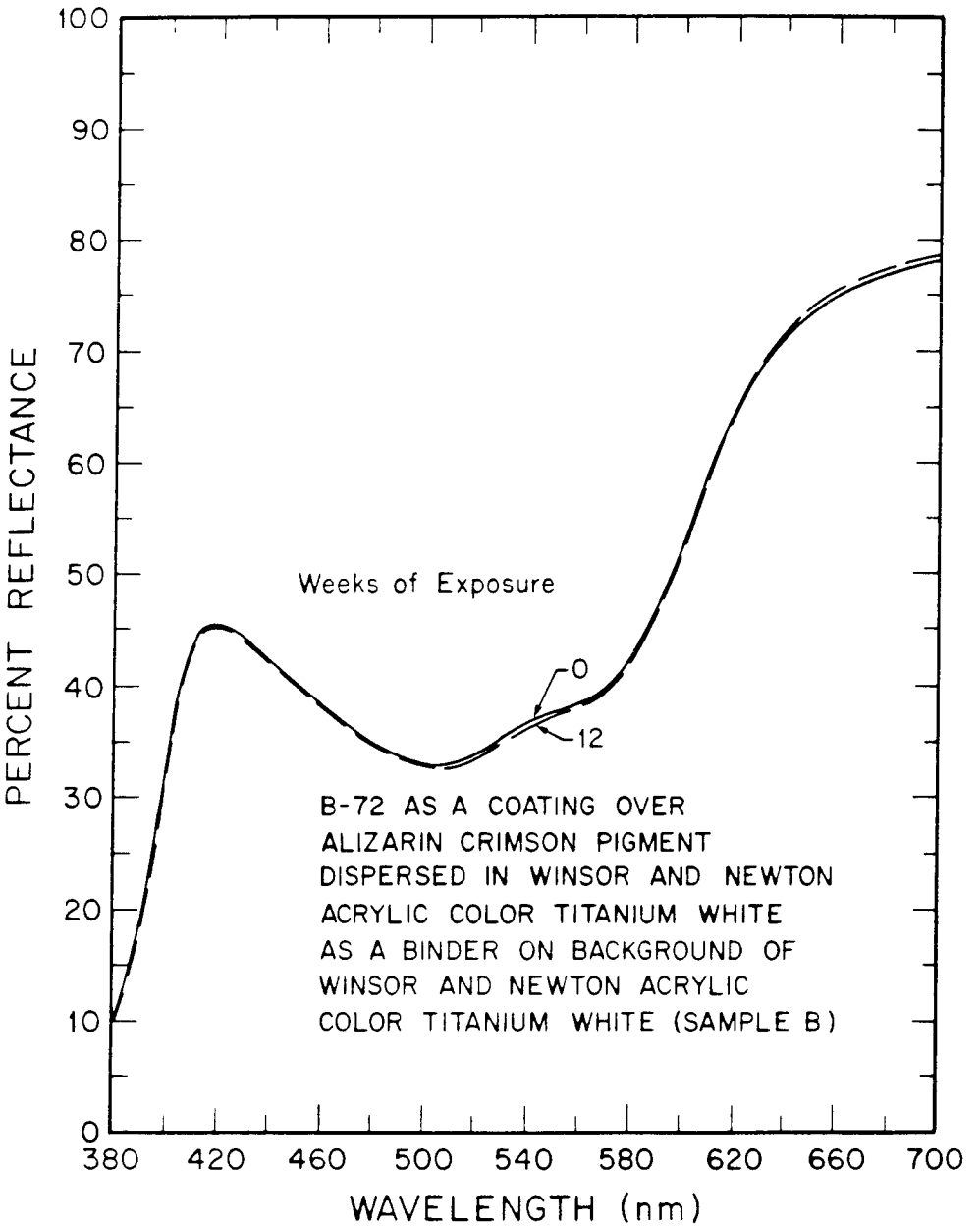

Figure 11.7. The reflectance spectrum of an ozone-sensitive Alizarin Crimson acrylic paint that has been coated with B-72, shown before and after exposure to 0.40 ppm ozone at 22°C, 52% RH, in the absence of light for 12 weeks.

sensitive pigment they contain. Studies of the ozone-induced changes in the intrinsic properties of these polymers must be left as areas of future research. The present work nevertheless has begun to address the quality of the protection of the colorants, surely a primary concern in any case.

CONCLUSION

The extent to which an ozone-fugitive pigment that has been placed in a binder and coating system will fade upon exposure to ozone has been examined. The results indicate that, for the ozone dosage used in this experiment (0.40 ppm over a twelve-week period), protecting the pigment by using a binder and/or coating can significantly reduce the rate of fading of the pigment. For the majority of the binders and coatings studied, little or no fading of the contained pigment was observed. There were, however, major exceptions to this trend. Of the binders and coatings studied, several of the acrylic media do not offer full protection from ozone-induced fading.

REFERENCES FOR CHAPTER 11

1. C.L. Shaver, G.R. Cass, and J.R. Druzik, "Ozone and the Deterioration of Works of Art," *Environmental Science and Technology, 17* (1983), 748-752.

2. K. Drisko, G.R. Cass, P.M. Whitmore, and J.R. Druzik, "Fading of Artists' Pigments due to Atmospheric Ozone," in *Wiener Berichte über Naturwissenschaft in Der Kunst,* Bd. 2/3, 1985/86, ed. A. Vendl, B. Pichler, and J. Weber. (Verlag ORAC, Vienna, 1985/86).

3. P.M. Whitmore, G.R. Cass, and J.R. Druzik, "The Ozone Fading of Traditional Natural Organic Colorants on Paper," *J. Amer. Inst. for Conservation, 26* (1987), 45-58.

4. P.M. Whitmore, and G.R. Cass, "The Ozone Fading of Traditional Japanese Colorants," *Studies in Conservation, 33* (1988), 29-40.

5. D. Grosjean, P.M. Whitmore, C.P. De Moor, G.R. Cass, and J.R. Druzik, "Fading of Alizarin and Related Artists' Pigments by Atmospheric Ozone: Reaction Products and Mechanisms," *Environmental Science and Technology, 21* (1987), 635-643.

6. D. Grosjean, P.M. Whitmore, G.R. Cass, and J.R. Druzik, "Ozone Fading of Natural Organic Colorants: Mechanisms and Products of the Reaction of Ozone with Indigos," *Environmental Science and Technology, 22* (1988), 292-298.

7. D. Grosjean, P.M. Whitmore, G.R. Cass, and J.R. Druzik, "Ozone Fading of Organic Colorants: Products and Mechanism of the Reaction of Ozone with Curcumin"; *Environmental Science and Technology* (in press).

8. D. Grosjean, P.M. Whitmore, G.R. Cass, and J.R. Druzik, "Ozone Fading of Triphenylmethane Colorants: Reaction Products and Mechanisms"; manuscript in preparation, California Institute of Technology, 1988.

9. J.B. Upham, and V.S. Salvin, "Effects of Air Pollutants on Textile Fibers and Dyes"; U.S. Environmental Protection Agency, Research Triangle Park, NC, 1975; EPA-650/3-74-008.

10. C.E. Bradley and A.J. Haagen-Smit, "The Application of Rubber in the Quantitative Determination of Ozone," *Rubber Chem. Technol., 24* (1951), 750-755.

11. H.H.G. Jellinek, and A.K. Chaudhuri, "Inhibited Degradation of Nylon 66 in Presence of Nitrogen Oxide, Ozone, Air, and Near-Ultraviolet Radiation," *J. Polymer Sci. Part A (Chemistry), 10* (1972), 1773-1778.

12. J. Peeling, M.S. Jazzar, and D.T. Clark, "An ESCA Study of the Surface of Polystyrene Film," *J. Polymer Sci. Part A (Chemistry), 20* (1982), 1797-1805.

13. G.G. Campbell, G.G. Schurr, D.E. Slawikoski, and J.W. Spence, "Assessing Air Pollution Damage to Coatings," *J. Paint Tech., 46* (1974), 59-71.

14. N. Grassie, and G. Scott, *Polymer Degradation and Stabilization* (Cambridge University Press, Cambridge, 1985) 194-195.

15. R.W. Murray, and P.R. Story, in E.M. Fettes, *Chemical Reactions of Polymers* (Interscience, New York, 1964) 672-721.

16. E.R. de la Rie, "Polymer Stabilizers: A Survey with Reference to Possible Applications in the Conservation Field," *Studies in Conservation, 33* (1988), 9-22.

17. A. Davis, and D. Sims, *Weathering of Polymers* (Applied Science, London, 1983) 261.

18. M. Matsui, and T. Kitao, "The Effect of Antiozonants on the Reaction of Dyes with Ozone: 1. Mechanism of Antiozonant Action," *J. Soc. Dyers and Colourists, 101* (1985), 334-336.

19. W.L. Hawkins, *Polymer Degradation and Stabilization* (Springer-Verlag, Berlin, 1984).

20. K. Raft, "A Preliminary Report on the Possibility of Using Bleached Beeswax to Improve the Resolubility of Picture Varnishes Based on Cyclohexanones," *Studies in Conservation, 30* (1985), 143-144.

21. P.M. Whitmore and G.R. Cass, unpublished results, California Institute of Technology, Pasadena, CA.

22. W.W. Nazaroff, and G.R. Cass, "Mathematical Modeling of Chemically Reactive Pollutants in Indoor Air," *Environmental Science and Technology, 20* (1986), 924-934.

23. R. Johnston-Feller, and C. Bailie, "An Analysis of the Optics of Paint Glazes: Fading," in N.S. Brommelle and G. Thomson, *Science and Technology in the Service of Conservation* (International Institute for Conservation, London, 1982) 180-185.

24. R. Massey, *Formulas for Painters* (Watson-Guptill, New York, 1979).

25. F.W. Billmeyer, Jr., and M. Saltzman, *Principles of Color Technology,* 2nd edition (John Wiley and Sons, New York, 1981).

26. "Standard Method of Specifying Color by the Munsell System," Designation D1535-80, American Society for Testing and Materials, Philadelphia, PA, 1980.

27. A. Carré, and H.B. Schreiber, "Dependence of Surface Properties in PMMA Coatings on Preparation History," *J. Coatings Technol., 54* (1982), 31-35.

28. R. Feller, N. Stolow, and E. Jones, "On Picture Varnishes and Their Solvents," (National Gallery of Art, Washington, DC, 1985), 218-225.

CHAPTER 12
PROTECTION OF WORKS OF ART FROM DAMAGE DUE TO ATMOSPHERIC OZONE

INTRODUCTION

Experiments conducted in controlled exposure chambers show that a variety of artists' pigments and colorants will fade severely if exposed to ozone at the levels found in Los Angeles photochemical smog (1-4). Pigments that are particularly sensitive to oxidation and fading by ozone include the anthraquinone lakes (including madder lakes), indigos, Dragon's Blood, curcumin (turmeric), saffron, and orpiment. Other materials that may be found in museum collections also are vulnerable to ozone attack, including textile fibers, textile dyes, cellulose, and polymers such as those found in rubber and in paint binders (5-17). Because of the recognized potential for damage to collections, the recommended limits on ozone concentrations in the indoor air of museums, libraries and archives are quite low, ranging from 0.013 ppm to 0.001 ppm, as seen in Table 12.1 (5,18-24). Most recommendations are that indoor ozone concentrations in such facilities be limited to about 0.001 ppm.

Ozone is produced in outdoor urban atmospheres by photochemical reactions involving hydrocarbons and the oxides of nitrogen (25). The Los Angeles area is widely known to have the highest ozone concentrations in the United States, but many other cities show outdoor ozone concentrations that exceed the air quality standards that have been set by the U.S. Environmental Protection Agency. The highest 1-hr average outdoor ozone concentration in the air basin that surrounds Los Angeles reached 0.35 ppm during 1986 (26), and the highest 1-hr average ozone concentration during the year averaged over all ozone monitoring sites in the United States exceeded 0.12 ppm in the early 1980's (27). Ozone concentrations averaged over all hours of the year are lower, in the range 0.02 to 0.054 ppm across the air monitoring sites located in the Los Angeles area (26). Average outdoor

Table 12.1. Suggested ozone concentration limits for art galleries, archives and libraries (after ref. 5)

Authority or Installation	Ozone Concentration Limit (ppm)	Reference
American National Standards Institute (draft)	0.001 ppm	(18)
British Museum Library	0.00 ppm	(5,19)
Canadian Conservation Institute	0.010 ppm	(5,20,21)
National Bureau of Standards	0.013 ppm	(19)
National Research Council	0.001 ppm	(22)
Newberry Library -Paul N. Banks	0.001 ppm	(5,23)
Royal Ontario Museum Workshop	use activated carbon	(5,19)
G. Thomson	reduce to trace levels (0-0.001 ppm)	(5,24)

ozone concentrations in the range 0.017 to 0.035 ppm are reported widely throughout the world, even at remote locations (28).

Measurement programs have demonstrated that high outdoor ozone concentrations can be transferred to the indoor atmosphere of museums. Shaver et al. (1) found that ozone concentrations inside an art gallery in Southern California that had a conventional air conditioning system were more than half as high as those outdoors. Davies et al. (29) reported ozone concentrations at 70% ± 10% of the outside ozone levels in a contemporary art gallery in rural eastern England. A recent comprehensive study of eleven museums, galleries, historical houses and libraries in Southern California showed that facilities with a high air exchange with the outdoors and no pollutant removal system have indoor ozone concentrations greater than two-thirds as high as those outdoors (see Chapter 10). Ozone concentrations as high as 0.143 ppm were measured inside one such museum. In that same survey, it was found that museums with conventional air conditioning systems showed indoor ozone concentrations about 30% to 40% of those outside, while museums with no forced ventilation system where slow air infiltration provides the only means of air exchange have indoor ozone levels typically 10% to 20% of those outdoors. Every museum facility studied that lacked a deliberate ozone removal system showed indoor ozone concentrations that were above 0.010 ppm at times (see Chapter 10 and reference 30).

The purpose of the present chapter is to examine a variety of methods that can be used to protect museum collections from damage due to atmospheric ozone. Control measures studied include elimination of pollutants from indoor air via ventilation system redesign, construction of display cases to protect the works, framing of paintings, prints and watercolors behind glass, selection of ozone-resistant pigments, and application of binders and coatings that will protect ozone-sensitive pigments. Each of these ozone damage prevention techniques will be discussed.

Ozone Removal Via Activated Carbon

Activated carbon air filtration systems have been employed for indoor pollutant control in a number of Southern California museums. An activated carbon system was installed at the Huntington Art Gallery on the Huntington Library grounds in the early 1950's. At present, similar systems are employed at the Los Angeles County Museum of Art, the J. Paul Getty Museum, the Norton Simon Museum, and at the Southwest Museum Library. The ventilation system at the Virginia Steele Scott Gallery on the Huntington Library grounds recently has been outfitted with activated carbon for the purpose of ozone removal.

The single-pass ozone removal efficiency of activated carbon beds in actual use is reported to be as high as 95 ± 5% when fresh, declining to 50% removal after 3600 hours of use (1000 kg of activated carbon used to filter 14,000 cfm of air during May-October in Pasadena, CA; ref. 31). The resultant indoor ozone concentrations will depend on the details of how the activated carbon beds are integrated into the building's ventilation system. Refering to the ventilation system schematic shown in Figure 12.1, activated carbon filters could be placed on the outdoor make-up air inlet only (filtering airstream f_{ox}), with no direct treatment of the recirculated air flow. That is the configuration used at the Norton Simon Museum in Pasadena, CA. Alternatively, both the outdoor make-up air and the recirculated air flow could be passed through activated carbon filters, as is the case at the new installation at the Scott Gallery. In addition, the ratio of recirculated air to outdoor make-up air can be varied, which will affect the ultimate indoor ozone concentration. To examine the effect of ozone removal efficiency and air recirculation options on indoor ozone concentrations an indoor air quality simulation model can be used.

In Chapter 9 of this work, a computer-based air quality model was developed for prediction of the indoor concentrations of photochemically-generated air pollu-

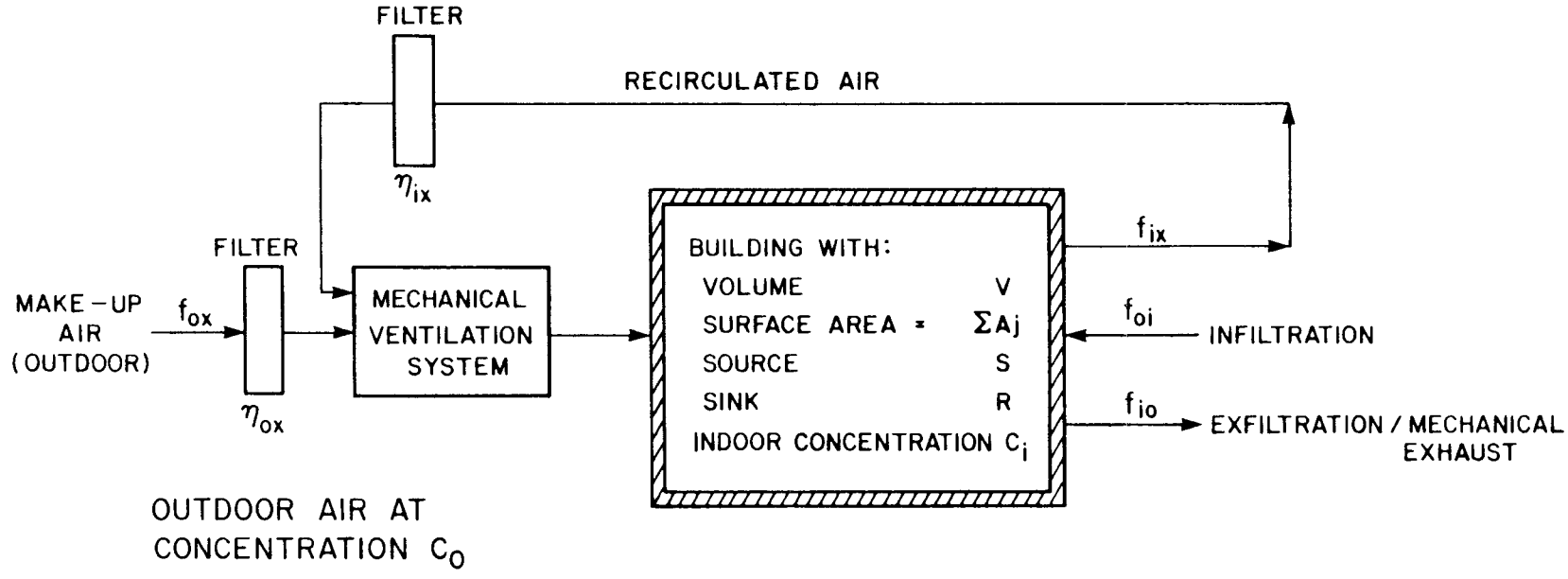

Figure 12.1. Schematic representation of a simple building ventilation system.

tants. In Chapter 10, a simplified version of that model was employed to determine that the indoor ozone concentrations observed in several museums were consistent with our present understanding of the effects of ventilation system design and ozone loss rates at interior surfaces. For a building that can be represented as a single well mixed volume with no indoor chemical reactions between pollutants and with a ventilation system that can be represented in the form of Figure 12.1, the model reduces to:

$$V\frac{dC_i}{dt}=(1-\eta_{ox})\,f_{ox}C_o+(1-\eta_{ix})\,f_{ix}C_i+f_{oi}C_o-f_{io}C_i+s-R \qquad (12.1)$$

where C_o and C_i are the outdoor and indoor pollutant concentrations. The parameters f_{ox}, f_{ix}, f_{oi}, and f_{io} denote the make-up air, recirculated air, infiltration air, and exfiltration plus exhaust air volumetric flow rates, respectively. The filtration efficiencies for pollutant removal are given at the make-up air supply (η_{ox}) and at the recirculated air supply (η_{ix}). R represents the removal rate of the pollutant by reaction at indoor surfaces, while s is the rate of indoor emission of that substance. For the museum gallery that will be studied here, there are no indoor sources. Ozone removal at building surfaces is described by

$$R=\sum_j v_{g_j}A_jC_i \qquad (12.2)$$

where v_{g_j} is the deposition velocity for ozone removal at the j^{th} surface that has surface area A_j. The ozone deposition velocity used for modeling purposes is 0.051 cm sec^{-1} (0.10 ft^3/ft^2-min) based on the experience of Hales et al. (32).

In Chapter 10, the model of Equations 12.1 and 12.2 was applied to study the causes of the ozone concentrations inside several Southern California museums. One of the sites studied was the Montgomery Gallery at Claremont, CA, which has a modern air conditioning system but no deliberate ozone removal system. Indoor

ozone concentrations in the Montgomery Gallery were predicted via modeling calculations to be about 47% as high as the outdoor peak ozone level, which is in close agreement with actual measurements made inside and outside of that building (see Figure 10.4). In Figure 12.2, the air quality model of Equations 12.1 and 12.2 is employed to compute the indoor ozone concentrations that would prevail in the Montgomery Gallery if activated carbon filters were placed on both the outdoor make-up air and on the recirculated air supply (air flows f_{ox} and f_{ix} in Figure 12.1), with no change from the base case air flow rates (6.48 air changes per hour total; 4.86 air changes per hour recirculated air; 1.62 air changes per hour outdoor make-up air). As seen in Figure 12.2, with 95% ozone removal during each pass through an activated carbon filter, peak indoor ozone levels in the Montgomery Gallery would drop to 0.0017 ppm versus a peak of 0.170 ppm outdoors. Greater than 99% removal relative to outdoor ozone concentrations could be achieved in that case by multiple passes of the indoor air through the activated carbon bed combined with ozone loss to interior building surfaces. Even with single pass filtration efficiencies, η_{ox} and η_{ix}, for ozone removal at the activated carbon bed of only 50%, the peak ozone concentration would drop from 0.171 ppm outdoors to 0.024 ppm indoors for the air flow conditions observed during our July 31, 1984 experiments at the Montgomery Gallery (see Figure 12.2).

The above analysis indicates that indoor peak ozone concentrations as low as 1% of that outdoors could be achieved at the Montgomery Gallery by addition of activated carbon filters alone under ideal conditions. However, experience gained through indoor measurements at other facilities where activated carbon systems are actually in use at present indicates that indoor ozone concentrations in the range of 3% to 37% of that outdoors are observed in practice (see Chapter 10, Table 10.7). Values at the higher end of this range apparently result from infiltration of untreated air through open doors or windows. When seeking to achieve very low

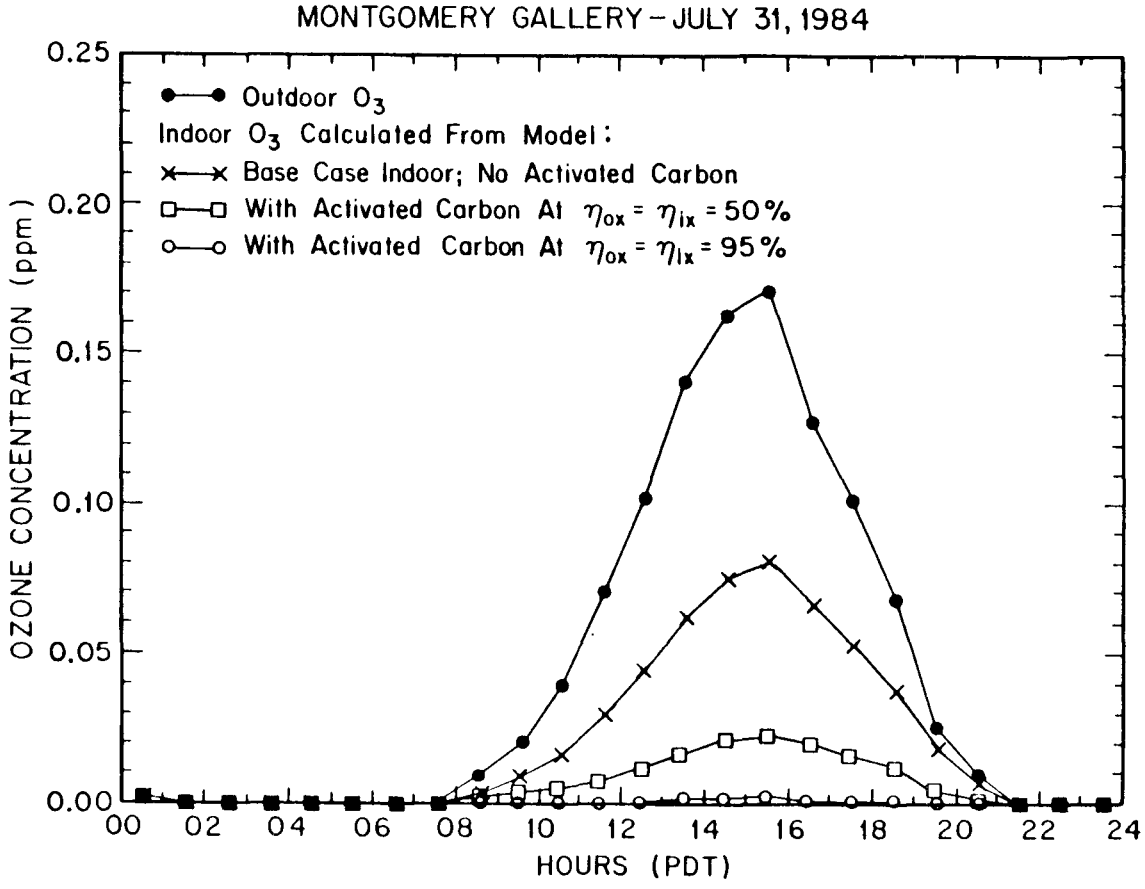

Figure 12.2. Air quality model predictions of the effect of activated carbon air filtration on ozone concentrations inside the Montgomery Gallery, Claremont, CA.

indoor ozone levels, prevention of extraneous infiltration of untreated air becomes a key factor in the overall system performance. If the building is pressurized such that air flows out the doors when they are opened, then infiltration will be reduced. Careful monitoring of the condition of the activated carbon bed also is required. As seen in Figure 12.2, a decrease in ozone removal efficiency (η_{ox} and η_{ix}) from 95% down to 50% is accompanied by a ten fold increase in indoor ozone levels. The activated carbon beds must be changed periodically when the ozone removal efficiency of the bed has fallen below design values.

The Effect of Reduced Outdoor Make-up Air

While activated carbon filters clearly can be used for ozone removal, the expense of their installation and maintenance may be beyond the budgets available to many museums. An alternative ozone control procedure that is available to some museums that have a conventional air conditioning system but no deliberate ozone removal system involves careful management of the ratio of recirculated air to outdoor make-up air, flows f_{ox} and f_{ix} in Figure 12.1.

As was discussed in Chapter 10, some of the lowest indoor ozone concentrations observed inside museums occur in private mansions that have been converted to museum use without the installation of a conventional air conditioning system of any kind. These buildings are operated with most doors and windows closed, and slow infiltration of outdoor air provides the only means of introduction of ozone into the building from outdoors. Outdoor air exchange rates from nearly zero up to one air exchange per hour are observed when these buildings are operated with the doors and windows mostly closed (see Chapter 10, Table 10.2 especially footnote f). Indoor ozone concentrations in the range of 10% to 20% of that outdoors are observed under these conditions (Table 10.4). This is significantly lower than the 30% to 40% ratio of indoor to outdoor ozone levels seen in most museums with conventional air conditioning systems. Careful study of this situation suggests that

it may be possible to attain the low indoor ozone levels found in buildings with slow air infiltration without sacrificing the temperature, humidity, and particulate pollutant control afforded by a conventional air conditioning system.

The approach that can be taken to achieve this result involves reducing the outdoor make-up air supply to the building's air conditioning system to the lowest value consistent with recommended ventilation codes, while increasing the recirculated air flow by a comparable amount. This air flow adjustment often can be accomplished by resetting existing mechanical dampers inside the system at no further capital expense. Any adjustment in this direction will reduce indoor ozone levels (in the absence of an indoor ozone source) because less ozone will be brought into the building from outdoors, while ozone removal at building surfaces will continue to deplete indoor ozone concentrations.

To illustrate the effect of rebalancing the air flows within a museum ventilation system, the indoor air quality model of Equations 12.1 and 12.2 will be used in conjunction with data from the Montgomery Gallery experiments. The Montgomery Gallery as tested has an interior volume of 2364 m^3 (83,475 ft^3) and an interior surface area of 2226 m^2 (23,964 ft^2). The total air flow through the ventilation system is 255.4 $m^3\ min^{-1}$ (9019 cfm), with one fourth of this flow (63.8 $m^3\ min^{-1}$) derived from outdoor air and three fourths of the air flow taken from recycled indoor air (191.5 $m^3\ min^{-1}$). At those airflow rates, the total air exchange rate for the building is 6.48 air changes per hour, with 1.62 changes per hour due to outdoor air plus 4.86 air changes per hour, due to recirculated indoor air. Standards for the minimum amount of make-up outdoor air for use in building ventilation systems are recommended by the American Society of Heating, Refrigerating, and Air-Conditioning Engineers (ASHRAE) (33). The minimum recommended outdoor make-up air flow rate is 8.5 m^3/hour per person occupying the building (33). Discussions with the Montomery Gallery personnel suggest that gallery occupancy is highly vari-

able. During the opening reception for a new exhibit, up to 300 persons may be in the building. Design guidelines for libraries (and museums) under normal operating conditions anticipate a design occupancy of 20 persons per 1000 ft^2 of floor space, which for the Montgomery Gallery is about 120 persons. At a design occupancy of 30 persons per 1000 ft^2 of floor area, the occupancy figure would be about 180 persons. However, on most days no more than 50 persons are actually present at the Montgomery Gallery. Much of the summer (the high ozone season), the gallery is closed to the public with only a few staff members present, and occupancy is even lower than 50 persons. At an air exchange rate of 8.5 $m^3\ hr^{-1}$ per person, these alternative occupancy figures for the Montgomery Gallery are translated into required outdoor make-up air flow rates in Table 12.2. The Montgomery Gallery as presently operated is configured to handle the few peak periods of high occupancy during a major reception, with some margin to spare. However, if such a facility were equipped with easiy adjustable dampers, the make-up air supply could be cut drastically from present settings during most hours of the year.

The effect that reduced outdoor make-up air would have on indoor ozone concentrations at the Montgomery Gallery was computed using the air quality model of Equations 12.1 and 12.2. Outdoor make-up air was reduced to the levels shown in Table 12.2, while recirculated air was increased to keep the total air exchange rate at the observed 6.48 air changes per hour. Calculations were based on the outdoor ozone levels measured during our July 31, 1984 experiments at the Montgomery Gallery. The results are shown in Figure 12.3. Under base case conditions, with 1.62 outdoor air exchanges per hour, a peak indoor O_3 concentration of 0.08 ppm is predicted, compared to an outdoor peak 1-hr average O_3 concentration of 0.171 ppm. At 1.08, 0.65, 0.43 and 0.18 outdoor exchanges per hour, the peak indoor ozone concentrations would drop to 0.065, 0.046, 0.033 and 0.016 ppm, respectively. If this building's outdoor air dampers were set for an occupancy of 50 per-

Table 12.2. Effect of occupancy on required outdoor make-up air supply at the Montgomery Gallery, Claremont, CA

Occupancy	Outdoor Air Flow (m^3/min)	Outdoor Air Exchanges per Hour
1. Base Case (building as tested July 31, 1984)	63.8	1.62
2. 300 persons	42.5	1.08
3. 180 persons	25.6	0.65
4. 120 persons	16.9	0.43
5. 50 persons	7.1	0.18

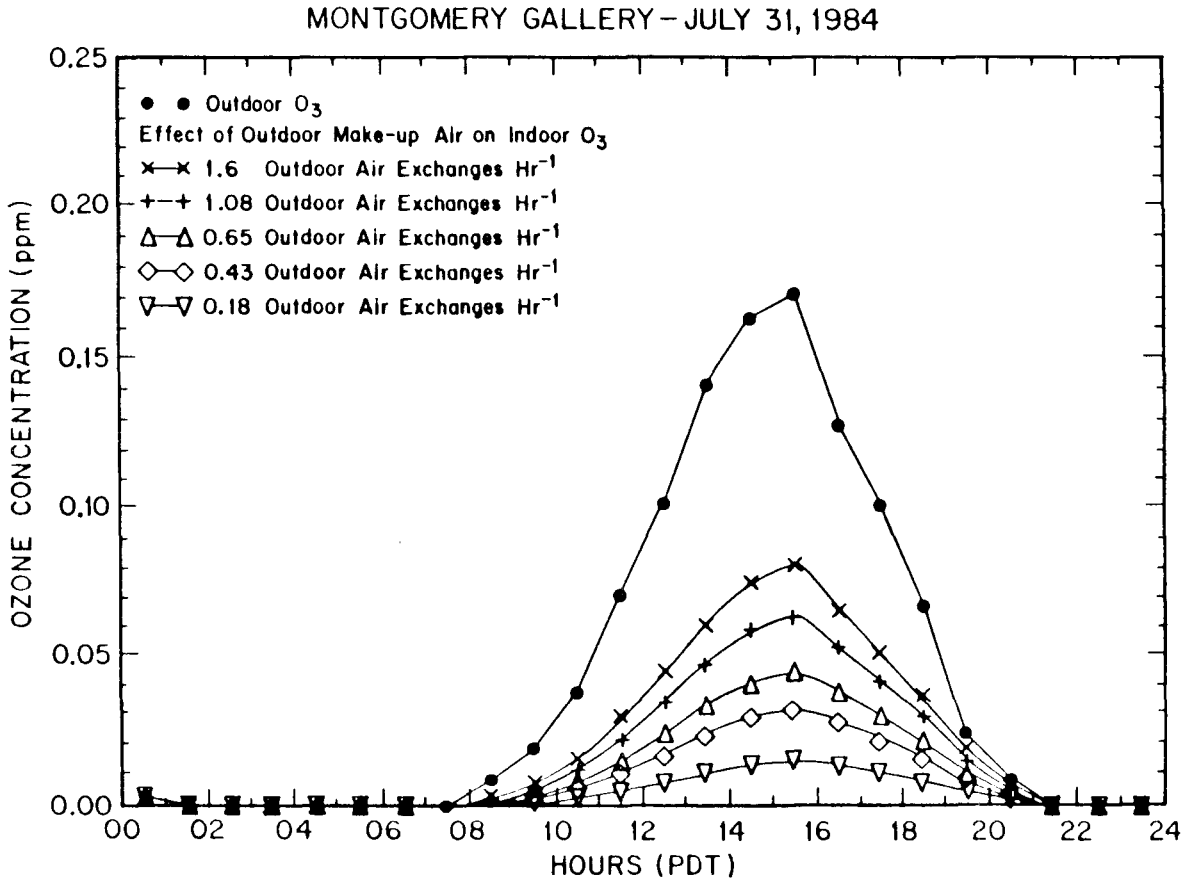

Figure 12.3. Air quality model predictions of the effect of altered outdoor make-up air flow rates on indoor ozone concentrations at the Montgomery Gallery, Claremont, CA.

sons or less most of the time, indoor ozone concentrations less than 10% of those outdoors could be maintained with little capital investment (as long as precautions are taken to minimize infiltration of outdoor air). Electro-mechanically driven dampers can be installed that are programmable by time of day, and that can be switched manually to a high make-up air flow condition during special events when the museum is unusually crowded.

Reduced make-up air and activated carbon filters, if used separately will each reduce indoor ozone levels. Both of these ventilation system modifications can be used simultaneously, for even greater ozone control. Indoor air quality modeling calculations for the Montgomery Gallery showing the effect of using activated carbon at $\eta_{ox} = \eta_{ix} = 95\%$ or 50% with various outdoor air exchange rates are displayed in Figures 12.4 and 12.5. With the outdoor air exchange rate reduced to comfortably accommodate 50 persons within the building (0.18 outdoor exchanges per hour) and with infrequent servicing of the activated carbon bed ($\eta_{ox} = \eta_{ix} = 50\%$), peak indoor ozone concentrations could be reduced to 0.003 ppm versus 0.171 ppm outdoors, an overall control efficiency of greater than 98%. With fresh activated carbon at $\eta_{ox} = \eta_{ix} = 95\%$, the same reduced make-up air flow and no infiltration, indoor ozone concentrations would drop to 0.0002 ppm (Figure 12.5). This is well below the most stringent indoor ozone air quality guideline (see Table 12.1), and would remain so even if outdoor ozone levels were increased to 0.40 ppm, which is approximately the highest outdoor value observed anywhere in the Los Angeles area in recent years.

A note of caution is in order. Reducing the flow of outdoor air will lead to reduced ozone concentrations in those cases where the ozone is supplied solely from outdoor air. It is possible for indoor ozone sources to occur due to the use of electrostatic precipitators for airborne particle removal, or through the use of duplicating machines or electric motors. If indoor sources are present, then reduc-

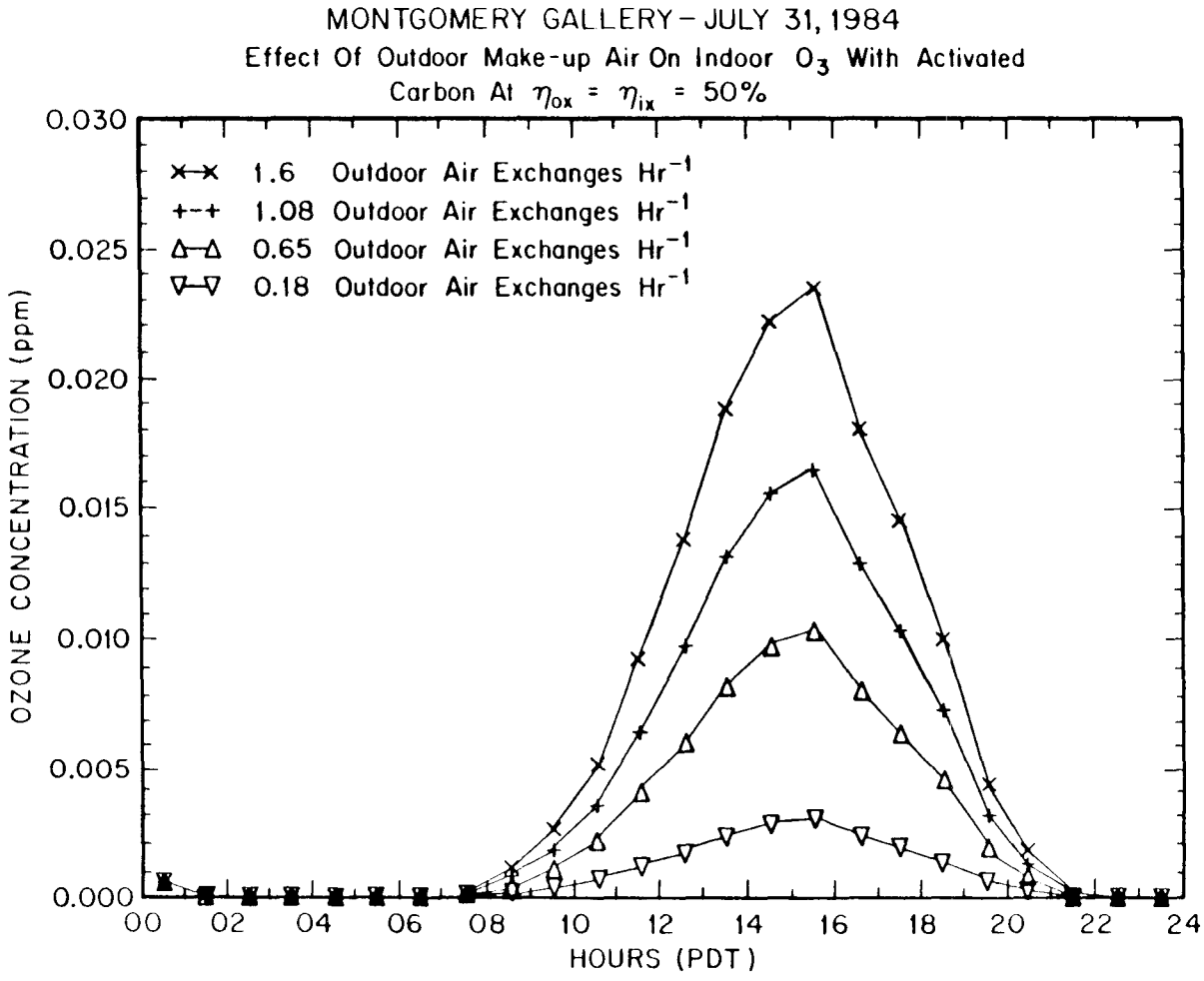

Figure 12.4. Air quality model predictions of the effect of the simultaneous use of activated carbon plus lowered outdoor make-up air on indoor ozone levels at the Montgomery Gallery: Case 1, activated carbon ozone removal efficiency is 50%.

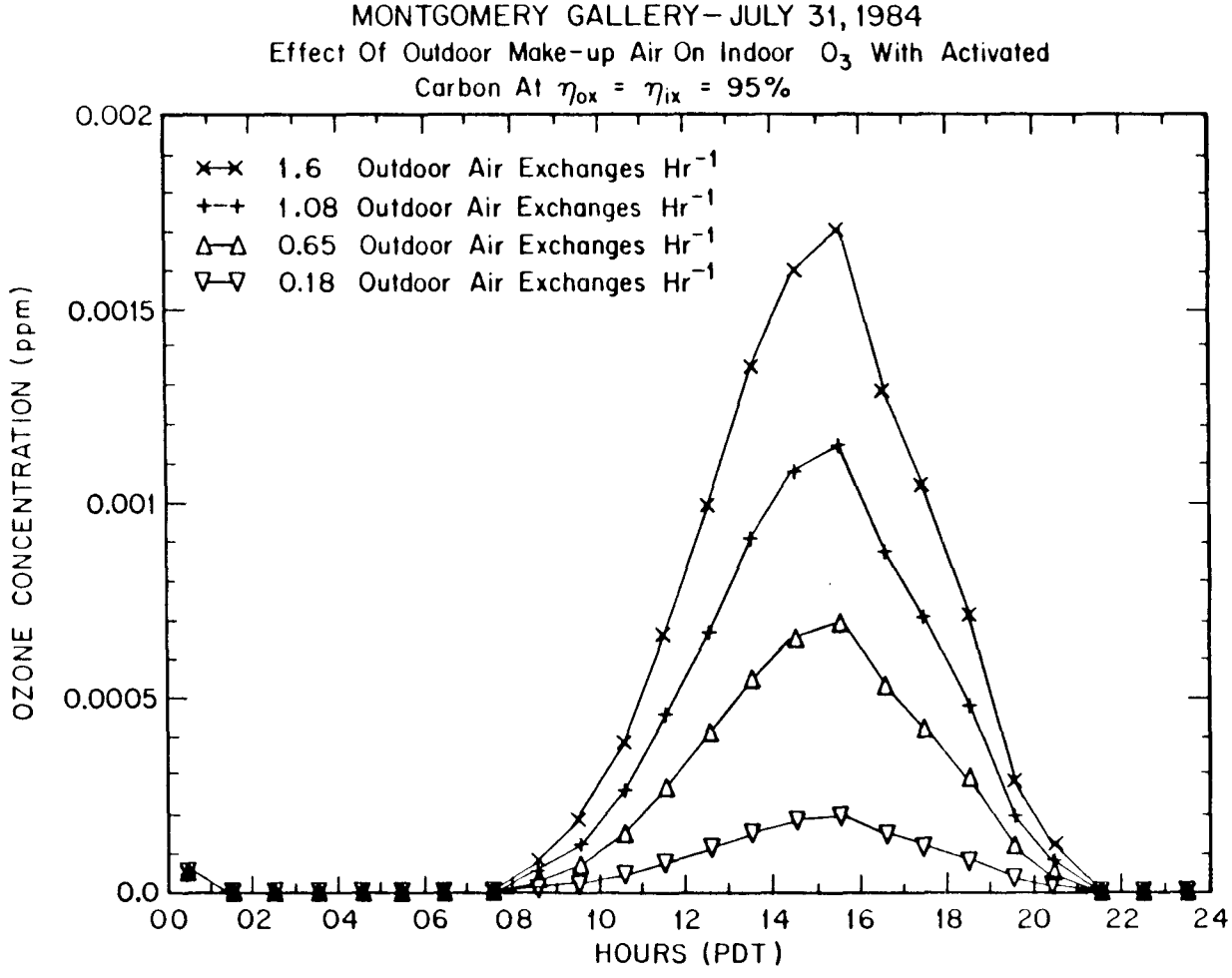

Figure 12.5. Air quality model predictions of the effect of the simultaneous use of activated carbon plus lowered outdoor make-up air on indoor ozone levels at the Montgomery Gallery: Case 2, activated carbon ozone removal efficiency is 95%.

ing the building's outdoor air supply may actually increase indoor ozone concentrations. Finally, any building that contains indoor sources of air pollutants other than ozone (e.g., formaldehyde emitted from particle board) should be analyzed carefully before the outdoor air exchange rate is reduced to ensure that other pollutant control problems are not aggravated.

The Effect of Display Cases

In situations where modifications to a museum's ventilation system are not practical, it may be possible to protect ozone-sensitive objects directly through the use of display cases. A display case can be viewed as another means for reducing the effective air exchange rate in the immediate vicinity of the object while allowing an extended time for ozone depletion by reaction with nearby interior surfaces.

Unusually high indoor ozone levels have been noted inside portions of the Southwest Museum, located in Los Angeles, CA (see Chapter 10, Table 10.3). Therefore, that museum was chosen as the site for testing the effect of display cases as a barrier between works of art and the indoor air.

A procedure for determining the air exchange rate between the room and a loosely fitted display case was developed, based on injection of SF_6 (an inert tracer gas measurable in ultra-small quantities) into the display case. These display cases selected for study, varying in size and construction, are described in Table 12.3. Approximately 1 cm^3 SF_6 was injected into each display case, and then air samples were withdrawn from the case periodically over a 110 to 140 min period using plastic syringes. These syringes were capped, and later analyzed for the SF_6 concentration in the air sampled by electron capture gas chromatography (35). Accompanying these experiments, ozone concentration measurements were made inside each display case and in the open room air surrounding each case using a matched pair of ultraviolet photometric ozone monitors (Dasibi, models 1003-AH and 1003-PC).

Table 12.3. Characteristics of three display cases tested for ozone removal at the Southwest Museum

Display Case	Interior Volume (m^3)	Interior Surface Area (m^2)	Surface Area of Air Gaps (m^2)	Comments
Display case 1	1.36	13.76	0.04	Painted drywall sides; painted wood inserts; track lighting on top of case. The front of the case has sliding glass doors, with an air gap between the doors.
Display case 2	4.75	19.09	0.06	Painted drywall sides; plastic lighting diffuser above; painted wood floor. The front of the case has three sliding glass doors with an air gap between the doors.
Display case 3	5.75	35.17	0.02	Painted drywall sides; painted wood ceiling with lights; painted wood floor and inserts. The front of the case is glass with a very small air gap running along the top edge of the glass front of the case.

The case of simple constant rate dilution of the SF_6 inside a display case by infiltration of the surrounding room air is governed by a differential equation of the form

$$\frac{dC}{dt}=-LC \tag{12.3}$$

where C is the SF_6 concentration inside the case and L is the air exchange rate (fraction of the display case air volume exchanged per unit time). For an initial SF_6 concentration, C_*, the solution to Equation 12.3 is

$$C(t)=C_* e^{-Lt} \tag{12.4}$$

and the characteristic time for air exchange between the display case and the surrounding room is L^{-1}. If Equation 12.4 holds, then a semi-logrithmic plot of SF_6 concentration against time should yield a straight line with concentration C_* at t=0 and a negative slope showing the value of the air exchange rate L. Experimental data for SF_6 exchange between Southwest Museum display case 3 that was described in Table 12.3 is shown in Figure 12.6. The characteristic time for air exchange between the display case and the surrounding room, L^{-1}, is 80.4 min. Analysis of similar data for display case 2 of Table 12.3 shows a characteristic time for air exchange of 23.1 min. SF_6 tests on display case 1 showed an air exchange pattern that was not log-linear, and therefore does not follow the form of Equation 12.4.

Ozone measurements made inside display case 3 and in the surrounding room air on September 22, 1985 are shown in Figure 12.7. While peak 1-hr average indoor ozone concentrations reached 0.079 ppm inside the Southwest Museum that day, corresponding ozone levels inside the display case never exceeded 0.008 ppm, a factor of ten lower. Display case 2 with its more rapid air exchange rate showed a peak ozone concentration of 0.009 ppm inside the case on a day with peak ozone concentrations of 0.065 ppm in the surrounding room air, or 14% of the room air

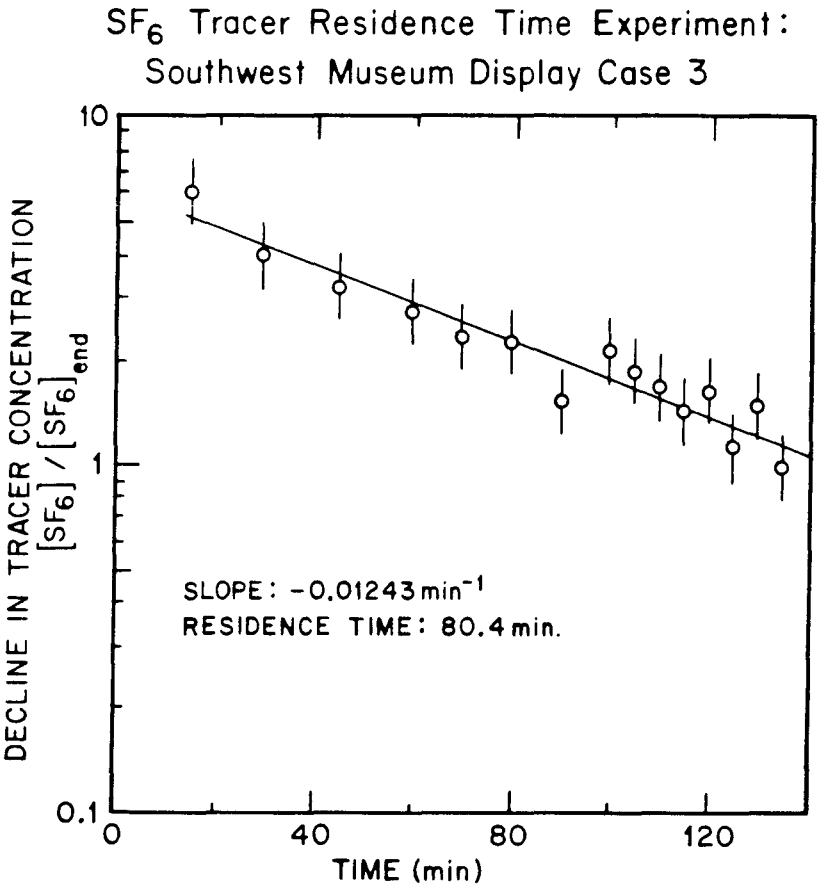

Figure 12.6. The decline in SF_6 concentration over time following injection of approximately 1 cm^3 of SF_6 into Southwest Museum display case 3. The SF_6 concentration has been normalized by dividing by the SF_6 concentration present at the end of the experiment (SF_{6end}).

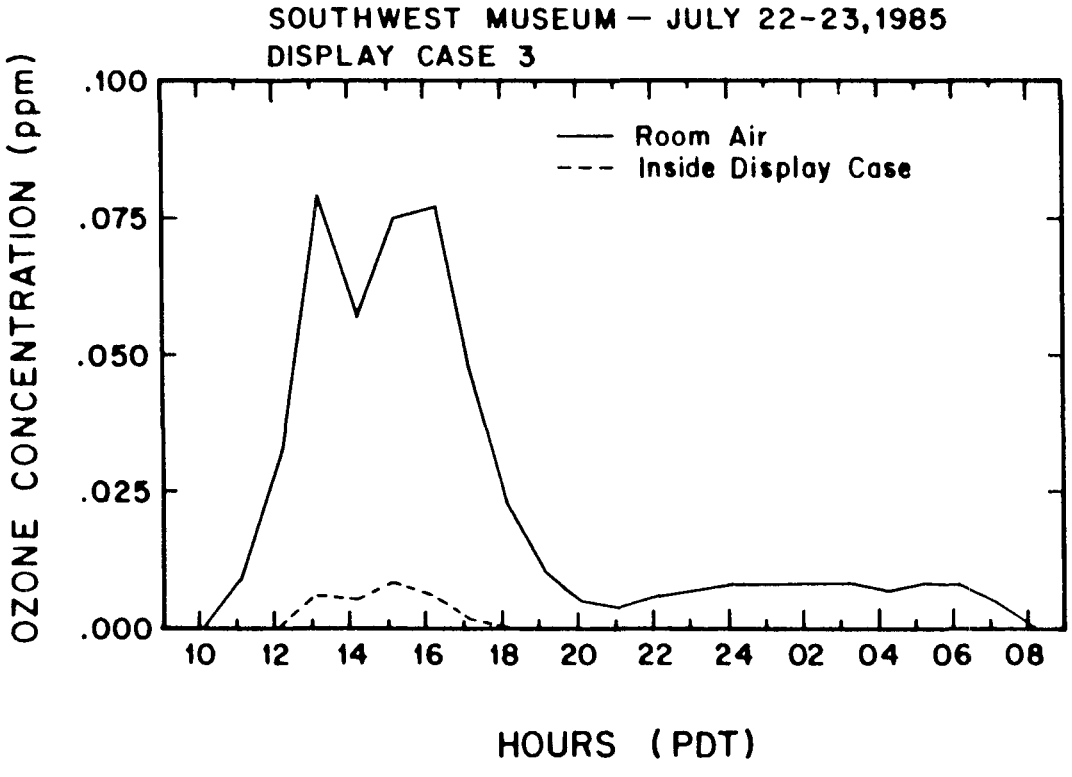

Figure 12.7. Ozone concentrations measured inside Southwest Museum display case 3 and in the surrounding room air, September 22, 1985.

ozone concentration found inside the display case.

It is clear that display cases can be used to greatly reduce the ozone levels in the immediate vicinity of sensitive objects as long as the characteristic time for air exchange between the room and the inside of the display case is sufficiently long.

The Effect of Framing

In the case of watercolors and paintings, the possibility exists to protect works of art from ozone damage by framing under glass. In order to test the protection afforded to an ozone-sensitive material by typical museum framing, a chamber exposure experiment was conducted in the laboratory.

Alizarin Crimson dry pigment is known to be one of the most ozone fugitive colorants typically used by artists (see Chapter 4). Two samples of Alizarin Crimson (Winsor and Newton) in methanol suspension were airbrushed onto Arches hot-pressed watercolor paper. Both samples were created at the same depth of shade, about 40% reflectance at the wavelength of maximum absorption. One sample was hinged to 4-ply acid-free mat board and mounted in a window mat (5cm x 5cm window). The matted sample was then enclosed in a standard wood frame (15.2cm x 20.3cm) with glass glazing, according to recommended practice (36). The framed and unframed samples then were exposed in the same chamber to 0.40 ppm O_3 at 50% RH, 22°C in the dark for 7 days according to the procedure described in Chapter 2. The diffuse reflectance spectra of these samples was measured before and after the ozone exposure using a Diano MatchScan II spectrophotometer. Color differences, ΔE, were calculated for CIE Illuminant C using the CIE 1976 L*a*b* formula.

As a result of that ozone exposure, the unframed sample experienced severe fading after 1 week (ΔE = 12.3), while the framed sample was essentially unchanged after exposure (ΔE = 0.3). It is concluded that conventional archival framing can act

to provide effective protection of vulnerable materials from ozone exposure (at least in the short term).

Selection of Ozone Resistant Pigments

Scientific research into the lightfastness of artists' pigments has resulted in permanence ratings that are widely available to the artist, both in standard reference works and in the literature furnished by the suppliers of artists' colors (37,38). In a similar fashion, protection against ozone-induced fading can be ensured for works of art that are yet to be created by selection of pigments that resist oxidation by ozone.

A large number of modern inorganic and organic artists' watercolors (1,2) and traditional organic pigments (3,4) have been tested for fading in the presence of atmospheric ozone. These experiments involved exposure to 0.3 to 0.4 ppm O_3 in the dark for three months at circa 22°C and 50% RH. That exposure (ozone concentration times duration) is roughly equivalent to a 6 to 8 year period inside a museum in the Los Angeles area that has conventional air conditioning but no deliberate pollutant removal system. Of the inorganic pigments tested, only the arsenic sulfides (e.g., orpiment), showed any definite color change due to ozone exposure (when judged by human observer Munsell color matches). Most of the traditional natural organic colorants tested show measurable fading when exposed to ozone. However, many of the modern synthetic organic colorants examined are relatively stable toward ozone exposure. Watercolors in the Winsor and Newton line containing quinacridone (PV 19), BON arylamide red (PR 10), chlorinated para red (PR 4), arylamide yellow (PY 1), and chlorinated copper phthalocyanine (PG 7) showed essentially no change in color before and after ozone exposure when judged by human observer Munsell color matches (2). While most organic colorants can be expected to react with ozone at some rate, modern synthetics can be found that react so slowly that their use should be considered as an alternative to the ozone-

fugitive traditional organic colorants, like the alizarin lakes.

The Effect of Binders and Coatings

In Chapter 11 of this report, binders and coatings were examined that might be used to protect ozone-sensitive pigments from oxidation by ozone or its reaction products. Binders studied included linseed oil, egg tempera, casein, beeswax, damar, alkyd enamel, acrylic polymer emulsions, and solvent-based acrylics, casein, damar, shellac, and Ethulose (a consolidant). It was found that most of the binders and coatings studied provided considerable protection from ozone induced fading in systems containing Alizarin Crimson as an example of an ozone-fugitive pigment. Important exceptions to this observaion were noted, however. Alizarin Crimson prepared as a paint in several acrylic binders faded severely, as did Alizarin Crimson dry pigment samples coated with some acrylic polymer emulsions. A change in the physical properties of damar varnish was noted upon ozone exposure. For selection of binder and coating systems that will protect ozone-sensitive pigments from fading, the interested reader should refer to the tables in Chapter 11.

CONCLUSION

It has been shown that a variety of approaches are available that can be used to protect museum collections from damage due to atmospheric ozone. Activated carbon filters placed in the building's ventilation system can be engineered to achieve very low indoor ozone levels. By this approach, ozone is removed from the room air, affording broad protection to all exhibits in the museum. In the absence of activated carbon filters, a strategy of reducing the outdoor make-up air to the building can be pursued that in many cases will reduce indoor ozone levels greatly. Display cases can be used to reduce the air exchange rate in the immediate vicinity of ozone-sensitive objects, thereby reducing ozone levels by extending the time available for ozone scavenging by indoor sufaces. Ozone levels inside display

cases can be cut by at least a factor of 10 relative to the room air, and a procedure for testing both the air exchange rate and ozone levels characteristic of such display cases has been demonstrated. Framing of sensitive watercolors behind glass has been shown experimentally to provide excellent protection against ozone-induced fading. Pigments have been identified that resist oxidation by ozone, and binder and coating systems have been described that will protect ozone-sensitive pigments if they must be used.

A wide range of alternative ozone control measures are available, many of which are both simple and inexpensive. With careful planning, most museum collections can be protected from damage due to atmospheric ozone.

REFERENCES FOR CHAPTER 12

1. C.L. Shaver, G.R. Cass, and J.R. Druzik, "Ozone and the Deterioration of Works of Art," *Environ. Sci. Technol., 17* (1983), 748-752.

2. K. Drisko, G.R. Cass, P.M. Whitmore, and J.R. Druzik, "Fading of Artists' Pigments due to Atmospheric Ozone," in *Wiener Berichte über Naturwissenschaft in Der Kunst,* Bd. 2/3, 1985/86, ed. A. Vendl, B. Pichler, and J. Weber. (Verlag ORAC, Vienna, 1985/86).

3. P.M. Whitmore and G.R. Cass, "The Ozone Fading of Traditional Natural Organic Colorants on Paper," *J. American Institute for Conservation, 26* (1987), 45-58.

4. P.M. Whitmore and G.R. Cass, "The Ozone Fading of Traditional Japanese Colorants," *Studies in Conservation, 33* (1988), 29-40.

5. N.S. Baer and P.N. Banks, "Indoor Air Pollution: Effects on Cultural and Historic Materials," *Int. J. Museum Manage. Curatorship, 4* (1985), 9-20.

6. L.S. Jaffe, "The Effects of Photochemical Oxidants on Materials," *J. Air Pollut. Control Assoc., 17* (1967), 375-378.

7. R.G. Newton, "Mechanism of Exposure Cracking of Rubber with a Review of the Influence of Ozone," *J. Rubber Res., 14* (1945), 27-39.

8. G.G. Campbell, G.G. Schurr, D.E. Slawikowski, and J.W. Spence, "Assessing Air Pollution Damage to Coatings," *J. Paint Technol., 46* (1974), 59-71.

9. N. Kerr, M.A. Morris, and S.H. Zeronian, "The Effect of Ozone and Lundering on a Vat-Dyed Cotton Fabric," *Am. Dyest. Rep., 58* (1969), 34-36.

10. A.A. Katai, and C. Schuerch, "Mechanism of Ozone Attack on α-methyl Glucoside and Cellulosic Materials," *J. Polymer Science; Part A-1, 4* (1966), 2683-2703.

11. V.S. Salvin, and R.A. Walker, "Service Fading of Disperse Dyestuffs by Chemical Agents Other than the Oxides of Nitrogen," *Textile Res. J., 25* (1955), 571-585.

12. V.S. Salvin, "Ozone Fading of Dyes," *Textile Chem. Color., 1* (1969), 245-251.

13. N.J. Beloin, "Fading of Dyed Fabrics Exposed to Air Pollutants," *Textile Chem. Color., 5* (1973), 128-133.

14. W.W. Lebensaft, and V.S. Salvin, "Ozone Fading of Anthraquinone Dyes on Nylon and Acetate," *Textile Chem. Color., 4* (1972), 182-186.

15. J.C. Haylock, and J.L. Rush, "Studies on the Ozone Fading of Anthraquinone Dyes on Nylon Fibers," *Textile Res. J., 46* (1976), 1-8.

16. F.M. Rowe, and K.A. Chamberlain, "Fading of Dyes on Cellulose Acetate Rayon," *J. Soc. Dyers. Colour., 53* (1937), 268-278.

17. V.S. Salvin, W.D. Paist, and W.J. Myles, "Advances in Theoretical and Practical Studies of Gas Fading," *Am. Dyest. Rep., 41* (1952), 297-302.

18. American National Standards Institute, "American National Standard Practice for Storage of Paper-Based Library and Archival Documents – Draft 4," ANSI z39.xx-1985 (American National Standards Institute, New York, 1985).

19. National Bureau of Standards, "Air Quality Criteria for Storage of Paper-Based Archival Records," NBSIR 83-2795 (National Bureau of Standards, Washington, D.C., 1983).

20. R.H. Lafontaine, "Recommended Environmental Monitors for Museums, Archives and Art Galleries," *Technical Bulletin (CCI), 3* (1978), 1-22.

21. R.H. Lafontaine, "Environmental Norms for Canadian Museums, Art Galleries and Archives," *Technical Bulletin (CCI), 5* (1979), 1-4.

22. Committee on Preservation of Historical Records, "Preservation of Historical Records," (National Research Council, National Academy Press, Washington, D.C., 1986).

23. P.N. Banks, *Addendum to Planning Report 7: Preliminary Statement on Environmental Standards for Storage of Books and Manuscripts* (The Newberry Library, Chicago, 1980).

24. G. Thomson, *The Museum Environment* (Butterworths, London, 1978).

25. J.H. Seinfeld, *Air Pollution: Physical and Chemical Fundamentals* (McGraw-Hill, New York, 1975).

26. California Air Resources Board "California Air Quality Data – Summary of 1986 Air Quality Data," (California Air Resources Board, Sacramento, CA, 1986).

27. U.S. Environmental Protection Agency, "National Air Quality and Emissions Trends Report, 1981," EPA-450/4-83-011 (Office of Air Quality Planning and Standards, U.S. Environmental Protection Agency, Research Triangle Park, N.C., 1983), p. 161.

28. Committee on Medical and Biologic Effects of Environmental Pollutants, "Ozone and Other Photochemical Oxidants," (National Academy of Sciences, Washington, D.C., 1977).

29. T.D. Davies, B. Ramer, G. Kaspyzok, and A.C. Delany, "Indoor/Outdoor Ozone Concentrations at a Contemporary Art Gallery," *J. Air Pollut. Control Assoc., 31* (1984), 135-137.

30. W.W. Nazaroff and G.R. Cass, "Mathematical Modeling of Chemically-Reactive Pollutants to Indoor Air," *Environ. Sci. Technol., 20* (1986), 924-934.

31. F.H. Shair, "Relating Indoor Pollutant Concentrations of Ozone and Sulfur Dioxide to Those Outside: Economic Reduction of Indoor Ozone through Selective Filtration of the Make-up Air," *ASHRAE Trans., 87* Part 1 (1981), 116-139.

32. C.H. Hales, A.M. Rollinson and F.H. Shair, "Experimental Verification of Linear Combination Model for Relating Indoor-Outdoor Pollutant Concentrations," *Environ. Sci. Technol., 8* (1974), 452-453.

33. American Society of Heating, Refrigerating and Air Conditioning Engineers, *ASHRAE Handbook - 1985 Fundamentals* (American Society of Heating, Refrigerating and Air Conditioning Engineers, Atlanta, GA, 1985).

34. R.A. Wadden and P.A. Scheff, *Indoor Air Pollution* (Wiley-Interscience, New York, 1983), p. 143.

35. P.J. Drivas, *Investigation of Atmospheric Dispersion Problems by Means of a Tracer Technique* (Ph.D. Thesis, California Institute of Technology, Pasadena, CA, 1974).

36. A.F. Clapp, *Curatorial Care of Works of Art on Paper* (Intermuseum Conservation Association, Oberlin, OH, 1978), pp. 71-80.

37. H.W. Levinson, *Artists' Pigments - Lightfastness Tests and Ratings* (Colorlab, Hallandale, FL, 1976).

38. Winsor and Newton, "Notes on the Composition and Permanence of Artists' Colours," (Winsor and Newton, Wealdstone, Harrow, Middlesex, HA3 5RH, England).